DISSERTATION

ANALYSIS OF EQUIVALENT WIDTHS OF ALLUVIAL CHANNELS AND APPLICATION FOR INSTREAM HABITAT IN THE RIO GRANDE

Submitted by

Claudia A. León

Department of Civil Engineering

In partial fulfillment of the requirements
For the Degree of Doctor of Philosophy
Colorado State University
Fort Collins, Colorado
Spring 2003

COLORADO STATE UNIVERSITY

1st February 2003

WE HEREBY RECOMMEND THAT THE DISSERTATION PREPARED UNDER OUR SUPERVISION BY CLAUDIA A. LEON ENTITLED "**ANALYSIS OF EQUIVALENT WIDTHS OF ALLUVIAL CHANNELS AND APPLICATION FOR INSTREAM HABITAT ON THE RIO GRANDE**" BE ACCEPTED AS FULFILLING PARTIAL REQUIREMENTS FOR THE DEGREE OF DOCTOR OF PHILOSOPHY.

Committee on Graduate Work

_____

_____

_____

_____

_____

_____

Adviser

_____

Department Head

ABSTRACT

ANALYSIS OF EQUIVALENT WIDTHS OF ALLUVIAL CHANNELS AND APPLICATION FOR INSTREAM HABITAT IN THE RIO GRANDE

Rivers are natural systems that adjust to variable water and sediment discharges. Channels with spatial variability in width that are managed to maintain constant widths over a period of time are able to transport the same water and sediment discharges by adjusting the bed slope. Methods developed to define equilibrium hydraulic geometry characteristics of alluvial channels are limited to steady state input variables.

This dissertation examines how the channel slopes adjust in sequential reaches with different widths to achieve continuity of steady and unsteady water and sediment discharges. The four objectives of this dissertation are: 1) to develop analytical relationships between equilibrium slope and width or width-depth ratio under steady water and sediment discharges; 2) to develop a transient numerical model for constant input variables to simulate the changes in channel slope with time; (3) to develop a transient numerical model for unsteady water and sediment discharges to simulate the transient solution of channel slope; and (4) to apply the model to the middle Rio Grande and integrate the results in the evaluation of potential fish habitat restoration activities.

Results of the analytical solutions indicate that wide channels require steeper slopes than narrow channels to transport the same water and sediment discharges. In addition, channel slope is highly dependent on sediment concentration. The analytical solutions are in good agreement with laboratory flume data previously

published and field measurements from the middle Rio Grande. Transient simulations under constant discharge show similar results. In addition, the model provides an estimate of the time to reach equilibrium under constant water discharge.

Transient simulations with variable discharge indicate that bed slope changes rapidly during floods. Long-term simulations of slope changes under variable water and sediment discharges compare better with the simulation under a constant flow close to the mean annual discharge than under constant large floods (e.g. discharge equalled or exceeded 10 % of the time, or discharge equal or close to the dominant discharge).

Field applications to the middle Rio Grande show that the wide channel reach of the Bosque del Apache has a steeper slope than the narrow reaches. Numerical simulations of the Bosque del Apache reach from 1992 to 1999 are in very good agreement with field measurements.

Despite the increase in slope in wide reaches, the results of the numerical simulations of the Bosque del Apache reach indicate that shallow depths and low velocities occur more frequently in wide and steeper reaches than in narrow reaches. It is likely that low velocities and shallow depths are more favorable for the habitat of the Rio Grande silvery minnow.

Claudia A. León
Department of Civil Engineering
Colorado State University
Fort Collins, CO 80523
Spring 2003

ACKNOWLEDGMENTS

I am very thankful for the guidance, encouragement and helpful suggestions of my adviser Dr. Pierre Y. Julien. I also would like to extend my appreciation to my committee member Ellen Wohl for her great comments and suggestions.

I am grateful to the U.S. Bureau of Reclamation for the funding, which make possible this research. I also would like to thank Drew Baird from the U.S. Bureau of Reclamation, Albuquerque, NM, for his comments and incentives. Paula Makar and Jan Oliver from the U.S. Bureau of Reclamation, Denver,CO, who provided many of the data sets used in this study.

Thanks to my friends Rosalia Rojas, Gigi Richard, Carmen Bernedo and Bellatrix Castelblanco for their friendship, support and smiles. Many thanks to my friend Angela Benedetti, for her friendship, support and invaluable help with Latex.

Thanks to my family, for their love, wisdom and support from a distance. Lastly but not least, I would like to thank Julio, my husband, for his love, support and patience. Thanks Julio for helping me to keep focus on my research and for pushing me to finish writing this dissertation.

Contents

List of Figures

List of Tables

LIST OF SYMBOLS

W	Channel width in m
S	Channel slope in m/m
ξ	Width-depth ratio in m/m
R_h	Hydraulic radius in m
Q	Water discharge in m^3/s
Q_s	Sediment discharge by volume in m^3/s
W_r	Width ratio
S_r	Slope ratio
h_r	Depth ratio
V_r	Velocity ratio
ξ_r	Ratio of width-depth ratios
n	Manning friction factor
f	Darcy-Weisbach friction factor
ϕ	Coefficient of Manning's resistance equation
	equal to 1 for SI units and 1.49 for English units
d_s	Particle size in mm
τ_*	Shields parameter
a	Coefficient in Brownlie's (1981) resistance equation
X, Y, Z, **and** T	Exponents of Brownlie's (1981) resistance equation
d_{50}	Bed material median grain size in mm
σ_g	Gradation coefficient of the bed material
G	Specific gravity of the sediment
g	Gravitational acceleration in m/s^2
S_o	Bed slope in m/m
S_f	Friction slope in m/m

F_r	Froude number
A_b	Area of the bed layer
t	Time
T_e	Trap efficiency
p_o	Porosity of the sediment
ω	Fall velocity of sediment particles in m/s
h_*	Trial value for the flow depth in m
H_*	Total energy corresponded to the trial flow depth in m
Δx	Space interval in m
Δt	Time interval in days
Z	Bed elevation in m
h_m	Minor losses in m
H_e	Total energy in m
c	Coefficient of expansion and/or contraction
Q_{10}	Flow discharge equalled or exceeded 10% of the time
C_w	Sediment concentration by weight
D_{gr}	Dimensionless grain diameter
ν	Kinematic viscosity in m^2/s
F_{gr}	Mobility number in Ackers and White transport equation
b	Transition exponent in Ackers and White transport equation
u_*	Shear velocity in m/s
C, A	Coefficients in Ackers and White transport equation
m	Exponent in Ackers and White transport equation
C_{ppm}	Sediment concentration by weight in ppm
q_{bv}	Unit sediment discharge by volume in m^2/s
ψ	Universal stream power in Molinas and Wu (2001) transport equation
ω_{50}	Fall velocity of sediment size d_{50}

ρ_s Mass density of solid particles in kg/m^3

ρ Water density in kg/m^3

p Exponent of the slope ratio vs. the ratio of the width-depth ratio relationship

q Exponent of the slope vs. width relationship

Chapter 1

Introduction and Objectives

Rivers are natural systems constantly changing as a result of the influence of many factors (water discharge, sediment load, climate, geology, vegetation, land-use and valley slope). The relationship between these variables depends on the time span and the size of the landscape (Schumm and Lichty, 1965). In the modern time span (Schumm and Lichty, 1965), rivers adjust their shape, form and gradient to accommodate the water and sediment discharge imposed upon them (Schumm and Lichty, 1965). Water and sediment load reflect changes in climate, geology, vegetation, soil and basin physiography (Knighton, 1998) and as such they are the two most important independent variables controlling river morphology. For the purposes of this dissertation, a channel is considered to be in equilibrium, when it develops a characteristic but not static form (gradient, shape, pattern and dimensions), in which the rate of transport and sediment supply are equal.

The alteration of the water and sediment regimes due to natural and/or human activities can cause changes in the river form. The magnitude of the changes in the input variables can trigger complex reactions of the river system that can lead the river to achieve a different equilibrium condition (Schumm and Lichty, 1965).

1.1 The Middle Rio Grande

Historically, humans have attempted to control rivers in order to protect surrounding lands and communities from flooding. The middle Rio Grande in New Mexico is an example of a river that has been highly managed to reduce aggradation rates

of the bed and halt flooding of the adjacent areas. The imbalance between the sediment entering the channel from tributaries and the capacity of the channel to remove sediment have caused the river to aggrade for many years (Crawford et al., 1993). Several dams in the main tributaries of the river and in the main stem have been constructed in an effort to control floods and induce degradation of the river bed. In addition, channel rectification works have been implemented (Woodson, 1961; Woodson and Martin, 1962; Lagasse, 1980). The end result of these measures consists of a less mobile channel (Richard, 2001) that does not shift across the floodplain.

Control of the middle Rio Grande has been successfully achieved from the engineering point of view. However, changes in the river do not provide the more desirable state from an ecological perspective. A more stable or less mobile channel uncouples important ecological processes (Stanford et al., 1996). The middle Rio Grande has evolved into a narrower and deeper channel than the historic channel (Lagasse, 1980, 1981, 1994; León, 1998; Bauer, 1999; Sanchez and Baird, 1997; Mosley and Boelman, 1998; Richard, 2001; Richard et al., 2001; León et al., 2002). These changes have been identified as one of the causes of the decline of the Rio Grande silvery minnow (*Hybognathus amarus*), a federally listed endangered species.

Large numbers of this native fish were found in the river between 1926 and 1978 (Bestgen and Platania, 1991). Remaining populations of this species are declining primarily due to the lack of warm, slow-moving, silt-sand substrate pools, dewatering of the river and abundance of non-native and exotic fish species (Platania, 1991; Bestgen and Platania, 1991; Burton, 1997; Robinson, 1995; Arritt, 1996).

Restoration of the channel to the previous or undisturbed conditions is unlikely to occur without further interference. The management of the river to restore a self-sustaining system similar to the pre-human-disturbance state, under the new regulated conditions, becomes a challenging task. Currently, some of the efforts to restore the habitat for the Rio Grande silvery minnow consist of creating wider and

shallower flow conditions (Baird, 2001).

1.2 Problem Statement

There is some evidence in the middle Rio Grande of channel reaches with alternating wide and narrow sections. One example is the Bosque del Apache Reach (BDA). Aerial photos of this reach show that the channel width of this stretch of the river has been almost constant from 1985 to the present. Additionally, the channel has not migrated across the existing floodplain. Therefore, it is presumed that the channel has accommodated the incoming water and sediment discharge by adjusting the channel slope. The wide section of this reach is the result of clearing the vegetation on the banks (Drew Baird, USBR, Albuquerque, NM, 2002 pers. comm.). The narrow sections developed after performing channel cuttings between 1949 and 1972 (U. S. Bureau of Reclamation, 2000).

The presence of such reaches in the middle Rio Grande provides an excellent opportunity to study the adjustment of the bed slope (vertical changes) due to changes in channel width (horizonal changes), to transport equivalent water and sediment discharges. One of the goals of restoration is to create wider channels (Baird, 2001). Therefore, the study of the adjustment of the channel slope in reaches like the Bosque del Apache can provide some insight to evaluate potential restoration activities in the river. The problems to be solved throughout this disseration are: 1) How does the channel slope adjust among channel reaches with different width to transport the same water and sediment load? 2) How is the habitat for the Rio Grande silvery minnow affected by the slope adjustment among channel reaches with different widths?

1.3 Previous Studies

For many years, methods were developed to predict equilibrium characteristics of alluvial channels. Formulation typically relates water discharge, sediment discharge,

sediment size, velocity, width, depth and slope. Three out of the seven variables are specified and the other variables are solved by means of three basic equations: water continuity equation, water resistance equation and sediment transport equation. The end result is a family of channel geometry characteristics that can transport the constant incoming steady state water and sediment discharges. Griffiths (1989) used this result to design gravel bed channels with different geometries and equivalent water discharge and sediment load. Others have also introduced a fourth condition (bank stability, extremal hypotheses, etc.) to explain the self-adjustment mechanism of alluvial channels and define a unique equilibrium channel geometry (Stevens, 1989; Kirkby, 1977; Chang, 1979, 1980; Carson and Griffiths, 1987; Yang, 1988; Huang and Nanson, 2000).

Existing methods are limited to steady state input variables to define equilibrium conditions. Furthermore, rivers are natural systems with large variability in water and sediment discharges. Therefore, there is a need to develop numerical and analytical methods that relate variable water discharge and sediment load with quantitative field data of hydraulic geometry of alluvial channels. Such methods need to be integrated for the evaluation of potential river restoration activities.

1.4 Dissertation Objectives

The main goal of this dissertation is to examine how the channel slope adjusts in sequential channel reaches with different widths under steady and unsteady water and sediment discharges. This goal is achieved through the following specific objectives:

1. To develop analytical relationships between equilibrium slope and width or width-depth ratio under steady state input water and sediment discharges.

2. To develop a one-dimensional numerical model to simulate the transient response of channels with variable widths under a constant flow discharge.

3. To develop a one-dimensional numerical model to simulate the transient behavior of channels with variable widths and variable water and sediment discharges.

4. To apply the numerical model to the middle Rio Grande and evaluate the changes in habitat conditions for the Rio Grande silvery minnow between wide and narrow reaches.

Chapter 2 provides background information about the different methods developed to predict equilibrium channel characteristics. Chapter 3 summarizes some of the main characteristics of the middle Rio Grande, including changes in water, sediment regime and channel morphology throughout time, as well as the ecological implications of these changes. Chapter 4 presents the development of steady state analytical solutions and numerical models for constant discharge developed to accomplish the specific objectives 1 and 2. Chapter 5 describes the numerical model for unsteady flows developed to achieve objective 3. The application of the numerical model to the middle Rio Grande and the comparison of the output of the model with the hydraulic conditions required by the Rio Grande silvery minnow are presented in Chapter 6. Chapter 7 summarizes the main conclusions of this dissertation. In addition, nine appendices that contain detailed procedures followed in different chapters are included at the end of this work.

Chapter 2

Background Information

Numerous definitions of equilibrium of alluvial rivers can be found in the literature, each one focusing on varying directions of channel adjustment in different spatial and temporal scales (Richard, 2001). Engineers are concerned with channel responses to storm events and man-induced changes, whereas geomorphologists focus on the study of evidence of long-term adjustments of river systems to changes in climate, tectonic activity and sea-level fluctuations (Schumm, 1969). The objective of the summary presented in the following section is to review some of the definitions of equilibrium that have taken root in the literature. This review will provide a single definition that will be used as a basis for the analysis to be conducted in this work. Then a summary of several quantitative and qualitative methods to characterize channel response to changes in water and sediment discharge is presented.

2.1 Concept of Equilibrium

The earliest usage of an equilibrium concept as applied to streams dated from the late 1600's and was proposed by Guglielmini, an Italian engineer who recognized that the slope of the channel will adjust such that neither erosion nor sedimentation will occur. He also pointed out that equilibrium is achieved when the force of the water and the resistance of the soil are in balance (Knox, 1975). The concept of equilibrium was later used by other engineers in the same manner as Guglielmini (Surell in 1841 and Dausee in 1872 in Knox,1975). In 1877, Gilbert recognized the equilibrium tendencies in streams and his research later served as a basis for the

concept of grade (Knox, 1975).

The design of stable canals began in the late 1800's and early 1900's, when British engineers developed the "regime theory". Kennedy, who pioneered this theory in 1895, proposed an equation to compute the velocity that will cause neither silting nor scouring of the bed of the channel (Simons and Albertson, 1963). His concept of equilibrium was similar to the previous definitions. In 1902, Davis introduced the term 'grade' into geomorphology as a "*balance between erosion and deposition attained by mature rivers*" (Knox, 1975). Davis' definition of grade was different from previous usage because he suggested that a period of geologic time was required to attain an equilibrium profile (Knox, 1975). Mackin (1948) stated that a graded stream is one "*in which, over a period of years, slope is delicately adjusted to provide, with available discharge and prevailing channel characteristics, just the velocity required for the transportation of the load supplied from the drainage basin*". Lane in 1953 defined a stable channel as "*an unlined earth channel for carrying water, the banks and bed of which are not scoured by the moving water, and in which objectionable deposits of sediment do not occur*" (Garde and Ranga Raju, 1977). Later, Lane (1954, 1955) proposed a qualitative relationship among water discharge (Q), bed-material load (Q_s), sediment size (D), and channel slope (S), as follows: $Q_S D \approx QS$.

This relationship shows that changes in sediment discharge, grain size and water discharge will induce adjustments of channel slope to achieve equilibrium (Lane, 1954, 1955). Lane's relationship is in agreement with Mackin's (1948) definitions of equilibrium state, which suggest that channel slope will be adjusted to convey the imposed water and sediment discharge.

It was later recognized that equilibrium could be achieved not only by adjusting the channel slope but also the cross-section shape and planform (Leopold and Maddock, 1953; Blench, 1957; Simons and Albertson, 1963; Schumm, 1969). Multiple studies have been performed on man-made and natural streams to describe qual-

itatively and quantitatively the relationship among water and sediment discharge, velocity, depth, width, slope and planform. Summary of these studies is deferred to Section 2.2.

Some other studies refer to the different degrees of stability in equilibrium state (stable equilibria and unstable equilibria) (Knighton, 1998). According to Vanoni et al. (1960) a river reach is in regime if "*its mean measurable behavior during a certain time interval do not differ significantly from its mean measurable behavior during comparable times before or after the given interval*". They also pointed out that a river reach could have an overall stability but not a local stability. Overall water and sediment balance could be achieved in a reach but local scour and deposition could occur at one point (e.g. meandering streams).

Conversely to the above definition, Schumm (1977) stated that rivers are not static and are constantly experiencing modifications with time. Eroding bends and local bank erosion are not necessarily instabilities in the channel, because rivers are continuously changing position as a result of hydraulic forces acting on the boundaries. Unstable channels are those that are "*adjusting dimension, gradient pattern, and shape rapidly and progressively to changed conditions*" (Schumm, 1977). Stable channels are those that have not shown progressive channel adjustment during the last 10 yr of record (Schumm, 1969).

Knighton (1998) stated that: "*Provided the controlling variables remain relatively constant in the mean, a natural river may develop characteristic or equilibrium forms, recognizable as statistical averages and associated with single-valued relationships to the control variables*". Different components of channel form (bed configuration, channel width and depth, meander wavelength, reach gradient, profile concavity, etc.) have different ability to absorb changes, implying that they are adjustable over different ranges of spatial and temporal scales (Knighton, 1998).

Other approaches to define equilibrium are based on the analogy between variational theories and fluvial systems (Langbein, 1964; Langbein and Leopold, 1964;

Kirkby, 1977; Chang, 1980; White et al., 1982; Huang and Nanson, 2000) These approaches rely on a type of variational argument in which the maximum or minimum of some variable is sought. The following hypotheses have been proposed as conditions for equilibrium (Knighton, 1998):

- Minimum unit stream power
- Minimum stream power
- Minimum energy dissipation rate
- Minimum Froude number
- Maximum sediment transport rate
- Maximum friction factor

Based on the previous discussion, the definition of equilibrium that will be considered in this work is: a condition in which the rate of change in gradient, shape, pattern and dimensions with time in response to imposed controlling variables is small, such that the river develops a characteristic but not static form. Each component of channel form will adjust at different temporal and spatial scales. Under equilibrium conditions, the rates of transport and sediment supply are equal. Therefore, the amount of sediment that comes into a reach is equal to the amount of sediment that comes out. Furthermore, this work is concerned with a time scale of about 10 to 20 years.

2.2 Predicting Channel Adjustment

The definition of dependent and independent variables in fluvial systems depends on the time and the size of the landscape (Schumm and Lichty, 1965). During geologic time (5,000 or 1,000 years ago), geology and climate are independent variables, whereas vegetation and relief are dependent (Schumm and Lichty, 1965). In the time

span termed modern, rivers adjust their shape, form and gradient to accommodate the water and sediment discharge imposed upon them (Schumm and Lichty, 1965). Water discharge and sediment load reflect the effects of climate, geology, vegetation, soil and basin physiography (Knighton, 1998) and as such they are the most important variables controlling channel adjustment.

In the present time (1 year or less), there is an apparent feedback from the dependent to the independent variables. For instance, the sediment transport could be adjusted by the flow velocity, or increase of discharge or slope. Therefore, only the instantaneous observations of water discharge, sediment discharge and flow characteristics are dependent variables, whereas mean discharge of water and sediment, channel morphology characteristics, valley dimensions, relief, vegetation, climate and geology are independent (Schumm and Lichty, 1965).

Most of the studies of stream morphology have been framed in the modern time span. Some of them have focused on the effect of type of sediment (Schumm, 1960, 1963; Simons and Albertson, 1963; Osterkamp, 1980; Osterkamp and Hedman, 1982), tectonic activity, change in base-level (Schumm, 1977; Knighton, 1998) and vegetation (Lawler et al., 1997; Millar, 2000; Abernethy and Rutherfurd, 2000) on the morphology of rivers.

Channel adjustment to external controls occurs in many directions (e.g. vertical or horizontal) and can be considered in terms of four degrees of freedom (cross sectional form, bed configuration, channel pattern, channel bed slope) (Knighton, 1998) up to nine degrees of freedom (bankfull width, depth, maximum depth, height, wavelength of bedforms, slope, velocity, sinuosity, meander arc length) (Hey, 1988).

Numerous studies have focused on predicting the responses of river systems to imposed input variables. These studies are either qualitative or quantitative.

2.2.1 Qualitative Approaches

Qualitative approaches to predict channel adjustment prove useful in understanding the direction of response to river regulation and/or climate changes. Lane's (1955) relationship (see section 2.1) predicts the long-term changes in channel slope to changes in median diameter, water and sediment discharge. For instance, direction of change in channel slope to increase in sediment load at tributary junctions or detention of sediment behind dams might be readily predicted with Lane's (1955) relationship.

Schumm (1969) proposed the concept of river metamorphosis to predict the response of channel slope, width, depth, width/depth ratio, meander wavelength and sinuosity to changing inputs (water and bed-material load discharge). Schumm (1969) proposed relationships based on the channel geometry and sediment characteristics of 36 stable alluvial rivers located in semiarid and subhumid regions of the Great Plains of the United States and the Riverine Plain of New South Wales, Australia. The following equations summarize Schumm's (1969) results. A plus (+) exponent indicates an increase in the magnitude of a parameter and a minus (-) indicates a decrease.

Decrease in bed material load:	$Q_s^- \sim \frac{W^- L^- S^-}{D^+ P^+}$
Increase in bed material load:	$Q_s^+ \sim \frac{W^+ L^+ S^+}{D^- P^-}$
Increase in water discharge:	$Q^+ \sim \frac{W^+ D^+ L^+}{S^-}$
Decrease in water discharge:	$Q^- \sim \frac{W^- D^- L^-}{S^+}$
Increase in water discharge and bed material load:	$Q^+ Q_t^+ \sim \frac{W^+ F^+ L^+ S^\pm D^\pm}{P^-}$

Decrease in water discharge and bed material load:	$Q^{-}Q_t^{-} \sim \frac{W^{-}F^{-}L^{-}S^{\pm}D^{\pm}}{P^{+}}$
Decrease in water discharge and increase in bed material load:	$Q^{-}Q_t^{+} \sim \frac{W^{\pm}L^{\pm}P^{-}D^{-}}{F^{+}S^{+}}$
Increase in water discharge and decrease in bed material load:	$Q^{+}Q_t^{-} \sim \frac{W^{\pm}L^{\pm}P^{+}D^{+}}{F^{-}S^{-}}$

where,

Q= water discharge, Q_s = bed material load,

Q_t= ratio of bedload (sand size or larger) to

total sediment load times 100 at mean annual discharge,

W = channel width, D = flow depth,

F = width/depth, L = meander wavelength,

P = sinuosity, and S = channel slope

Richardson et al. (1990) developed qualitative equations by directly relating the bed material sediment transport (Q_s) to stream power ($\tau_o V$) and inversely relating Q_s to the fall diameter of bed material (d_{50}). The use of fall diameter of bed material is preferred over the physical diameter because it accounts for the effect of temperature on the transportability of the bed material. In addition, Richardson et al.'s (1990) equation incorporates the volumetric concentration of wash load C_f, which accounts for the changes in apparent viscosity of the flow and transportability of bed material. Richardson et al.'s (1990) relationship is: $Q_s \propto \frac{\tau_o V w C_f}{d_{50}}$.

Brookes in 1992 (from Richard 2001) developed equations similar to Schumm's river metamorphosis model. However, his model does not account for changes in sinuosity, meander wavelength and width/depth ratio but includes changes in median particle size of bed material. Brookes' model makes distinctions among different degrees of changes in inputs to the channel (no change, increase, decrease, considerable increase or decrease).

According to all of the above-mentioned methods, channel width is directly proportional to water discharge and sediment load. Flow depth is directly proportional to water discharge but inversely proportional to sediment load, and slope is directly proportional to sediment load but inversely proportional to water discharge. However, when water and sediment discharges change simultaneously in the same or opposite directions, the direction of channel responses will depend on the relative magnitude of the changes in water and sediment. Thus, a quantitative approach is necessary to predict the channel response.

2.2.2 Quantitave Approaches

Different methods have been used to quantitatively predict channel adjustments to variations in input. These methods include: hydraulic geometry equations, extremal hypotheses and rational or mechanistic approaches (ASCE Task Committee on Hydraulics and of River Width Adjustment, 1998).

Hydraulic geometry equations are empirical and semi-analytical equations developed from data of flumes, canals and rivers in equilibrium. Rational methods link dependent and independent variables through the simultaneous solution of physical deterministic process equations (ASCE Task Committee on Hydraulics and of River Width Adjustment, 1998). Extremal hypothesis approaches combine the basic laws of mechanics with variational principles to obtain the equilibrium width and slope of channels.

Hydraulic Geometry Equations

Downstream hydraulic geometry deals with spatial variation in channel properties at some reference discharge (Leopold and Maddock, 1953; Knighton, 1998). Detailed summary of the existing downstream hydraulic geometry equations have been surveyed by Julien and Simons (1984) and Wargadalam (1993). In addition, Ferguson (1986a) presents a critical review of most hydraulic geometry equations.

The traditional hydraulic geometry problem is to solve width, depth, slope and velocity as function of water discharge, sediment load and sediment size. Slope is considered as a dependent variable, because it is locally adjusted when sediment transport capacity and supply are imbalanced.

The first regime equation was proposed by Kennedy in 1895 (Simons and Albertson, 1963). Many other equations, such as Lindley 1919 (from Wargadalam 1993), Lacey 1920 (from Wargadalam 1993), Blench (1957), and Simons and Albertson (1963), were proposed after Kennedy's equation in an attempt to improve and enhance their performance.

Kennedy's (1985, from Simons and Albertson 1963) equation is a simple power function of velocity as a function of flow depth. This equation lacks general applicability since its coefficient and exponent are site specific (Simons and Albertson, 1963). Lindley's (1919, from Wargadalam 1993) equations introduce bed width as a regimen variable for the first time and relate it to flow depth. Lacey's (1920, from Wargadalam 1993) equations are slightly more complex than the previous equations, because they account for the effect of flow discharge and sediment size on velocity, wetted perimeter, hydraulic radius, area and slope. The sediment size effect was incorporated into a silt factor for the bed and side of the channel. Chien (1955) proposed functional relationships between Lacey's silt factor and sediment size and concentration. Blench (1957) modified Lacey's approach by introducing side and bed factors, which distinguish between the material of the bed and banks. Simons and Albertson (1963) relate wetted perimeter, hydraulic radius, and cross section to water discharge for five different types of bed and bank material.

Lacey's (1920, from Wargadalam 1993) and Blench's (1957) equations indicate that channel slope is directly proportional to the silt factors and inversely proportional to water discharge. In addition, water discharge has a greater influence over the channel width than over the flow depth and slope.

Geomorphologists use natural stream and laboratory data to develop power law

hydraulic geometry equations (ASCE Task Committee on Hydraulics 1998). Leopold and Maddock (1953) pioneered this approach by correlating width, depth and velocity with mean annual discharge, which is roughly the discharge equaled or exceeded about one day in every four over a long period of time. Leopold and Maddock (1953) proposed the following power equations: $W = aQ^b$, $d = cQ^f$,$v = kQ^m$. Where W=width, d = depth, and v=velocity.

The exponent of the equations,b,f and m are on average equal to 0.5, 0.4 and 0.1 regardless of the flow regime, sediment characteristics and physiographic location of the rivers (ASCE Task Committee on Hydraulics and of River Width Adjustment, 1998). Conversely, regression coefficients (a,c and k) vary widely from one location to the other, which suggests that there are other variables that control channel form (Knighton, 1998; Ferguson, 1986a; Maddock, 1970). Ferguson (1986a) noted that the empirical $W = f(Q)$ and $d = f(Q)$ trends are parallel for artificial canals but not for natural rivers. Klassen and Vermeer (1988) developed a relationship for braided rivers based on data from the Jamuna River, Bangladesh. The exponents of the Klassen and Vermeer (1988) equations are very close to the exponent original proposed by Leopold and Maddock (1953). Many other equations, such as Lacey (1920, from Wargadalam 1993), Blench (1957), Simons and Albertson (1963), Henderson (1966), etc., confirm that channel width varies approximately as the square root of discharge.

Magnitude of discharge is not the only factor that controls geometry of channels. Variability of water discharges proves to affect significantly natural river geometry (Yu and Wolman, 1987). Yu and Wolman showed that easily deformed rivers (e.g. sand bed and banks) are narrower in the mean when the flow is highly variable. Stevens et al. (1975) noted that differences in peak-flood discharge between two rivers in the same geological settings are responsible for differences in river forms (straight and sinuous planforms). Nouh (1988) found that the ratio of annual peak flood for a return period of 50 years to annual mean flood best correlates with width,

depth and slope of ephemeral channels in an extremely arid zone of Saudi Arabia.

In addition, type of load is related to the shape of the channel, whereas amount of load is related to the size. Schumm (1960) demonstrated that the shape of cross sections expressed as the width-depth ratio depends on sediment type (amount of silt-clay in bed and banks). Channels containing little silt and clay are wide and shallow, whereas high silt-clay content is related to narrow and deep channels. Osterkamp and Hedman (1982) found similar results as Schumm (1960).

Several researchers have quantified the relationship between sediment load with channel width, depth, slope and velocity (Chien, 1955; Maddock, 1970; Maza-Alvarez and Cruickshank-Villanueva, 1973). The results vary widely. For example, according to Chien (1955)and Maddock (1970), water discharge correlates better than sediment load with channel slope. But, according to Maza-Alvarez and Cruickshank-Villanueva (1973), sediment load is more important than water discharge in defining channel slope.

In summary, there are many hydraulic geometry equations that have been developed to predict the equilibrium geometry of alluvial channels. Most of the equations are empirical and as such, their use is restricted to their range of application. According to most of the equations, channel width varies as the squared root of water discharge. Channel slope is directly proportional to sediment load and inversely proportional to water discharge, as indicated by the qualitative approaches. Some of the studies indicate that water discharge drives the changes in channel slope. Conversely, other results show that sediment load is the dominant factor that defines channel slope.

Rational or Mechanistic Approach

As previously mentioned, alluvial channels have from four (Knighton, 1998) to nine degrees of freedom (Hey, 1988). Dependent and independent variables are linked by physically deterministic process equations, and the simultaneous solution of these

equations will result in the prediction of the morphology of channels. This method is referred as the rational or mechanistic approach. Currently, solutions can be obtained for up to four degrees of freedom (Julien and Wargadalam, 1995) based on flow continuity, flow resistance, secondary flow and sediment transport equations. In the case of channels with fixed bed (no sediment transport), the fourth equation will be critical shear stress or Shields criterion.

Many mechanistic approaches have been developed. They can be classified into two groups: those methods that predict a single solution or single stable channel configuration (Garde and Ranga Raju, 1977; Henderson, 1966; Maza-Alvarez and Cruickshank-Villanueva, 1973; Parker, 1978a,b, 1979; Julien and Wargadalam, 1995; Huang and Nanson, 1995; Cao and Knight, 1998; Julien, 2002), and those approaches that predict a range of possible width-slope combinations that can transport the incoming water and sediment load (Stevens, 1989; Griffiths, 1989).

Lane (1953, from Garde and Ranga Raju 1977) developed the tractive force method to design stable channels in coarse noncohesive material with no sediment supply from upstream. The stability method consisted of designing a channel such that the shear forces on the perimeter of the channel are below the resistive forces of the material. Three equations were used in the design: limiting tractive force in the bed (Lane and Carlson, 1953), critical shear stress on the banks and flow resistance equations similar to the Manning-Strickler equation (Garde and Ranga Raju, 1977). This method leads to the design of a cosine cross section.

Henderson (1966) developed regime equations based on the tractive force method. Parker (1978a, 1978b, 1979) developed a cosine bank profile for straight wide channels based on the idea that bank erosion due to gravity is counteracted by the deposition of suspended sediment originating from the center of the channel and moved to the banks by lateral diffusion. Cao and Knight (1998) extended Parker's approach to account for secondary currents.

Maza-Alvarez and Cruickshank-Villanueva (1973) developed regime equations to

predict width, depth and slope based on a flow resistance equation, a sediment transport equation and a width to depth ratio relationship. The independent variables are flow discharge, sediment load, and sediment size. According to Maza-Alvarez and Cruickshank-Villanueva (1973), channel width and depth are driven by water discharge, whereas channel slope is dominated by sediment load.

Julien and Wargadalam (1995) derived analytical downstream hydraulic geometry relationships that include the concepts of secondary flows in curved channels and the three dimensional mobility of noncohesive particles. Later, Julien (2002) included the effect of sediment concentration on the downstream hydraulic geometry relationships. According to his results, sediment concentration drives the change in slope, whereas discharge is the dominant factor for channel width. This result is in agreement with the results of Maza-Alvarez and Cruickshank-Villanueva (1973).

Huang and Nanson (1995) related the width-depth ratio of alluvial channels with rectangular cross sections to the ratio of shear stress acting on the walls to bed shear stress. Combining the resulting equation with water continuity and Manning's resistance equation, the width, depth, area, velocity and width-depth ratio were expressed as power functions of flow discharge, friction factor, slope and sediment composition of the channel boundary. Huang and Nanson (1995) concluded that sediment composition of the channel perimeter has a significant effect on channel shape (width-depth ratio) and their results are in agreement with Schumm's (1960) observations. Discharge is the dominant factor in the width, depth, area and velocity relations. Channel roughness is the second most important factor in determining the power functions. Huang and Nanson (1995) concluded that, when the variability of channel roughness (Manning n) and channel slope is not significant, as in stable channels, the results of their work are consistence with the regime equations developed from stable canal data.

Stevens (1989) extended Lane's work by combining the tractive force method with a sliding strength criterion that prevents channel banks from having geotech-

nical failures. These two criteria were combined with water and sediment continuity equations, Darcy-Weisbach's resistance equation and Colby's sediment transport equation to obtain the width of a trapezoidal cross section in a straight alluvial channel. Stevens (1989) concluded that there is a range of stable or regime channel widths rather than one stable width. The bank height controls the minimum width, and the meandering tendency that creates bank erosion controls the maximum width.

Griffiths (1989) predicted the characteristics of a stable single-thread channel equivalent in water and bedload transport capacity to a given braided gravel-bed river. His approach is based on the concept of river training developed in New Zealand (Henderson, 1966; Nevins, 1969; Davies and Lee, 1988), which consists of confining gravel braided streams laterally to a width smaller than the unconfined original width, in order to induce degradation of the bed and create single thread channels. Griffiths (1989) proposed five different design methods for the conversion of braided to single thread rivers. Water discharge and sediment size were always assumed known in the single-thread channel together with at least two of width, depth, bed slope, gravel discharge and resistance coefficient (Griffiths, 1989). The Meyer-Peter and Müller (1948, from Julien 1995) formula for bedload transport and Manning's resistance equation were used. Four cases were developed for steady state conditions and one for unsteady state conditions. From the five cases, Case 4 for steady state conditions solves a problem similar to the one stated in this work, in which two channels of different configuration transport the same water discharge and sediment load. However, Case 4 is specifically concerned with a change from a gravel bed braided channel to a single thread channel, both transporting the same gravel load. The solution was obtained following lengthly numerical iterations. Griffith (1989) used laboratory data (run 1) from Ashmore (1985; 1988) to validate his method. Based on the width of a braided channel, the flume slope and the sediment size, Griffiths (1989) predicted the channel slope of an equivalent single

thread channel of prescribed width. The same trends observed in his results were observed in the laboratory data: the narrower reach had a flatter slope than the wider reach.

Griffith (1989) also developed an approach (Case 5) for unsteady flow using a flow discharge/sediment-rating curve method (Julien, 1995). The objective was to find out the width of a single thread channel that could transport the same gravel load as a braided channel. In this case, the slope of both reaches were unknown.

Carson and Griffiths (1987) recognized the importance of determining the changes in sediment load (specifically gravel load) due to a new imposed channel width under discharges different from the dominant discharge. Their comments are supported by Nordin and Beverage (1965), who compared the total bed-material discharge to water discharge at confined and unconfined sections in the Rio Grande, New Mexico. For any discharge below 1,000 cfs, more sediment is transported at the narrow sections than at the wide sections. The opposite happens at discharges greater than 4,000 cfs (Nordin and Beverage, 1965).

In summary, many different rational approaches have been developed to come up with regime relationships. In general, it has been concluded that channel width varies as the squared root of discharge, as observed with empirical hydraulic geometry equations. Also, it has been proposed that there are multiple channel geometries rather than a single stable channel that can transport the imposed water and sediment load (Nevins, 1969; Stevens, 1989; Griffiths, 1989).

Extremal Hypotheses

Researcher propose extremal hypotheses by combining mechanistic approaches with variational principles in an effort to select a unique stable channel configuration from the multiple solutions obtained by the application of some rational approaches. The extremal hypotheses are based on the idea that channels adjust to convey the maximum possible bedload, given the slope, water discharge and sediment size or

to carry the sediment load with the available discharge on the lowest possible slope (Ferguson, 1986a).

Kirkby (1977) first quantified the hypothesis of maximum sediment efficiency, which says that rivers will adjust to carry the sediment load imposed upon them as efficiently as possible in the medium term. Kirkby (1977) used the Meyer-Peter and Müller equation for bedload transport, the Darcy-Weisbach resistance equation and the water continuity equation to develop a set of curves that represent the relationship between sediment concentration and channel slope, depth and grain size. Except for very high concentrations, the curves reflect minimum slopes that correspond to sediment transport of maximum efficiency. According to Kirkby (1977), the region to the right of maximum sediment efficiency is one of unstable channels (braided channels). On the other hand, the region to the left of maximum sediment efficiency is one of stable channels, typified by meandering channels.

Nanson and Huang (1999) observed that anabranch rivers are very common in arid regions of Australia, where gradient cannot increase, systems are overloaded with sediment, discharge is decreasing and river banks are very stable. Based on river data of anabranch rivers in Australia, Nanson and Huang showed that anabranch rivers are more efficient than a wide, single-thread system, because the decrease in aggregate width and increase in flow depth produces an increase in velocity that will increase or at least maintain its sediment transport. Increase in flow resistance of about 10% will still increase the velocity of the anabranch channel with respect to a wide single channel (Nanson and Huang, 1999). This result is of great applicability in river systems that cannot increase the slope when they widen.

Yang developed the minimum unit stream power hypothesis in 1971 based on the theory of minimum rate of energy dissipation (Yang, 1988). He stated that a system will adjust itself in such a way that its rate of energy dissipation will reach a minimum value. Chang (1979; 1980) introduced the hypothesis of minimum stream power in alluvial channels based on the theorem of least work. The min-

imum stream power theory is as follows: "*For an alluvial channel, the necessary and sufficient condition for equilibrium is when the stream power is a minimum subject to given constraints. Hence, an alluvial channel with given water discharge and sediment inflow tends to establish its width, depth and slope such that the stream power or slope is a minimum*". The difference between unit stream power VS and stream power QS is the cross section area, where V is the velocity, Q is the water discharge and S is the slope. Chang (1980) demonstrated that the two minimization techniques produce different results, predicting different stable channel width, depth and slope. Chang (1979) also pointed out that possible multiple channel geometries with identical water discharge and sediment load must be associated with different flow regimes, stream-bed roughness, velocity, etc. For example, by using the Engelund and Hansen resistance formula for upper and lower regimes in rivers, the Lacey resistance equation for lower flow regimes in canals, and three different sediment transport equations (DuBoys, Engelund and Hansen, Einstein-Brown), Chang (1979) developed slope-width curves for different water discharge and sediment load values that reflect two minimum slopes: one for the lower regime and another for the upper regime. The global minimum is a more stable condition than the local minimum (Chang 1979). However, the local minimum also represents a stable configuration (Chang 1979). Chang (1979) argued that channel geometry and river pattern are closely related. A meandering channel is more stable than a straight channel and it represents minimization of sediment load and stream power (Chang 1979).

White et al. (1982) analytically demonstrated that extreme values of the sediment concentration lead to extreme values for the slope. However, White et al. (1982) were not able to demonstrate whether the extreme values were maxima or minima. White et al. (1982) used Ackers and White sediment transport theory, and the frictional characteristics were computed using White, Paris and Bettess linear relationship between mobility factors related to total shear stress and to effective

shear stress. Figure 2.1 shows the slope and sediment concentration versus width relationship from White et al. (1982).

Huang and Nanson (2000) solved the problem of indeterminacy of channel adjustment by reducing the number of dependent variables to three (width to depth ratio, slope and velocity) and using three basic equations (continuity, Lacey's resistance equation and DuBoys' sediment transport equation). Huang and Nanson developed the following relationship:

$$Q_s = K_1 \frac{\xi^{10/11}}{(\xi+2)^{7/11}} \left[K_2 \frac{\xi^{5/11}}{(\xi+2)^{9/11}} - \tau_c \right]$$

Where, $K_1 = \rho C_d N_a^{8/11} S^{7/11} Q^{8/11}$ and $K_2 = \rho N_a^{4/11} S^{9/11} Q^{4/11}$, $N_a = 0.0225 f^{1/4}$, f is Lacey's silt factor related to sediment size d in mm as $f = 1.6 d^{1/2}$, $C_d = 0.17 d^{-3/4}$ in $m^3 kg^{-1} s^{-1}$ and $\tau_c = 0.061 + 0.093 d$ in $kg\ m^2$. The approach followed to obtain this equation is similar to the approach followed in this work. However, the sediment transport equation used (Duboy's equation) is more appropriate for gravel bed channels (Julien, 1995) than for sand bed channels. The approach followed in this work uses a sand sediment transport equation. Huang and Nanson (2000) identified an optimum condition for sediment transport by adjusting the width/depth ratio for given flow discharge, channel slope and sediment size. The optimum condition is maintained in the range of 2.5 to 30 for the width to depth ratio. The optimum condition for sediment transport reveals high levels of consistency with the downstream hydraulic geometry equations developed by Julien and Wargadalam (1995) and Huang and Nanson (1995). However, the results obtained by Huang and Nanson were not validated with field or laboratory data.

Carson and Griffiths (1987) identified some drawbacks in applying the maximum sediment transport hypothesis in gravel bed rivers. Some of them are: 1) difficulties to select an appropriate resistance and transport equation; 2) variation of resistance and sediment transport at different width-depth ratios (e.g. wide braided, meander); 3) utilization of a fixed dominant discharge; and 4) reduction of dominant discharge

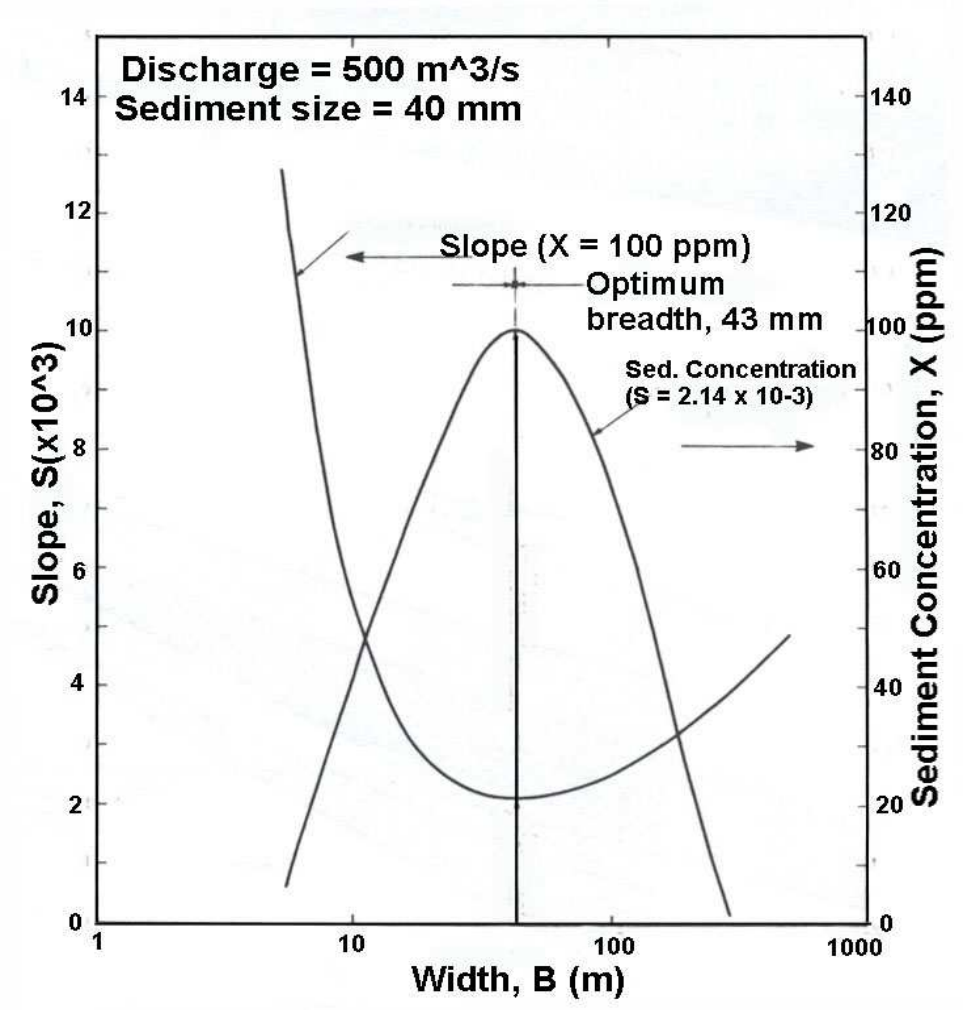

Figure 2.1: Sediment load, slope and channel width relationships (After White et al. 1982).

due to overbank flow.

According to Carson and Griffiths (1987), the relationship between sediment load and width in wide braided gravel channels might be similar to the modelling of bedforms in sand bed channels as proposed by Chang (1979) (Carson and Griffiths, 1987). It is expected to find a double peak (two maxima) in the sediment load-

width relationship for wide braided channels (Carson and Griffiths, 1987). Bed load transport in braided channels is poorly understood (Ashmore, 1985) and it is more difficult to model than the changes in roughness due to bedforms (Carson and Griffiths, 1987).

According to Carson and Griffiths (1987), the physical explanation for the existence of a peak in the sediment load-width relationship is due to the inclusion of a threshold shear stress in the transport equations. Carson and Griffiths (1987) also noticed that different researchers have used different sediment transport and resistance equations, and all of the equations include a threshold shear stress. Ferguson (1986a) found that an extremum in the sediment-load and width-depth ratio relationship does not exist when using the Strickler resistance equation and Einstein-Brown transport equation for shear stress greater than 0.1, which does not include a threshold shear stress in the equation. Ferguson's (1986a) finding is in agreement with Carson and Griffiths's (1987) conclusion. However, according to Carson and Griffiths (1987), the optimum width for maximum sediment transport will emerge if the three equations developed by Einstein-Brown are used, because these equations represent the curvilinear nature of the data.

Furthermore, Carson and Griffiths (1987) show that an optimum width for a maximum sediment transport exists in all cases when $c > m$, assuming wide channels ($Rh = D$), where c is the exponent of the flow depth factor in the resistance equation ($BD^c = \frac{nQ}{S^{0.5}}$) and m is the exponent of the excess shear stress factor in the sediment transport equation. The width is B, the flow depth is D, the friction factor is n, the water discharge is Q, and the slope is S.

2.2.3 Summary

Channel adjustment to imposed changes in water discharge and sediment load is a complex problem not fully understood yet. Throughout this review, several methods to predict equilibrium configurations of channels have been presented. Several

aspects related to channel adjustments are worthy of further investigation. In particular, the following aspects have been identified and are pursued in this dissertation:

- There are many methods that demonstrate numerically and analytically that there are multiple channel geometries that can transport the same water and sediment discharge. These results have been validated with laboratory data but not with quantitative field data. In addition, these results have not been used for the evaluation of river restoration activities.

- All the methods developed to predict multiple channel geometries with equivalent water and sediment discharge used only steady state input variables. In addition, the solutions represent the condition of equilibrium and not the evolution of the slope of the channel with time.

Chapter 3

Rio Grande Background

The Middle Rio Grande (MRG), NM begins about 56 kilometers north from Albuquerque at Cochiti Pueblo and continues to the headwaters of Elephant Butte Reservoir (see Figure 3.1). Historically, the river was relatively straight with a braided planform (Baird, 1996). The maximum degradation of the Rio Grande occurred about 22,000 years ago (Sanchez and Baird, 1997). Since then, the Rio Grande has been aggrading due to the imbalance between the sediment input from tributaries and the capacity of the channel to transport the sediment (Crawford et al., 1993). Water shortage and increasing sediment input from tributaries and arroyos increased the sedimentation of the river bed around 1850 (Scurlock, 1998). The aggradation trend caused severe flooding, waterlogged lands and failing irrigation facilities (Scurlock, 1998).

The Middle Rio Grande Conservancy District was organized in 1925 with the objective of improving drainage, irrigation and flood control in the middle valley (Woodson and Martin, 1962). Levees were built along the channel in the early 1930's to provide flood protection and prevent avulsion to the adjacent irrigated lands and urban areas. The confinement of the river into a smaller area induced more sedimentation in the bed. As a result, the levees had to be raised (Sanchez and Baird, 1997). The Middle Rio Grande Conservancy District also built El Vado Dam on a tributary of the river (Rio Chama) in 1935, four diversion dams along the main stem, two canal headings and many miles of drainage and irrigation canals (Lagasse, 1980).

Due to continued aggradation of the bed, the Corps of Engineers and the U.S.

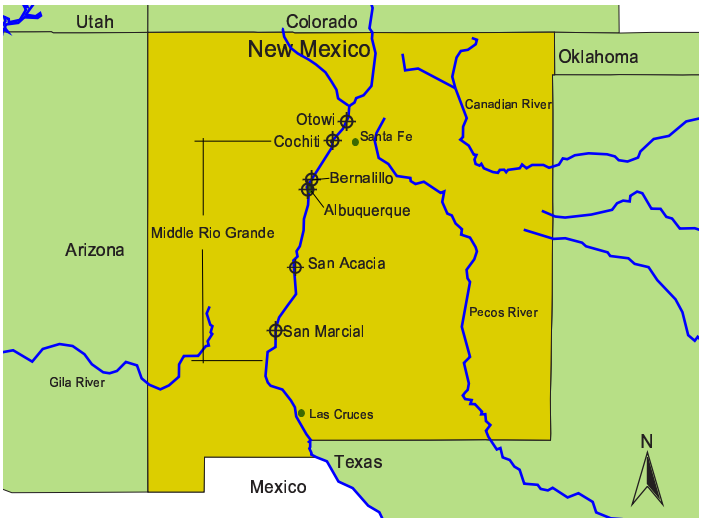

Figure 3.1: Location map of the Middle Rio Grande,NM. Large circles indicate the locations of USGS gage stations. Map not to scale.

Bureau of Reclamation together with other Federal, State and local agencies recommended a Comprehensive Plan of Improvement for the Rio Grande in New Mexico in 1948 (Pemberton, 1964). The plan consisted of constructing a system of reservoirs on the Rio Grande (Cochiti) and its tributaries (Abiquiu, Jemez, Galisteo), as well as improving the conditions of the floodway constructed by the Middle Rio Grande Conservancy District in 1935 (Woodson, 1961; Woodson and Martin, 1962).

Cochiti Dam, built in the Rio Grande, began operating in November 1973 (Lagasse, 1980). This dam was intended to control floods and sediment, preventing further aggradation of the river bed and inducing degradation (Lagasse, 1980). The response of the river to construction of the dams as well as to system-wide changes during longer time periods, has been investigated in several studies (Lagasse, 1980, 1981, 1994; León, 1998; Bauer, 1999; Sanchez and Baird, 1997; Mosley and Boelman, 1998; Massong et al., 2000; Richard, 2001; Richard et al., 2001; León et al., 2002). These studies have focused on the characterization of the response of the river to

changes in hydrologic and sediment regimes. The following sections summarize some of the characteristics of the hydrologic and sediment regimes along the middle Rio Grande as well as some of the river changes and ecological problems that have been observed.

3.1 Hydrologic Regime

The flow in the Rio Grande follows a typical seasonal pattern. However, operations of reservoirs and diversion dams alter the natural variability of the flow. Snowmelt and rain in the mountains provide flow during the spring and early summer, from about April to June. Irrigators begin to withdraw water from about March, decreasing the spring runoff peak (U. S. Bureau of Reclamation, 2000). Heavy local rains in tributary areas provide the flow during the summer season. After the summer rains end, the flows remain fairly constant throughout the winter season (U. S. Bureau of Reclamation, 2000).

Several United States Geological Survey (USGS) stream gages are located along the river (Figure 3.1). In the downstream order, some of the stations are: Rio Grande at Otowi Bridge (upstream from Cochiti Dam)(08-3145-00), Rio Grande at Cochiti (just downstream from Cochiti Dam)(08-3145-00), Rio Grande below Cochiti (08-3174-00), Rio Grande near Bernalillo (08-3295-00), Rio Grande at Albuquerque (08-3300-00), Rio Grande at San Acacia (08-3549-00) and Rio Grande at San Marcial (08-3584-00). Analysis of the streamflow gage data allows a characterization of the changes in discharge regime. Several studies have identified dam construction and climate changes as responsible for the major changes in water regime along the Rio Grande.

Figure 3.2 shows the flow discharge mass curves at the above-mentioned gages. The changes in slopes of the curves between the mid 1940's and the late 1970's indicate a decline in water volume along the river. The change in slope is more pronounced in the stations downstream from Albuquerque (see Figure 3.2). Large

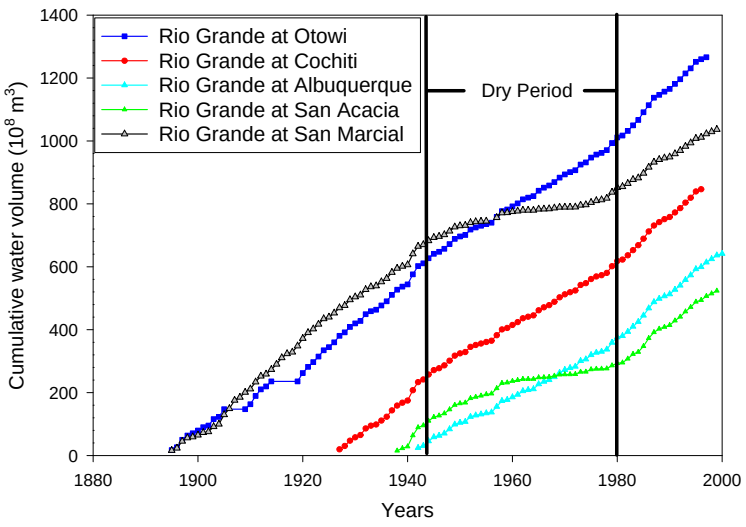

Figure 3.2: Flow discharge mass curves at USGS gage stations.

floods occurred in the Rio Grande before the early 1940's (Woodson, 1961; Lagasse, 1980). The construction of flood and sediment control reservoirs in the mid 1950's could have contributed to the decline of water volume. In addition, variations in climate over the upper Rio Grande basin might have caused this extended dry period (U. S. Bureau of Reclamation, 2000). Molnár (2001) analyzed the recent trends in precipitation and streamflow in the Rio Puerco, one of the largest tributary arroyos of the Middle Rio Grande. According to Molnár (2001), annual maximum precipitation events seem to produce lower annual maximum runoff events in the Rio Puerco basin in the last 50 years, consequently decreasing water input into the Middle Rio Grande. Furthermore, long-term precipitation trends in the Rio Puerco Basin are strongly related to sea surface temperature anomalies in the Northern Pacific (Molnár, 2001).

Flood and sediment control dams in the system play an important role in defining the flow regime. Richard (2001) analyzed the impact of Cochiti Dam on the natural flow regime of the river and concluded that the operation of the dam affects peaks in

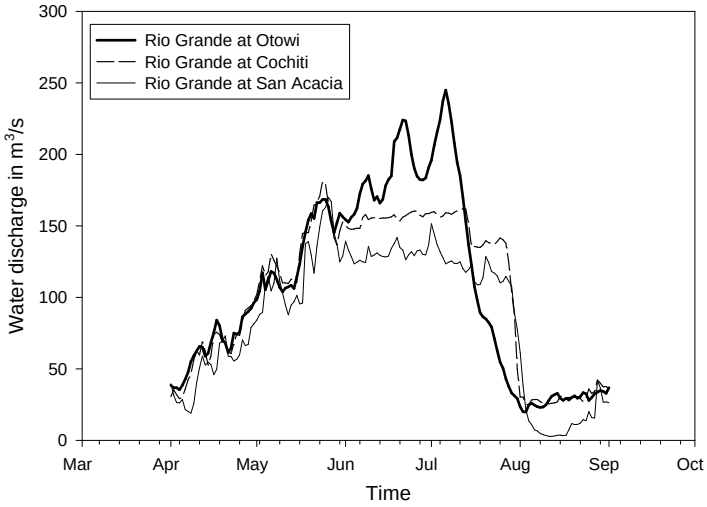

Figure 3.3: Spring runoff hydrograph in 1995.

excess of 142 m^3/s (5,000 cfs). Also, flood waves are attenuated and the duration of the annual peak is increased (see Figure 3.3). The historical unregulated two-year return period peak of 316 m^3/s (11,166 cfs) decreased to the regulated two-year return period flow of 160 m^3/s (5,650 cfs) after flow regulation began at Abiquiu Dam on the Rio Chama in 1963 and Cochiti Dam on the Rio Grande in 1973 (Bullard and Lane, 1993). Water for irrigation is withdrawn from the Rio Grande, reducing the spring runoff peak. Figure 3.3 shows the decline in the peak between Cochiti Dam and San Acacia gages.

Flow duration curves (Salas et al., 1999) of the pre-dam and post-dam periods at Otowi, Cochiti, Albuquerque and San Acacia gages reveal increased low flows and decreased high flows between the two periods (see Figure 3.4). Otowi gage, located upstream from Cochiti Dam, observes the same behavior as the other stations downstream from Cochiti Dam. Therefore, these changes in flow regime between the pre-dam and post-dam periods are not due to the construction of the dam. The water delivery from the San Juan-Chama Project to the Otowi gage since 1971

might be responsible for the changes in flow regime between the pre-dam and post-dam periods in all gages. The San Juan-Chama project provides about 67x10^6 m^3 (54,600 acre-feet) of the San Juan River water annually to the Otowi gage (Mussetter Engineering, 2002). Another source of water to the river is the wastewater discharge from the City of Albuquerque, which averages about 74x10^6 m^3 (60,000 acre-feet) annually (Mussetter Engineering, 2002).

3.2 Sediment Regime

The sediment regime in the Rio Grande has changed with time, as well. Gellis (1991) reported decreasing trends of suspended sediment loads relative to annual runoff at streamflow-gaging stations and decreasing sedimentation rates in selected reservoirs in New Mexico through time. It is believed that the decreasing trend is partly due to the reduction of sediment delivery from tributary arroyos, which coincides with arroyo evolution in the Southwest (Gellis, 1991).

In addition, Cochiti Dam alters the sediment regime in the river. Richard (2001) observed that the greatest impact of Cochiti Dam on suspended sediment supply to the river is seen at the Cochiti gage, located directly downstream from the dam, where the sediment concentration decreases as much as 99 % from the pre-dam to the post-dam period. Figure 3.5 is a plot of the cumulative suspended sediment from Otowi to San Marcial gages. Suspended sediment discharge started to decline at San Acacia and San Marcial before Cochiti Dam was constructed in 1973. However, there is an evident break in slope at the Albuquerque gage in 1973.

Figure 3.6 shows the double mass curve of annual water and sediment discharge at USGS gage stations. The curves were adjusted to the San Marcial gage for comparison. Averaged suspended sediment concentrations were computed at the beginning and end of the period of records of each gage, where a constant trend was observed. The slopes of the curves were computed for the indicated periods and the appropriate conversion factor was used to present the results in milligrams per liter

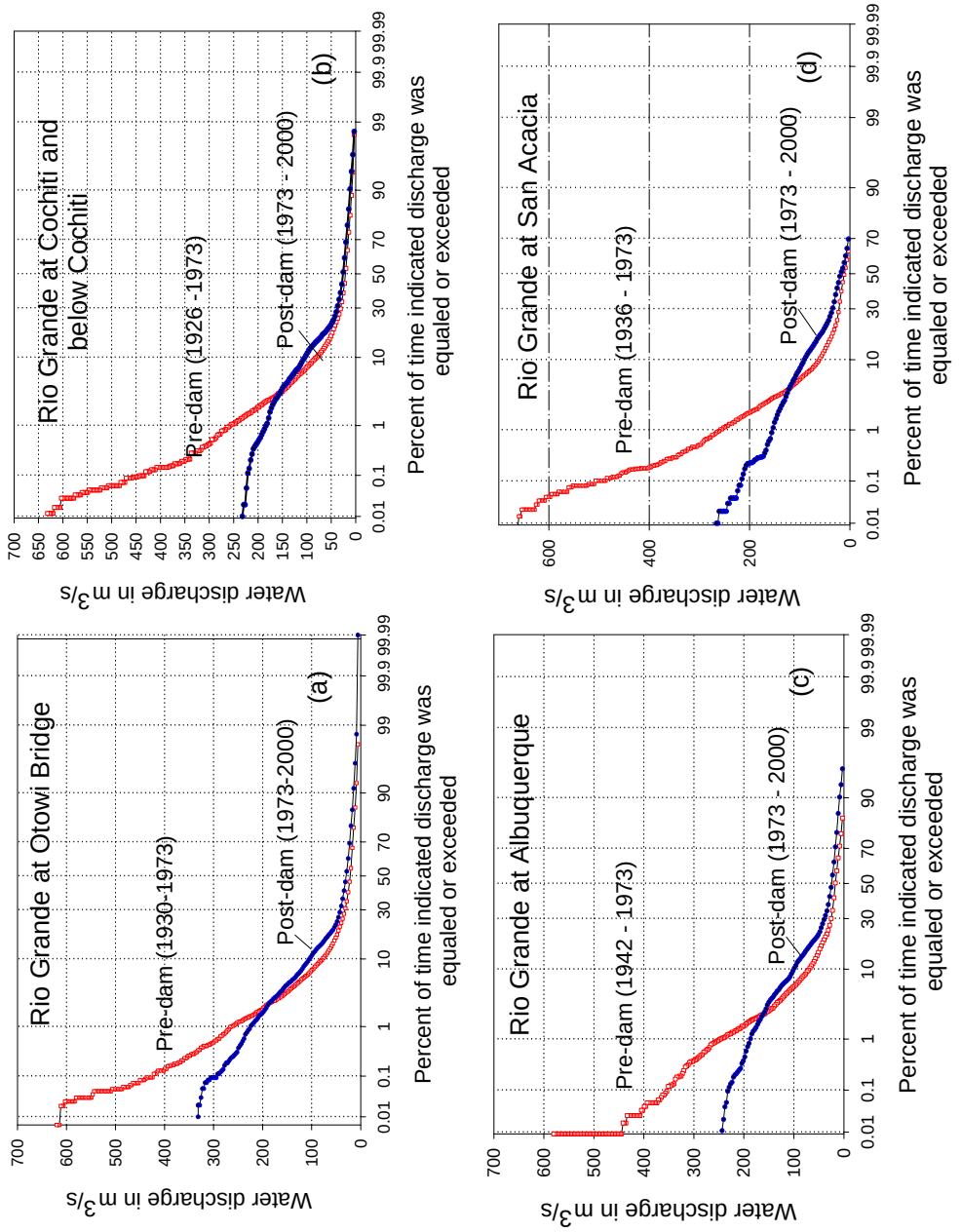

Figure 3.4: Pre-dam and post-dam flow duration curves at (a)Otowi, (b)Cochiti, (c)Albuquerque and (d)San Acacia.

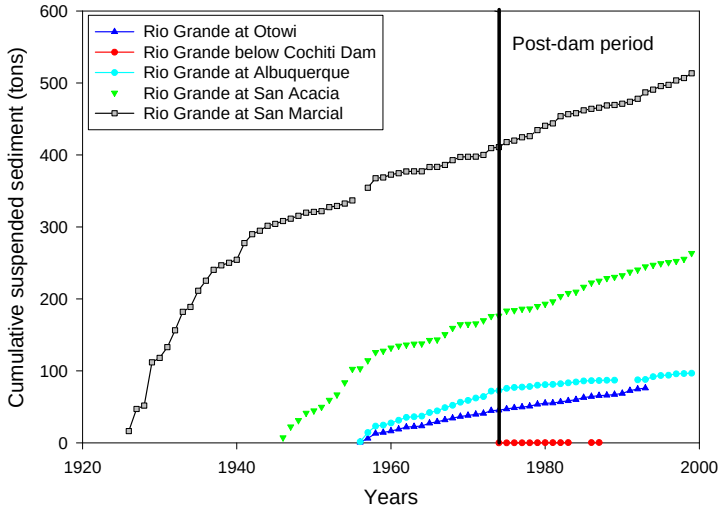

Figure 3.5: Cumulative mass curve of annual suspended sediment at USGS gage stations.

(mg/l). Table 3.1 summarizes the concentration values.

Sediment concentration started to decline at the San Marcial gage before Cochiti dam was built. The decline in sediment load at San Marcial after 1936 could be partially due to the completion of El Vado dam in the Rio Chama, one of the tributaries of the river upstream from Cochiti dam. According to Rittenhouse (1944), about 2 to 8 per cent of the channel sand material comes from the Rio Grande upstream from Cochiti Dam. In addition, the decrease in suspended sediment loads in the river coincides with the arroyo evolution of the Southwest. Arroyos that delivered large amounts of sediment to the river in the beginning of the 19^{th} century, due to incision, have been aggrading and delivering less sediment to the channel (Gellis, 1991).

The sediment concentration was reduced by almost half at the Otowi gage after 1973. The same trend is evident at Albuquerque, San Acacia and San Marcial, downstream from Cochiti Dam (see white dots in Figure 3.6). The reduction of

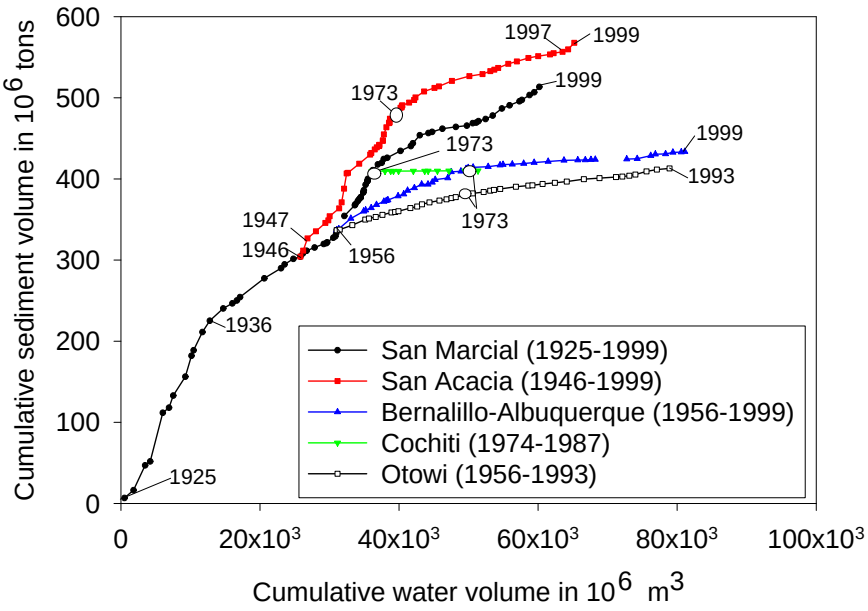

Figure 3.6: Double mass curve of annual water and sediment discharge at USGS gage stations. White circles indicate year of completion of Cochiti Dam.

sediment concentration at Otowi gage might be due to changes in land use in the watershed, climate, etc. The change in sediment concentration downstream from Cochiti Dam might be the result of the effect of the same factors affecting Otowi plus the retention of sediment behind the dam.

Table 3.1 shows that concentration increases with increasing distance downstream from Cochiti dam. Sediment is delivered to the river from tributaries and is mined from the bed and banks along the channel.

Gage Station	Concentration in mg/l	
Otowi	(1956-1973) 2,400	(1973-1993) 1,150
Cochiti	(1974-1987) 38	–
Albuquerque	(1956-1973)4,000	(1973-1999) 950
San Acacia	(1925-1936)17,800	(1991-1999) 5,100
San Marcial	(1946-1947)22,000	(1997-1999) 6,000

Table 3.1: Summary of suspended sediment concentration at USGS gage stations. The time periods used for the estimations of the concentrations are in parentheses.

3.3 Bed Material

Bed material varies along the channel and with time. Prior to the construction of Cochiti Dam, the middle Rio Grande was a sand bedded channel with some coarse material (gravel and cobbles) in the upper reach (Nordin and Beverage, 1965). Bed material has been coarsened in several reaches through time. Gravel bed is found from Cochiti Dam to Bernalillo Bridge from 1985 to the present (Richard, 2001). The sediment is sand and gravel downstream from Bernalillo (León et al., 2002). The Rio Salado, upstream from San Acacia Diversion Dam, inputs large quantities of gravel sized particles. The material is stored in the pool upstream of the dam and periodically flushed downstream (Mussetter Engineering, 2002). About 18 kilometers downstream from the San Acacia dam, a sand layer of about 0.60 - 0.90 meters of depth overlays a layer of gravel (Massong et al., 2000). Downstream from this reach, the bed material consists of very fine sand. In the headwaters of Elephant Butte reservoir, it consists of sand together with clay and silt.

3.4 Changes in Channel Morphology

The morphologic characteristics of the river vary along the channel depending on geologic, geomorphic and man-made controls. However, some characteristics can be

generalized for the entire river. For example, the active channel width, defined as the width of the sand bed channel where the vegetation has been cleared away by the flows (U. S. Bureau of Reclamation, 2000), has decreased since at least 1918. Furthermore, the rate of decrease has not been exacerbated by the construction of Cochiti Dam (Sanchez and Baird, 1997; Richard et al., 2001; León et al., 2002). The sinuosity of the Rio Grande has been generally lower than 1.2 (U. S. Bureau of Reclamation, 2000; Sanchez and Baird, 1997; Richard et al., 2001; León et al., 2002), indicative of a straight river. Downstream from the San Acacia Diversion Dam, the river develops a very particular planform of a sequence of alternating wide and narrow reaches followed by a man-made narrow reach that extends to Elephant Butte Reservoir.

In addition, the river has incised throughout most of its length. River reaches upstream from Elephant Butte Reservoir are highly affected by the reservoir surface elevation. Therefore, river bed aggradation occurs when the reservoir delta moves upstream with the reservoir pool (U. S. Bureau of Reclamation, 2000). Channel aggradation has occurred as far as 76 Kilometers upstream from the headwaters of the reservoir, at the town of San Antonio (U. S. Bureau of Reclamation, 2000).

In general, the river has changed from a relatively straight, wide, braided and aggrading channel to a narrow, incised channel. Recent aerial photos of the river, taken at low flows, show a single thread channel with some split-flow reaches from Cochiti Dam to Bernalillo. Bank-attached alternate bars and mid-channel braid bars are common downstream from Bernalillo. There are also some dense vegetated mid-channel bars in this reach.

Table 3.2 summarizes some of the characteristics of the middle Rio Grande based on the data collected at the USGS gage stations. The time periods selected to compute these values correspond to the time span of the most recent trends.

The mean annual flow ($\overline{Q}$) was computed from the mean daily discharge records from 1978 to 2000. The hydrologic regime did not change during this period (1978-

2000), as evidenced by the constant slopes of the curves in Figure 3.2. The Mann-Whitney test (Salas et al., 1999) was used to determine the significance of the difference between the time series before and after the change in mean annual streamflow at the San Acacia gage. The lag-1 coefficient of the time series before and after the probable point of shift (1978) demonstrated that the time series were independent, which is a condition to apply this method. The Mann-Whitney test was applied for different periods to detect the most probable point of the change in the mean. The change occurred in 1978, and the means are significantly different at a significance level of $\alpha = 0.05$.

The annual sediment loads (L_a) were computed from Figure 3.5 during the periods of time indicated in parentheses in the Table 3.2. The median grain sizes (d_{50}) correspond to the surface bed material samples taken at the gage stations for the dates indicated in parenthesis. The median grain size at Cochiti corresponds to the surface bed material sample collected at cross section CO-3, about 5.5 kilometers downstream from Cochiti Dam, and the median grain size at San Acacia is a value reported by Massong et al. (2000). The dominant discharge (Q_d) was estimated by taking the average of the peak daily flows of the five previous years to 1999 (Richard, 2001). The rationalization behind this method of estimating the dominant discharge is that the peak flows (high magnitude, low frequency flows) are responsible for shaping the channel in arid regions (Knighton, 1998). In addition, the dominant discharge at San Acacia is comparable with the value estimated by Massong et al. (2000) based on recurrence interval data and field data ($Q_d = 142\ m^3/s$). Similarly, the dominant discharge at Cochiti is comparable with values estimated by Richard (2001) based on frequency analysis ($Q = 145\ m^3/s$) and the effective discharge method ($Q = 153\ m^3/s$) (Wolman and Miller, 1960).

Gage Station	$\overline{Q}$	L_a	d_{50}	Q_d
	m^3/s	tons/year	mm	m^3/s
Otowi	(78-2000)	(1958-1993)	-	(1995-1999)
	48	1.8 x 10^6	-	150
Cochiti	(78-2000)	(1974-1987)	(1998)	(1995-1999)
	45	0.06 x 10^6	16	133
Albuquerque	(1987-2000)	(1995-1999)	(1999)	(1995-1999)
	40	0.08 x 10^6	0.50	128
San Acacia	(1978-2000)	(1971-1999)	(1996)	(1995-1999)
	35	3.5 x 10^6	0.40	139
San Marcial	(1978-2000)	(1991-1999)	(2000-2001)	(1995-1999)
	32	4.9 x 10^6	0.22	104

Table 3.2: Summary mean annual flow ($\overline{Q}$), annual sediment load L_a,median grain size (d_{50}) and dominant discharge Q_d at USGS gage stations. Values were averaged over the period indicated in parentheses.

3.5 Environmental Implications and Restoration Efforts

The changes in water and sediment regime in the middle Rio Grande and the subsequent changes in river morphology through time have affected the biodiversity of the aquatic and riparian habitat (Platania, 1991; Bestgen and Platania, 1991; Burton, 1997; Robinson, 1995; Arritt, 1996). Human perturbations such as water pollution, food-web manipulation by harvest, stocking and exotic invasions and alteration of water temperature and flux of material by dams, diversions and revetments uncouple important ecological processes (Stanford et al., 1996). Several of these factors, if not all of them, are present along the middle Rio Grande.

3.5.1 Fish Habitat

The native fishes of the New Mexican portion of the Rio Grande consisted of 16 species (Platania, 1991). Of these, four species have been extirpated and five appear to be declining in both range and abundance (Platania, 1991). Currently, the only endemic of the Rio Grande surviving in New Mexico is the Rio Grande silvery minnow (*Hybognathus amarus*) (Platania, 1991), a species historically occurring from Española, New Mexico, to the Gulf of Mexico (Bestgen and Platania, 1991) and in major tributaries of the river (Burton, 1997). Large numbers of Rio Grande silvery minnow were found in the middle Rio Grande between 1926 and 1978 (Bestgen and Platania, 1991). Remaining populations of this species continue to decline primarily due to the lack of warm, slow-moving, silt-sand substrate pools, dewatering of the river and abundance of non-native and exotic fish species (Platania, 1991; Bestgen and Platania, 1991; Burton, 1997; Robinson, 1995; Arritt, 1996).

Generally, the Rio Grande silvery minnow prefers shallow water with flow depths less than 0.4 m and velocities less than 0.1 m/s (U. S. Fish and Wildlife Service, 2001). Few fish have been found in water greater than 0.5 m and velocities greater than 0.4 m/s (U. S. Fish and Wildlife Service, 2001). According to some flume experiments with the fish, the fish can swim in waters with velocities up to 0.4 m/s and perform some short springs of up to 1 m/s (Mike Porter, USBR, Albuquerque, NM, 2002 pers. comm.).

The most common mesohabitats of the silvery minnow were debris piles (41%), pools (36%), and backwaters (14%). Small minnows are found in shorelines, backwaters, and pools. Large minnows are found in the main channel and in side channel runs. Moderate sized minnows are found close to debris piles in the winter. However, the majority of all size-classes are found in low-velocity habitats (U. S. Fish and Wildlife Service, 2001). Platania (1991) documented the longitudinal distribution of fishes in the Rio Grande based on samples taken in 1984. The river was divided into five sections within which similar physical attributes were observed (Figure 3.7).

Sections I to III were cool-water reaches and sections IV and V were warm-water reaches. Section III, just downstream from Cochiti Dam, was the most species-rich reach of the river with 17 species. The Rio Grande silvery minnow reached its most upstream distribution in this section. The Rio Grande silvery minnow was present at all sections III, IV and V, but was more abundant in section IV and in the lowermost sites in section V (Platania, 1991). Figure 3.8 represents the longitudinal distribution and relative abundance of five cyprinids in the Rio Grande.

Currently, the Rio Grande silvery minnow occurs only in less than 10 % of its original range (Bestgen and Propst, 1996). In 1999, the U.S. Fish and Wildlife Service (USFWS) designated the middle Rio Grande, New Mexico from just downstream of Cochiti Dam to the railroad bridge at San Martial as critical habitat for the silvery minnow, a federally listed endangered species (U. S. Fish and Wildlife Service, 1999).

3.5.2 Riparian Vegetation and Bird Habitat

The degradation trend of the bed of the middle Rio Grande has halted overbank flooding in recent decades (Umbreit, 2001). As a result, wetlands, particularly cottonwood-willow riparian habitat, have been degraded. Frequent overbank flooding ensures widespread seed dispersal and germination (U. S. Bureau of Reclamation, 2000). Furthermore, non-native vegetation such as saltcedars and Russian olives have contributed to this process (Taylor and McDaniel, 2001). Saltcedars have longer seed dispersal periods, which enables them to germinate with flows that decline later in the summer (U. S. Bureau of Reclamation, 2000).

Large-scale loss of cottonwood-willow riparian habitat is the main reason for the decline of the southwestern willow flycatcher (SWWF) (*Empidonax trailli extimus*). In 1995, the U.S Fish and Wildlife Service listed the SWWF as an endangered species (U. S. Fish and Wildlife Service, 2000) and the State of New Mexico also classified it as endangered. However, no critical habitat has been designated along

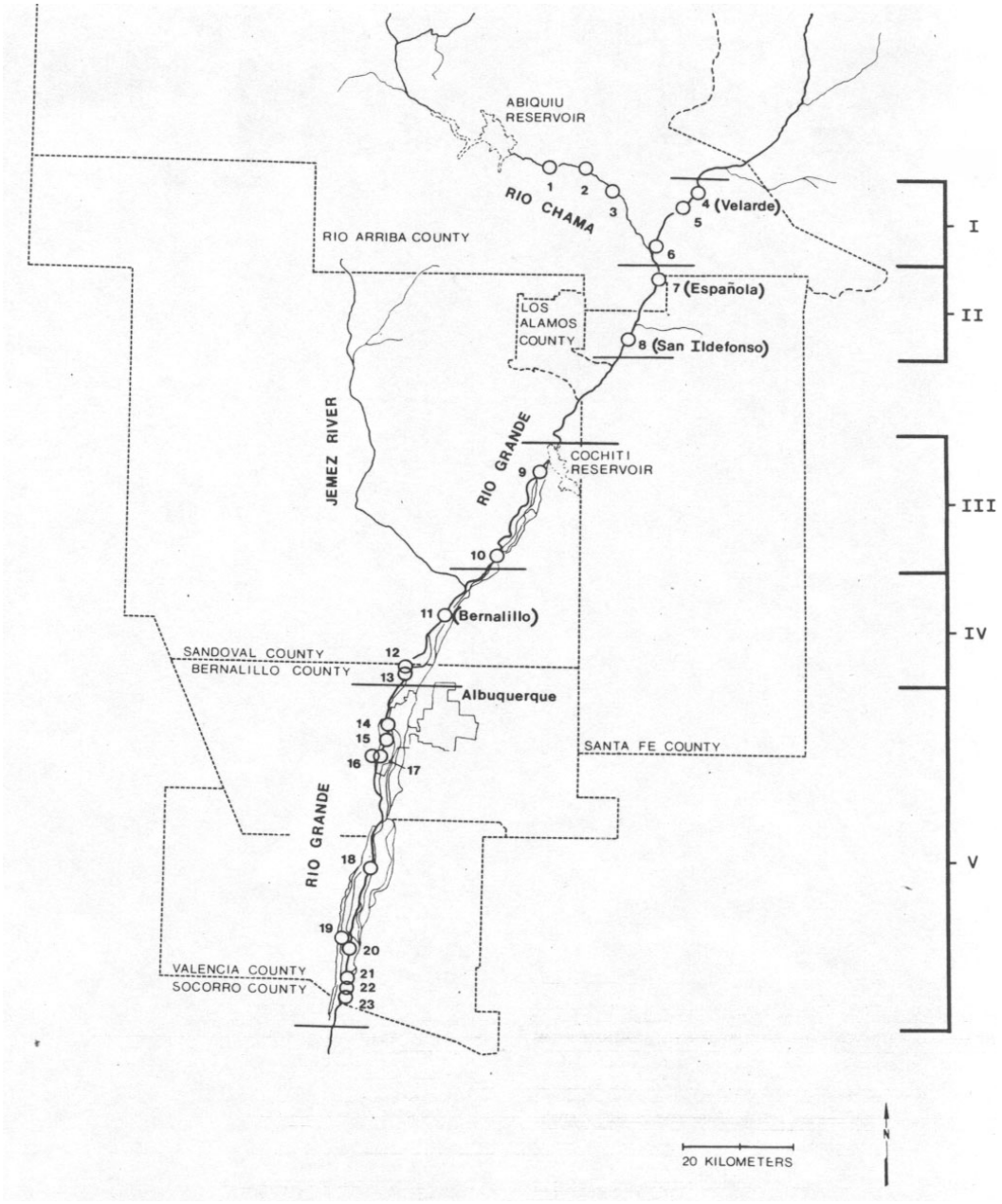

Figure 3.7: Map of the Middle Rio Grande indicating the longitudinal distribution of the cyprinids (After Platania 1991).

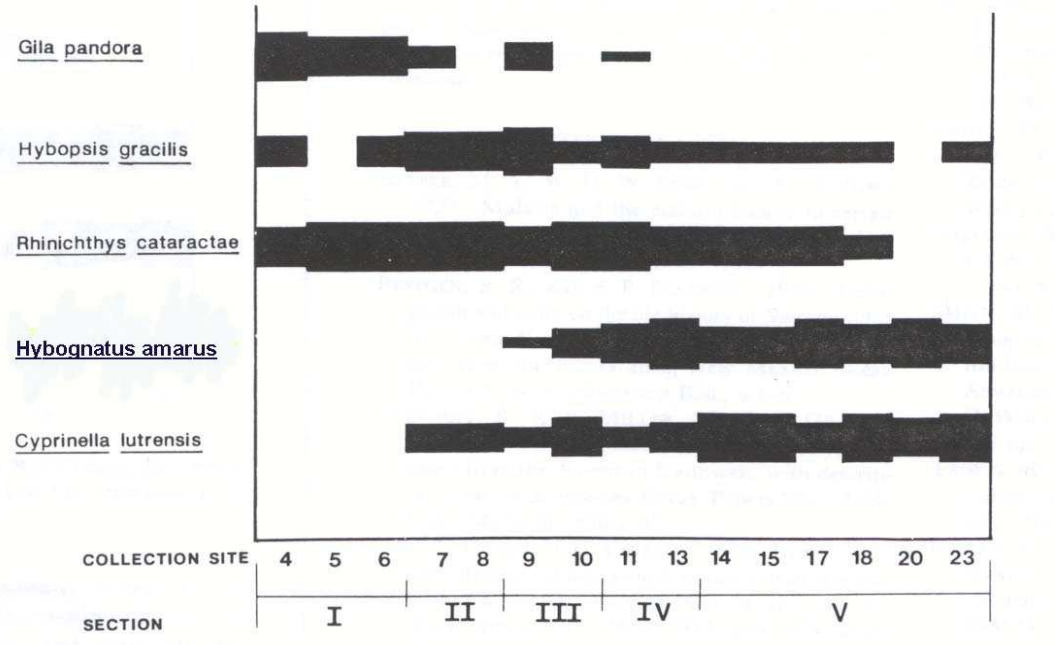

Figure 3.8: Longitudinal distribution and relative abundance of five cyprinids in the Rio Grande. Bar width (one of five thicknesses) indicates abundance, relative to the other four species. Thickest bar represents most common of the five species. Collection sites and sections correspond to those in Figure 3.7 (After Platania 1991).

the Rio Grande (U. S. Bureau of Reclamation, 2000).

Cottonwood and willows also provide habitat for many neotropical migrant landbirds during the migration and the breeding periods (U. S. Bureau of Reclamation, 2000). More than 100 bird species rest and forage in this habitat during the spring and fall migration (U. S. Bureau of Reclamation, 2000).

The goal of ecological restoration is to produce a self-sustaining system as similar as possible to the native biota (Whitney, 2001). Additionally, restoration goals must meet social, political and biological constraints (Whitney, 2001; Booker and Ward, 1999), which makes their implementation a complex problem. Currently, restoration efforts in the Rio Grande consist of creating wider shallower flow conditions, lowering

overbank areas to re-connect the main channel with floodplains and establishing native riparian species (Baird, 2001). Moreover, environmental groups, water users and federal agencies are trying to negotiate the appropriate allocation of water that will prevent the river from dewatering.

3.6 Summary

Changes in water and sediment regimes in the Rio Grande due to climate changes and human activities have produced changes in the morphology of the middle Rio Grande. The habitat of the native biota has been altered, causing the decline of the Rio Grande silvery minnow, a federally listed endangered species.

The majority of all size-class silvery minnows are found in low-velocity habitats (U. S. Fish and Wildlife Service, 2001), with flow depths less than 0.4 m and velocities less than 0.1 m/s. Few fish have been found in water greater than 0.5 m and velocities greater than 0.4 m/s (U. S. Fish and Wildlife Service, 2001). Current narrow and deep channels in some reaches of the Rio Grande do not provide the appropriate habitat for the minnow. One of the proposed means to restore the habitat for the fish is to create wide channels that provide slow-moving and shallow flows (Baird, 2001).

Changes in channel width under current water and sediment regimes will induce channel form adjustments. It is the intent of this work to provide some insight about the mechanisms of channel slope adjustment due to imposed changes in channel width. Also, to evaluate how adjustments in slope due to imposed changes in channel width will influence habitat for the silvery minnow.

Chapter 4

Steady State and Transient Models

As pointed out in the previous chapter, there are several reaches of the Rio Grande characterized by straight wide channels that alternate between single thread narrow stretches. The Bosque del Apache (BDA) reach is an example of these reaches that has maintained the same width from about 1985 and has not migrated across the floodplain. Therefore, this reach has been transporting the imposed or incoming water and sediment discharges by adjusting the bed slope. The objective of this chapter is to develop a steady state model to predict the adjustment of channel slope due to changes in width along the channel. Two analytical approaches are developed. The first approach approximates the hydraulic radius to the flow depth (wide channels) (see Section 4.1) and the second approach does not approximate the hydraulic radius to the flow depth (see Section 4.1). A numerical model for constant water discharge input is developed to simulate the transient behavior of the system (see Section 4.2). Finally, the results of the analytical and numerical approaches are compared.

4.1 Analytical Approach for Steady State Condition

The problem to be solved consists of estimating the channel slope of two sequential channel reaches with different widths able to transport the same sediment load and water discharge. This approach will be explained by means of the following hypothetical example: the initial width (W_1) of a rectangular channel of slope (S) is changed from (W_1) to (W_2) at a distance (L_1)(see Figure 4.1). In order to main-

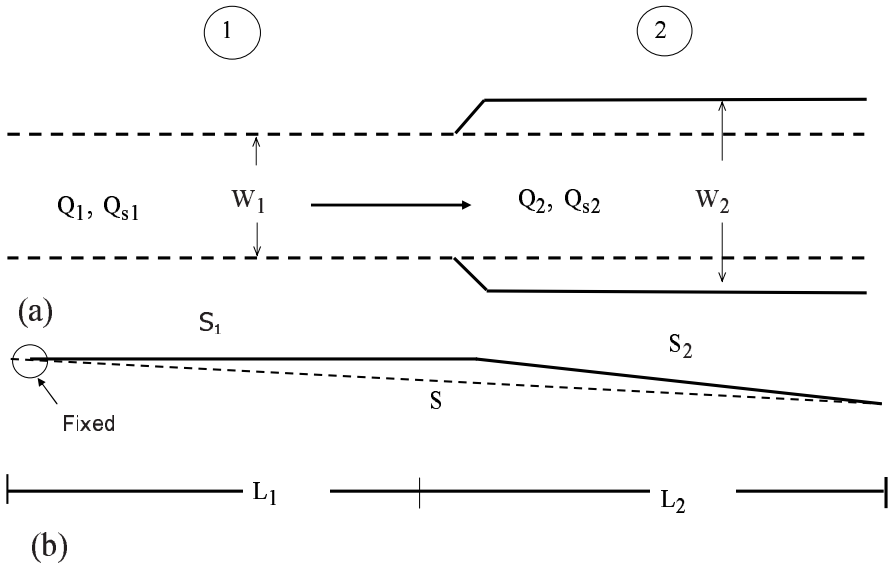

Figure 4.1: (a) Plan view of an example channel. Dashed line represents the width of the original channel. Continued line represents the width of the new imposed channel. (b) Profile of reaches 1 and 2. Dashed line represents the profile of the original channel. Continued line represents the width of the new imposed channel. W = width, S = slope, L = length, Q = water discharge, Q_s = sediment discharge.

tain the same sediment load ($Q_{s1} = Q_{s2}$) through both reaches (denoted 1 and 2 respectively), the slope, velocity and depth will adjust (see Figure 4.1)

The known variables in reach 1 are: water discharge (Q_1), sediment discharge (Q_{s1}), channel width (W_1), mean flow depth (h_1), mean flow velocity (V_1)and the initial channel slope (S). The known variables in reach 2 are: water discharge (Q_2), sediment discharge (Q_{s2}), channel width (W_2) and the initial slope (S). If the channel width does not change with time, the slope of both subreaches will adjust to accommodate the water and sediment discharge, until sediment transport equilibrium is reached ($Q_{s1} = Q_{s2}$).

The following assumptions are made to solve this problem:

- Both reaches have rectangular cross-sections

- Both reaches are straight
- Sediment size (d_s) and friction factor (n) are the same for both reaches
- Sand bed channel
- Water discharge (Q) and sediment discharge (Q_s) are constant
- The overall slope of the channel is able to pass the input sediment load. The upstream node is fixed.

4.1.1 Case A: Simplified Analytical Approach: hydraulic radius is approximated to flow depth ($R_h \approx h$)

The following three basic equations are used to solve the problem:

1. Water mass continuity for steady flow conditions: $Q = VA$. Where Q is the water discharge, V is the mean velocity and A is the cross sectional area
2. Manning's flow resistance equation: $V = \frac{\phi}{n} R_h^{2/3} S^{1/2}$. Where ϕ is 1.49 for English units and 1 for metric units, n is the friction factor, R_h is the hydraulic radius and S is the energy grade line slope.
3. Julien's (2002) simplified sediment transport equation: $Q_s = 18W\sqrt{g}d_s^{3/2}\tau_*^2$. Where Q_s is the sediment discharge by volume, W is the channel width, g is the gravitational acceleration, d_s is the particle size and $\tau_* = \frac{\tau}{(\gamma_s - \gamma)d_s}$, τ is the bed shear stress, γ_s is the specific weight of the sediment and γ is the specific weight of the water-mixture. Julien's (2002) simplified sediment transport equation was developed for $0.1 < \tau_* < 1.0$.

Under sediment transport equilibrium the following conditions are met: $Q_1 = Q_2$ and $Q_{s1} = Q_{s2}$. Replacing the resistance equation into the continuity equation, we obtain:

$$Q = VA = \frac{\phi}{n} R_h^{2/3} S^{1/2} A$$

For very wide channels $R_h \approx h$, then:

$$Q = \frac{\phi}{n} h^{2/3} S^{1/2} hW = \frac{\phi}{n} h^{5/3} S^{1/2} W$$

Thus the ratio of Q_1 and Q_2 is:

$$\frac{Q_2}{Q_1} = 1 = \frac{W_2 h_2^{5/3} S_2^{1/2}}{W_1 h_1^{5/3} S_1^{1/2}} = W_r h_r^{5/3} S_r^{1/2}$$

Solving for S_r we get:

$$S_r = \frac{1}{W_r^2 h_r^{10/3}} \tag{4.1}$$

Where W_r is the ratio of the widths, h_r is the ratio of the flow depths, and S_r is the ratio of the slopes.

The ratio of Q_{s2} and Q_{s1} is:

$$\frac{Q_{s2}}{Q_{s1}} = 1 = \frac{W_2 h_2^2 S_2^2}{W_1 h_1^2 S_1^2} = W_r h_r^2 S_r^2$$

Solving for S_r we get:

$$S_r = \frac{1}{W_r^{1/2} h_r} \tag{4.2}$$

Then, making equation 4.1 equal to equation 4.2 we obtain:

$$\frac{1}{W_r^2 h_r^{10/3}} = \frac{1}{W_r^{1/2} h_r} \Rightarrow h_r = W_r^{-9/14} \tag{4.3}$$

Replacing equation 4.3 into equation 4.1 we obtain:

$$S_r = W_r^{1/7} \tag{4.4}$$

$$S_r = h_r^{-2/9} \tag{4.5}$$

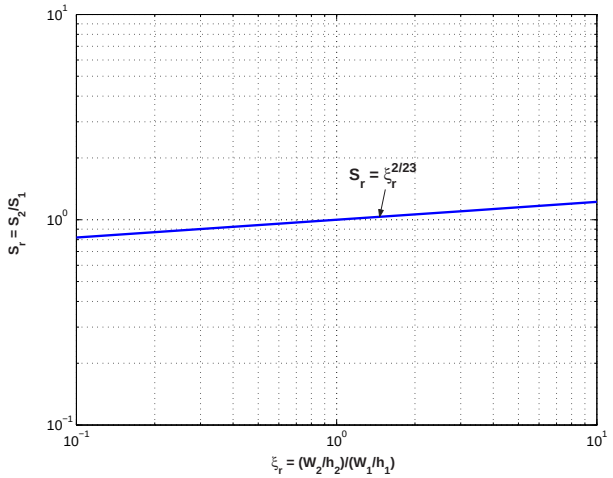

Figure 4.2: Relationship between the ratio of the slopes and the ratio of the width-depth ratios according to equation 4.6

$$S_r = \left(\frac{W_r}{h_r}\right)^{2/23} = (\xi_r)^{2/23} \tag{4.6}$$

The ratio of the velocities is equal to:

$$\frac{V_2}{V_1} = h_r^{2/3} S_r^{1/2} \Rightarrow V_r = S_r^{-5/2} \tag{4.7}$$

In practice, equations 4.6 and 4.4 indicate that an increase in channel width will require an increase in channel slope to satisfy continuity of sediment transport. Figure 4.2 represents equation 4.6. The coordinate (1,1) corresponds to a channel of one width and slope. As the channel width is increased (move to the right of the curve), the channel slope has to increase to transport the same sediment load.

4.1.2 Case B: Detailed Analytical Approach: hydraulic radius is not approximated to the flow depth ($R_h \neq h$)

This approach consists of determining the relationship between slope and width-depth ratio of a channel, when the hydraulic radius is not approximated to the flow depth. The following three dependent variables are considered: width to depth ratio

(ξ), mean flow velocity (V) and channel slope (S). The steady state independent variables are: flow discharge (Q), sediment discharge (Q_s), sediment size (d_s) and friction factor (n). The same basic equations used in sub-section 4.1.1 are used in this approach.

The cross section area (A) and the hydraulic radius (R_h) can be expressed as function of the width-depth ratio (ξ), then: $A = Wh = \xi h^2$ and $R_h = \frac{Wh}{W+2h} = \frac{\xi h}{\xi+2}$. Substituting R_h, A and V into the continuity and resistance equations the following expression is obtained:

$$\frac{Q}{A} = V = \frac{\phi}{n}\left(\frac{\xi h}{\xi+2}\right)^{2/3} S^{1/2}$$

Solving for h:

$$\frac{Q}{\xi h^2} = V = \frac{\phi}{n}\left(\frac{\xi h}{\xi+2}\right)^{2/3} S^{1/2}$$

$$h^{8/3} = \frac{Qn}{\phi S^{1/2}}\frac{(\xi+2)^{2/3}}{\xi^{5/3}} \Rightarrow h = \frac{Q^{3/8}n^{3/8}}{\phi^{3/8}S^{3/16}}\frac{(\xi+2)^{1/4}}{\xi^{5/8}}$$

Then, W can be written as:

$$W = \xi\frac{Q^{3/8}n^{3/8}}{\phi^{3/8}S^{3/16}}\frac{(\xi+2)^{1/4}}{\xi^{5/8}} = \frac{Q^{3/8}n^{3/8}}{\phi^{3/8}S^{3/16}}(\xi+2)^{1/4}\xi^{3/8}$$

Replacing W and h into the sediment transport equation:

$$Q_s = 18g^{1/2}d_s^{3/2}W\frac{R_h^2S^2}{(G-1)^2d_s^2}$$

$$Q_s = 18g^{1/2}d_s^{3/2}\left[\frac{Q^{3/8}n^{3/8}}{S^{3/16}\phi^{3/8}}(\xi+2)^{1/4}\xi^{3/8}\right]\frac{S^2}{(G-1)^2d_s^2}\frac{\xi^2}{(\xi+2)^2}h^2$$

$$Q_s = 18g^{1/2}d_s^{3/2}\left[\frac{Q^{3/8}n^{3/8}}{S^{3/16}\phi^{3/8}}(\xi+2)^{1/4}\xi^{3/8}\right]\frac{S^2}{(G-1)^2d_s^2}\frac{\xi^2}{(\xi+2)^2} \text{ x } \left[\frac{Q^{6/8}n^{6/8}}{S^{6/16}\phi^{6/8}}\frac{(\xi+2)^{1/2}}{\xi^{5/4}}\right]$$

Solving for S

$$S = \left(\frac{Q_s}{Q}\right)^{16/23} \frac{(G-1)^{32/33} d_s^{8/23} \phi^{18/23}}{Q^{2/23} 18^{16/23} g^{8/23} n^{18/23}} \frac{(\xi+2)^{20/23}}{\xi^{18/23}} \tag{4.8}$$

The above equation can be expressed as a function of the volumetric sediment concentration C_v as:

$$S = C_v^{16/23} \frac{(G-1)^{32/33} d_s^{8/23} \phi^{18/23}}{Q^{2/23} 18^{16/23} g^{8/23} n^{18/23}} \frac{(\xi+2)^{20/23}}{\xi^{18/23}} \tag{4.9}$$

For large width-depth ratios ($\xi \rightarrow \infty$), the hydraulic radius R_h approximates the flow depth h and equation 4.8 reduces to:

$$lim_{\xi \rightarrow \infty} S = \left(\frac{Q_s}{Q}\right)^{16/23} \frac{(G-1)^{32/33} d_s^{8/23} \phi^{18/23}}{Q^{2/23} 18^{16/23} g^{8/23} n^{18/23}} (\xi+2)^{2/23} \tag{4.10}$$

This equation is similar to equation 4.6, where the slope is a function of the width-depth ratio to the power of 2/23. Figure 4.3 compares the results of Case A and Case B. The input data used to develop these curves are: water discharge ($Q = 139\ m^3/s$), sediment discharge ($Q_s = 0.082\ m^3/s$), particle size ($d_s = 0.3\ mm$), friction factor ($n = 0.023$), specific gravity of the sediment ($G = 2.65$) and gravitational acceleration ($g = 9.81\ m/s^2$). Both cases yield the same solutions for width-depth ratios greater than 70. For the above set of data, the Shields parameter is greater than 1 at width-depth ratios less than about 490. The Shields parameter is about 2.7 at a width-depth ratio of 18 (at minimum slope). At this value of Shields parameter, Julien's (2002) simplified sediment transport equation is expected to over-estimate the transport. However, the accuracy of the equation for Shields parameter greater than 1 has not yet been tested. For practical purposes, the portion of the curve that corresponds to the Shields parameter between 0.1 and 1 should only be used.

The minimum of the curve for Case B can be calculated analytically by taking the derivative of equation 4.9 with respect to ξ and equating it to zero, as shown below:

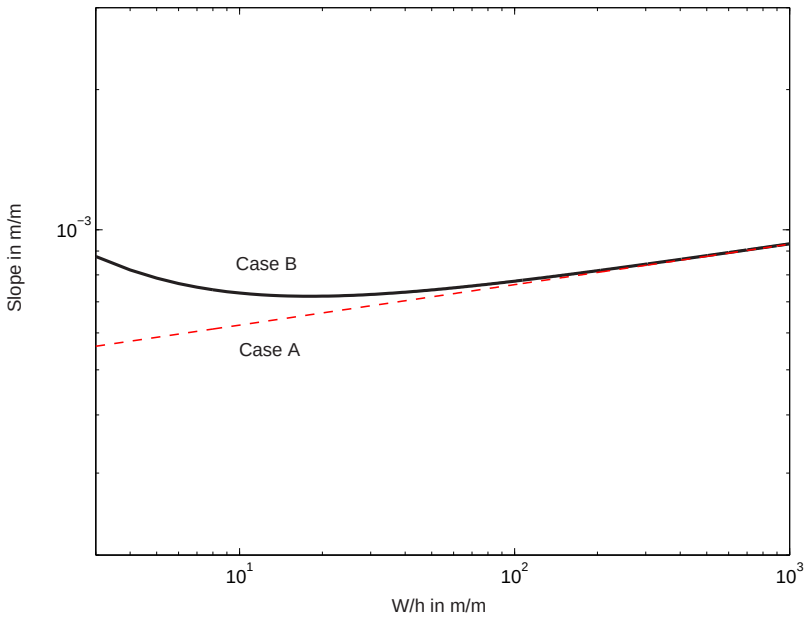

Figure 4.3: Slope versus width-depth ratio relationships for cases A and B. This curve was generated with the following data: $Q = 139\ m^3/s$, $Q_s = 0.082\ m^3/s$, $d_s = 0.3\ mm$, $n = 0.023$, $G = 2.65$, and $g = 9.81\ m/s^2$.

$$\begin{aligned}\frac{dS}{d\xi} &= K\frac{d}{d\xi}\left[\frac{(\xi+2)^{20/23}}{\xi^{18/23}}\right] = \\ &= K\left[\frac{20}{23}(\xi+2)^{-3/23}\xi^{-18/23} + (\xi+2)^{20/23}\left(\frac{-18}{23}\right)\xi^{-41/23}\right] = 0\end{aligned} \tag{4.11}$$

Where $K = \left(\frac{Q_s}{Q}\right)^{16/23}\frac{(G-1)^{32/33}d_s^{8/23}\phi^{18/23}}{Q^{2/23}18^{16/23}g^{8/23}n^{18/23}}$. Solving for ξ in equation 4.11, the minimum slope occurs always at $\xi = 18$.

The maximum width a channel could develop will be limited to the excess of shear stress. When the available shear stress is less than the critical shear required to entrain the sediment particles of the bed, all the sediment will deposit. Therefore, the solution for large width-depth ratios is limited to this condition.

Analytical Solutions with Different Resistance to Flow Equations

The solutions presented in Sections 4.1.1 and 4.1.2 were developed from Manning's resistance equation and Julien's (2002) simplified sediment transport equation. Similar solutions were also developed using Darcy-Weisbach's and Brownlie's resistance equations. The detailed procedure is outlined in Appendix B.

The following set of equations represents the solutions developed from Darcy-Weisbach's resistance equation for the simplified case, when the hydraulic radius is approximated to the flow depth ($R_h \approx h$).

The slope versus width relationship is:

$$S_r = W_r^{1/4} \tag{4.12}$$

The slope versus depth relationship is:

$$S_r = h_r^{-1/3} \tag{4.13}$$

The slope versus width-depth ratio relationship is:

$$S_r = \left(\frac{W_r}{h_r}\right)^{1/7} = (\xi_r)^{1/7} \tag{4.14}$$

And the slope versus velocity relationship is:

$$S_r = V_r^{-1} \tag{4.15}$$

The following equation is the detailed analytical solution for the slope versus the width-depth ratio relationship, when the hydraulic radius is not approximated to the flow depth ($R_h \neq h$):

$$S = \frac{Q_s^{5/7}}{Q^{6/7}} \frac{d_s^{5/14} g^{1/14} (G-1)^{10/7}}{18^{5/7}} \left(\frac{8}{f}\right)^{3/7} \frac{(\xi+2)}{\xi^{6/7}} \tag{4.16}$$

As opposed to the solution obtained with Manning's resistance equation, the minimum of the function represented by equation 4.16 is always at $\xi = 12$.

Brownlie (1981) developed two flow resistance equations, one for lower regime and another for upper regime, for large width-depth ratios ($R_h \approx h$). The following equation is the detailed analytical solution developed from Brownlie's (1981) resistance equations:

$$S = \frac{Q_s^{\frac{1+X}{b}}}{Q^{\frac{3X}{b}}} \left[\frac{(G-1)^2}{18}\right]^{\frac{1+X}{b}} \frac{d_s^{\frac{10X-6T+1}{2b}} \xi^{\frac{2X-1}{b}}}{g^{\frac{1-2X}{2b}} a^{\frac{3}{b}} \sigma_g^{\frac{3Z}{b}}} \tag{4.17}$$

where $b = 2(1+X)+3Y$ and a,X,Y,Z and T are the coefficient and exponents of the resistance equation as indicated in the following equation:

$$h = a\left(\frac{Vh}{\sqrt{gd_{50}^3}}\right)^X S^Y \sigma_g^Z d_{50}^T$$

The values of the coefficient and exponents depend on the flow regime. For lower regime $a = 0.3724$, $X = 0.6539$, $Y = -0.2542$, $Z = 0.1050$, and $T = 1$. For upper regime $a = 0.2836$, $X = 0.6248$, $Y = -0.2877$, $Z = 0.08013$, and $T = 1$.

The function represented by equation 4.17 does not have a minimum. For large width-depth ratios, the slope tends to: $S \propto \xi^p$, where $p = \frac{2X-1}{b}$ and is equal to $p = 0.1209$ for lower regime and $p = 0.1046$ for upper regime.

Figure 4.4 shows the solutions of equations 4.8, 4.16, and 4.17 for the following data set: water discharge ($Q = 139\ m^3/s$), sediment discharge ($Q_s = 0.082\ m^3/s$), particle size ($d_s = 0.3\ mm$), Manning friction factor ($n = 0.023$), Darcy-Weisbach friction factor $f = 0.03$, specific gravity of the sediment ($G = 2.65$) and gravitational acceleration ($g = 9.81\ m/s^2$). In order to plot equation 4.17, a flow regime was assumed and then it was verified that the results correspond to the assumed flow regime (see Appendix 7.1 for the conditions of each flow regime).

Numerical Solutions with Different Sediment Transport Equations

The analytical solutions presented at the beginning of this chapter were developed from Julien's (2002) simplified sediment transport equation. Other sediment trans-

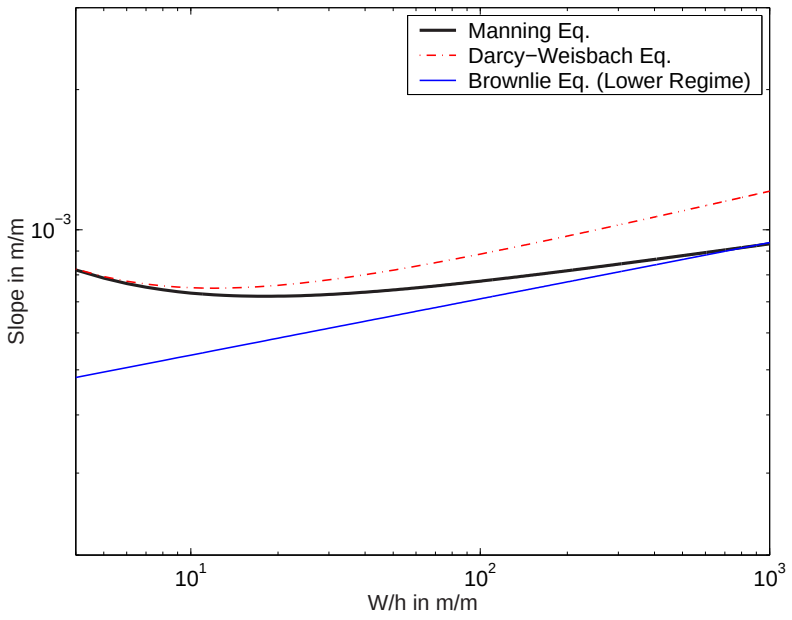

Figure 4.4: Slope versus width-depth ratio relationships developed from Julien simplified sediment transport equation and Manning, Darcy-Weisbach and Brownlie flow resistance equations. These curves were generated with the following data: $Q = 139\ m^3/s$, $Q_s = 0.082\ m^3/s$, $d_s = 0.3\ mm$, $n = 0.023$, $f = 0.03$, $G = 2.65$, and $g = 9.81\ m/s^2$.

port equations were also used to develop slope versus width-depth ratio relationships for comparison. The sediment transport equations used were: Yang (1973), Engelund and Hansen (1967, from Julien 1995), Molinas and Wu (2001), Brownlie 1981, and Ackers and White (1973). These equations are included in Appendix 7.1.

Analytical solutions cannot be developed with these equations. Therefore, numerical solutions were produced by performing numerical iterations. Given the flow discharge (Q), the sediment discharge (Q_s), the sediment size (d_s), the friction factor (n or f), and the channel width (W), the resistance equation and the sediment transport equation were solved simultaneously for the channel slope S by solving for the flow depth h. These iterations were performed with Visual Basic for Microsoft

Excel.

The numerical solutions were developed using three resistance equations (Manning, Darcy-Weisbach, Brownlie) (see Appendix 7.1). The solutions were found for the same data used to develop Figure 4.4. Figures 4.5 and 4.6 present the results. The analytical solution developed from Julien's simplified transport equation is also plotted for comparison.

Figures 4.5 and 4.6 show that the slope versus width-depth ratio relationships change with the different transport and resistance equations. The width-depth ratios at the minimum slopes vary from about 1.5 to 25 in Figure 4.5. Multiple slope solutions for the same value of width-depth ratio are generated when using Brownlie's (1981) equation.

Similar solutions can be obtained for the slope versus width relationships. Figures 4.7 and 4.8 contain the results of these relationships for all the sediment transport and resistance equations. The solution of slope versus width relationship obtained from Julien's (2002) simplified sediment transport equation and without approximation of the the hydraulic radius equal to the flow depth can only be obtained numerically. Figure 4.7 shows that the width at minimum slope varies from about 10 to 50.

The SAM hydraulic Design Package for Flood Control Channels (v. 3.07, 10 August 1994), developed by the US Army Corps of Engineers, was used to generate similar curves to the relationships in Figures 4.5 to 4.8 for comparison. This program uses composite hydraulic parameters, which consist of computing the cross section as a function of the bed hydraulic radius and the side slope hydraulic radius. The bed hydraulic radius is computed with Brownlie's flow resistance equation and the side slope hydraulic radius with Manning's flow resistance equation. In addition, Brownlie's transport equation is used to compute the sediment concentration. Figure 4.9 presents the results obtained from SAM. The width and the width-depth ratio at minimum slope are 5.6 m and 4.6 m, respectively.

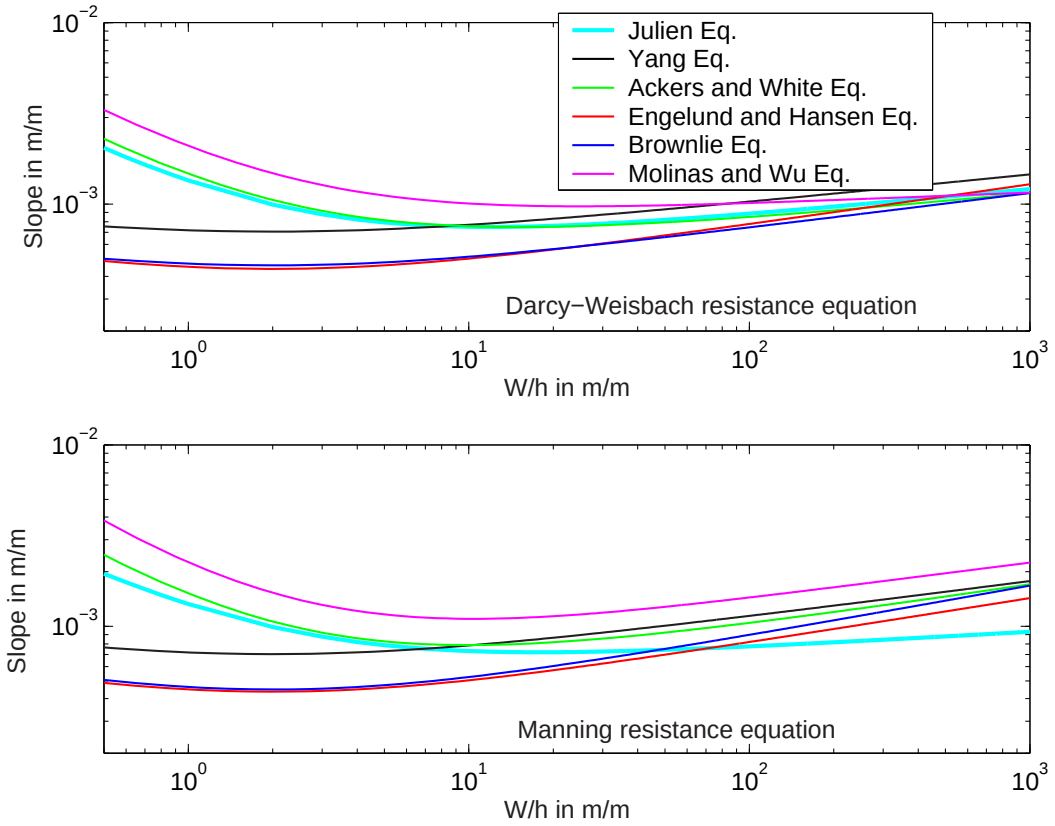

Figure 4.5: Slope versus width-depth ratio relationships developed from six different sediment transport equations and Manning and Darcy-Weisbach flow resistance equations. These curves were generated with the following data: $Q = 139\ m^3/s$, $Q_s = 0.082\ m^3/s$, $d_s = 0.3\ mm$, $n = 0.023$, $f = 0.03$, $G = 2.65$, and $g = 9.81\ m/s^2$.

In order to achieve a better understanding of these relationships, a sensitivity analysis of the slope versus width-depth ratio and slope versus width relationships was performed. Two different analyses were carried out. In one the sediment discharge was considered dependent on water discharge. In this case water discharge (Q), sediment size (d_s) and friction factor (n) were perturbed and the sediment discharge was estimated according to the bed material rating curve at San Marcial (see Appendix 7.1) for each value of water discharge. The bed material load was used instead of the bedload, because there are no bedload measurements at San Marcial

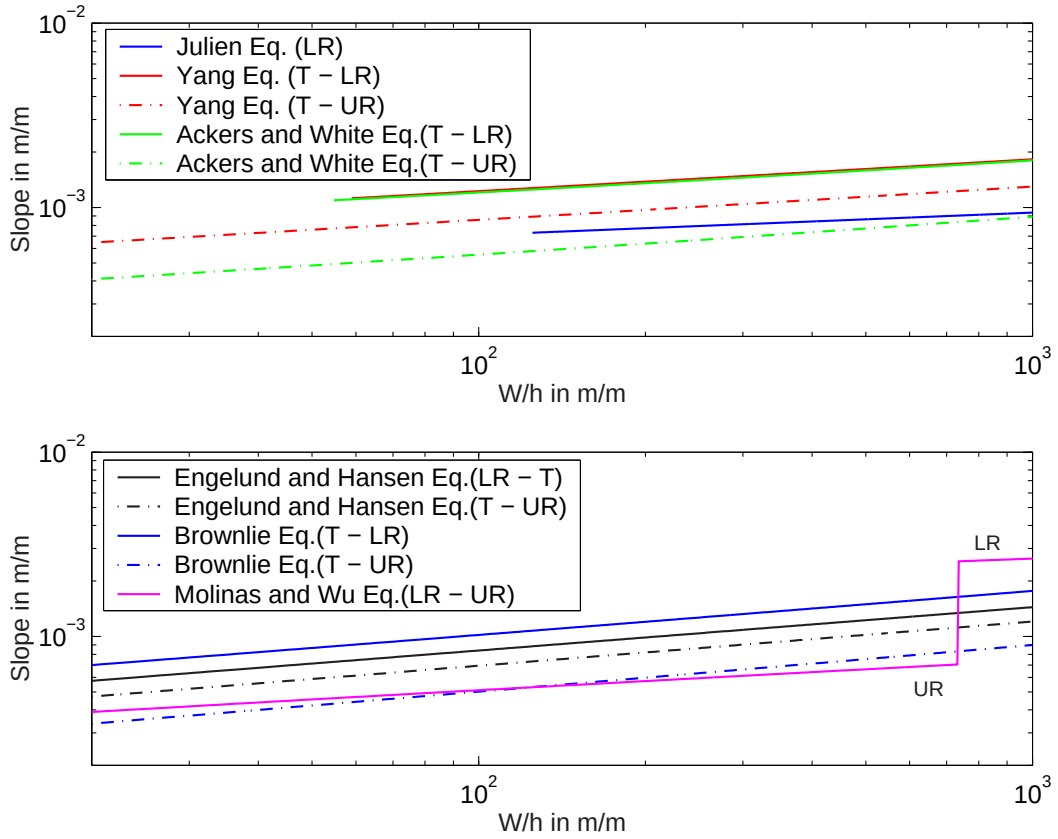

Figure 4.6: Slope versus width-depth ratio relationships developed from six different sediment transport equations and Brownlie flow resistance equation. These curves were generated with the following data: $Q = 139\ m^3/s$, $Q_s = 0.082\ m^3/s$, $d_s = 0.3\ mm$, $G = 2.65$, and $g = 9.81\ m/s^2$. T = Transition; LR = Lower regime; UR = Upper regime.

gage. The second analysis consisted of changing only the sediment discharge and keeping the water discharge constant. Four different responses were measured. The width-depth ratio at minimum slope, the width at minimum slope and the exponents p and q of the following relationships: $S_r = \left(\frac{W_r}{h_r}\right)^p$, and $S_r = W_r^q$, for large widths. The details of the procedures followed and the results of the sensitivity analysis are in Appendix C.

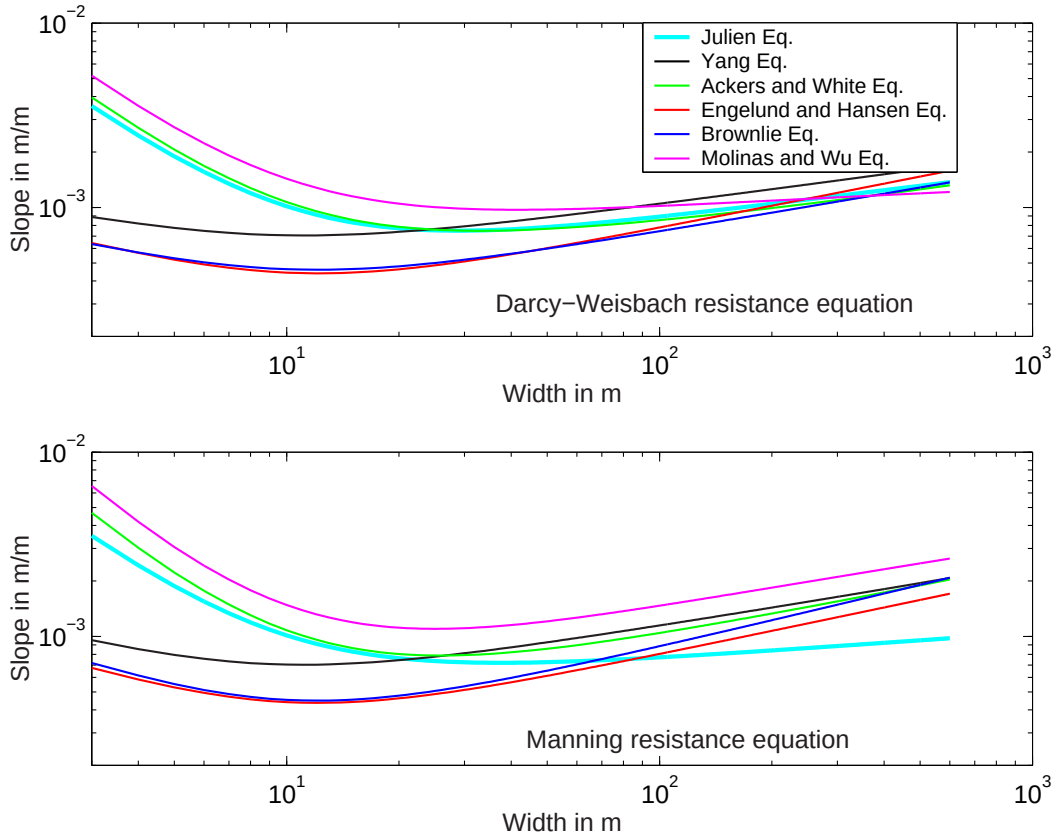

Figure 4.7: Slope versus width relationships developed from six different sediment transport equations and Manning and Darcy-Weisbach flow resistance equations. These curves were generated with the following data: $Q = 139\ m^3/s$, $Q_s = 0.082\ m^3/s$, $d_s = 0.3\ mm$, $n = 0.023$, $f = 0.03$, $G = 2.65$, and $g = 9.81\ m/s^2$.

Even though the slope versus width-depth ratio and slope versus width relationships change with different equations (see Figure 4.5 to 4.8) and different levels of the input variables, there are some common trends in the results of the sensitivity analysis. The exponents p and q never change for any level of water discharge, sediment size and friction factor, when using the Engelund and Hansen equation. For example, the exponents p and q are always equal to 0.22 and 0.40, respectively, for the Engelund and Hansen sediment transport equation and the Darcy-Weisbach re-

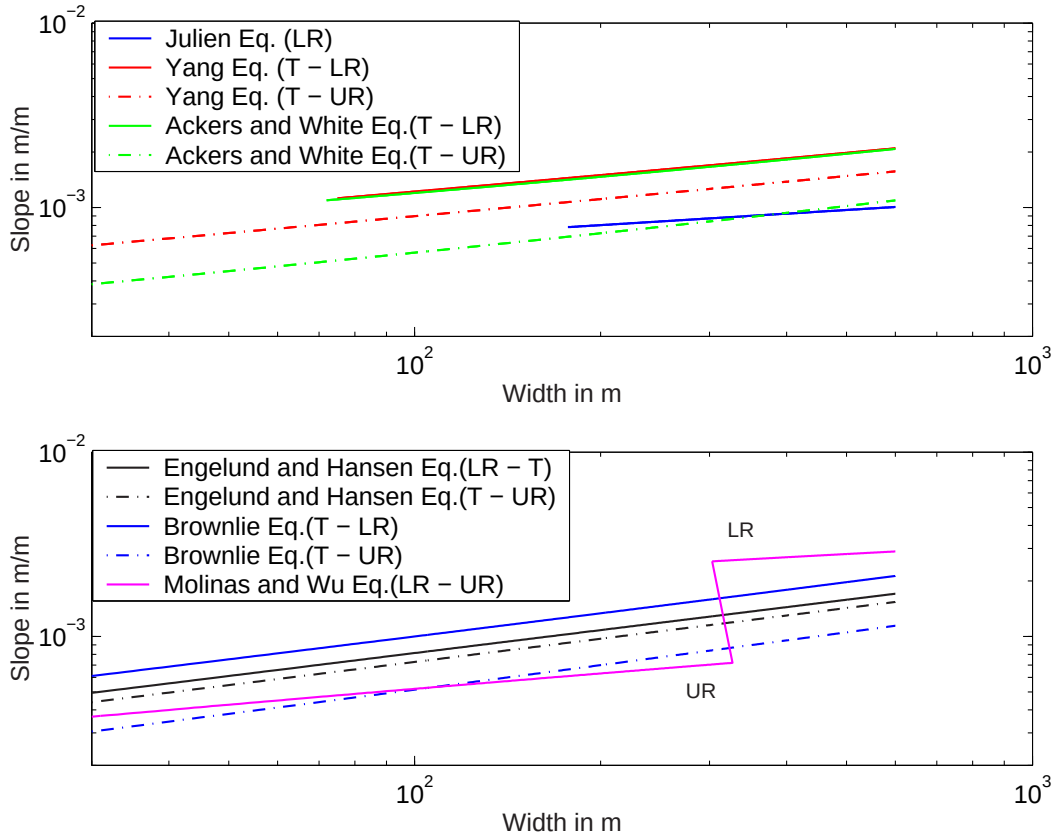

Figure 4.8: Width versus slope relationships developed from six different sediment transport equations and Brownlie flow resistance equation. These curves were generated with the following data: $Q = 139\ m^3/s$, $Q_s = 0.082\ m^3/s$, $d_s = 0.3\ mm$, $n = 0.023$, $f = 0.03$, $G = 2.65$, and $g = 9.81\ m/s^2$. T = Transition; LR = Lower regime; UR = Upper regime.

sistance equation. Similarly, p and q are always equal to 0.24 and 0.42 respectively, when using the Manning resistance equation. It can be noticed from these results that p and q are almost the same in both cases.

In general, the exponents p and q are more sensitive to the combined changes in water and sediment discharge than to the changes in sediment size, and friction factor, when using Yang's and Brownlie's equations.

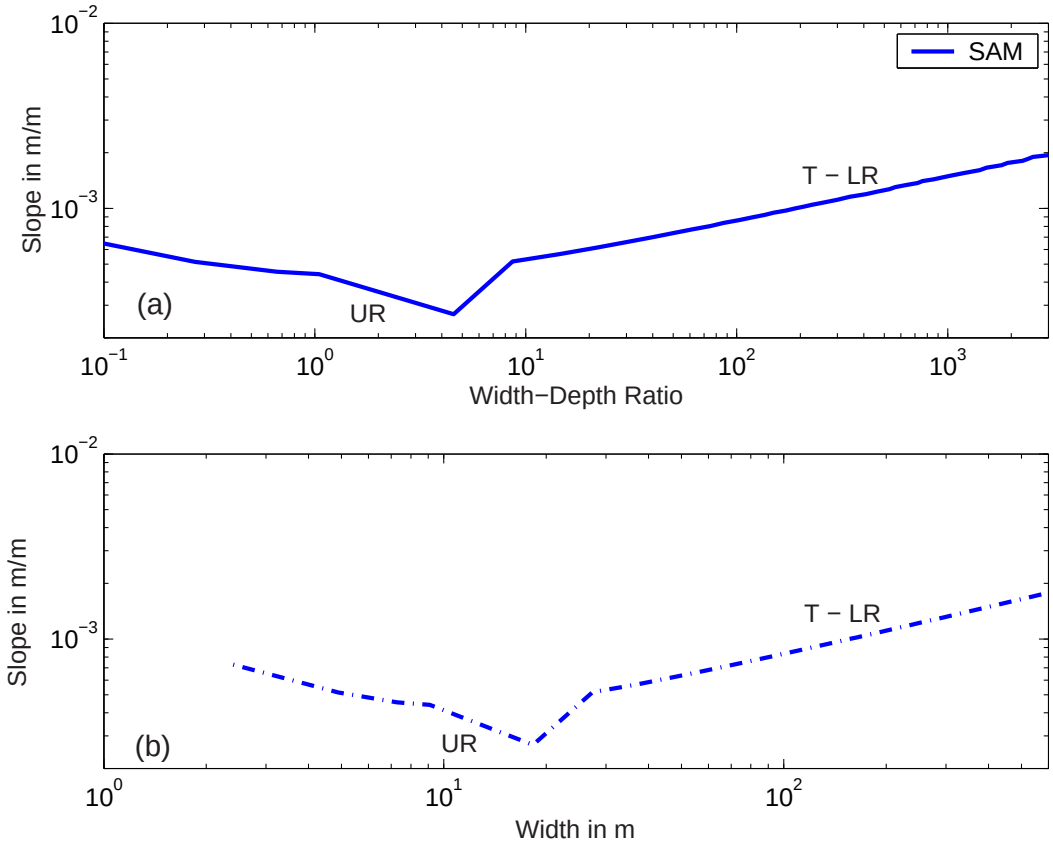

Figure 4.9: Results from SAM hydraulic Design Package for Flood Control Channels. (a) Width-depth versus slope relationship. (b) Width versus slope relationship. These curves were generated with the following data: $Q = 139\ m^3/s$, $Q_s = 0.082\ m^3/s$, $d_s = 0.3\ mm$ and $n = 0.023$.

The outcomes of the model developed with Ackers and White's equation are more sensitive to the perturbations of the input variables than the outcomes produced with any other transport equations.

Another interesting result is that none of the response variables change for the different levels of friction factor n, when using the Molinas and Wu sediment transport equation.

For all the different input conditions and all the sediment transport equations,

the exponents p range from 0.09 to 0.29 when using the Manning resistance equation and from 0.02 to 0.22 when using the Darcy-Weisbach equation. Similarly, q ranges from 0.14 to 0.56, when using the Manning equation and from 0.05 to 0.40, when using the Darcy-Weisbach resistance equation.

4.2 Transient Solution with Constant Discharge

In the previous section analytical solutions were developed between the equilibrium slope and the width-depth ratio for steady state input variables. The transient solution of the channel slope changes from the initial condition to the equilibrium condition in a channel like the one depicted in Figure 4.1, which can be simulated with a numerical model. This section summarizes the characteristics of the numerical model used and the results of the simulations.

4.2.1 Model Overview

A one-dimensional numerical model was developed to compute bed aggradation and degradation processes driven by constant water discharge (Q). This model provides the changes in bed slope of a sequence of channel reaches with different widths (see Figure 4.1) under constant discharge. The model consists of fully uncoupled hydraulic and sediment components solved by an explicit finite difference scheme, forward in time and backward in space (FTBS) (Hoffmann and Chiang, 2000).

The backwater profile for one-dimensional steady gradually varied flow was calculated with the following equation of motion (Chow, 1959; Henderson, 1966):

$$\frac{dh}{dx} = \frac{S_o - S_f}{1 - F_r^2} \tag{4.18}$$

where S_o is the bed slope, S_f is the friction slope, F_r is the Froude number, h is the flow depth and x is the distance along the channel.

Changes in channel bed elevation were computed with the equation of conservation of sediment without sediment source (Vanoni, 1977; Julien, 1995) given by:

$$\frac{\partial A_b}{\partial t} + \frac{T_e}{(1-p_o)}\frac{\partial Q_s}{\partial x} = 0 \tag{4.19}$$

Where A_b is the area of the bed layer, p_o is the porosity of the sediment, Q_s is the sediment discharge and T_e is the trap efficiency, defined as $T_e = 1 - e^{x\omega/hV}$. Where, ω is the sediment fall velocity, h is the flow depth, V is the flow velocity and x is the distance along the channel. The first term in equation 4.19 expresses the rate of deposition and/or erosion in the bed and the second term provides the change in sediment discharge along the channel. Because the width of the channel changes with distance x, equation 4.19 was expressed as:

$$\frac{\partial Z_b}{\partial t} + \frac{T_e}{W(1-p_o)}\frac{\partial Q_s}{\partial x} = 0 \tag{4.20}$$

where Z_b is the elevation of the bed and W is the width of the channel.

Julien's (2002) simplified sediment transport equation was used to compute the sediment discharge along the channel. Appendix G contains the flow chart, the Matlab computer code of the model and typical input and output files. A more detailed description of the model follows in the next section.

Backwater Profile

The model was developed for subcritical flow. Therefore, the flow is controlled at the downstream end of the channel. The downstream flow depth must be provided to start the computation of the backwater profile. The program computes the normal depth at the first downstream node to start the backwater computation. It is assum that a normal flow develops in the reach downstream from the study reach. If an adverse slope develops in the first downstream node, the model will stop. The normal depth does not exist on adverse slopes.

The standard step method (Chow, 1959; Henderson, 1966) is used to integrate equation 4.18. This method consists of computing the flow depth at a specified

distance Δx along the channel. For a given discharge, the flow depth at the downstream node is known (h_1). Then a trial value of the unknown depth upstream from the first node is chosen(h_*), and the total energy ($H_{*1} = z + v^2/2g + h_*$) is computed based on this value. Manning's resistance equation is used to compute the friction slopes (S_{f1} and S_{f*}) at each node and from the mean value ($\overline{S_f}$) a second value of the total energy (H_{*2}) at the second node is calculated. If the difference of H_{*1} and H_{*2} is less than or equal to a specified error (error = 0.001), the trial flow depth is the solution. Otherwise a new trial flow depth will be computed, as the previous trial depth plus an increment. Henderson's (1966) method is used to compute the increment in flow depth for the new trial value. The increment in flow depth (Δh_2) is computed with the following equation:

$$\Delta h_2 = \frac{H_E}{1 - Fr_2^2 + \frac{3S_{f2}\Delta x}{2R_2}} \tag{4.21}$$

where H_E is the change in total energy ($H_{*2} - H_{*1}$), and Fr_2 is the Froude number at node 2.

Once a solution has been found, the program checks that the flow depth is greater than the critical flow. Otherwise, the model sets the solution equal to the critical flow. In addition, if there is a contraction in the channel, the model checks that the flow has enough energy to pass the constriction. If the flow is choked, the water upstream from the constriction has to back up. Therefore, a new flow depth upstream of the constriction is computed based on the minimum energy at the constriction.

This program computes the backwater profile using an algorithm for gradually varied flow. There are some cases in which rapidly varied flow occurs and some of the characteristics are approximated with a gradually varied flow algorithm. For example, when there is a change in channel width, rapidly varied flow occurs and the curvature of the flow is more pronounced than in gradually varied flow. In addition, the friction losses become less important in rapidly varied flow than in the

gradually varied flow. In these cases, it might be difficult to find a solution of the equation of motion. The program keeps track of all the trial values of the flow depth at each station as well as the number of iterations and the computed errors (H_E). If the minimum error (0.001) has not been met after 50 iterations, the program uses the flow depth that produced the minimum error as the solution and continues computing the backwater profile in the next upstream node. The backwater routing was validated with published data in the Open-Channel Flow book by Chaudhry (1993, p.136).

This model works with a constant roughness coefficient. Under this condition, it is better to assume a constant Manning roughness coefficient (n) than a constant Darcy-Weisbach roughness coefficient (f). The comparison of both equations shows that $\sqrt{\frac{8g}{f}} = \frac{R_h^{1/6}}{n}$. Therefore, even though n is constant, the factor that accounts for roughness in Manning resistance equation changes with changes in hydraulic radius R_h. In addition, the Manning roughness coefficient (n) has been used as a calibration parameter in sediment transport models in the middle Rio Grande (Drew Baird, USBR, Albuquerque, NM, 2002 pers. comm.). The results of the roughness coefficient from the calibration(n) are used as a reference value in this dissertation (see Chapter 6).

Hydraulic geometry characteristics of the channel can be computed for trapezoidal or rectangular cross sections. The side slope (z) has to be specified in either case. If z is zero, the cross section is rectangular. The component of the program that computes the backwater profile works for rectangular and/or trapezoidal cross sections. However, the component that computes the changes in bed elevation only works for rectangular cross sections.

Aggradation/Degradation

The results of the backwater profile are input into the sub-routing that computes aggradation/degradation along the channel. The equation of conservation of sed-

iment (equation 4.20) was discretized as: $Z_{j+1}^{t+1} = Z_{j+1}^{t} - \frac{T_e}{(1-p_o)} \frac{(Q_{sj+1}^{t} - Q_{sj}^{t})\Delta t}{W_{j+1}\Delta x}$. The super-index t refers to time and the sub-index j refers to space. The sub-index j increases in the downstream direction. The median grain size (d_{50}) is used to compute the sediment load. The sediment size (d_{50}) and the friction factor (n) do not change along the channel.

It is assumed that the bed elevation at the first upstream node does not change with time, meaning that the channel is able to transport the sediment coming into the reach. Due to the numerical scheme used (backward in space), the change in elevation computed between the first upstream node (j) and the adjacent node downstream from it ($j+1$) will be assigned to the node $j+1$. Therefore, the upstream elevation has to be specified. The bed slope at each node is computed with the elevation of subsequent nodes. The slope at node j is the slope computed with the elevations of nodes j (upstream) and $j+1$ (downstream). The slope of the first downstream node is assumed equal to the slope of the node upstream from it.

The scheme of discretization of the equation of conservation of sediment that produces more stable results depends on the type of sediment transport equation (Julien, 2002). In addition, the stability of the model also depends on the time step (Δt) and space intervals (Δx) specified. The stability of the model is checked at each node with the Courant-Friedrich-Levy condition. The Courant-Friedrich-Levy number is $C = \frac{\Delta t}{\Delta x}\frac{5}{3}V$, when using Manning's resistance equation (Julien, 2002). The mean flow velocity is V. If C exceeds 1, the model produces a warning message to indicate that numerical instability is likely to occur.

4.2.2 Model Limitations

Natural processes are complex and not fully understood. Consequently, numerical models are generalizations of the reality and therefore do not account for all the factors that might affect a given process. This section summarizes the limitations of the numerical model:

- Backwater profile and changes in bed elevation are modelled as one dimensional processes. Therefore, three dimensional flows, that occur in braided channels, cannot be simulated with this model.

- The model does not account for changes in channel width with time. The changes in channel width will depend, among other factors, on the resistance of the banks to erosion. Some reaches of the middle Rio Grande (e.g. Bosque del Apache Reach) have not changed significantly their widths since about 1985, likely due to the vegetation on the banks and the almost constant water and sediment regimes (see Figures 3.2 and 3.5).

- The model does not account for point sources of sediment, such as tributaries.

- The model does not account for coarsening or fining of the bed material with erosion or deposition of sediment in the channel bed.

- The model does not account for infiltration and/or exfiltration along the channel.

- The model does not account for changes in roughness with discharge due to bedforms.

4.2.3 Simulation with Constant Discharge

A sequence of two channel reaches with different widths similar to Figure 4.1 was modelled. The total length of the channel was 32 kilometers. The following data were input into the model: upstream and downstream channel widths: $W_1 = 100$ m and $W_2 = 200$ m, respectively, initial channel slope $S = 0.0008$ m/m, constant water discharge: $Q = 139$ m^3/s, Manning friction factor: $n = 0.023$ and sediment size: $d_s = 0.3$ mm. The space interval was $\Delta x = 200$ m and the time step $\Delta t = 0.2$ day. The channel width changes from 100 m to 200 m over a distance of 200 m. The lengths of the subreaches are $L_1 = 12.2$ km and $L_2 = 19.6$ km for subreaches 1 and

2, respectively. These channel geometry, sediment and roughness characteristics are typical values for the middle Rio Grande downstream from the San Acacia gage.

The normal flow depth downstream was used as a boundary condition. In addition, the elevation of the first upstream nodes was fixed. The model was run until the sediment transport rate was equal in the upstream and downstream reaches. It took a long time (about 18 model-years) to reach this condition. Figure 4.10 shows the results of the hydraulic component of the model. Figure 4.11 shows the results of the sediment component of the model. The slope of the wide reach ($W_2 = 200\ m$) steepened and the slope of the narrow reach ($W_1 = 100\ m$) flattened until continuity of sediment was achieved (see Figure 4.11(b)). In consequence, the velocity of the wide reach increases with time. However, it remained less than the velocity of the narrow reach.

Sensitivity analysis of the model to the time to reach equilibrium indicates that for a reduction of about 50% of dx and dt, the time to reach equilibrium decreases about 6%. In addition, the time to reach equilibrium decreases with decrease in reach length, increase in roughness coefficient (n) and increase in water discharge. The decrease in sediment size from 1.00 mm to 0.5 mm also decreased the time to reach equilibrium, even though, the trap efficiency is decreased with the finer sediment size. Appendix F contains the results of the model for different reach lengths, sediment sizes, roughness coefficients and water discharges. The time to reach equilibrium is expected to vary with the square of the reach length (L^2), because this time is a function of the volume of sediment storage in the reach.

The changes in slope with time at the narrow and wide reaches are plotted in Figure 4.12. The increase in the slope in the narrow reach during the first 100 days is due to the water profile upstream (Type M2) from the transition. The channel transition produces a pronounced curvature of the flow in the narrow reach. In consequence, the friction and water surface slopes increase, producing higher transport rates in the narrow reach than in the wide reach, creating a scour hole.

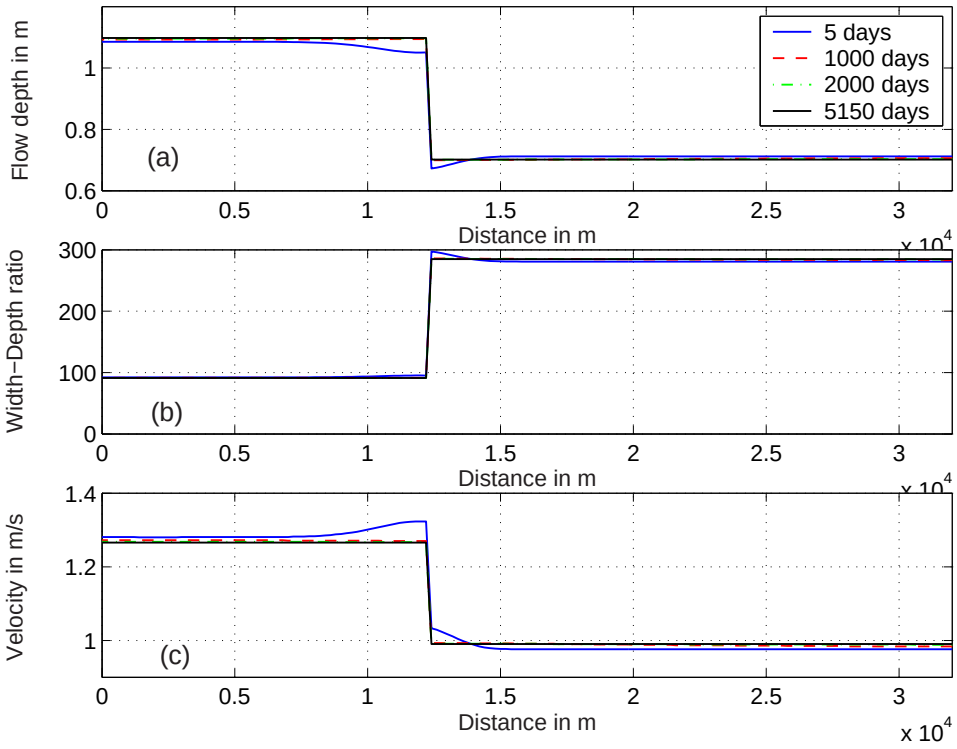

Figure 4.10: Results of the hydraulic component of the numerical model with constant discharge . (a) Flow depth along the channel, (b) Width-depth ratio along the channel,(c)Flow velocity along the channel.

This discontinuity is evident in Figure 4.11(a), where the curve for t = 5 days has a spike. The spike attenuates with time and for this example it took about 100 days. The initial spike was $30,000\ m^3/s$. If the transition is longer, the initial spike decreases. For example, for a transition of 400 m, the spike is about $20,000\ m^3/s$ and attenuates during the first 50 days. However, in either case the time of attenuation of the spike is very small compared to the time to reach sediment transport equilibrium. Therefore, the time to equilibrium is not significantly affected by the length of the transition and the final results are not different. It is worthwhile noticing that the definition of the curves in Figure 4.12 depends on the nodes selected to compute the reach-averaged slopes. The closer the node is to the transition, the steeper will be

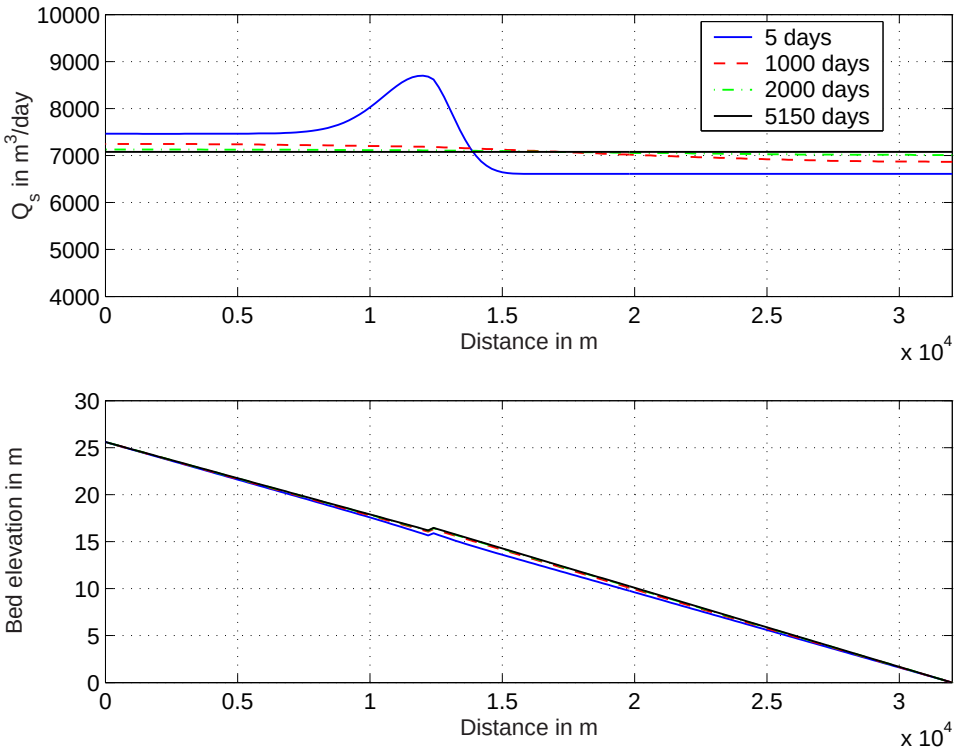

Figure 4.11: Results of the sediment component of the numerical model with constant discharge. Top Figure: Sediment discharge along the channel. Bottom Figure: Bed elevation profile.

the reach-averaged slope of the narrow reach.

An exponential model was fit to the data of Figure 4.12 in order to describe the slope change as function of time. Richard (2001) and Williams and Wolman (1984) performed similar analyses to describe the changes in channel width with time. The detailed procedure and the results are included in Appendix F.

The results of the numerical model are compared with the results of the analytical approach in Figure 4.13. Numbers 1 and 2 identify reach 1 and reach 2, respectively. The ratio of the final bed slopes is $S_r = 1.09$ and the ratio of the width-depth ratios is $\xi_r = 3.13$. Then, equation 4.6 is satisfied.

Figure 4.14 represents a scheme of the slope versus width-depth ratio relation-

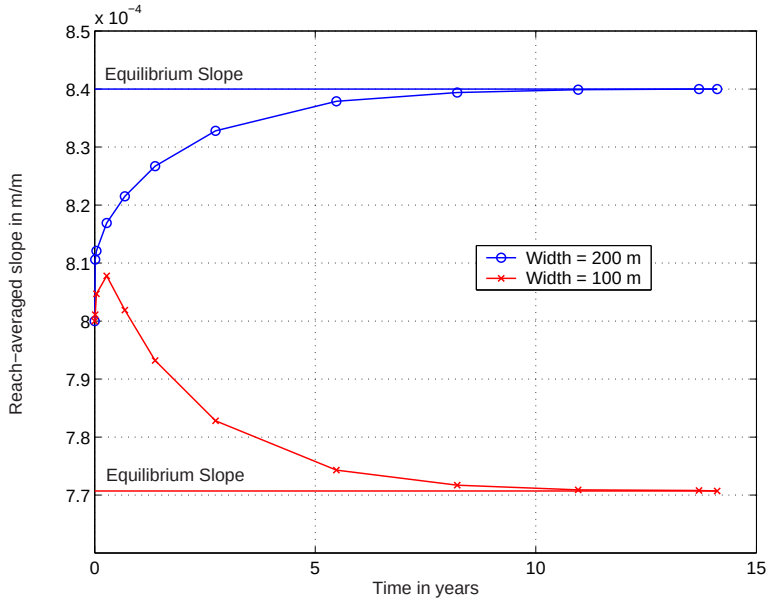

Figure 4.12: Change in reach-averaged slope with time in reach 1 ($W_1 = 100\ m$) and reach 2 ($W_2 = 200\ m$).

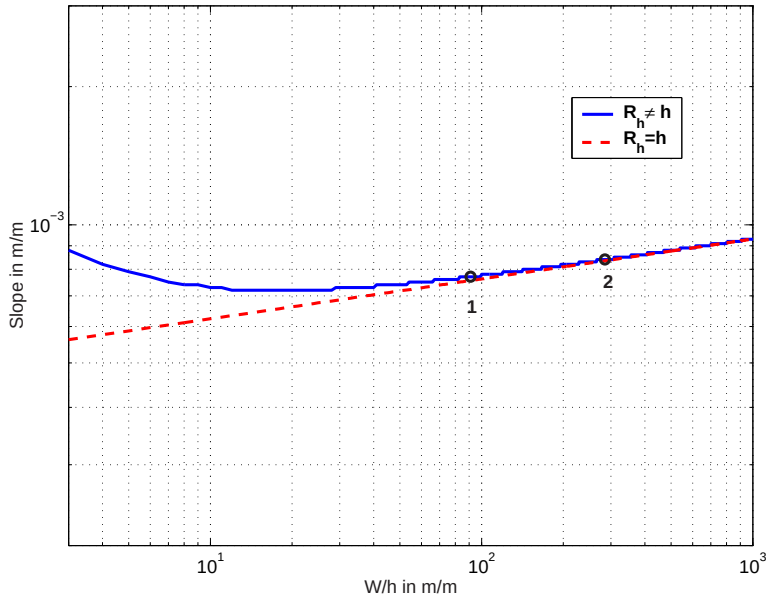

Figure 4.13: Comparison of the results of the analytical and numerical approaches. Number 1 represents reach 1 and number 2 represents reach 2.

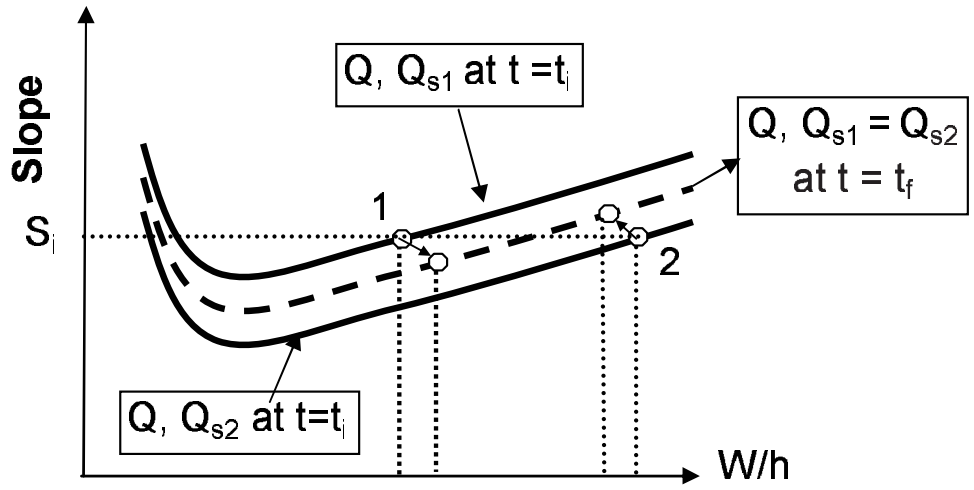

Figure 4.14: Scheme of the change in slope versus width-depth ratio relationship between reach 1 and 2. Solid lines represents the initial conditions. Dashed line represents the final relationship for both reaches. Q_{s1} and Q_{s2} are the sediment loads at reach 1 and 2, respectively. The white dots represents the initial and final conditions of each reach.

ships of the two reaches and how this relationship changes with time. At the initial time (t_i), both reaches have the same slope, and they transport the same water discharge but different sediment loads. Therefore, the slope and width-depth ratio for each reach plots in different curves (solid lines). As the time passes, the narrow reach develops a flatter slope and the wide reach develops a steeper slope. In consequence, the narrow reach decreases the sediment load and the wide reach increases it. The characteristics of the two reaches (width-depth ratio and slope) plot in the same curve (dashed line), when both reaches transport the same sediment load at time ($t = t_f$). The arrows indicate the change in conditions at each reach with time.

4.3 Validation of the Steady State Analytical Solution

Laboratory flume data of Bigillon (1997) were used to validate the analytical solution developed in section 4.1.1 of this Chapter. Bigillon (1997) conducted 20 flume runs involving five different flume slopes, two water discharges and ten sediment discharges. Two different types of test were performed. One type of test, in which the sediment injected in the channel was smaller than the sediment discharge, corresponded to the initial experimental conditions, such that erosion of the bed was induced. The other type of test consisted of injecting a sediment discharge higher than the sediment discharge resulted from the initial experimental conditions. In both cases, the experiments were run until equilibrium conditions were reached. Ten of the runs were performed from a narrow (W = 15 cm) to a wide reach (W = 30 cm), and the other ten from a wide (W = 30 cm) to a narrow (W = 15 cm) reach. In both cases, the channel transition had a length of 60 cm.

The widths of the channels and the equilibrium slopes at the end of each run are compared with equation 4.4 in Figure 4.15. The downstream reach is numbered 2 and the upstream reach is numbered 1. The results for both cases (channel widening and narrowing) are summarized in box plots and represented in Figure 4.16. Both cases are compared with the analytical solution.

The laboratory results are in good agreement with equation 4.4, except for two runs for the case of channel widening and three runs for the case of channel narrowing (Figure 4.15). Most of the results indicate that the wide reach develops a steeper slope than the narrow reach (see Figure 4.16. The laboratory flume data show the same trend indicated by the analytical solution.

4.4 Summary

Analytical solutions developed in Section 4.1 indicate that a change in channel width from a narrow to a wide section causes a decrease in slope in the narrow reach and

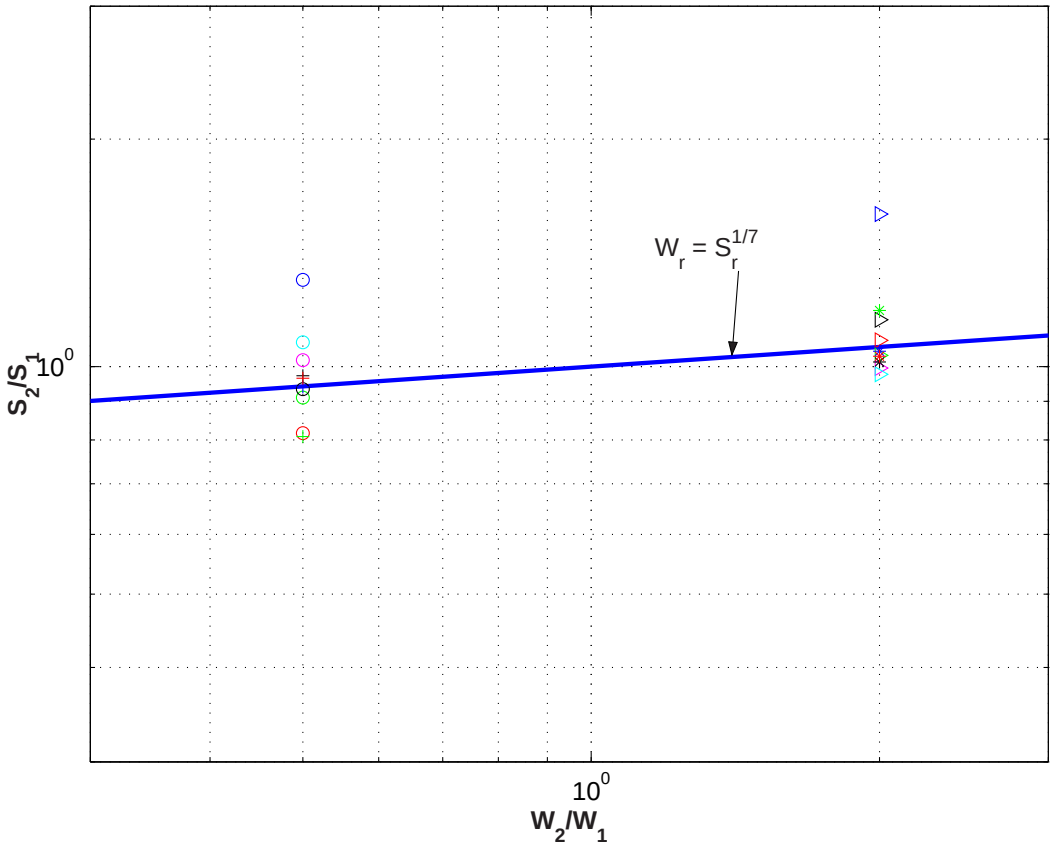

Figure 4.15: Comparison of the slope versus width-depth ratio relationship in equation 4.4 with the laboratory flume data of Bigillon (1997).

an increase in slope in the wide reach. This result is in agreement with laboratory flume data of Bigillon (1997) and the literature of hydraulic geometry equations (see Chapter 2).

Equation 4.9 shows that the change in slope depends more on the sediment concentration by volume (C_v) than on the flow discharge (Q). This result is in agreement with Julien (2002), Huang and Nanson (2000), and Maza-Alvarez and Cruickshank-Villanueva (1973).

Slope versus width-depth and slope versus width relationships depend on the sediment transport and resistance equation used. The exponents p and q of the

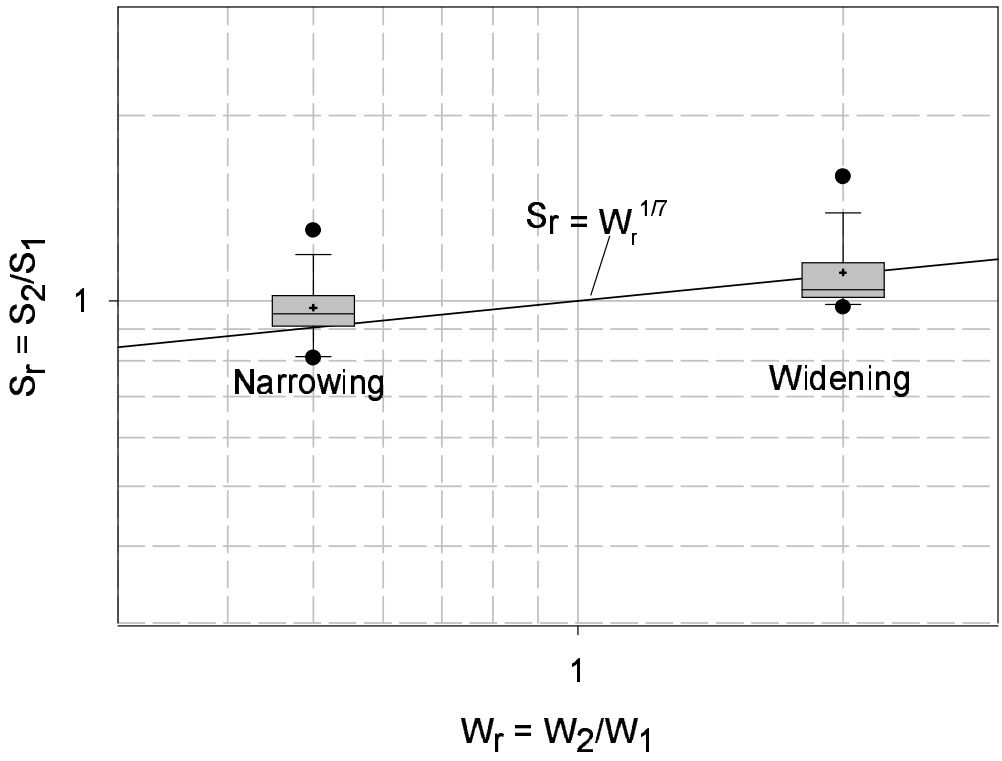

Figure 4.16: Comparison of the width ratio versus slope ratio relationship in equation 4.4 with the box plots for the results of the laboratory flume data of Bigillon (1997).

following relationships $S_r = \left(\frac{W_r}{h_r}\right)^p$, and $S_r = W_r^q$ vary with different equations.

A numerical model was developed to simulate the evolution of the channel bed of a sequence of two channel reaches with different widths under constant water discharge. The results of the numerical model are in agreement with results of the analytical solution. This model can be used to estimate the time to reach equilibrium under constant water discharge.

Chapter 5

Numerical Model with Variable Discharge

It is a common practice in engineering to use a dominant discharge for designing river works. However, the definition of this dominant discharge is not a simple task. Each component of the channel form adjusts at different time scales (Knighton, 1998) over a range of discharges. The objective of this Chapter is to simulate the evolution of the bed elevation under unsteady flows rather than under a constant discharge, then compare the long-term changes in channel slope with the equilibrium slope predicted for constant discharges. In the first part of this chapter a description of the model is presented. Then the results of the model simulations are presented and compared with the simulations of the numerical model with constant discharge.

5.1 Description of the Model

5.1.1 Backwater Computation

The same algorithm developed for the numerical model for constant discharge was used in the numerical model for variable discharge. However, the flow discharge is allowed to change every time step. This algorithm implies that the local acceleration term ($\frac{dV}{dt}$) in the momentum equation is neglected (Chow et al., 1988).

In order to validate this assumption, the terms of the momentum equation were estimated using flow depth and flow velocity data reported at the San Acacia and San Marcial gages during two consecutive days (Table 5.1). The San Acacia gage is located upstream from the San Marcial gage (Figure 3.1). The momentum equation is as follows: $S_f = S_o - \frac{\partial h}{\partial x} - \frac{\partial V^2/2g}{\partial x} - \frac{1}{g}\frac{\partial V}{\partial t}$. (Chow et al., 1988). Where, S_f is the

Station	Dates	Q in m^3/s	Depth (m)	Velocity (m/s)
San Acacia	5/22/01	40	1.1	0.74
San Marcial	5/23/01	98	1.8	1.02

Table 5.1: Flow discharge, depth and velocity at San Acacia and San Marcial gages for May 22 and 23 of 2001.

friction slope, S_o is the bed slope, h is the flow depth, V is the flow velocity, g is the gravitational acceleration, x is the length of the channel, and t is the time.

The flow data of May 22 and 23 of 2001 were used to estimate the terms of the momentum equation. Table 5.1 summarizes these data. The two gage stations are about 76 km apart. The averaged bed slope in this reach is about $S_o = 7\ x\ 10^{-4}$. The change in flow depth Δh between the two stations $\Delta h = 1.8 - 1.1 = 0.7m$. Then, the change in flow depth over the reach is $\frac{\Delta h}{\Delta x} = \frac{0.7\ m}{76{,}000\ m} = 9.21\ x\ 10^{-06}$. The convective acceleration can be evaluated as: $\frac{\Delta V^2}{2g\Delta x} = \frac{(1.02^2 - 0.74^2) m^2/s^2}{2*9.81*76{,}000\ m^2/s^2} = 3.28\ x\ 10^{-07}$. The local acceleration term can be evaluated as: $\frac{\Delta V}{g\Delta t} = \frac{(1.02-0.74) m/s}{9.81\ m/s^2 * 86400 s} = 3.31\ x\ 10^{-07}$.

The local acceleration term is of the order of 10^{-07}, whereas the bed slope (S_o) is of the order of 10^{-04}. Therefore, the local acceleration term was neglected and a non-uniform, steady state model was developed.

Other variables that are allowed to change with time are the water temperature, kinematic viscosity of the flow and fall velocity of the sediment particles. The temperature data are input to the model. Then, the kinematic viscosity and the fall velocity are computed for each time step.

The original steady state model was also modified to account for other factors. For example, contraction and expansion losses were added to the model. The program compares the velocity between two consecutive stations. If the velocity downstream is greater than the velocity upstream a contraction occurs. If the opposite happens an expansion occurs. The coefficient of contraction is $c = 0.1$ and the coefficient of expansion is $c = 0.4$, which are typical coefficients recommended

by the U. S. Army Corps of Engineers (1998).

Minor losses due to expansion and contraction are evaluated in the following manner:

$$h_m = c\left|\frac{V_d^2}{2g} - \frac{V_u^2}{2g}\right|$$

where, V_d and V_u are the downstream and upstream velocities and g is the gravitational acceleration.

The equation of Henderson (Henderson, 1966) for the solution of the energy equation was also changed to account for the expansion and contraction coefficients and is as follows:

$$\Delta h_i = \frac{H_E}{1 - Fr_i^2(1 - 0.5c) + \frac{3S_{fi}\Delta x}{2R_i}}$$

where Δh_i is the increment of flow depth at node i, H_E is the change in total energy $(H_{*i} - H_{*i-1})$, and Fr_i is the Froude number at node i.

5.1.2 Aggradation/Degradation Computations

The aggradation/degradation module of the program was modified to limit the maximum bed degradation, in order to account for the existence of man-made or geologic controls in the bed of the channel. In order to do this, the user has to specify the minimum bed elevation at each node. Then, the initial available sediment volume that can be eroded in the channel is computed as:

$$\begin{aligned} volume_i =& (1 - po)\left(\frac{(elevation_i - minelev_i) + (elevation_{i+1} - minelev_{i+1})}{2}\right) * \\ & * d_x\left(\frac{width_i + width_{i+1}}{2}\right) \end{aligned}$$

where, $elevation_i$ is the bed elevation at node i, $minelev_i$ is the minimum elevation the bed can have at node i, $width_i$ is the width of the channel at node i and po is the porosity of the sediment.

The sediment transport capacity is computed at each node (i). The difference in sediment discharge between two adjacent nodes yields the amount of sediment

that will be aggraded or degraded between them. If there is aggradation, the change in bed elevation is computed as explained in Chapter 4 and the available volume is recomputed as the volume that already exists in the bed plus the volume that will be stored. If there is degradation, there are two options: 1) the amount of sediment to be degraded is greater than the available volume in the bed. In this case, all the sediment is moved downstream and the bed elevation takes the value of the minimum elevation. Or, 2) the amount of sediment to be degraded is less than the available volume in the bed. In this case, the change in bed elevation is computed as explained in Chapter 4 and the available sediment volume left in the bed is recomputed as the available volume that existed in the previous time step minus the volume of sediment moved downstream in the present time step. Appendix G contains the flow chart of the model.

5.2 Long-term Simulations

The numerical model for variable discharge was run for 20 years. The flow discharge data at the San Acacia gage from 1979 to 1999 were routed through the channel. This period was selected because the flow regime did not change during this time span (see Figure 3.2).

The channel characteristics are the same as the characteristics used in the example presented in Chapter 4, Section 4.2.3, where the channel is widened from 100 m to 200 m. The following data were input into the model: initial channel slope $S = 0.0008$, Manning friction factor: $n = 0.023$ and sediment size: $d_s = 0.3\ mm$. The space interval was $\Delta x = 200\ m$ and the time step $\Delta t = 0.2\ day$. The channel width changes from 100 m to 200 m over a distance of 200 m. The lengths of the subreaches are $L_1 = 12.2\ km$ and $L_2 = 19.6\ km$ for subreaches 1 and 2, respectively.

Figure 5.1 (a) contains the hydrograph input to the model, and Figure 5.1 (b) presents the change in reach-averaged slope with time. The values of the reach-averaged slope depend on the nodes used to compute them. Then, rather than a

unique curve a family of curves is more representative of the averaged value. Figure 5.1 (b) shows the reach-averaged slope computed with five different sets of nodes.

The slope of the wide reach increases, whereas the slope of the narrow reach decreases. The slope changes rapidly during high peak flows and stays almost constant during low flows. This result is in agreement with the results of the steady state model for different flow discharges (see Appendix F), where the rate of change in slope with time is faster with steady state high flows than with steady state low flows. The increase in sediment discharge also increases the sediment concentration. Therefore, the channel slope changes rapidly during high flows. Another interesting result is that the larger the discharge, the larger the equilibrium slopes.

Appendix D contains the analysis performed to explore the effect of the sediment concentration on the time to equilibrium with variable discharge.

Figures 5.2 to 5.4 compare the results of the numerical model with variable discharge with the results of the numerical model with constant discharge for three different discharges: the dominant discharge ($Q = 139\ m^3/s$) (see Chapter 3), discharge equalled or exceeded 10 percent of the time ($Q_{10} = 97\ m^3/s$) (see Appendix E) during the period 1979-1999 and mean annual discharge ($Q = 35\ m^3/s$) during the same time period. The dominant discharge was estimated as the average of the peak daily flows of the five previous years to 1999 (Richard, 2001).

5.3 Summary

Numerical simulations with variable discharge of a sequence of two channel reaches with different widths and constant initial channel slope indicate that the slope of the wide reach increases, whereas the slope of the narrow reach decreases. The rate of change of slope with time is faster at high flows and is almost zero at low flows.

The long-term changes in channel slope with time due to variable water discharges are better approximated by the numerical simulation with a constant discharge close to the mean annual flow than with the flood discharges (e.g., discharge

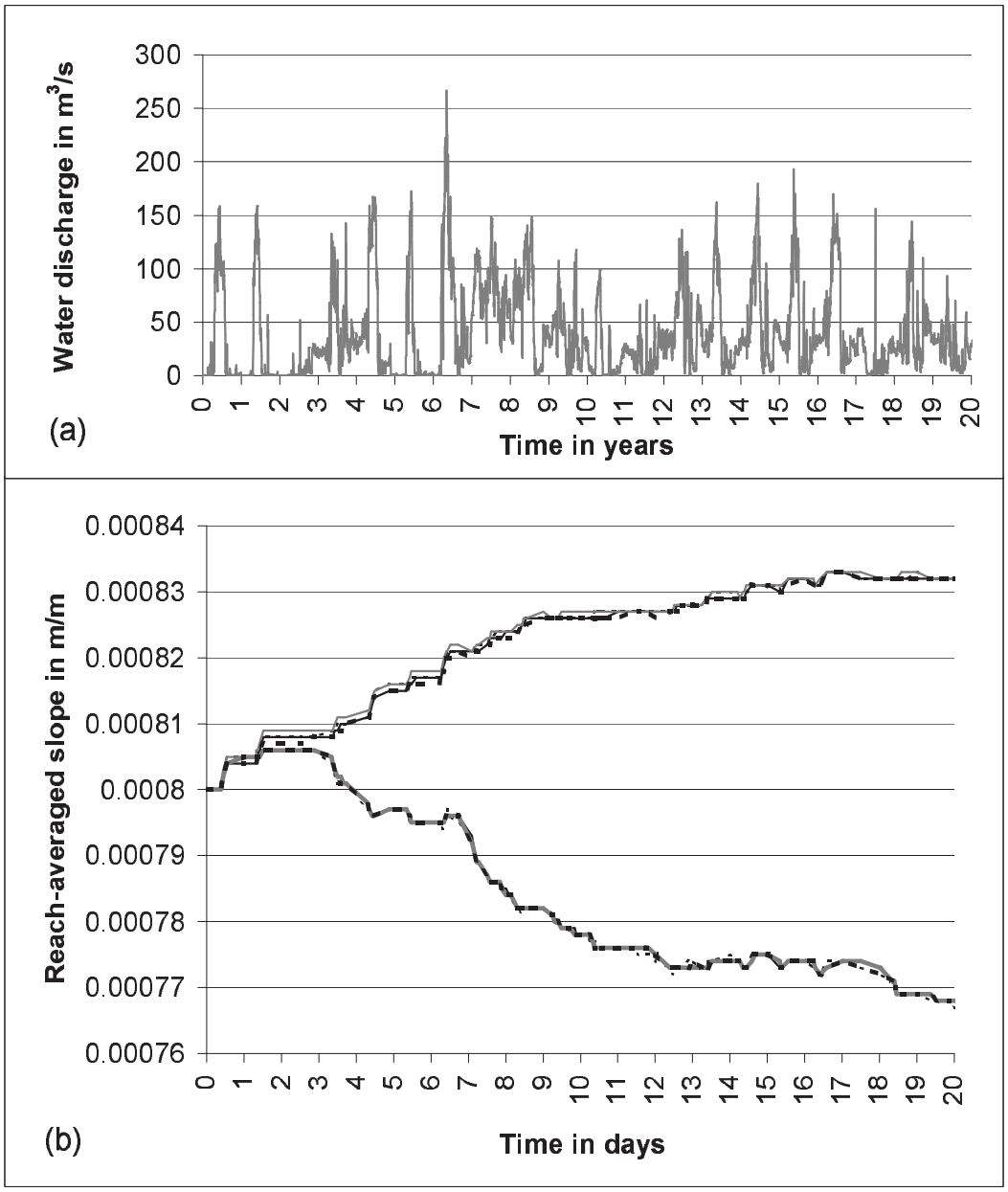

Figure 5.1: Results of the numerical model with variable discharge. (a) Input hydrograph from the San Acacia gage from 1979 to 1999, (b) Change in reach-averaged slope with time.

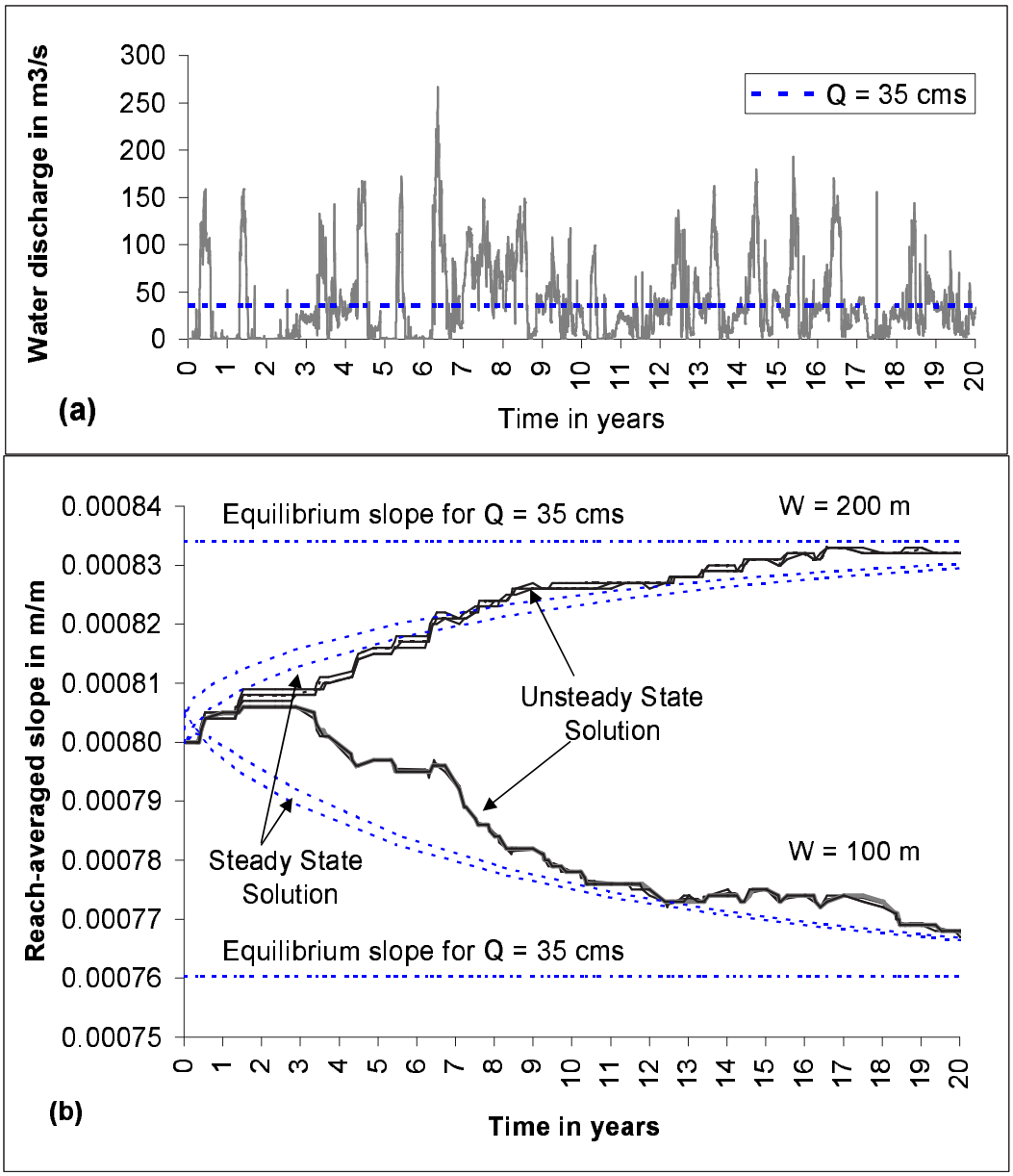

Figure 5.2: Results of the numerical model with variable and constant discharges. (a) Input hydrograph from the San Acacia gage from 1979 to 1999, (b) Change in reach-averaged slope with time from the numerical model with variable discharge and from the numerical model with a constant discharge equal to the mean annual flow of $Q = 35\ m^3/s$.

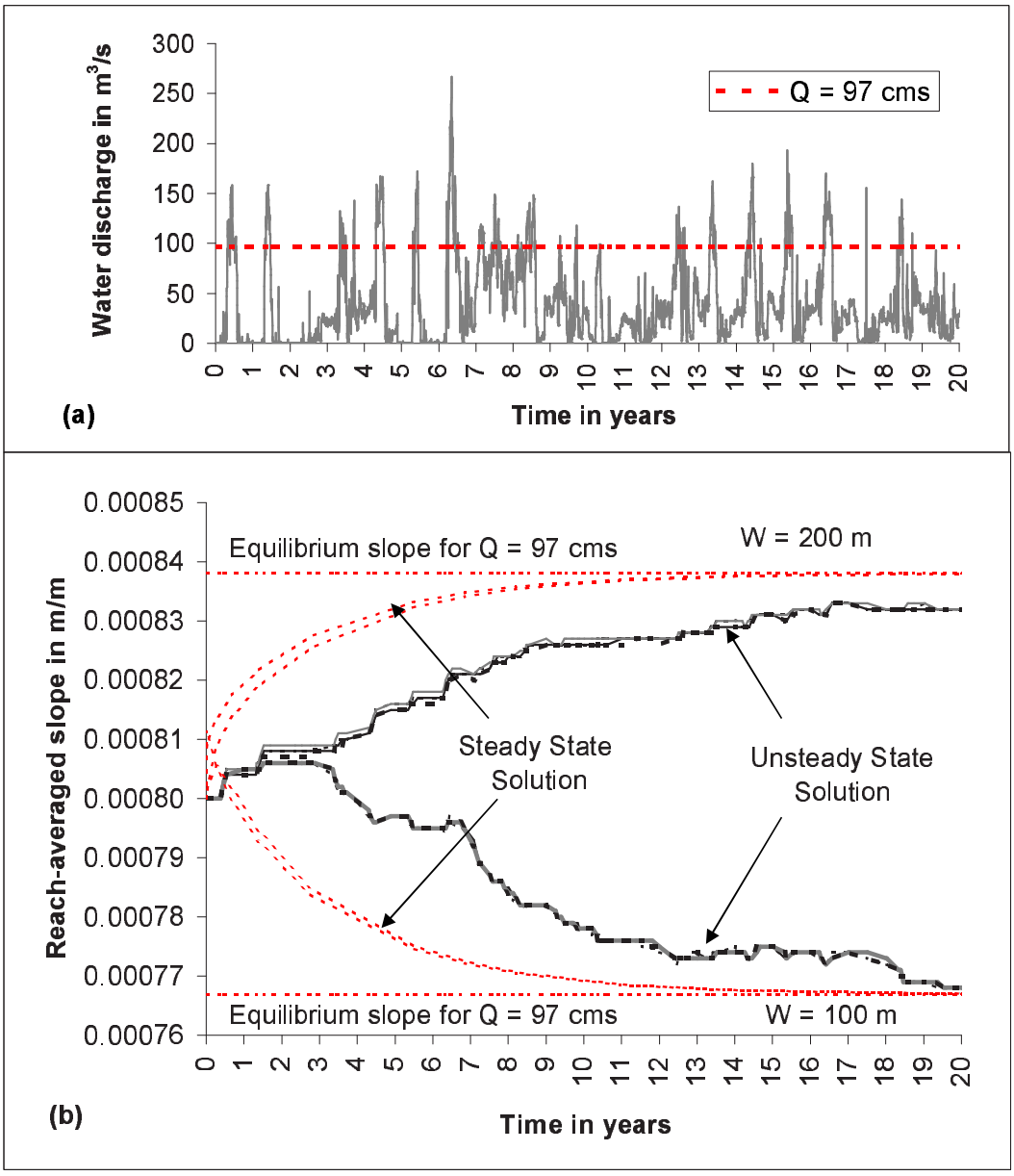

Figure 5.3: Results of the numerical model with variable and constant discharges. (a) Input hydrograph from the San Acacia gage from 1979 to 1999, (b) Change in reach-averaged slope with time from the numerical model with variable discharge and from the numerical model with a constant flow equal to the discharge equal of exceeded 10% of the time ($Q = 97\ m^3/s$).

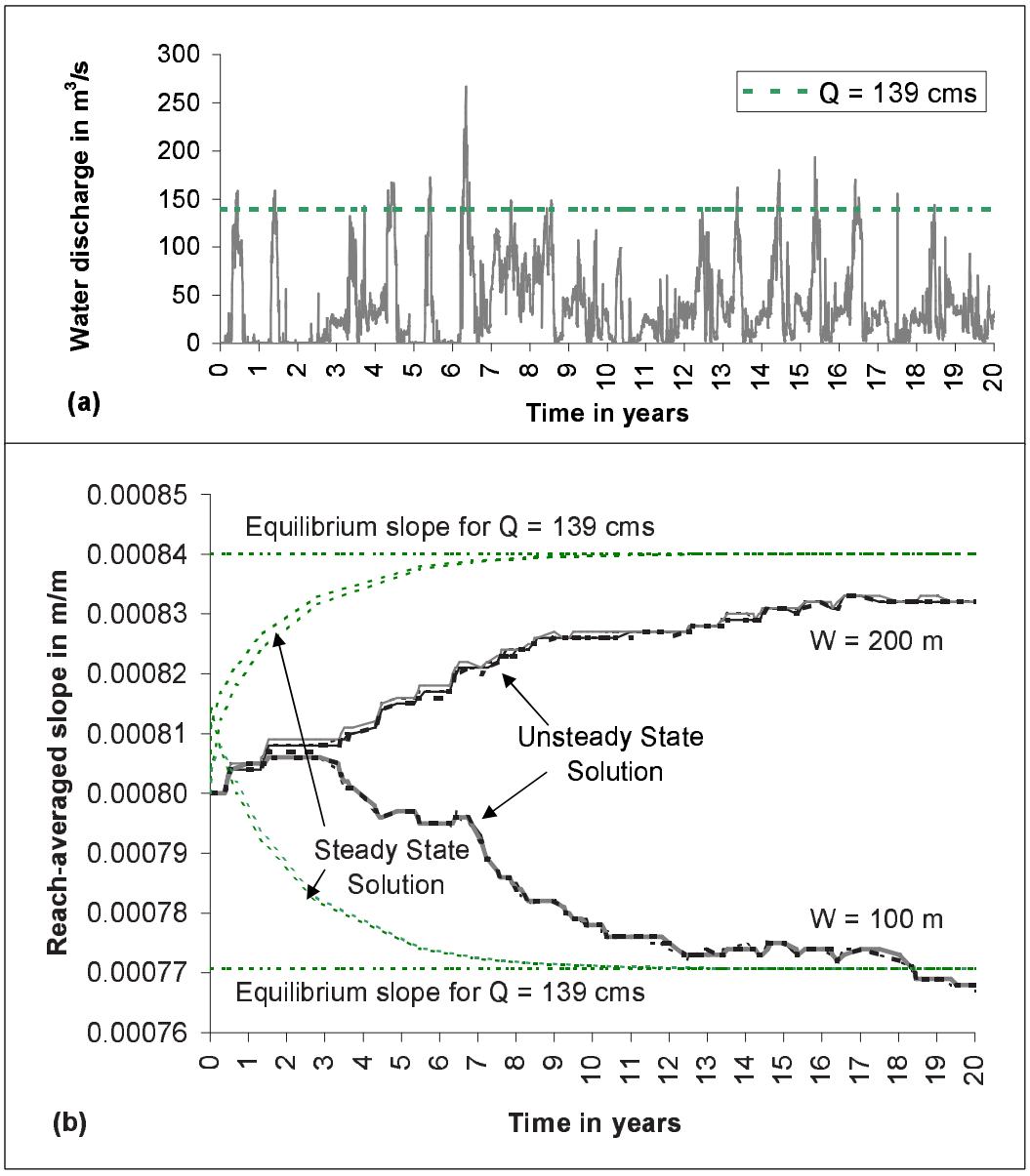

Figure 5.4: Results of the numerical model with variable and constant discharges. (a) Input hydrograph from the San Acacia gage from 1979 to 1999, (b) Change in reach-averaged slope with time from the numerical model with variable discharge and from the numerical model with a discharge equal to the dominant discharge ($Q = 139\ m^3/s$).

equalled or exceeded 10 % of the time, dominant discharge).

The rate of change of slope with time decreases after about 10 years. The sequence of high flow peaks between the year 12 and 19 did not change the channel slope as much as the sequence of peaks from year 1 to 9. This indicates that the channel slope is approaching an equilibrium slope asymptotically.

Chapter 6

Field Application to the Middle Rio Grande

Wide braided reaches and alternating narrow straight channels are common in some stretches of the middle Rio Grande. The numerical model for variable discharges was used to simulate the slope adjustment of a river stretch characterized by reaches of different widths. The study reach is located in the southern end of the middle Rio Grande, which includes the Bosque del Apache National Wildlife Refuge (see Figures 6.1 and 6.3). The following section describes the characteristics of the study reach. The data input into the model are summarized in Section 6.2. Section 6.3 presents the model results and Section 6.6 presents the applications of the results to river restoration.

6.1 Description of the Study Reach

The study reach starts about 47 kilometers downstream from the San Acacia diversion dam (Figure 6.1). This reach comprises the Bosque del Apache Reach National Wildlife Refuge and consists of three subreaches; one wide section located between two narrow, straight reaches.

This reach was selected because its width has remained almost constant since about 1985. In addition, it has not migrated across the floodplain. Digitized aerial photos of the active channel or non-vegetated channel show that this reach narrowed from 1918 to 1972 (Figure 6.2). Channel cuts took place in this reach between 1949 and 1972 (U. S. Bureau of Reclamation, 2000). Much of this narrowing is due to human intervention (U. S. Bureau of Reclamation, 2000). The wide reach

Figure 6.1: Approximate location of the Bosque del Apache reach in the middle Rio Grande. Map not to scale.

observed in the planform plots after 1972 is the result of clearing the vegetation on the banks. The width of the channel corresponds to the channel clearing width (Drew Baird, USBR, Albuquerque, NM, 2002 pers. comm.). This wide reach has remained the same since then (Figure 6.3). The banks have not widened as a result of the vegetation that was not cleared (Drew Baird, USBR, Albuquerque, NM, 2002 pers. comm.). In addition, the cohesive banks of the downstream narrow reach have remained fairly stable (Figure 6.3).

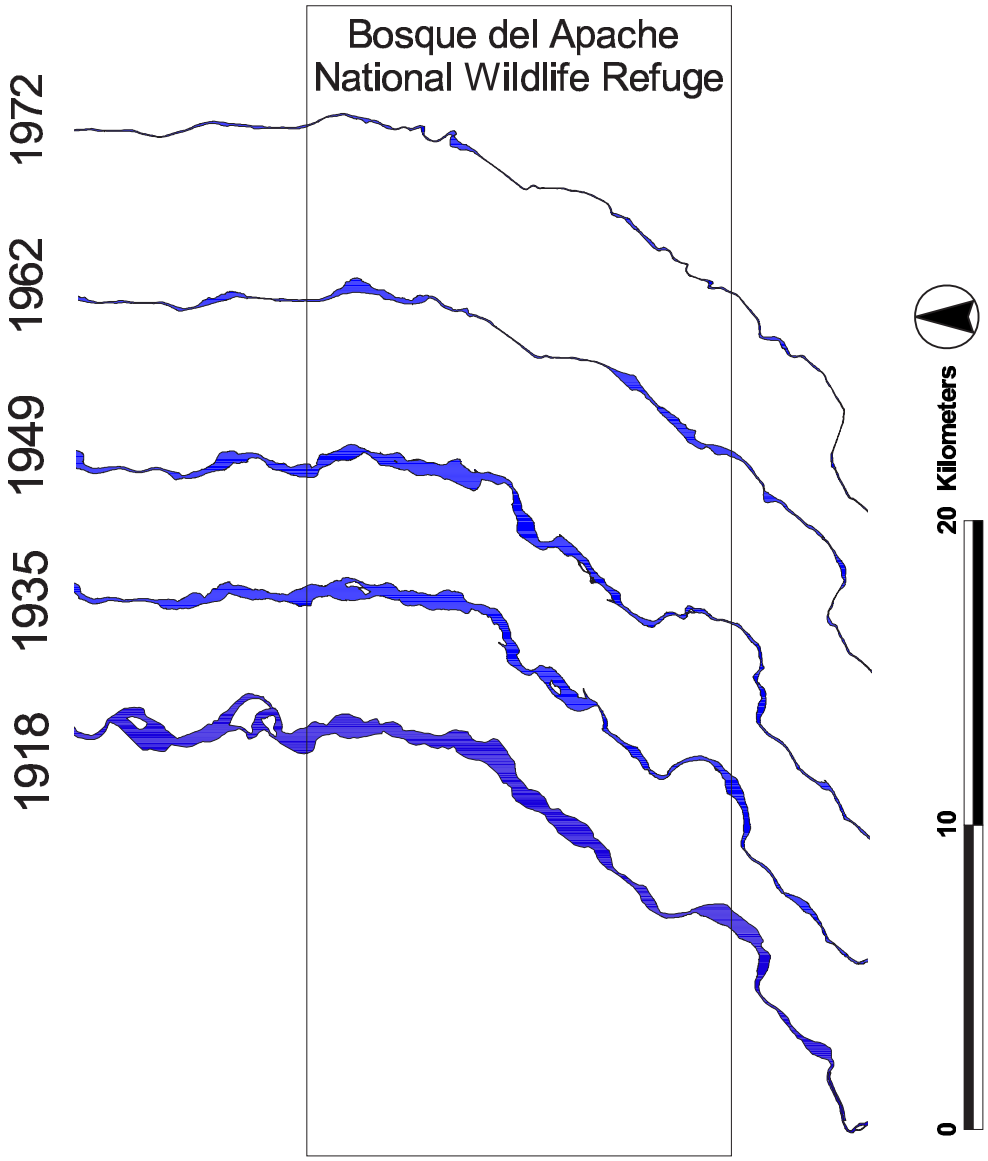

Figure 6.2: Non-vegetated channel from 1918 to 1972.

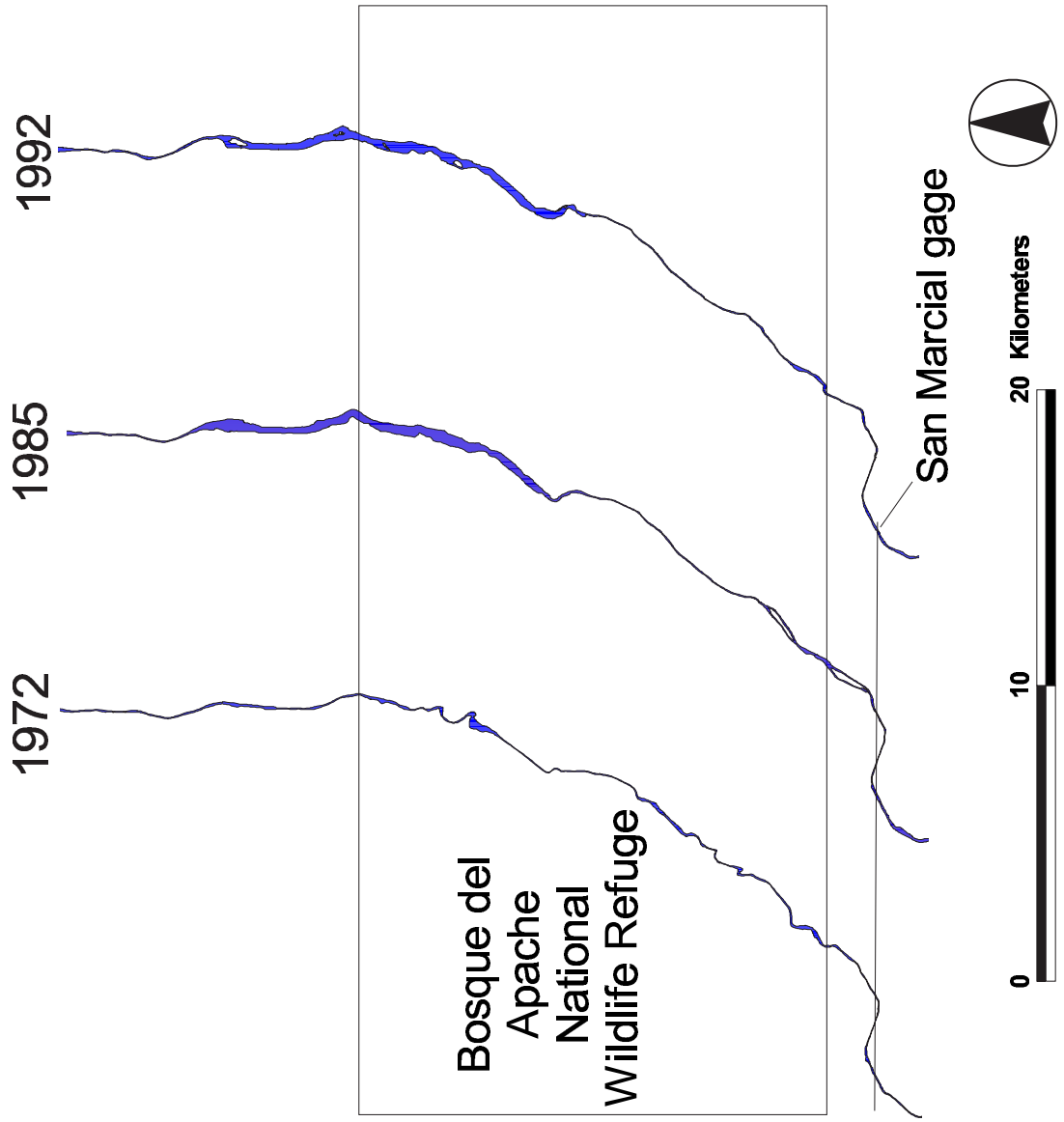

Figure 6.3: Non-vegetated channel from 1972 to 1992.

6.1.1 Cross Section Surveys

Field surveyed cross section data along the study reach (Socorro-lines or SO-lines) have been collected since 1987. Figure 6.4 shows three typical cross sections at each of the subreaches.

Figures 6.5 and 6.6 contain the thalweg profiles for February 1992 and July to September of 1999, respectively. Linear regressions were fit to the available data, with one regression per subreach. The slopes of the regression lines were estimated for each subreach and are indicated in Figures 6.5 and 6.6. These slopes show that the wide reach is steeper than the two narrow reaches for both surveys. Similar results are obtained from the cross section data collected in 1993, 1997 and 1998 (see Appendix I).

6.1.2 Active Channel Width

The active channel width corresponds to the non-vegetated channel delineated by the GIS and Remote Sensing Group of the USBR, Denver, CO, from aerial photos and topographic maps. The active channel width definition is based on the idea that high flows for the five or so years prior to the survey will clear away the newly established vegetation (Richard, 2001). The non-vegetated channel width was measured at each cross section (SO-line) along the reach. These measurements were performed with ArcView by clipping the cross section line coverage with the active channel polygon coverage. Figure 6.7 shows the active channel width at the SO cross sections in 1985 and 1992. The non-vegetated channel width has not changed significantly during this period, except for two short stretches in the upstream and downstream narrow sections. The narrow reach downstream from Bosque del Apache (Figures 6.2 and 6.3) is completely a man-made channel (Mussetter Engineering, 2002). Aerial photos of the study reach taken in the winter of 2000 show that the channel width has not changed from 1992 to 2000. Figures 6.8 and 6.9 show the digitized non-vegetated planform in 1992 and the 2000 aerial photo of the upstream section (narrow) and a

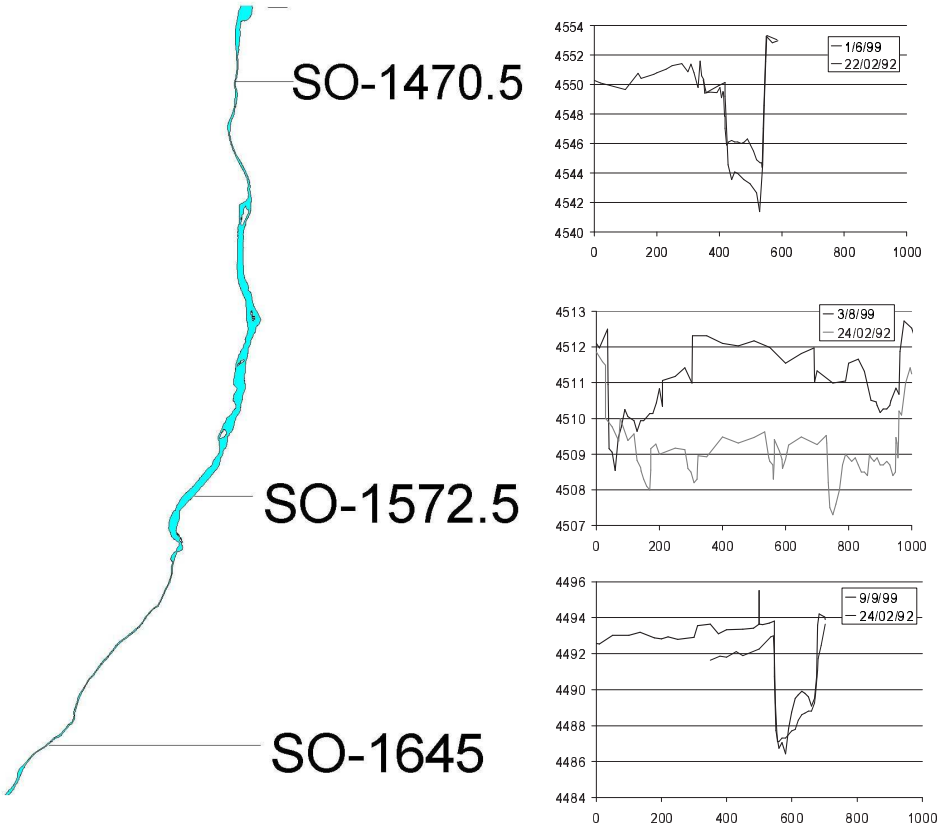

Figure 6.4: Typical cross sections in the study reach.

section of the middle reach, respectively. The location of the reach in Figure 6.8 is between the letters A and B in the 1992 longitudinal profile (Figure 6.5). Similarly, the location of the wide channel section in Figure 6.9 is between letters B and C in the same profile.

6.1.3 Width-Depth Ratios

The width-depth ratios were computed from the cross section surveys, which include water surface elevations. The surveys were collected when the flow discharges were between 9 and 32 m^3/s in 1999. The mean annual flow is 39 m^3/s at the San Acacia gage between 1992 and 1999. Therefore, all the measurements were performed during flows less than or close to the mean annual flow. Unfortunately, there are

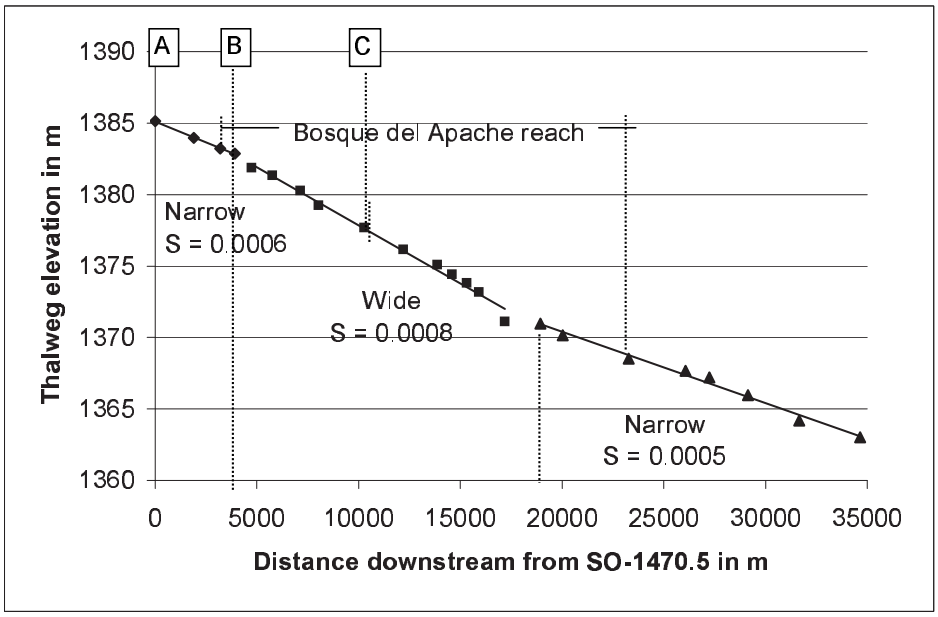

Figure 6.5: Thalweg profile of the study reach for 1992. Bed slopes in m/m are indicated in the plot. The letters A,B, and C identify the location of the aerial photos shown in Figures 6.8 and 6.9.

not cross section measurements during high flows.

The upstream, narrow reach has an averaged width-depth ratio of 163 with a standard deviation of 89, when the flow discharge is 9 m^3/s. The middle, wide reach has an averaged width-depth ratio of 337 with a standard deviation of 28, for a flow discharge of 32 m^3/s. The downstream, narrow reach has an averaged width-depth ratio of 91 with a standard deviation of 58 for a flow discharge of 18 m^s/s.

6.1.4 Bed material

The banks and bed of the Bosque del Apache reach consist of sand-sized material (Drew Baird, USBR, Albuquerque, NM, 2002 pers. comm.). Bed material particle size distributions have been collected at the SO-lines from 1990 to 1999. Bed material data collected in 1992 were input into the model. Several samples were collected

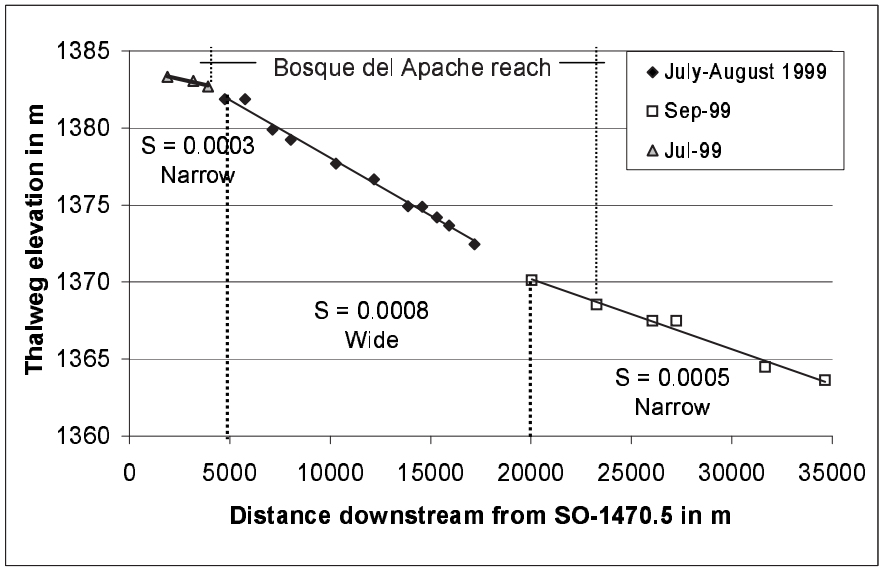

Figure 6.6: Thalweg profile of the study reach for 1999. Bed slopes in m/m are indicated in the plot.

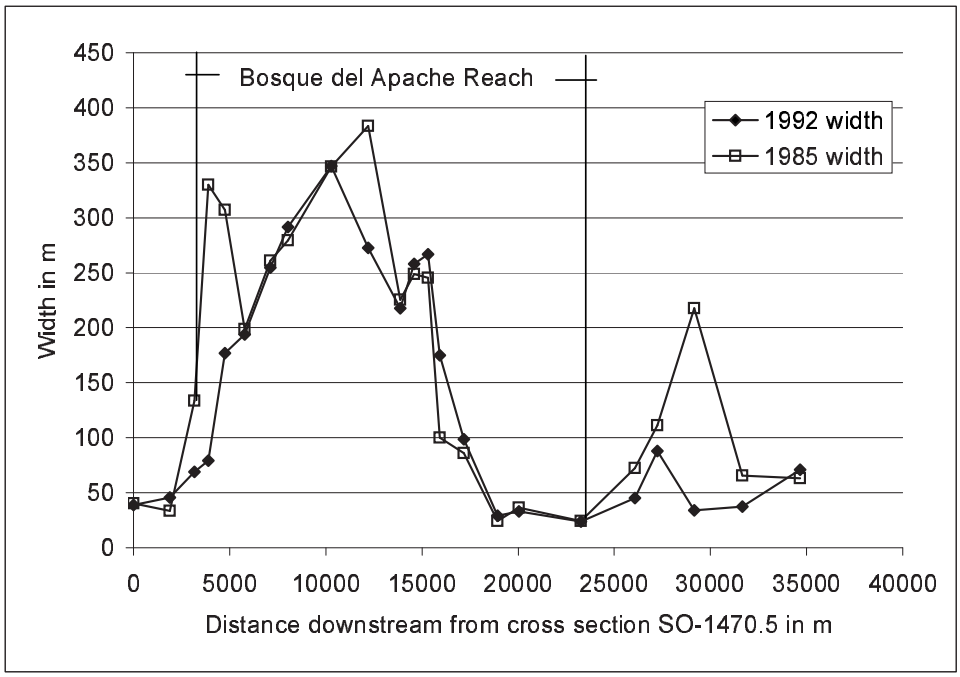

Figure 6.7: Non-vegetated channel width for 1985 and 1992.

across cross section SO-1470.5 in April and May of 1992 (see Figure 6.4). The arithmetic average of the values of percentages finer than a given size were computed to generate an average curve (Nordin and Culbertson, 1961). The averaged particle size distribution for SO-1470.5 in 1992 is shown in Figure 6.10. The median grain size is 0.26 mm and the $d_{84} = 0.43$ mm. Bed material data collected at different SO-lines and at different times of the flow regime in 1999 indicated variability of the median size between 0.1 mm and 0.3 mm, with the majority of the samples between 0.2 mm and 0.3 mm. This indicates that the bed material has not changed between 1992 and 1999. Mussetter Engineering (2002) reported median grain size of 0.3 mm in this reach according to bed material surveys performed in September of 2001.

6.1.5 Roughness Coefficient

The San Acacia gage is located upstream from the study reach. Measurements at the gage between 1988 to 1999 were used to estimate Manning roughness coefficient (n). This period of record was selected, because the sediment and water regime has not changed during this time period (Massong et al., 2000).

The data collected at the gage consist of flow discharge, channel width, cross sectional area and mean flow velocity. In addition, reported channel slope estimates indicate that the slope in the 5.6 kilometer reach below the San Acacia Diversion dam varies from 0.0006 m/m to 0.0008 m/m (Massong et al., 2000), with a mean value of 0.0007 m/m. Manning roughness coefficient at the gage was estimated based on these data. Figure 6.11 shows the Manning n as a function of discharge. The roughness coefficient varies from about 0.010 to 0.05. There is no trend between discharge and roughness coefficient in this plot. However, it is expected to find bedforms in a fine-grained sand bed river, like this one. It has been observed that the water surface elevation can drop during high flows (U. S. Bureau of Reclamation, 2000), probably because of reduction of the resistance to flow during the development of upper regime plane bed. Unfortunately, there are not enough data to use a

bedform predictor and estimate the roughness coefficient as a function of discharge in this reach.

6.1.6 Water Temperature

Water temperatures affect the transport of fine sediment particles. The decrease in water temperatures increases the kinematic viscosity, the resistance to flow and therefore the total load. Nordin and Beverage (1965) observed that changes in concentration are usually accompanied by changes in water temperature during spring runoff, whereas changes in concentration might be independent of temperature changes during late summer or fall in the Rio Grande. Sporadic water temperature samples from 1982 to 1997 at the San Acacia gage were used to estimate monthly averaged temperature values. Figure 6.12 shows the sample data as well as the monthly averaged values of water temperature in degrees Celsius. Averaged temperatures vary from about 5 to 25 degrees Celsius, with the maximum temperatures in July and August.

6.2 Data Input into the Model

The data input into the model correspond to the 1992 data collected in the river. The data consist of channel thalweg elevation at each cross section included in Figure 6.5, channel width at each cross section included in Figure 6.7, monthly averaged temperatures presented in Figure 6.12, and an overall roughness coefficient of $n = 0.026$ obtained from Figure 6.11. This overall roughness coefficient input into the model is in good agreement with the roughness coefficient ($n = 0.024$) obtained from the calibration of sediment transport models in the upper reach of Elephant Butte Reservoir (Drew Baird, USBR, Albuquerque, NM, 2002 pers. comm.).

The model was run with one sediment size equal to the median bed material size (d_{50}) obtained from the sediment gradation curve in Figure 6.10, because the bed material is almost uniform. This conclusion is supported with the analysis presented

in Appendix H.

The initial channel slope was computed at each node based on the initial thalweg elevation and the distance between cross sections. In addition, the mean daily flow discharge record at the San Acacia gage from 1992 to 1999 was routed. The 1999 reach-averaged slopes predicted by the model were compared to the slopes computed from the measurements (Figure 6.6).

The upstream boundary condition consists of the historical thalweg elevation at the first upstream cross section (SO-1470.5). A total of 38 elevation measurements were available from 1992 to January of 1999. Daily bed elevation values were estimated from the available data by linearly interpolating the missing elevations. The model was run until January 6, 1999.

The thalweg elevation profiles of the study reach from 1987 to 1999 show that the channel has aggraded and degraded above a channel elevation close to but slightly lower than the 1992 channel elevation. The lower end of the study reach is affected by the backwater profile from the Elephant Butte Reservoir during wet periods (U. S. Bureau of Reclamation, 2000). In addition, there are some stretches of the lower end of the study reach that have a significant amount of cohesive material in the bed (Kristi Smith, USBR, Albuquerque, NM, 2002 pers. comm.). The lower end of the study reach was moved to the east side of the valley between 1949 and 1962 and relocated to an overbank area that had a higher clay content than the previous main channel (U. S. Bureau of Reclamation, 2000). The cohesion of the bed explains the low degradation observed in the lower part of the study reach. However, it is not clear why the upper part of the study reach behaves in the same manner as the lower reach.

Two different simulations were performed. In one simulation, the bed degradation was controlled in the last two downstream cross sections of the study reach. The bed was not allowed to degrade below the lowest elevation recorded at those stations during the 1987 to 1999 period. In the other simulation, the bed of the

Year	a	b
1992	0.156	0.363
1993	0.105	0.475
1994	0.178	0.348
1995	0.109	0.490
1998	0.230	0.254
1999	0.215	0.291

Table 6.1: Regression coefficients of depth-discharge relationships at the San Marcial gage.

entire study reach was not allowed to degrade below the lowest elevation recorded during the 1987 to 1999 period.

For the downstream boundary condition the initial downstream water depth was estimated from depth-discharge relationships developed at the San Marcial gage. Based on flow discharge, channel width and cross sectional area measurements at the gage from 1992 to 1999, the mean flow depth was estimated and plotted against the discharge. One depth-discharge relationship was developed for each year, because the bed elevation changes with the flow regime and the stage-discharge relationships shift with time. There were few data values for 1996 and 1997. Therefore, the 1995 equation was used for these years. The equations are of the following form: $h = aQ^b$, where h is the flow depth in m, Q is the flow discharge in m^3/s and a and b are coefficients determine with a non-linear regression. Table 6.1 summarizes the regression coefficients.

Yang's (1973) sediment transport equation was used in the simulation. This equation has been used in sediment transport modelling in the upper end of Elephant Butte Reservoir and its results are in good agreement with field measured transport rates (Drew Baird, USBR, Albuquerque, NM, 2002 pers. comm.). The bed material measurements at the San Acacia gage are close to the predicted values

with this equation, for discharges greater than about 10 m^3/s (see Appendix 7.1). However, the measurements at the San Acacia gage are less than the capacities computed with Yang's equation. This gage is located downstream from the San Acacia diversion dam, and therefore the sediment is trapped behind the dam, reducing the bed material load downstream.

An attempt was made to compute the incoming sediment load to the channel with the bed material rating curves developed at San Acacia and San Marcial gages. However, the incoming sediment loads from the rating curves and the potential transport rates from Yang's (1973) equation were not in balance. Therefore, the rating curves were not used in the simulations. Even though the bed material measurements were close to the potential transport capacities computed with Yang's (1973) equation based on the historical hydraulic and sediment data at San Acacia gage (see Appendix 7.1), the regression lines (rating curves) do not fit the data (measurements) very well and therefore they do not compare very well with the predictions made with Yang's (1973) equation during the simulations.

6.3 Model Results

The model was run from February of 1992 to January of 1999, which corresponds to the dates for which bed elevations in the upstream node are available. Comparison of the results was made with the bed elevation profiles for September 1993, July 1997, May-June 1998 and July-September of 1999. The comparison of the results with the 1999 data is presented in this chapter. The other results are included in Appendix I.

Figures 6.13 (a) and (b) compare the resulting channel profiles from the model with the 1999 measurements. Figure 6.13 (a) shows the results for the case in which the channel degradation was only controlled in the last two downstream nodes. Figure 6.13 (b) shows the results when the maximum degradation was controlled along the entire reach.

The results obtained with the condition of controlling the maximum degradation along the entire reach seem to better reproduce the 1999 channel profile. Similarly, the results for 1993, 1997 and 1998 are best approximated when the maximum degradation is controlled (Appendix I). If the degradation is not controlled in the entire channel, a deeper and larger pool is predicted in the narrow downstream reach (Figure 6.13 (a)).

Figures 6.14 (a) and (b) show the reach-averaged slopes obtained from the profiles in Figures 6.13. Linear regressions were fit to the data. The slopes of the regression lines were estimated for each subreach. The results show that the wide reach is steeper than the two narrow reaches. In addition, the reach-averaged slopes from the simulations are in good agreement with the reach-averaged slopes obtained from the field data.

6.4 Comparison of Model Simulations with Variable and Constant Flows with the Field Measurements of 1999

Numerical simulations were performed in the study reach with two different steady flow discharges and with the mean daily flows at the San Acacia gage from 1992 to 1999. Figures 6.15 and 6.16 show the comparison of the 1999 field data with the three different runs for the case in which the channel degradation was controlled in the last two downstream nodes and the case in which the maximum degradation was controlled along the entire channel, respectively. For both cases, the results of the runs with the mean annual discharge Q = 39 m^3/s are in good agreement with the results of the runs with the mean daily flows at the San Acacia gage from 1992 to 1999. Conversely, the results of the runs with the dominant discharge (Q = 139 m^3/s) are not in good agreement with the solution obtained with variable flows. These results are in agreement with the results obtained in Chapter 5. The long-term changes in bed elevation with time due to variable water discharges are better approximated by the numerical simulations with a constant discharge close

to the mean annual flow.

6.5 Comparison of the Steady State Solution with the Field Measurements of 1999

Figures 6.17 and 6.18 compare the steady state solutions of slope versus width and slope versus width-depth ratio, respectively, with the field measurements of 1999. The steady state solutions were obtained for a mean annual flow of $Q = 39\ m^3/s$ between 1992 and 1999, a sediment load of about $Q_s = 4,000\ tons/day$ (see Figures A.1 and A.2 in Appendix 7.1), a median grain size of $d_s = 0.26\ mm$, and a Manning friction coefficient of $n = 0.026$. The steady state solutions were developed with Julien's (2002) simplified sediment transport and Manning resistance equations.

The reach-averaged width of the wide section is 229 m, whereas the reach-averaged width of the narrow downstream section is 46 m. The weighting factor used to compute these averages was one half of the distances to each of the adjacent upstream and downstream cross-sections. The reach-averaged slopes are indicated in Figure 6.6. The width-depth ratios were estimated from the measured reach-averaged widths and the computed normal depths at each reach corresponding to the reach averaged slopes, the mean annual discharge of $Q = 39\ m^3/s$, and the Manning friction coefficient of $n = 0.026$. The results of the steady state solutions for the mean annual discharge and the corresponding averaged sediment discharge are in good agreement with the field measurements.

6.6 Application to River Restoration in The Middle Rio Grande

Reach-averaged mean flow velocity and mean flow depth were computed for each day from the results of the simulations presented in the previous section. The weighting factor used in the reach averaging was one half of the distances to each of the adjacent upstream and downstream cross-sections.

Flow depth and mean flow depth duration curves were developed with the averaged data. Figure 6.19 (a) shows the comparison of the flow depth duration curves of the narrow (upstream) reach and the wide (middle) reach. Figure 6.19 (b) shows the curves for the wide (middle) reach and the narrow (downstream) reach. The results include the two cases considered in the previous section: not controlling the maximum degradation along the entire channel, and controlling the maximum degradation along the entire channel.

Figure 6.20 (a) shows the comparison of the flow velocity duration curves of the upstream (narrow) reach and the middle (wide) reach. Figure 6.20 (b) shows the curves for the wide (middle) reach and the narrow (downstream) reach. The results include the two cases considered in the previous section: controlling the maximum degradation at the downstream end of the channel, and controlling the maximum degradation along the entire channel.

These plots show the estimated flow depth ($h = 0.4\ m$) and flow velocity ($V = 0.1\ m/s$) below which the greatest population of Rio Grande silvery minnows have been found (U. S. Fish and Wildlife Service, 2001). Also the maximum flow depth ($h = 0.5\ m$) and maximum flow velocity ($V = 0.4\ m/s$), where fewer minnows have been found (U. S. Fish and Wildlife Service 2001, Mike Porter, USBR, Albuquerque, NM, 2002 pers. comm.), is indicated. Tables 6.2 and 6.3 summarize the percent of time the indicated flow depths and flow velocities have been equalled or non-exceeded at the three reaches for the two conditions (controlling degradation, and not controlling degradation). The average value is also summarized.

The flow depths and flow velocities needed by the Rio Grande silvery minnow occur more frequently in the wide reach than in the two narrow reaches. Flow depths less than or equal to 0.4 m occur about 1.5 to 2 times more in the wide reach than in the narrow reaches, whereas flow velocities less than or equal to 0.1 m/s occur approximately 10 times more in the wide reach than in the narrow reaches.

Flow depths less than or equal to 0.5 m and flow velocities less than or equal to

Reach	h≤ 0.4 m (%)	average	V≤ 0.1 m/s (%)	average
Narrow (u/s)(control)	15.8		1.2	
		16.7		0.8
Narrow (u/s)(no control)	17.5		0.3	
Wide (m) (control)	33.0		6.28	
		30.4		11.7
Wide (m) (no control)	27.8		7.7	
Narrow (d/s) (control)	16.7		0.4	
		14.6		1.2
Narrow (d/s) (no control)	12.4		2	

Table 6.2: Summary of percent of time the flow depth and the flow velocity equal or non-exceed $h = 0.4\ m$ and $V = 0.1\ m/s$, respectively. Upstream reach is u/s, middle reach is m, downstream reach is d/s. Control represents the results when controlling the maximum degradation along the entire channel. No control represents the results when the maximum degradation was controlled at the downstream end of the channel.

0.4 m/s occur more frequently in the wide than in the two narrow reaches. However, the percent of times these conditions are equalled or non-exceeded are high in all three reaches, when compared with the more strict conditions summarized in Table 6.2.

It is worthwhile mentioning that this analysis was performed with mean cross sectional velocities and flow depths and do not account for the variation of velocity and flow depth across the cross sections due to the development of middle bars and multiple channels. Small minnows are found in shorelines, backwaters, and pools, whereas large minnows are found in the main channel and in side channel runs (U. S. Fish and Wildlife Service, 2001). The analysis performed with the mean flow velocity and depth duration curves do not distinguish the changes in velocity

Reach	h≤ 0.5 m (%)	average	V≤ 0.4 m/s (%)	average
Narrow (u/s)(control)	27		15	
		26		16.5
Narrow (u/s)(no control)	25		18	
Wide (m) (control)	50		68	
		47		67.5
Wide (m) (no control)	44		67	
Narrow (d/s) (control)	24		15	
		20.5		23.5
Narrow (d/s) (no control)	17		32	

Table 6.3: Summary of percent of time the flow depth and the flow velocity equal or non-exceed $h = 0.5\ m$ and $V = 0.4\ m/s$, respectively. Upstream reach is u/s, middle reach is m, downstream reach is d/s. Control represents the results when controlling the maximum degradation along the entire channel. No control represents the results when the maximum degradation was controlled at the downstream end of the channel.

between backwaters and pools in the same cross section. Therefore, the results of this analysis are an approximation.

6.7 Summary

Field data of the middle Rio Grande indicate that two narrow reaches upstream and downstream from a wide river section have developed slopes that are flatter than the slope of the wide reach. Results of the model simulations of the study reach are in good agreement with the field measurements.

Results of the numerical model obtained with a constant discharge equal to the mean annual flow are in good agreement with the results obtained with variable discharges.

The steady state slope versus width and slope versus width-depth ratio for the mean annual flow and the corresponding sediment discharge are in agreement with the field measurements collected in 1999.

Flow depth and flow velocity duration curves indicate that the wide reach provides shallower and lower velocity flows than the two narrow reaches, which might be more favorable for the fish habitat. The flow conditions ($h \leq 0.4\ m$ and $V \leq 0.1\ m/s$), where the majority of Rio Grande Silvery Minnow have been found in the river (U. S. Fish and Wildlife Service, 2001), are met less than 30 % of the time at all reaches.

The percent of time a flow depth of $h = 0.5\ m$ is non-exceeded or equalled is about 50 % in the wide reach. In the case of a mean flow velocity of $V = 0.4\ m/s$, this condition is equalled or non-exceeded about 70 % of the time in the wide reach. In the narrow reaches, the percent of time the flow depth and velocity occur or are less than $h = 0.5\ m$ and $V = 0.4\ m/s$ respectively is less than 30 %.

Figure 6.8: Digitized non-vegetated channel in 1992 (left) and 2000 aerial photo (right) of the upstream, narrow reach. This reach is located between A and B in Figure 6.5.

Figure 6.9: Digitized non-vegetated channel in 1992 (left) and 2000 aerial photo (right) of a section of the middle, wide reach. This reach is located between B and C in Figure 6.5.

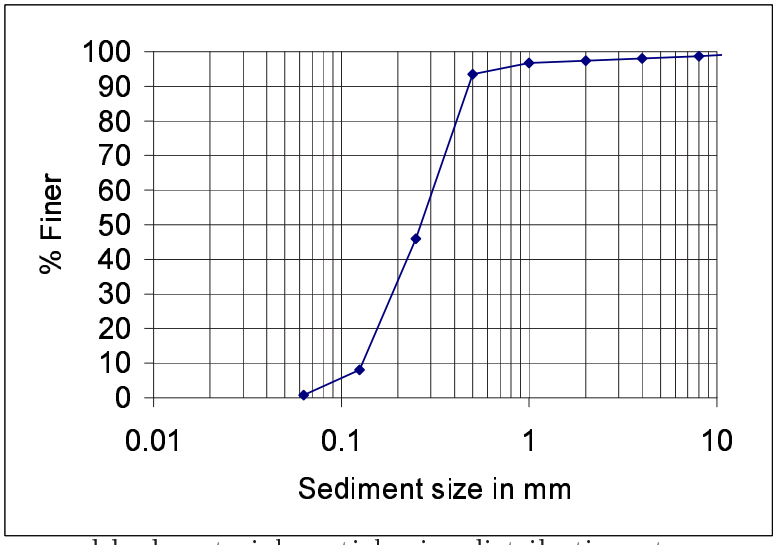

Figure 6.10: Averaged bed material particle size distribution at cross section SO-1470.5 in 1992.

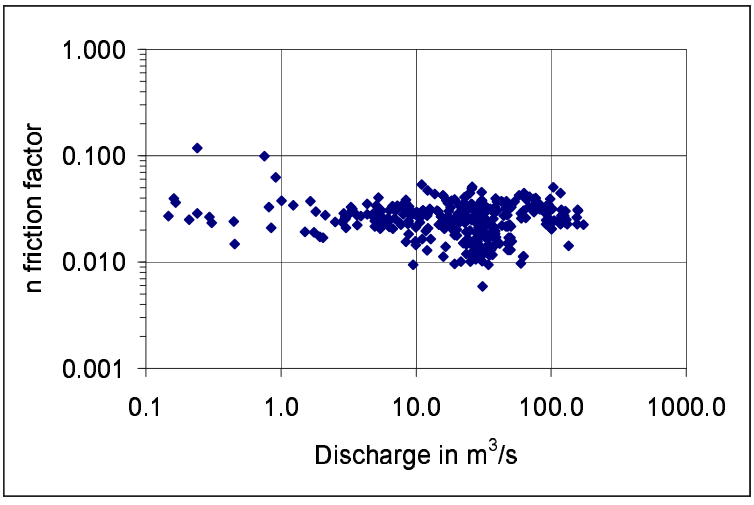

Figure 6.11: Manning n as function of flow discharge at San Acacia gage. Period of record: 1988-1999.

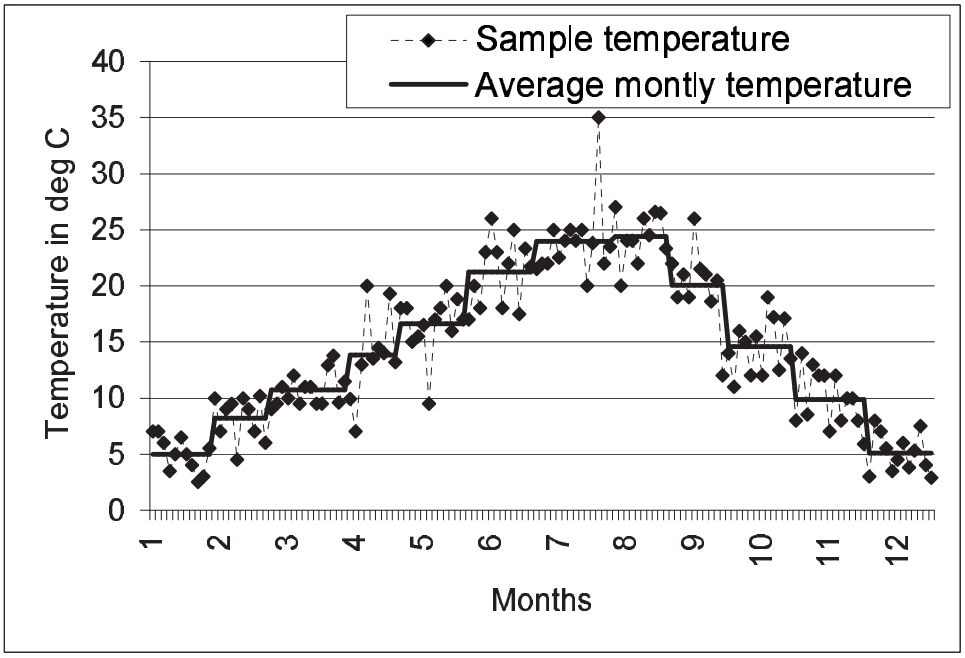

Figure 6.12: Water temperature as function of time at the San Acacia gage.

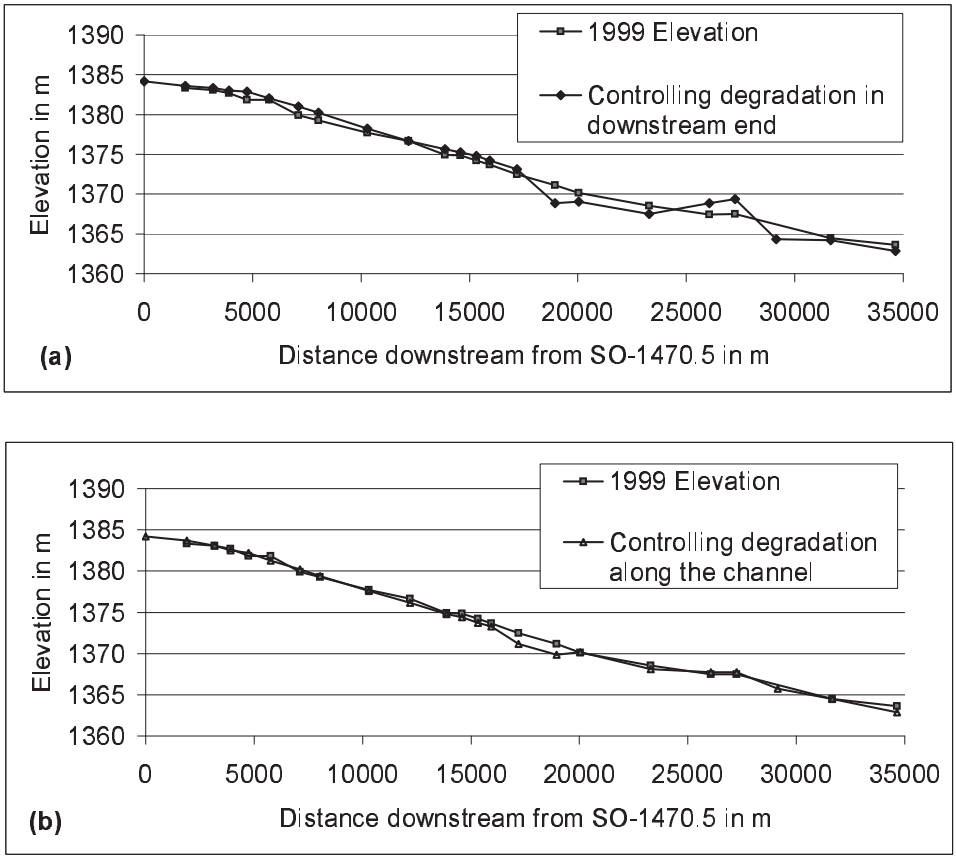

Figure 6.13: Resulting channel profile from the sediment transport model. (a) Channel degradation is controlled in the last two downstream nodes of the reach. (b) Channel degradation is controlled along the entire channel.

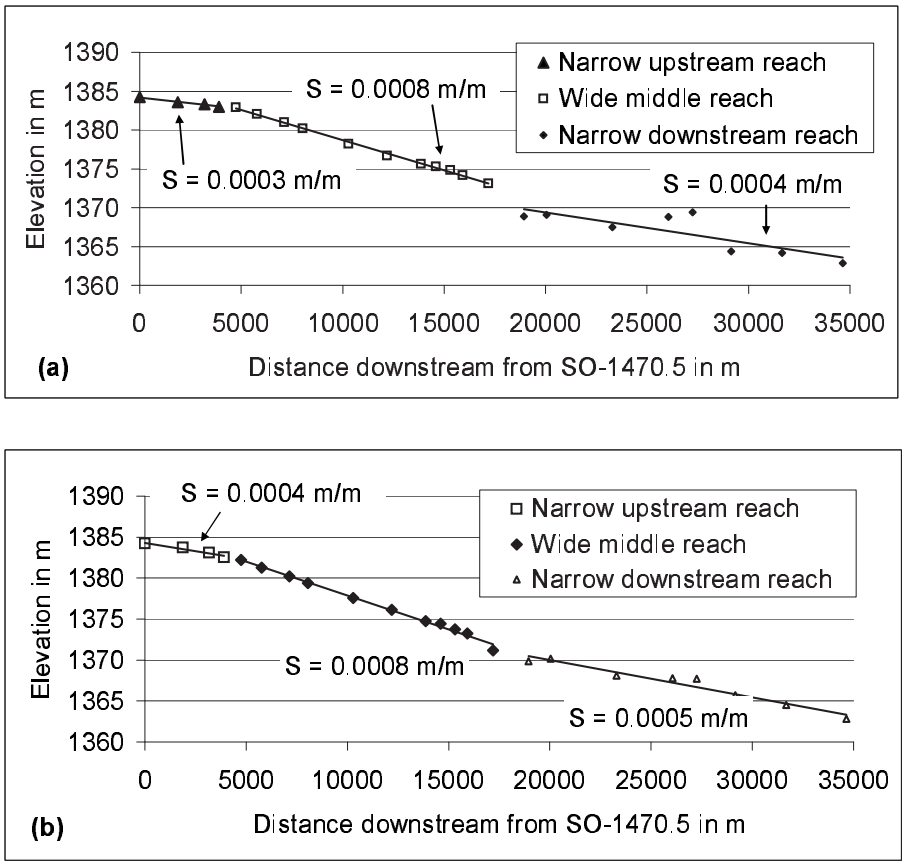

Figure 6.14: Reach-averaged slopes of each subreach from the simulations. (a) Results of the simulations when the degradation of the last two downstream nodes were controlled. (b) Results of the simulations when the maximum degradation along the entire channel was controlled.

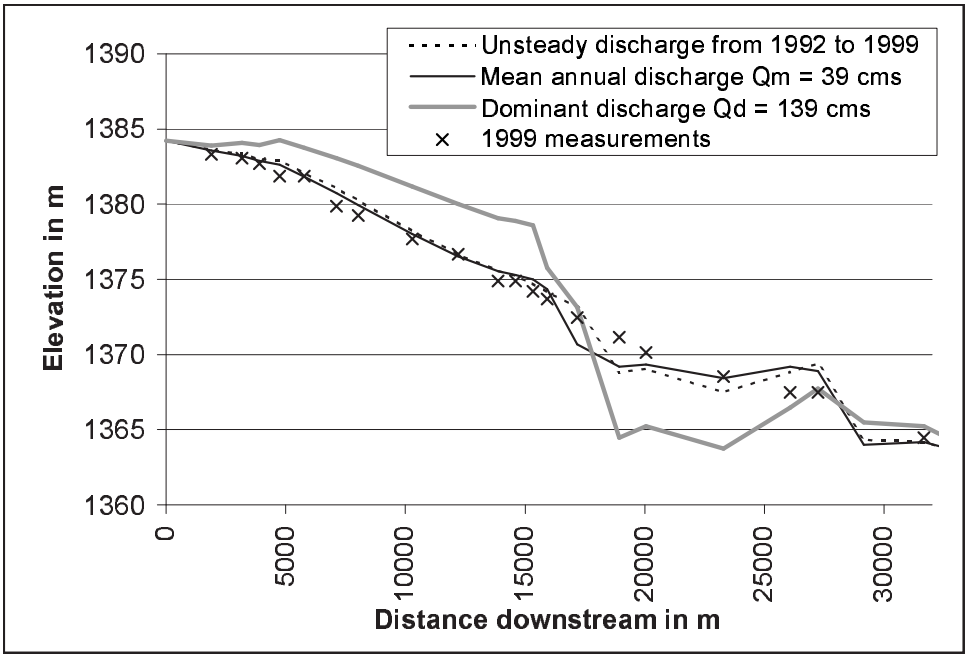

Figure 6.15: Comparison of the field data collected in 1999 with the results of the sediment transport model with the mean daily flows at the San Acacia gage from 1992 to 1999, the mean annual flow at the San Acacia gage from 1992 to 1999 (Q = 39 m^3/s) and the dominant discharge (Q = 139 m^3/s). Channel degradation is controlled in the last two downstream nodes of the reach.

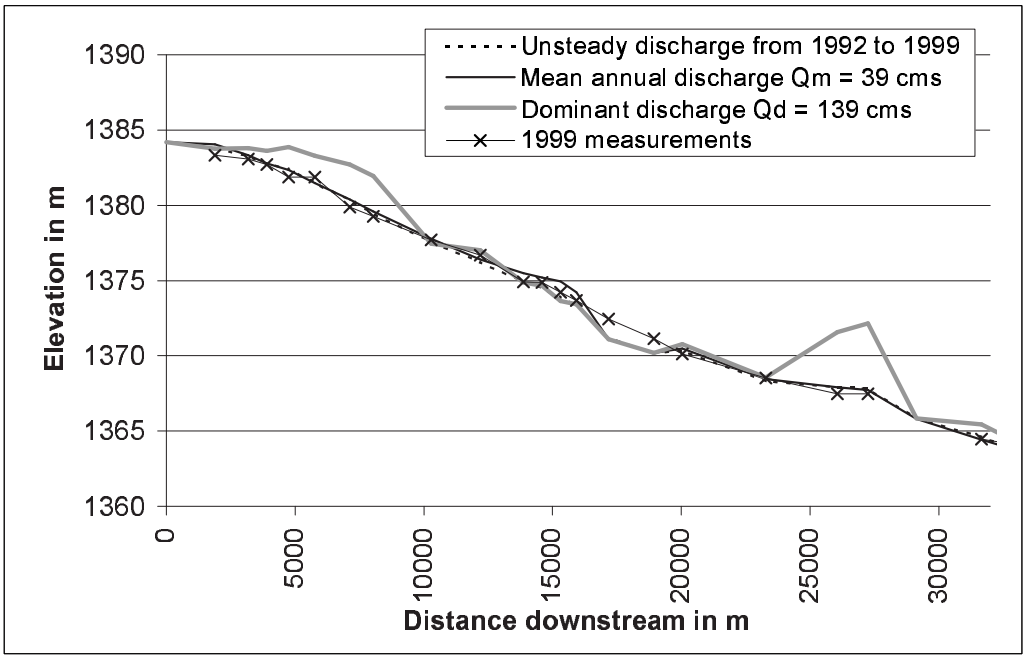

Figure 6.16: Comparison of the field data collected in 1999 with the results of the sediment transport model with the mean daily flows at the San Acacia gage from 1992 to 1999, the mean annual flow at the San Acacia gage from 1992 to 1999 (Q = 39 m^3/s) and the dominant discharge (Q = 139 m^3/s). Channel degradation is controlled along the entire reach.

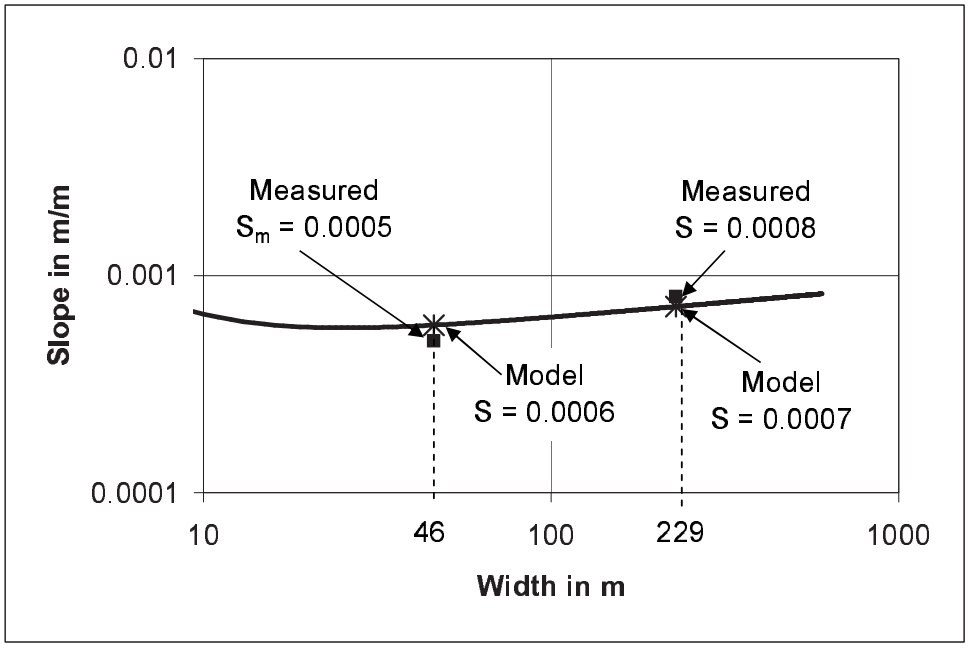

Figure 6.17: Comparison of the field data collected in 1999 with the results of the steady state slope versus width relationship obtained for a mean annual flow of Q = 39 m^3/s, a sediment discharge of $Q_s = 4,000 tons/day$, a median grain size of $d_s = 0.26\ mm$, and a Manning friction coefficient of $n = 0.026$.

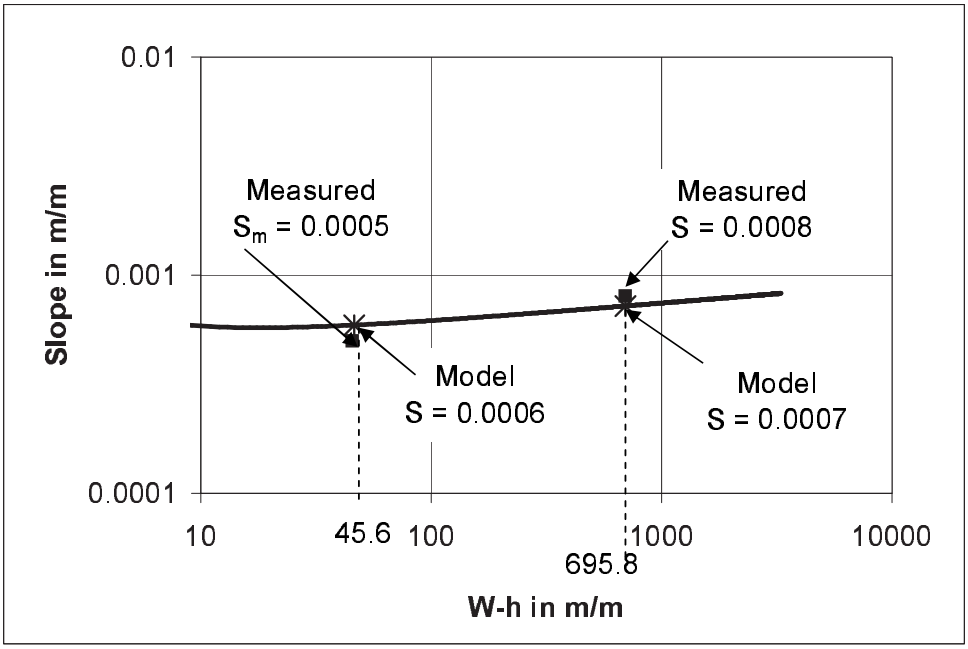

Figure 6.18: Comparison of the field data collected in 1999 with the results of the steady state slope versus width-depth ratio relationship obtained for a mean annual flow of Q = 39 m^3/s, a sediment discharge of $Q_s = 4,000 tons/day$, a median grain size of $d_s = 0.26\ mm$, and a Manning friction coefficient of $n = 0.026$.

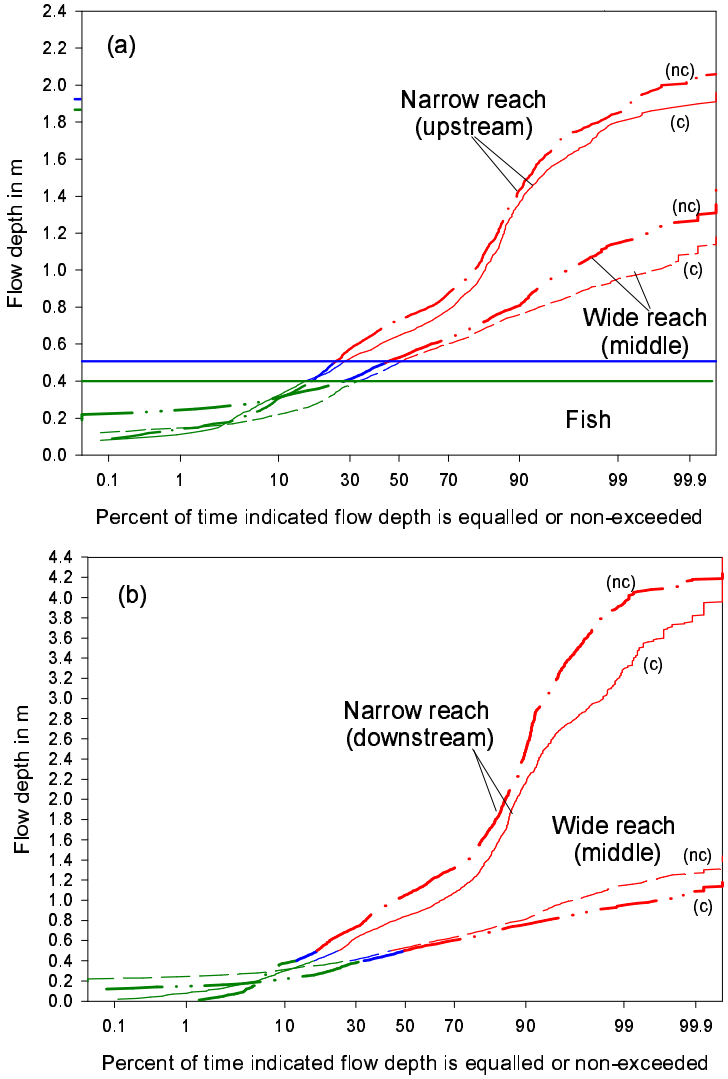

Figure 6.19: Flow depth duration curves. (a) Comparison of the curves at the narrow (upstream) and wide (middle) reaches. (b) Comparison of the curves at the wide (middle) and narrow (downstream) reaches. nc = no controlling degradation along the entire channel; c = controlling degradation along the entire channel.

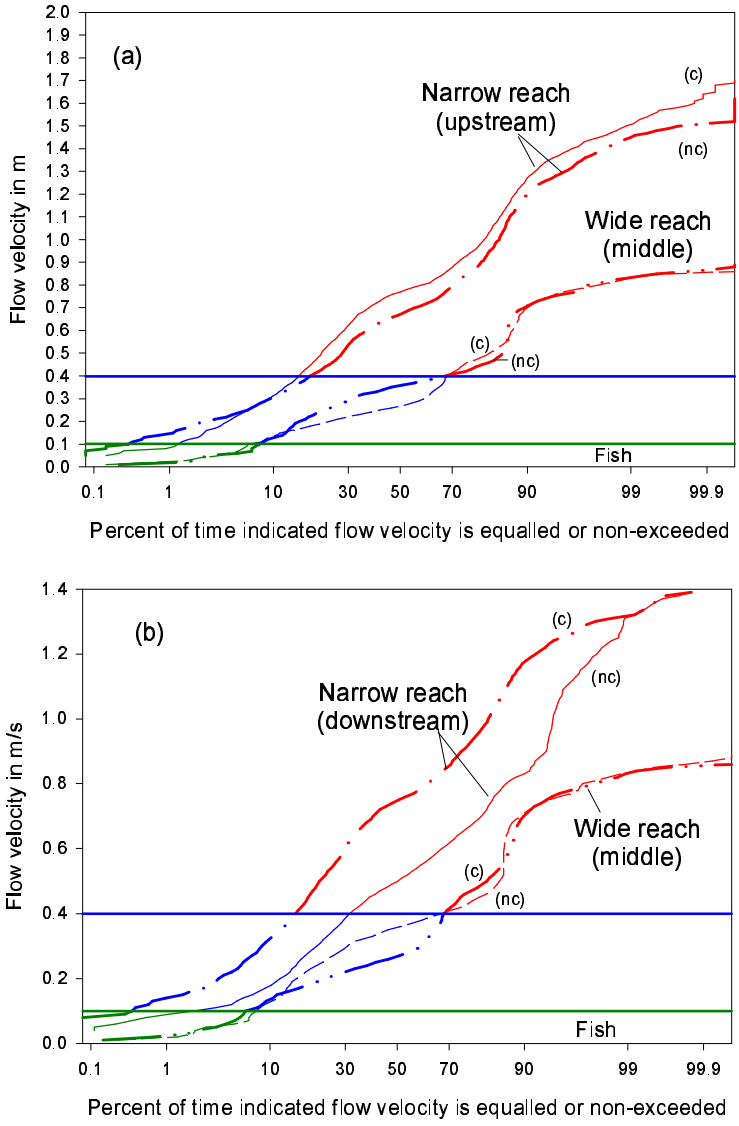

Figure 6.20: Flow velocity duration curves. (a) Comparison of the curves at the narrow (upstream) and wide (middle) reaches. (b) Comparison of the curves at the wide (middle) and narrow (downstream) reaches. nc = no controlling degradation along the entire channel; c = controlling degradation along the entire channel.

Chapter 7

Conclusions and Recommendations

The Bosque del Apache reach, located in the middle Rio Grande, NM, provided an excellent case to study the adjustment of bed slope in sequential sand bed channels with different widths and equivalent water and sediment discharge. The primary conclusions of this work are as follows:

1. Analytical solutions of the slope versus width and width-depth ratio of channels in equilibrium under steady state input water and sediment discharges were developed in Chapter 4. These relationships indicate that an increase in channel width will require an increase in channel slope to satisfy continuity of sediment transport.

   The following relationships are the analytical solutions for the case when the hydraulic radius is approximated to the flow depth (wide channels):

$$S_r = W_r^{1/7}$$

$$S_r = \left(\frac{W_r}{h_r}\right)^{2/23} = (\xi_r)^{2/23}$$

   The following relationship is the analytical solutions for the case when the hydraulic radius is not approximated to the flow depth:

$$S = C_v^{16/23} \frac{(G-1)^{32/33} d_s^{8/23} \phi^{18/23}}{Q^{2/23} 18^{16/23} g^{8/23} n^{18/23}} \frac{(\xi+2)^{20/23}}{\xi^{18/23}}$$

The above equation indicates that the channel slope is directly proportional and highly dependent on sediment concentration. The analytical solutions for both cases ($R_h \approx h$ and $R_h \neq h$) yield the same results for width-depth ratios greater than or equal to 70.

The analytical solution of the width ratio versus the slope ratio for large widths is in good agreement with the laboratory flume data of Bigillon (1997). Similarly, the analytical solutions of slope versus width and slope versus width-depth ration are in good agreement with field measurements of the middle Rio Grande.

2. The transient solutions for constant discharge are in agreement with the results of the analytical solutions. The numerical simulations allow estimation of the time to reach equilibrium under constant discharge.

3. The transient solution of the slope under variable flow and sediment discharges indicates that the slope changes more rapidly under large flows than under low flows.

   The long term simulations with variable flows compare better with the transient solutions under a constant discharge close to the mean annual flow than under flood discharges (e.g. discharge equalled or exceeded 10 % of the time, or discharge equal or close to the dominant discharge).

4. Quantitative field data from the study reach, which include the Bosque del Apache in middle Rio Grande, indicate that the two narrow reaches have flatter slopes than the wide reach. Simulations of a study reach of the middle Rio Grande with the transient numerical model with both variable discharges and mean annual flow are in good agreement with the field data.

   It is likely that the wide reach of the study reach provides better habitat for the Rio Grande silvery minnow than the two narrow reaches, as indicated by

the flow and velocity duration curves. Mean cross-sectional flow depths less than or equal to 0.4 m occur about 1.5 to 2 times more in the wide reach than in the narrow reaches, while mean cross-sectional flow velocities less than or equal to 0.1 m/s occur approximately 10 times more in the wide reach than in the narrow reaches.

Flow conditions such as $h \leq 0.5\ m$ and $V \leq 0.4\ m/s$, where some silvery minnow have been found in the river (U. S. Fish and Wildlife Service, 2001), occur more than 40 % of the time in the case of the flow depth and 70 % of the time in the case of the mean flow velocity in the wide reach.

7.1 Recommendations and Future Work

The dynamic nature of rivers does not easily allow humans to force rivers into controllable and more manageable conditions. Restoration of the Rio Grande is a challenging task that should be carefully implemented. This dissertation provides a tool to understand and evaluate the adjustment of channel slope with time due to spatial changes in channel width and to estimate the degree of change of hydraulic variables (mean cross sectional velocity and depth) between wide and narrow reaches.

The methodology proposed in this work could be used in other sectors of the Rio Grande and in other rivers to evaluate restoration activities. However, the assumptions made in this work must apply. The width of the channel has to be managed in order to maintain it almost constant with time, as in the case of the Bosque del Apache reach. The vegetation on the banks of this reach has not allow the channel to widen. It seems that the constant flow regime for the last 20 years has also contributed in the maintenance of an almost constant channel width. New establish vegetation in the bed of the river during low flows seem to be removed by the high flows during the wet periods.

Even though the study reach has maintained an almost constant width for about a period of 20 years, other reaches of the Rio Grande or other rivers might not

responde in the same manner to management of the vegetation on the banks. In these cases, the change in channel width with time is a factor that might need to be considered and could be explored in future works. Empirical relationships that describe the change in channel width with time such as the one developed by Richard (2001), could be included in the numerical models developed in this dissertation. This empirical width model accounts for channel narrowing and new relationships must be developed for channel widening. Therefore, appropriate data should be collected to develop the relationships that account for increase in width.

Other factor that might be considered when designing the increase in channel width is the downstream and upstream control imposed by the current conditions of the channel. For example, the increase in width will cause degradation of the downstream narrower reach. This degradation will be controlled by the type of bed material and existing geologic controls in the bed of the channel. If erosion is limited, the channel downstream might response by increasing the width to accommodate the imposed water and sediment discharges. This change in channel width will depend on the resistance of the banks to absorb the changes in flows. If the changes in the downstream reach exceed the natural inherent variability of the river, the disturbance will result in the channel becoming unstable (Werritty, 1997). Also, a nickpoint could form and migrate upstream. Creating instabilities in the channel. It these types of changes occur, the modelling of the changes in width with time might be required to obtain better results.

The equivalent results obtained with the mean annual flow and the variable discharge during the same period of time suggest that different water management strategies could be used in the river. The increase in mean annual discharge, by increasing the base water level, could produce equivalent results (changes in bed elevation) to the increase of flow peaks. However, other channel characteristics, such as channel width, might be more responsive to the increase in flow peaks than to the increase in base water levels, because channel width is highly dependent on

water discharge. Therefore, if dam operating regime in the Rio Grande is desired to be changed to increase the flows, the simultaneous adjustment of width and slope should be assessed under both conditions: increase in base level, and increase of flow peaks. Other factors such as the increase in elevation of the water table due to the increase in base level in the channel, should be considered in a new proposed management strategy. Because, the increase in elevation of the water table could effect negatively the agricultural lands adjacent to the channel.

Channel widening is desired to restore the habitat of the Rio Grande silvery minnow. River widening could be promote by increasing the flows or removing the vegetation. Previous experiences in the Rio Grande showed that channel widening could be achieved by managing the vegetation. If changes in water regime are proposed, the considerations outlined in the previous paragraph should be taken into account.

The majority of silvery minnows are found in low-velocity habitats such as debris piles, backwaters and pools (U. S. Fish and Wildlife Service, 2001). If the channel is widened, a braided morphology could develop if the width-depth ratio exceeds a threshold. For example, theoretical analyzes indicate that braiding occurs when the width-depth ratio exceeds 50 (Knighton, 1998). It is possible that the minnow not only needs wide channels but also braided planforms. Therefore, to restore the habitat of the minnow both conditions should be seek.

Finally, it is of crucial importance to try to identify the ability of the river to resist and accommodate the imposed disturbance or changes in the channel. This is not an easy task. However, previous experiences in the river and historical data should be used as a start point for the design of restoration activities. It is recommended to continue the data collection in the Rio Grande for the specific purposes of river restoration. Bed load data will allow to develop appropriate sediment rating curves. In addition, daily flow depth and velocity measurements will allow to estimate or simulate the changes in channel roughness due to the development of bedforms.

Bibliography

Abernethy, B. and I. Rutherfurd: 2000, Does the weight of riparian trees destabilize riverbanks? *Regulated Rivers: Research & Mangement*, **16**, 565–576.

Ackers, P. and W. R. White: 1973, Sediment transport: New approach and analysis. *Journal of the Hydraulics Division. ASCE*, **99**, 2041–2060.

Arritt, S.: 1996, Rio Grande silvery minnow: Symbol of an embattled river. *New Mexico Wildlife*, **41**, 8–10.

ASCE Task Committee on Hydraulics, B. M. and M. of River Width Adjustment: 1998, River width adjustment i: Processes and mechanisms. *Journal of Hydraulics Engineering*, **124**, 881–902.

Ashmore, P.: 1985, *Process and Form in Gravel Braided Streams: Laboratory Modelling and Field Observations*. Ph.D. Dissertation, University of Alberta.

— 1988, Bed load transport in braide gravel-bed stream models. *Earth Surface Processes and Landforms*, **13**, 677–695.

Baird, D.: 1996, River mechanics experience on the middle Rio Grande. *Proceedings of the 6th Federal Interangency Sedimentation Conference*, volume 1, III–9 – III–16.

— 2001, River restoration on the middle Rio Grande: Opportunities and challenges. *Proceedings of the 7th Federal Interangency Sedimentation Conference*, volume II, 81–88.

Bauer, T.: 1999, *Morphology of the Middle Rio Grande from Bernalillo Bridge to the San Acacia Diversion Dam, New Mexico*. Master's thesis, Colorado State University.

Bestgen, K. and S. Platania: 1991, Status and conservation of the Rio Grande silvery minnow, *Hibognathus Amarus*. *The Southwestern Naturalist*, **36**, 225–232.

Bestgen, K. and D. Propst: 1996, Redescription, geographic variation and taxonomic status of Rio Grande silvery minnow, *Hybgnathus amarus* (girard 1856). *Copeia*, 41–55.

Bigillon, F.: 1997, *Evolution d'un lit torrentiel a section transversale graduellement variee*. Master's thesis, Universite Joseph Fourier, Cemagref de Grenoble, Grenoble, France.

Blench, T.: 1957, *Regime Behaviour of Canals and Rivers*. Butterworths Scientific Publications, London.

Booker, H. and F. Ward: 1999, Instream flows and endangered species in an international river basin. the upper Rio Grande. *American Journal of Agricultural Economics*, **81**, 1262–1267.

Brownlie, W.: 1981, Prediction of flow depth and sediment discharge in open channels. Technical Report Report No. KH-R-43A, W.M. Keck Laboratory of Hydraulics and Water Resources. Division of Engineering and Applied Science. California Institute of Technology, Pasadena, California.

Bullard, K. and W. Lane: 1993, Middle Rio Grande peak flow frequency study. Technical report, U. S. Department of the Interior, Bureau of Reclamation, Flood Hydrology Group, Denver, CO.

Burton, G.: 1997, *America's National Wildlife Refuges... Where Wildlife Comes Naturally! Rio Grande Silvery Minnow*. Web Page Avalilable: http://refuges.fws.gov/NWRSFiles/Wildli.../Fish/Rio$_{G}rande_{S}ilvery_{M}innow.html$.

Cao, S. and D. W. Knight: 1998, Design for hydraulic geometry of alluvial channels. *Journal of Hydraulic Engineering*, **124**, 484–492.

Carson, M. and G. Griffiths: 1987, Gravel transport rates and yields related to channel width. *Journal of Hydrology (N.Z.)*, **26**, 81–108.

Chang, H.: 1980, Stable alluvial canal design. *Journal of the Hydraulics Division, ASCE*, **106**, 873–889.

Chang, H. H.: 1979, Minimum stream power and river channel patterns. *Journal of Hydrology*, **41**, 303–327.

Chaudhry, M. H.: 1993, *Open-Channel Flow*. Prentice-Hall,Inc., New Jersey.

Chien, N.: 1955, A concept of the regime theory. *Transactions of the American Society of Civil Engineers*, **Paper No. 2884**, 785–793.

Chow, V., D. Maidment, and L. Mays: 1988, *Applied Hydrology*. McGraw-Hill.

Chow, V. T.: 1959, *Open-Channel Hydraulics*. McGraw-Hill Book Company, Inc.

Crawford, C., A. Cully, R. Leutheuser, M. Sifuentes, L. White, and J. Wilber: 1993, Middle Rio Grande ecosystem: Bosque biological management plan. Technical report, U. S. Fish and Wildlife Service, Albuquerque, NM.

Davies, T. and A. Lee: 1988, Physical hydraulic modelling of width reduction and bed level change in braided rivers. *Journal of Hydrology (N.Z.)*, **27**, 113–127.

Ferguson, R.: 1986a, Hydraulics and hydraulic geometry. *Progress in Physical Geography*, **10**, 1–31.

— 1986b, River loads underestimated by rating curves. *Water Resources Research*, **22**, 74–76.

Garde, R. J. and K. G. Ranga Raju: 1977, *Mechanics of Sediment Transportation and Alluvial Stream Problems*. Halsted Press, A Division of John Wiley & Sons, Inc, New York.

Gellis, A.: 1991, Decreasing trends of suspended sediment concentration at selected stream-flow stations in New Mexico. *New Mexico Water Resources Research Institute*, **11**, 77–93.

Griffiths, G. A.: 1989, Conversion of braided gravel-bed rivers to single-thread channels of equivalent transport capacity. *Journal of Hydrology (N.Z.)*, **28**, 63–75.

Helse, D. and R. Hirsch: 1995, *Statistical Methods in Water Resources. Studies in Environmental Science 49*. Elsevier Science B.V.

Henderson, F.: 1966, *Open Channel Flow*. Prentice-Hall, Inc.

Hey, R.: 1988, *Mathematical Models of Channel Morphology*, John Wiley & Sons Ltd., chapter 5. 99–123.

Hoffmann, K. and S. Chiang: 2000, *Computational Fluid Dynamics. Volume I. Fourth Edition*. Engineering Education System.

Huang, H. and G. Nanson: 1995, The multivariate controls of hydraulic geometry: A casual investigation in terms of boundary shear distribution. *Earth Surface Processes and Landforms*, **20**, 115–130.

Huang, H. Q. and G. Nanson: 2000, Hydraulic geometry and maximum flow efficiency as products of the principle of least action. *Earth Surface Processes and Landforms*, **25**, 1–16.

Julien, P.: 1995, *Erosion and Sedimentation*. Cambridge University Press.

— 2002, *River Mechanics*. Cambridge University Press.

Julien, P. and B. D. Simons: 1984, Analysis of hydraulic geometry relationships in alluvial channels. Technical report, Civil Engineering Department. Engineering Research Center. Colorado State University, Fort Collins, Colorado.

Julien, P. and J. Wargadalam: 1995, Alluvial channel geometry: Theory and applications. *Journal of Hydraulics Engineering*, **121**, 312–325.

Kirkby, M.: 1977, *Maximum Sediment Efficiency as a Criterion for Alluvial Channels*, John Wiley & Sons, Ltd., Belfast, N. Ireland, chapter 27. 429–442.

Klassen, G. and K. Vermeer: 1988, Channel characteristics of the braiding jamuna river, bangladesh. *International Conference on River Regime*, W.R.White, ed., John Wiley & Sons, Ltd., Wallingford, England, 55–66.

Knighton, D.: 1998, *Fluvial Forms and Processes*. John Wiley & Sons, Inc., New York, NY.

Knox, J.: 1975, Concept of the graded stream. *Theories of Landform Development: A Proceedings Volume of the Sixth Annual Geomorphology Symposia Series*, R. C. F. Wilton N. Melhorn, ed., Binghamton, New York, 170–198.

Lagasse, P.: 1980, An assessment of the response of the Rio Grande to dam construction - cochiti to isleta reach. Technical report, A Technical Report for the U. S. Army Engineer District, Albuquerque Corps of Engineers, Albuquerque, New Mexico.

— 1981, Geomorphic response of the Rio Grande to dam construction. *Geological Society, Special Publication*, **10**, 27–46.

— 1994, *Variable Response of the Rio Grande to Dam Construction*, ASCE Press, chapter 18. 395–420.

Lane, E. W.: 1954, The importance of fluvial morphology in hydraulic engineering. Technical Report Hydraulic Laboratory Report no. 372, United States Department of the Interior Bureau of Reclamation, Denver, Colorado.

— 1955, The importance of fluvial morphology in hydraulic engineering. *American Society of Civil Engineers. Proceedings*, **81**, 62–79.

Lane, E. W. and E. Carlson: 1953, Some factors affecting the stability of canals constructed in course granular materials. *Proceedings of International Association for Hydraulic Research, 5th International Hyd. Conv.*, Minneapolis, 37–48.

Langbein, W.: 1964, Geometry of river channels. *Journal of the Hydraulics Division, ASCE*, **90**, 301–311.

Langbein, W. and L. Leopold: 1964, Quasi-equilibrium states in channel morphology. *American Journal of Science*, **262**, 782–794.

Lawler, D. M., C. R. Thorne, and J. M. Hooke: 1997, *Bank Erosion and Instability*, John Wiley & Sons Ltd, England.

León, C.: 1998, *Morphology of the Middle Rio Grande from Cochiti Dam to Bernalillo Bridge, New Mexico*. Master's thesis, Colorado State University.

León, C., M. Sixta, and P. Julien: 2002, Hydraulic modeling on the middle Rio Grande, NM. Bernalillo Bridge reach. Technical report, Prepared for the U. S. Bureau of Reclamation,

Albuquerque, NM. Colorado State University. Engineering Research Center. Department of Civil Engineering., Fort Collins, Colorado.

Leopold, L. and T. J. Maddock: 1953, The hydraulic geometry of stream channels and some physiographic implications. *U. S. Geological Survey Professional Paper 252*, 57.

Mackin, J.: 1948, Concept of the graded river. *Bulleting of the Geological Society of America*, **59**, 463–512.

Maddock, T. J.: 1970, Indeterminate hydraulics of alluvial channels. *Journal of the Hydraulics Division*, **96**, 2309–2323.

Massong, T., T. Bauer, and M. Nemeth: 2000, Geomorphologic assessment of the Rio Grande. San Acacia Reach. DRAFT. Technical report, U. S. Department of the Interior. Bureau of Reclamation, Albuquerque, NM.

Maza-Alvarez, J. A. and C. Cruickshank-Villanueva: 1973, Stable channels in alluvium. *Sediment Transportation Proceedings of the International Association for Hydraulic Research. International Symposium on River Mechanics*, Asian Institute of Technology, Bangkok, Thailand, A61–1–A61–8.

Millar, R.: 2000, Influence of bank vegetation on alluvial channel patterns. *Water Resources Research*, **36**, 1109–1118.

Molinas, A. and B. Wu: 1998, Effect of size gradation on trasport of sediment mixtures. *Journal of Hydraulic Engineering*, **124**, 786–792.

— 2001, Transport of sediment in large sand-bed rivers. *Journal of Hydraulic Research*, **39**, 135–146.

Molnár, P.: 2001, *Precipitation and Erosion Dynamics in the Rio Puerco Basin*. Ph.D. Dissertation, Colorado State University. Fort Collins, CO.

Mosley, H. and S. Boelman: 1998, Santa Ana geomorphic report - DRAFT. Technical report, U. S. Bureau of Reclamation, Albuquerque, NM.

Mussetter Engineering, I.: 2002, Geomorphic and sedimentologic investigations of the middle Rio Grande between Cochiti dam and Elephant Butte reservoir. Technical report, Submitted to New Mexico Interstate Stream Commission, Albuquerque, New Mexico, Fort Collins, Colorado.

Nanson, G. and H. Huang: 1999, *Anabranching Rivers: Divided Efficiency Leading to Fluvial Diversity*, John Wiley & Sons, Ltd., chapter 19. 477–494.

Nevins, T.: 1969, River training. the single-thread channel. *New Zealand Engineering*, **24**, 367–373.

Nordin, C. and J. Beverage: 1965, Sediment transport in the Rio Grande New Mexico. Technical report, U. S. Geological Survey Professional Paper 462-F.

Nordin, C. and J. Culbertson: 1961, Particle-size distribution of stream bed material in the middle Rio Grande basin, New Mexico. *Short Papers in the Geologic and Hydrologic Sciences*, **Article 147-292**, C–323–C326.

Nouh, M.: 1988, Regime channels of an extremely arid zone. *International Conference on River Regime*, W. White, ed., John Wiley & Sons, Ltd., Wallingford, England, 55–66.

Osterkamp, W.: 1980, Sediment-morphology relations of alluvial channels. *Proceedings of the Symposium on Watershed Management*, American Society of Civil Engineers, 188–199.

Osterkamp, W. and E. Hedman: 1982, Perennial-streamflow characteristics related to channel geometry and sediment in missouri river basin. *U. S. Geological Survey Professional Paper 1242*, 37.

Parker, G.: 1978a, Self-formed straight rivers with equilibrium banks and mobile bed. part 1: The sand-silt river. *Journal of Fluid Mechanics, Cambridge, UK*, **89**, 109–125.

— 1978b, Self-formed straight rivers with equilibrium banks and moble bed. part 2: The gravel river. *Journal of Fluid Mechanics, Cambridge, UK*, **89**, 127–146.

— 1979, Hydraulic geometry of active gravel rivers. *Journal of the Hydraulics Division*, **105**, 1185–1201.

Pemberton, E. L.: 1964, Sediment investigations - middle Rio Grande. *Journal of the Hydraulics Division. ASCE*, **90**, 163–185.

Platania, S.: 1991, Fishes of the Rio Chama and upper Rio Grande, new mexico, with preliminary comments on their longitudinal distribution. *The Southwestern Naturalist*, **36**, 186–193.

Richard, G., C. León, and P. Julien: 2001, Hydraulic modelling on the middle Rio Grande, NM. Rio Puerco reach. Technical report, Prepared for the U. S. Bureau of Reclamation. Colorado State University. Engineering Research Center. Department of Civil Engineering, Fort Collins, Colorado.

Richard, G. A.: 2001, *Quantification and Prediction of Lateral Channel Adjustments Downstream from Cochiti Dam, Rio Grande, NM*. Ph.D. Dissertation, Colorado State University. Fort Collins, CO.

Richardson, E., D. Simons, and P. Julien: 1990, Highways in the river environment. Technical report, Prepared for the U. S. Department of Transportation. Federal Highway Administration. Civil Engineering Department. Engineering Research Center, Fort Collins, Colorado.

Rittenhouse, G.: 1944, Sources of modern sands in the middle Rio Grande valley, New Mexico. *The Journal of Geology*, **52**, 145–183.

Rivera-Trejo, F. and G. Soto-Cortés: 2002, Análisis comparativo del transporte de sedimentos con cambio granulométrico. *Ingeniería del Agua*, **9**, 73–79.

Robinson, S.: 1995, The life & times of Rio Grande minnows. *New Mexico Wildlife*, **40**, 2–5.

Salas, J., R. Smith, G. Tabios, and J. Heo: 1999, *Statistical Computing Techniques in Water Resources and Environmental Engineering*. Department of Civil Engineering. Colorado State University.

Sanchez, V. and D. Baird: 1997, River channel changes downstream of Cochiti dam. middle Rio Grande, New Mexico. *Proceedings of the Conference on Management of Landscapes Disturbed by Channel Incision*, E. J. L. Sam S. Y. Wang and F. D. S. Jr., eds.

Schumm, S.: 1977, *The Fluvial System*. Wiley, New York.

Schumm, S. and W. Lichty: 1965, Time, space, and causality in geomorphology. *American Journal of Science*, **263**, 110–119.

Schumm, S. A.: 1960, The shape of alluvial channels in relation to sediment type. *U. S. Geological Survey Professional Paper 352-B*, 18.

— 1963, A tentative classification of alluvial river channels. Technical Report Cicular 477, U. S. Geological Survey.

— 1969, River metamorphosis. *Journal of the Hydraulics Division, ASCE*, **95**, 255–273.

Scurlock, D.: 1998, From the rio to the sierra. an environmental history of the middle Rio Grande basin. Technical Report General Technical Report RMRS-GTR5, USDA. Forest Service, Rocky Mountain Research Station, Fort Collins, Colorado.

Simons, D. and M. Albertson: 1963, Uniform water conveyance channels in alluvial material. *Journal of the Hydraulics Division, ASCE. Proceedings Paper 3399*, **128**, 65–107.

Stanford, J., J. Ward, W. Liss, C. Frissel, R. Williams, J. Lichatowich, and C. Coutant: 1996, A general protocol for restoration of regulated rivers. *Regulated Rivers: Research & Management*, **12**, 391–413.

Stevens, H. J. and C. Yang: 1989, Summary and use of selected fluvial sediment-discharge formulas. Technical report, U. S. Geological Survey, Water Resources Report 89-4026.

Stevens, M.: 1989, Width of straight alluvial channels. *Journal of hydraulicsEngineering*, **115**, 309–326.

Stevens, M., D. Simons, and E. Richardson: 1975, Nonequilibrium river form. *Journal of the Hydraulics Division*, **101**, 557–566.

Taylor, J. and K. McDaniel: 2001, *Restoration of Saltcedar Infested Flood Plains on the Bosque del Apache national Wildlife Refuge*. Web Page Available at: http://bhg.fws.gov/Literature/newpage12.htm.

U. S. Army Corps of Engineers: 1998, *Hydrologic Engineering Center-River Analysis System. User's Manual. Version 2.2*. Hydrologic Engineering Center, Davis, California.

U. S. Bureau of Reclamation: 2000, Rio Grande and Low Flow Conveyance Channel Modifications. DRAFT environmental impact statement. Technical report, U. S. Department of the Interior. Bureau of Reclamation. Albuquerque Area Office, Albuquerque, New Mexico.

U. S. Fish and Wildlife Service: 1999, Final designation of critical habitat for the Rio Grande Silvery Minnow, 50 CFR part 17, federal register. v.64, no.128. Technical report, U. S. Fish and Wildlife Service.

U. S. Fish and Wildlife Service: 2000, *Southwestern Willow Flycatcher*. Web Page Available at: http://pacific.fws.gov/vfwo/SpeciesAccount/birds/SWWF.htm.

U. S. Fish and Wildlife Service: 2001, *Endangered Species Information*. Web Page Available at: http://ifw2ex.fws.gov/EndangeredSpecies/Lists/SpeciesInfo.cfm?speciesID=168.

Umbreit, N.: 2001, *Revegetation of Point Bars. Albuquerque Overbank Project*. Web Page Available at: http://bhg.fws.gov./point%20bars.htm.

Vanoni, V.: 1977, *Sedimentation Engineering*. The ASCE Task Committee for the Preparation of the Manual on Sedimentation of the Sedimentation Committee of the Hydraulics Division, New York.

Vanoni, V. A., N. Brooks, and J. Kennedy: 1960, Lecture notes on sediment tranportation and channel stability. Technical Report No. KH-R1, California Institute of Technology, Pasadena, California.

Wargadalam, J.: 1993, *Hydraulic Geometry Equations of Alluvial Channels*. Ph.D. Dissertation, Colorado State University.

Werritty, A.: 1997, *Short-term Changes in Channel Stability*, John Wiley & Sons Ltd, England.

White, W., R. Bettess, and E. Paris: 1982, Analytical approach to river regime. *Journal of the Hydraulics Division, ASCE*, **108**, 1179–1193.

Whitney, J.: 2001, *Observations on Southwestern Riparian Ecosystems*. Web Page Available at: http://bhg.fws.gov/Literature/whit1.htm.

Williams, G. and M. Wolman: 1984, Downstream effects of dams on alluvial rivers. *USGS Professional Paper 1286. U.S. Government Printing Office, Washington, D.C.*.

Wolman, M. and J. Miller: 1960, Magnitude and frequency of forces in geomorphic processes. *Journal of Geology*, **68**, 54–74.

Woodson, R. C.: 1961, Stabilization of the middle Rio Grande in New Mexico. *Journal of the Waterways and Harbors Division. ASCE*, **87**, 1–15.

Woodson, R. C. and J. Martin: 1962, The Rio Grande comprehensive plan in New Mexico and its effects on the river regime through the middle valley. *Control of Alluvial Rivers by Stell Jetties. American Society of Civil Engineers Proceedings, Water Ways and Harbors Division Journal 88*, E. Carlson and E. A. Dodge, eds., American Society of Civil Engineers, NY, NY, 53–81.

Yang, C. T.: 1973, Incipient motion and sediment transport. *Journal of the Hydraulics Division. ASCE*, **99**, 1679–1704.

— 1988, Dynamic adjustments of channel width and slope. *International Conference on River Regime*, W. White, ed., John Wiley & Sons, Ltd., 17–28.

Yu, B. and G. Wolman: 1987, Some dynamic aspects of river geometry. *Water Resources Research*, **23**, 501–509.

Appendix A

Sediment Transport and Resistance Equations

A summary of the sand-bed material sediment transport equations and the resistance equations that are used in this work is presented in this section. Also, the estimated bed material rating curves at the San Acacia and San Marcial gages are compared with the different sediment transport equations presented at the beginning of the appendix.

A.1 Sediment Transport Equations

- Engelund and Hansen

Engelund and Hansen (1967, from Julien 1995) developed the following equation to obtain sediment concentration by weight:

$$C_w = 0.05 \left(\frac{G}{G-1} \right) \frac{VS_f}{[(G-1)gd_s]^{\frac{1}{2}}} \frac{R_h S_f}{(G-1)d_s}$$

where S_f is the friction slope, d_s is the grain size, R_h is the hydraulic radius, V is the depth averaged velocity, g is the gravitational acceleration and G the specific gravity of sediment. This equation can be used with moderately sorted bed materials having mean fall diameter larger than 0.15 mm (Stevens and Yang, 1989).

- Ackers and White

Ackers and White (1973) developed a sediment transport equation in terms of three dimensionless groups: dimensionless grain diameter (D_{gr}), sediment mobility

($F_{gr}R$) and sediment transport (G_{gr}). Coarse sediment is considered to be transported mainly as a bed load and only part of the shear stress of the bed causes the movement of the sediment. Fine sediments are transported in suspension and the total shear stress causes the movement of fine particles.

The dimensionless grain diameter is defined as the cube root of the ratio of immersed weight to viscous forces:

$$D_{gr} = d_s \left[\frac{g(G-1)}{\nu^2}\right]^{\frac{1}{3}}$$

Where d_s is the particle size, g is the acceleration of gravity, G the specific gravity of the sediment and ν the kinematic viscosity.

The mobility number is defined as:

$$F_{gr} = \frac{u_*^b}{\sqrt{(g-1)d_s g}} \left[\frac{V}{\sqrt{32}\log\frac{10h}{d_s}}\right]^{1-b}$$

Where u_* is the shear velocity, V the mean velocity, h the mean depth, and b the transition exponent that depends on sediment size. For coarse sediment $b = 0$ and for fine sediments $b = 1$. The total sediment concentration by weight is expressed as:

$$C_w = CG\frac{d_s}{h}\left(\frac{V}{u_*}\right)^b \left[\frac{F_{gr}}{A} - 1\right]^m$$

for $1.0 < D_{gr} < 60.0$ (e.g.0.04 mm to 2.5 mm)

$n = 1.0 - 0.56 \log D_{gr}$

$\log C = 2.86 \log D_{gr} - \log {D_{gr}}^2 - 3.53$

$A = \frac{0.23}{D_{gr}^{\frac{1}{2}}} + 0.14$ and $m = \frac{9.66}{D_{gr}} + 1.34$

for $D_{gr} > 60.0$, $n = 0$, $C = 0.025$, $A = 0.17$, and $m = 1.50$

Ackers and White's equation overestimate the sediment transport of fine and very fine sands (Julien, 1995).

- Yang

Yang (1973) stated that the unit stream power of the time rate of potential energy expenditure per unit weight of water in an alluvial channel is the dominant factor in determining the total sediment concentration. The dimensionless regression equation for the total sediment concentration (Ct) in ppm by weight for sand is:

$$\begin{aligned}\log C_{ppm} &= 5.435 - 0.286 \log \frac{\omega d_s}{\nu} - 0.457 \log \frac{u_*}{\omega} \\ &\quad + \left(1.799 - 0.409 \log \frac{\omega d_s}{\nu} - 0.314 \log \frac{u_*}{\omega}\right) \\ &\quad x \log \left(\frac{VS}{\omega} - \frac{V_c S}{\omega}\right)\end{aligned}$$

Where C_{ppm} is the total sediment concentration in ppm by weight, V_c is the average flow velocity at incipient motion, VS is the unit stream power, VS/ω is the dimensionless unit stream power and V_c/ω is the dimensionless critical velocity expressed as:

$\frac{V_c}{\omega} = \frac{2.5}{\log u_* d_s/\nu} - 0.06 \quad \text{for } 1.2 < \frac{u_* D}{\nu} < 70$

and

$\frac{V_c}{\omega} = 2.05 \quad \text{for } \frac{u_* d_s}{\nu} \geq 70$

The data used to test the above equations cover the following ranges: particle size from 0.15 mm to 1.71 mm; channel width from 0.44 ft (0.134 m) to 1,746 ft (532 m); channel depth from 0.037 ft (0.011 m) to 49.9 ft (15.21 m) ; water temperatures between 0 C and 34.3 C; average water velocity from 0.75 fps (0.23 m/s) to 6.45 fps (1.96 m/s) ; slope from 0.000043 to 0.0279; and total sediment concentration between 10 ppm to 585,000 ppm (Yang, 1973).

- Julien

Julien (2002) proposed a simplified sand bed load transport formula. The equation expresses the unit sediment discharge by volume as a simple power function of the Shields parameter (τ_*) as follows:

$q_{bv} = 18\sqrt{g} d_S^{3/2} \tau_*^2 \quad \text{for } 0.1 < \tau_* < 1$

Where q_{bv} is the unit sediment discharge by volume, g is the gravitational acceleration, d_s is the particle size and $\tau_* = \frac{\tau}{(\gamma_s - \gamma)d_s}$, τ is the bed shear stress, γ_s is the specific weight of the sediment and γ is the specific weight of the water-mixture.

- Molinas and Wu

Molinas and Wu (2001) recently developed a sediment transport equation for large rivers, using the stream power concept and a large data set of field measurements, which include data from the Rio Grande (Molinas and Wu, 2001). The bed material concentration by dry-weight in parts per millions (C_t(ppm)) is given by the following equation:

$$C_t(ppm) = \frac{1430(0.86 + \sqrt{\psi})\psi^{1.5}}{0.016 + \psi} \tag{A.1}$$

Where ψ is the universal stream power given by

$$\psi = \frac{V^3}{(s_g - 1)gh\omega_{50}\left[\log\left(\frac{h}{d_{50}}\right)^2\right]} \tag{A.2}$$

V is the mean flow velocity, s_g is the relative density $= \rho/\rho_s$, g is the gravitational acceleration, h is the flow depth, and ω_{50} is the fall velocity of sediment corresponding to particle size d_{50}.

- Brownlie

Brownlie (1981) proposed the following equation to compute the sediment concentration in parts per million (C_{ppm}):

$$C_{ppm} = 7115C_F(F_g - F_{go})^{1.978}S^{0.6601}\left(\frac{r}{d_{50}}\right)^{-0.3301}$$

Where $C_F = 1$ for laboratory data and $C_F = 1.268$ for field data. F_g is the grain Froude number and F_{go} is the critical grain Froude number given by the following equations:

$$F_g = \frac{V}{\sqrt{\left(\frac{\rho_s - \rho}{\rho}\right) g d_{50}}}$$

$$F_{go} = 4.596 \tau_{*0}^{0.5293} S^{-0.1405} \sigma^{-0.1606}$$

Where $\tau_{*0} = 0.22Y + 0.06(10)^{-7.7Y}$, which defines the transformed Shields curve $\tau_{*0} = f(R_g)$, where R_g is the grain Reynolds number, $Y = (\sqrt{(\rho_s - \rho)/\rho} R_g)^{-0.6}$, r is the hydraulic radius, S is the friction slope, and d_{50} is the mean grain size.

A.2 Resistance Equations

This section presents a summary of the three different resistance equations used in this work.

- Manning

The Irish engineer Robert Manning developed the following resistance equation in 1889 (Chow, 1959):

$$V = \frac{\phi}{n} R_h^{2/3} S^{1/2}$$

Where ϕ is 1.49 for English units and 1 for metric units. R_h is the hydraulic radius, S is the friction slope, n is the Manning friction factor, and V is the mean velocity of the flow.

- Darcy-Weisbach

The Darcy-Weisbach resistance equation is as follows (Chow, 1959):

$$V = \sqrt{\frac{8g}{f}} R_h^{1/2} S^{1/2}$$

Where f is the Darcy-Weisbach friction factor, g is the gravitational acceleration, R_h is the hydraulic radius, S is the friction slope, and V is the mean velocity of the flow.

- Brownlie

Brownlie 1981 developed two resistance equations for lower and upper regimes, based on dimensionless analysis of nine variables and calibrating the equation coefficients and exponents with laboratory and field data for wide channels and rivers. The two proposed equations are:

For lower flow regime

$$\frac{rS}{d_{50}} = 0.3724(q_* S)^{0.6539} S^{0.09188} \sigma_g^{0.1050}$$

For upper flow regime

$$\frac{rS}{d_{50}} = 0.2836(q_* S)^{0.6248} S^{0.08750} \sigma_g^{0.08013}$$

Where r is the hydraulic radius, S is the slope, g is the gravitational acceleration, σ_g is the gradation coefficient of the bed material, d_{50} is the median grain size and $q_* = q/\sqrt{gD_{50}^3}$.

To determine the type of flow regime (upper or lower) under existing set of hydraulic conditions, Brownlie proposed a discriminator based on the slope (S), the grain Froude (F_g) number and a variable F_g'. Lower regime occurs when $F_g < 0.8F_g'$, where $F_g' = 1.74S - 1/3$. Upper regime occurs when $S > 0.006$ or $F_g > 1.25F_g'$.

A.3 Bed Material Rating Curves

Bed material data at the San Acacia and San Marcial gages were estimated from the total load reported by the U.S.G.S. (United States Geological Survey) from 1990 to 1997. In general, the washload comprises the fine particles not found in large quantities in the bed. One of the criteria to define the proportion of the bed material that consists of fine particles is to estimate the percentage of material in suspension that is finer than the d_{10} (particle size at which 10 % of the material by

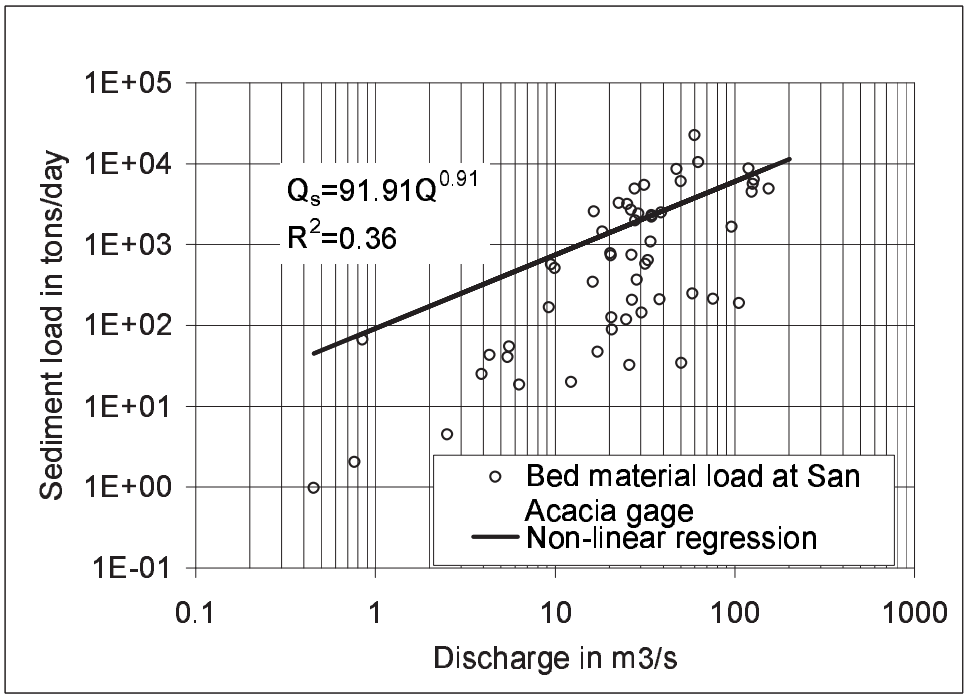

Figure A.1: Bed material data measured at the San Acacia gage from 1990 to 1997. The rating curve fitted to the data is indicated.

weight is finer) of the bed material (Julien, 1995). Therefore, the d_{10} of each bed material sample was determined. Then, the percent of material in suspension finer than the d_{10} of the bed corresponds to the percent of washload. The bed material is estimated as the total load minus the washload.

The following rating curves were generated from the data. A non-linear regression was fit to the data to avoid the problem of underestimating the sediment load predicted by the fitted equations (Ferguson 1986b, Duan (1983, from Helse and Hirsch 1995). The resulting bed material sediment load rating curves are $Q_s = 91.91Q^{0.91}$ and $Q_s = 18.38Q^{1.35}$ for San Acacia gage and San Marcial gage respectively. Figures A.1 and A.2 show the bed material load data and the non-linear regressions. In both cases there is a lot of scatter around the regression lines.

The sediment transport capacity was computed with the different sediment trans-

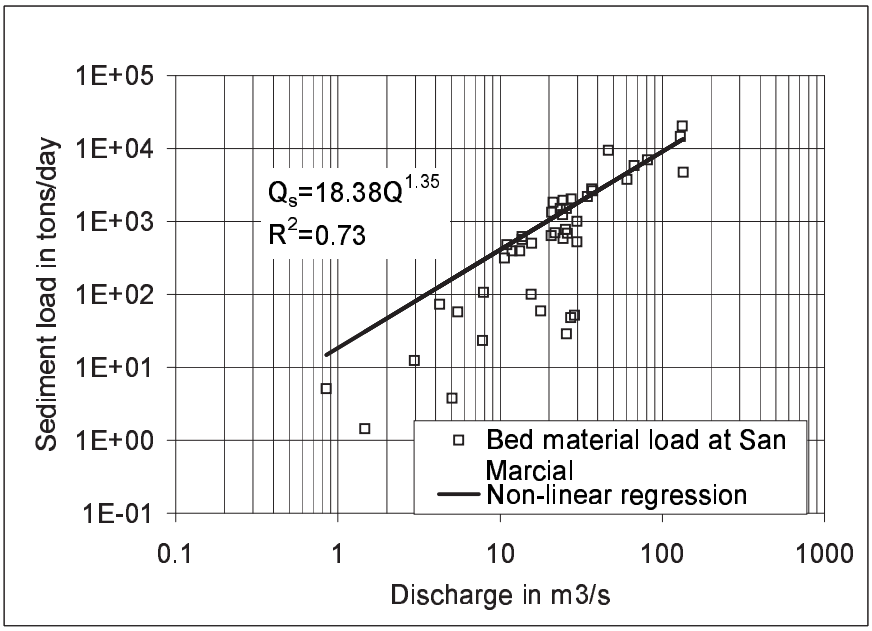

Figure A.2: Bed material data measured at the San Marcial gage from 1990 to 1997. The rating curve fitted to the data is indicated.

port equations presented in the previous section of this appendix and the hydraulic and sediment data at the San Acacia gage from 1990 to 1997. The results are plotted together with the bed material measurements at both stations in Figure A.3. The sediment transport capacities were compared with the bed material data, because there are not bed load measurements at these gages.

Regression lines were fit to the potential transport capacities predicted with each equation. Even though linear regressions underestimate the sediment load predicted by the fitted equations, they graphically represent better the data than the non-linear regression methods. The objective of fitting the regression lines was to summarize the data into single relationships for each sediment transport equation and compare them with the measurements, and not to make predictions with the regression equations. Figure A.4 shows the linear regression lines generated from the potential capacities predicted with each equation. For flow discharges greater

than about 20 m^3/s, all the equations, but Ackers and White's equation, converge to the same solutions.

Yang's (1973) equation was selected to perform the simulations for the field application in the Rio Grande, because this equation has been used previously in sediment transport modelling in the Rio Grande and its results have been in good agreement with field measured transport rates (Drew Baird, USBR, Albuquerque, NM, 2002 pers. comm.).

Figure A.5 shows the comparison between the potential transport capacity computed with Yang's equation based on the hydraulic and sediment data at San Acacia from 1997 to 1990 and the bed material loads at San Acacia and San Marcial gages during the same period. The comparison of the potential transport capacity values computed with Yang's equation (Figure A.5 show good agreement with the measurements.

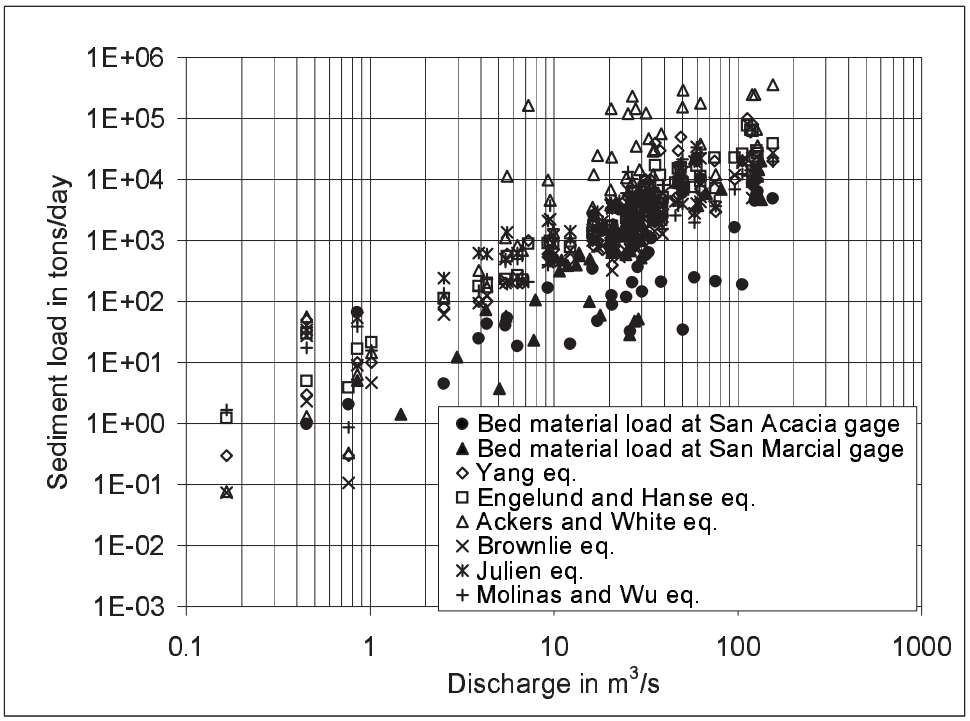

Figure A.3: Comparison of the bed material data measured at the San Acacia and San Marcial gages from 1990 to 1997 with the potential transport capacities computed with different sediment transport equations.

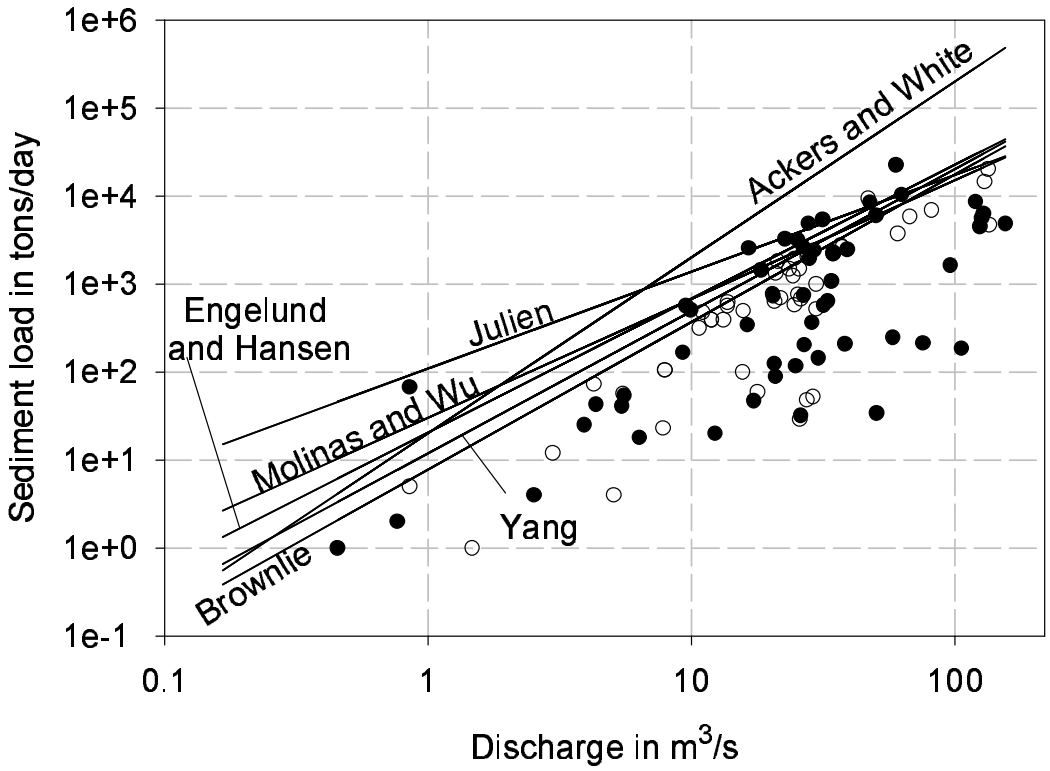

Figure A.4: Comparison of the bed material data at collected the San Acacia and San Marcial gages from 1990 to 1997 with the regression lines generated from the potential transport capacities computed with different sediment transport equations.

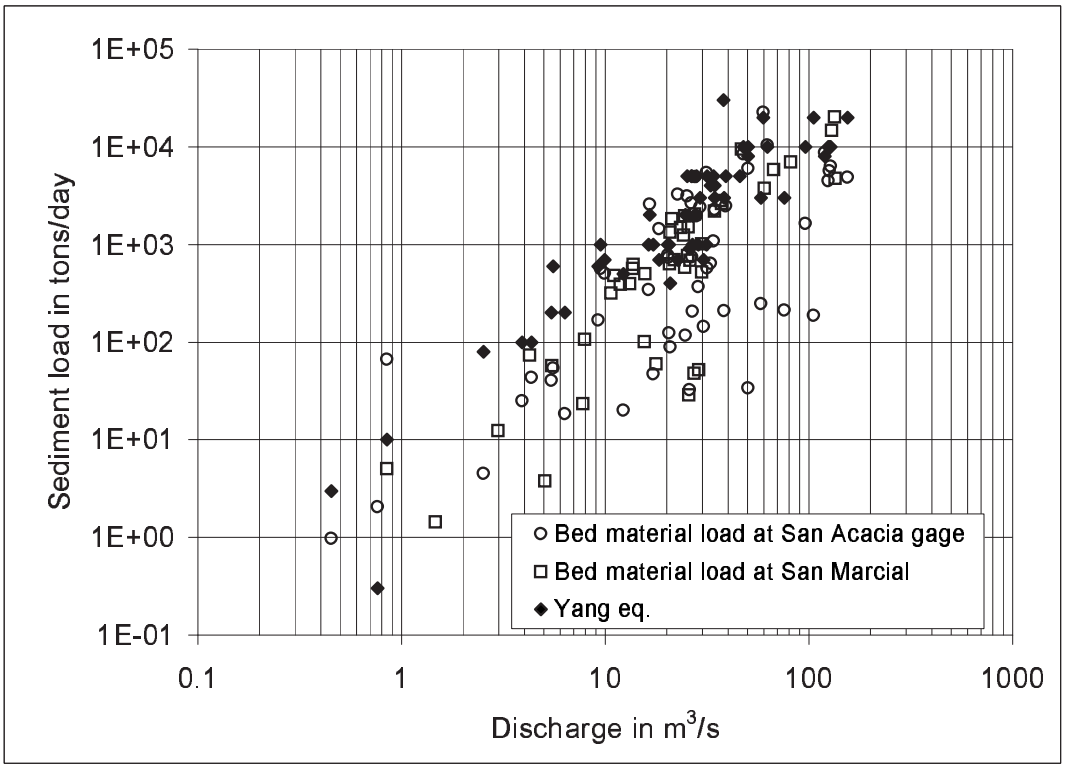

Figure A.5: Comparison of the bed material data measured at the San Acacia and San Marcial gages from 1990 to 1997 with the potential transport capacities computed with Yang's (1973) sediment transport equation.

Appendix B

Other Analytical Solutions

The developement of the width-depth ratio versus slope relationship using Julien's (2002) simplified transport equation and Darcy-Weisbach and Brownlie resistance equations are presented in this appendix.

B.1 Analytical Solution with Darcy-Weisbach Resistance Equation. Hydraulic Radius is approximated to the flow depth $R_h = h$

Under sediment transport equilibrium the following conditions are met: $Q_1 = Q_2$ and $Q_{s1} = Q_{s2}$. Replacing the resistance equation into the continuity equation, we obtain:

$$Q = VA = W\sqrt{\frac{8g}{f}}h^{3/2}S^{1/2}$$

The ratio of Q_1 and Q_2 is:

$$\frac{Q_2}{Q_1} = 1 = \frac{W_2 h_2^{3/2} S_2^{1/2}}{W_1 h_1^{3/2} S_1^{1/2}} = W_r h_r^{3/2} S_r^{1/2}$$

Solving for S_r we get:

$$S_r = \frac{1}{W_r^2 h_r^3} \tag{B.1}$$

Where W_r is the ratio of the widths, h_r is the ratio of the flow depths, and S_r is the ratio of the slopes.

The ratio of Q_{s2} and Q_{s1} is:

$$\frac{Q_{s2}}{Q_{s1}} = 1 = \frac{W_2 h_2^2 S_2^2}{W_1 h_1^2 S_1^2} = W_r h_r^2 S_r^2$$

Solving for S_r we get:

$$S_r = \frac{1}{W_r^{1/2} h_r} \tag{B.2}$$

Then, making equation B.1 equal to equation B.2 we obtain:

$$\frac{1}{W_r^2 h_r^3} = \frac{1}{W_r^{1/2} h_r} \Rightarrow h_r = W_r^{-3/4} \tag{B.3}$$

Replacing equation B.3 into equation B.1 we obtain:

$$S_r = W_r^{1/4}$$

$$S_r = h_r^{-1/3}$$

$$S_r = \left(\frac{W_r}{h_r}\right)^{1/7} = (\xi_r)^{1/7}$$

The ratio of the velocities is equal to:

$$\frac{V_2}{V_1} = h_r^{1/2} S_r^{1/2} \Rightarrow V_r = S_r^{-1}$$

B.2 Detailed Analytical Solution with Darcy-Weisbach Resistance Equation. Hydraulic Radius is different from the flow depth $R_h \neq h$

The cross section area (A) and the hydraulic radius (R_h) can be expressed as function of the width-depth ratio (ξ), then: $A = Wh = \xi h^2$ and $R_h = \frac{Wh}{W+2h} = \frac{\xi h}{\xi+2}$. Substituting R_h, A and V into the continuity and resistance equations the following expression is obtained:

$$\frac{Q}{A} = V = \sqrt{\frac{8g}{f}} \left(\frac{\xi h}{\xi + 2}\right)^{1/2} S^{1/2} \Rightarrow \frac{Q}{\xi h^2} = V = \sqrt{\frac{8g}{f}} \left(\frac{\xi h}{\xi + 2}\right)^{1/2} S^{1/2}$$

Solving for h:

$$h = \frac{Q^{2/5}}{S^{1/5}} \left(\frac{f}{8g}\right)^{1/5} \frac{(\xi+2)^{1/5}}{\xi^{3/5}}$$

Then, the width is:

$$W = \xi h = \frac{Q^{2/5}}{S^{1/5}} \left(\frac{f}{8g}\right)^{1/5} (\xi+2)^{1/5} \xi^{2/5}$$

Replacing W and h into the sediment transport equation:

$$Q_s = 18 g^{1/2} d_s^{3/2} W \frac{R_h^2 S^2}{(G-1)^2 d_s^2}$$

$$Q_s = \frac{18 g^{1/2}}{d_s^{1/2}(G-1)^2} W S^2 \frac{\xi^2}{(\xi+2)^2} h^2 \tag{B.4}$$

$$Q_s = \frac{18 g^{1/2}}{d_s^{1/2}(G-1)^2} W S^2 \frac{\xi^2}{(\xi+2)^2} \left[\frac{Q^{2/5}}{S^{1/5}} \left(\frac{f}{8g}\right)^{1/5} \frac{(\xi+2)^{1/5}}{\xi^{3/5}}\right]^2$$

$$Q_s = \frac{18 g^{1/10}}{d_s^{1/2}(G-1)^2} S^{8/5} Q^{4/5} \left(\frac{f}{8}\right)^{2/5} \frac{\xi^{4/5}}{(\xi+2)^{8/5}} W$$

$$Q_s = \frac{18 g^{1/10}}{d_s^{1/2}(G-1)^2} S^{8/5} Q^{4/5} \left(\frac{f}{8}\right)^{2/5} \frac{\xi^{4/5}}{(\xi+2)^{8/5}} \left[\frac{Q^{2/5}}{S^{1/5}} \left(\frac{f}{8g}\right)^{1/5} (\xi+2)^{1/5} \xi^{2/5}\right]$$

$$Q_s = \frac{18}{d_s^{1/2}(G-1)^2 g^{1/10}} S^{7/5} Q^{6/5} \left(\frac{f}{8}\right)^{3/5} \frac{\xi^{6/5}}{(\xi+2)^{7/5}}$$

Solving for S

$$S = \frac{Q_s^{5/7}}{Q^{6/7}} \frac{d_s^{5/14} g^{1/14} (G-1)^{10/7}}{18^{5/7}} \left(\frac{8}{f}\right)^{3/7} \frac{(\xi+2)}{\xi^{6/7}}$$

B.3 Analytical Solution with Brownlie Resistance Equation. Hydraulic Radius is approximated to the flow depth $R_h = h$

Brownlie (1981) developed one flow resistance equation for lower regime and another one for upper regime. Both equations are of the same form but with different coefficients and exponents. These resistance equations can be expressed as:

$$r = h = a\left(\frac{Vh}{g^{1/2}d_s^{3/2}}\right)^X S^Y \sigma_g^Z d_s^T \tag{B.5}$$

Replacing the continuity equation into the above equation and solving for h:

$$h = a\frac{Q^X}{h^X W^X}\frac{h^X}{g^{X/2}d_s^{3X/2}} S^Y \sigma_g^Z d_s^T$$

$$h = a\frac{Q^X}{W^X g^{X/2}d_s^{3X/2}} S^Y \sigma_g^Z d_s^T$$

Replacing channel width as $W = \xi h$:

$$h = a\frac{Q^X}{\xi^X h^X g^{X/2}d_s^{3X/2}} S^Y \sigma_g^Z d_s^T$$

And solving for h:

$$h = \frac{a^{\frac{1}{1+X}} Q^{\frac{X}{1+X}} S^{\frac{Y}{1+X}} \sigma_g^{\frac{Z}{1+X}}}{\xi^{\frac{X}{X+1}} g^{\frac{X}{2(X+1)}} d_s^{\frac{3X-2T}{2(1+X)}}}$$

Replacing $W = \xi h$ and h into sediment transport equation we obtained:

$$Q_s = \frac{18g^{1/2}S^2}{d_s^{1/2}(G-1)^2} h^3 \xi$$

$$Q_s = \frac{18g^{1/2}S^2}{d_s^{1/2}(G-1)^2} \frac{a^{\frac{3}{1+X}} Q^{\frac{3X}{1+X}} S^{\frac{3Y}{1+X}} \sigma_g^{\frac{3Z}{1+X}}}{\xi^{\frac{3X}{1+X}} g^{\frac{3X}{2(1+X)}} d_s^{\frac{9X-6T}{2(1+X)}}} \xi$$

$$Q_s = \frac{18 g^{\frac{1-2X}{2(1+X)}} S^{\frac{2(1+X)+3Y}{1+X}} a^{\frac{3}{1+X}} Q^{\frac{3X}{1+X}} \sigma_g^{\frac{3Z}{1+X}}}{d_s^{\frac{10X-6T+1}{2(1+X)}} (G-1)^2 \xi^{\frac{3X}{1+X}-1}}$$

Solving for S:

$$S = \frac{Q_s^{\frac{1+X}{b}}}{Q^{\frac{3X}{b}}} \left[\frac{(G-1)^2}{18}\right]^{\frac{1+X}{b}} \frac{d_s^{\frac{10X-6T+1}{2b}} \xi^{\frac{2X-1}{b}}}{g^{\frac{1-2X}{2b}} a^{\frac{3}{b}} \sigma_g^{\frac{3Z}{b}}} \tag{B.6}$$

where $b = 2(1 + X) + 3Y$. For lower regime $a = 0.3724$, $X = 0.6539$, $Y = -0.2542$,$Z = 0.1050$ and $T = 1$, and for upper regime $a = 0.2836$, $X = 0.6248$, $Y = -0.2877$,$Z = 0.08013$ and $T = 1$.

Appendix C

Sensitivity Analysis

This appendix summarizes the procedure and the results of the sensitivity analysis of the width-depth ratio versus slope and width-versus slope relationships. This analysis was performed with the results obtained from all sediment transport equations (see Appendix 7.1) and Manning's and Darcy-Weisbach's resistance equations. The sensitivity analysis was not performed with Brownlie's resistance equations, because these equations produced multiple solutions for the same input data set making difficult the selection of the response variables.

C.1 Methodology

The effects of water discharge (Q), sediment size (d_s) and friction factor n, were tested. Sediment discharge (Q_s), which is an input to the models, was considered dependent of water discharge. For each water discharge (Q), a sediment discharge (Q_s) was estimated from the bed-material rating curve at the San Acacia gage (see Appendix 7.1 and Table C.1). However, to determine the sensitivity of the model to sediment discharge (Q_s) separately, for a single water discharge (Q) value, two different sediment discharge (Q_s) values were tested.

The water discharge values in Table C.1 correspond to the dominant discharge ($Q = 139\ m^3/s$), as defined in Chapter 3, the discharge equalled or exceeded 10 % of the time ($Q_{10} = 97\ m^3/s$), according to the flow duration curve at San Acacia from 1986 to 2000 (see Appendix E) and the mean annual flow at San Acacia ($\overline{Q} = 35\ m^3/s$) during the same period.

Q (m^3/s)	Q_s (ppm)
139	1179
97	730
35	272

Table C.1: Water discharge Q and sediment concentration Q_s values used in the sensitivity analysis.

Model solutions were compared to a reference solution. To determine the sensitivity to each input variable, each input variable was modified separately, and the model solution was compared to the reference solution. Figure C.1 is a scheme of all the input variable levels tested.

There were different reference solutions. When comparing the effect of changing the flow discharge from $Q = 139\ m^3/s$ to $Q = 97\ m^3/s$, the reference solution corresponds to the solution at $Q = 139\ m^3/s$ and from $Q = 97\ m^3/s$ to $Q = 35\ m^3/s$ the reference solution was at $Q = 97\ m^3/s$. When comparing the effect of the change in sediment size, the reference solution corresponds to the solution obtained with $d_s = 0.3\ mm$ and when comparing the effect of changing the friction factor from $n = 0.010$ to $n = 0.023$, the reference solution was the solution obtained with $n = 0.010$ and from $n = 0.023$ to $n = 0.040$, the reference solution was at $n = 0.023$.

The width versus slope and width-depth ratio versus slope relationships were characterized with four variables. These response variables were: the width at minimum slope, the width-depth ratio at minimum slope, and the exponents p and q of the following relationships $S_r = \left(\frac{W_r}{h_r}\right)^p$, and $S_r = W_r^q$, for large widths.

In a log-log plot of width (W) versus slope (S), the slope of the curve for large widths represents the exponent p. Similarly, the slope of the width-depth ratio (W/h) versus slope (S) curve, in log-log scale, for large width-depth ratios represents the exponent q. In order to estimate these exponents (p and q), the second derivative of the curves were computed numerically. Then, a straight line was defined as the

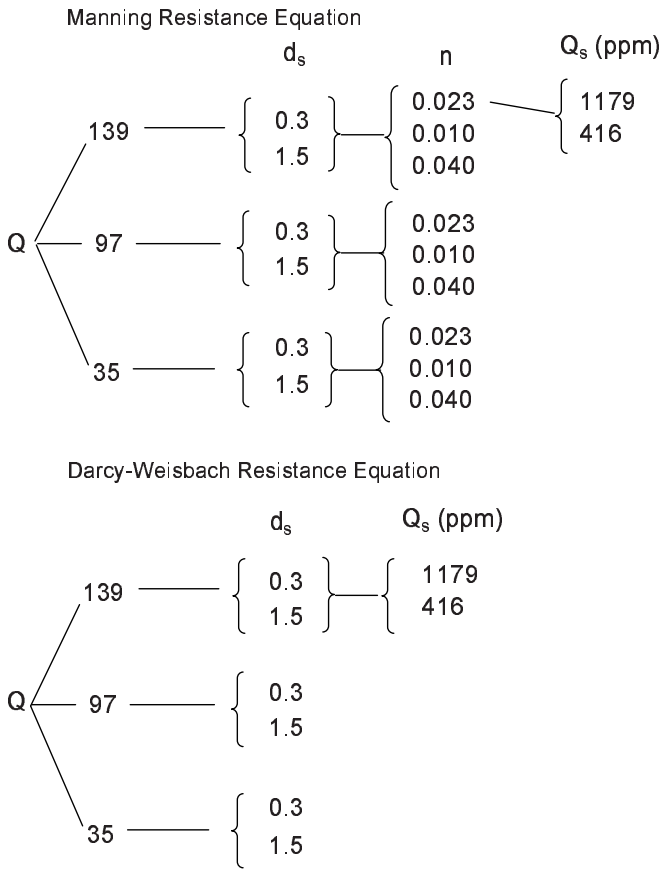

Figure C.1: Scheme showing the values of the input variables tested in the sensitivity analysis.

stretch of the function where the second derivative was less than 0.05. Once the straight part of the function was identified, the slope of was determined with a linear regression.

The effect of each input variable (x_j) into each one of the solution of the models (f_i) was evaluated with a Jacobian matrix (J). Each element of the matrix represents the partial derivative of the outcome variable with respect to the reference solution. The partial derivative is expressed as:

$$\frac{\partial f_i}{\partial x_i} = \frac{\frac{f_i' - f_i}{f_i'}}{\frac{x_j' - x_j}{x_j'}} \tag{C.1}$$

where, f_i ($i = 1 \ldots$ number of outcomes) is the outcome of the model and x_j ($j = 1 \ldots$ number of inputs)is the input. The superscript ' represents the reference state of the model.

The Jacobian matrix is defined by:

$$J(x_1 \ldots x_n) = \begin{bmatrix} \frac{\partial f_1}{\partial x_1} & \cdots & \frac{\partial f_1}{\partial x_n} \\ \vdots & \ddots & \vdots \\ \frac{\partial f_n}{\partial x_1} & \cdots & \frac{\partial f_n}{\partial x_n} \end{bmatrix} \tag{C.2}$$

C.2 Results

Tables C.2 to C.11 summarize the model responses to the different input values tested. These results correspond to the combined effect of changing sediment discharge as function of water discharge. Tables C.12 to C.15 summarize the model responses due to changes in sediment concentration only.

Tables C.16 and C.17 are the Jacobian matrixes for all sediment transport and Darcy-Weisbach and Manning resistance equations respectively. Each one of the elements of the matrix represents the partial derivative of the response variable with respect to a reference solution. These changes were considered negligible if its value was lower than 5 percent. A negative value means an increase in the response

Input variables			Width at minimum slope in m					
Q (m^3/s)	d_s (mm)	f	Julien	Yang	A and W	E and H	Brownlie	M and W
139	0.3	0.03	30	11	32	13	13	44
97	0.3	0.03	26	10	29	11	11	39
35	0.3	0.03	18	7	18	7	7	28

Input variables			Width at minimum slope in m					
Q (m^3/s)	d_s (mm)	f	Julien	Yang	A and W	E and H	Brownlie	M and W
139	1.5	0.03	27	11	369	11	11	47
97	1.5	0.03	23	10	223	9	9	42
35	1.5	0.03	16	7	63	6	6	32

Table C.2: Summary of the width values at minimum slope for all sediment transport equations, Darcy-Weisbach resistance equation and two different sediment sizes ($d_s = 0.3$ mm and 1.5 mm).

variable with respect to the reference solution.

Input variables			Width at minimum slope in m					
Q (m^3/s)	d_s (mm)	n	Julien	Yang	A and W	E and H	Brownlie	M and W
139	0.3	0.01	25	9	23	10	11	26
97	0.3	0.01	22	8	20	8	9	23
35	0.3	0.01	16	5	13	6	6	16

Input variables			Width at minimum slope in m					
Q (m^3/s)	d_s (mm)	n	Julien	Yang	A and W	E and H	Brownlie	M and W
139	0.3	0.023	39	11	27	12	12	26
97	0.3	0.023	35	10	23	11	11	23
35	0.3	0.023	24	7	15	7	7	16

Input variables			Width at minimum slope in m					
Q (m^3/s)	d_s (mm)	n	Julien	Yang	A and W	E and H	Brownlie	M and W
139	0.3	0.04	52	13	29	15	14	26
97	0.3	0.04	46	12	26	13	12	23
35	0.3	0.04	32	8	17	9	8	16

Input variables			Width at minimum slope in m					
Q (m^3/s)	d_s (mm)	n	Julien	Yang	A and W	E and H	Brownlie	M and W
139	1.5	0.023	35	11	51	11	11	25
97	1.5	0.023	31	10	41	9	9	22
35	1.5	0.023	22	7	23	6	6	16

Table C.3: Summary of the width values at minimum slope for all sediment transport equations and Manning resistance equation for two different sediment sizes and friction factors.

Input variables			Width-depth ratio at minimum slope in m					
Q (m^3/s)	d_s (mm)	f	Julien	Yang	A and W	E and H	Brownlie	M and W
139	0.3	0.03	12	1.84	13.49	2.13	2.16	24.95
97	0.3	0.03	12	2.02	14.4	2.05	2.06	25.19
35	0.3	0.03	12	2.19	12.37	1.9	1.87	26.3
Input variables			Width-depth ratio at minimum slope in m					
Q (m^3/s)	d_s (mm)	f	Julien	Yang	A and W	E and H	Brownlie	M and W
139	1.5	0.03	12	1.92	1265.4	2.19	2.1	32.92
97	1.5	0.03	12	2.09	672.94	1.96	1.88	33.64
35	1.5	0.03	12	2.25	147.5	2	1.88	38.62

Table C.4: Summary of the width-depth ratio values at minimum slope for all sediment transport equations, Darcy-Weisbach resistance equation and two different sediment sizes.

Input variables			Width-depth ratio at minimum slope in m					
Q (m^3/s)	d_s (mm)	n	Julien	Yang	A and W	E and H	Brownlie	M and W
139	0.3	0.01	18	1.95	9.31	2.18	2.06	10.15
97	0.3	0.01	18	2.02	9.22	1.84	1.81	10.21
35	0.3	0.01	18	1.69	8.48	2.27	1.76	10.11

Input variables			Width-depth ratio at minimum slope in m					
Q (m^3/s)	d_s (mm)	n	Julien	Yang	A and W	E and H	Brownlie	M and W
139	0.3	0.023	18	1.86	9.97	1.85	1.85	10.15
97	0.3	0.023	18	2.01	9.51	2.06	2.06	10.21
35	0.3	0.023	18	2.1	8.74	1.82	1.83	10.11

Input variables			Width-depth ratio at minimum slope in m					
Q (m^3/s)	d_s (mm)	n	Julien	Yang	A and W	E and H	Brownlie	M and W
139	0.3	0.04	18	1.92	9.85	2.04	2.11	10.15
97	0.3	0.04	18	2.14	10.24	2.02	2.05	10.21
35	0.3	0.04	18	2.04	9.43	2.12	2	10.11

Input variables			Width-depth ratio at minimum slope in m					
Q (m^3/s)	d_s (mm)	n	Julien	Yang	A and W	E and H	Brownlie	M and W
139	1.5	0.023	18	1.93	48.28	2.19	2.11	11.25
97	1.5	0.023	18	2.08	40.84	1.93	1.86	11.21
35	1.5	0.023	18	2.16	27.39	1.88	1.83	11.91

Table C.5: Summary of the width-depth ratio values at minimum slope for all sediment transport equations, Manning resistance equation and two different sediment sizes and friction factors.

			Julien			Yang		
Q (m^3/s)	d_s (mm)	f	q	r^2	range	q	r^2	range
139	0.3	0.03	0.3	1.000	180-600	0.27	1.000	94-600
97	0.3	0.03	0.3	1.000	157-600	0.28	1.000	84-600
35	0.3	0.03	0.3	1.000	106-600	0.3	1.000	62-600

			A and W			E and H		
Q (m^3/s)	d_s (mm)	f	q	r^2	range	q	r^2	range
139	0.3	0.03	--	--	--	0.4	1.000	111-600
97	0.3	0.03	--	--	--	0.4	1.000	96-600
35	0.3	0.03	--	--	--	0.4	1.000	63-600

			Brownlie			M and W		
Q (m^3/s)	d_s (mm)	f	q	r^2	range	q	r^2	range
139	0.3	0.03	0.4	1.0000	122-600	0.10	1.000	136-600
97	0.3	0.03	0.4	0.9999	108-600	0.10	1.000	119-600
35	0.3	0.03	0.4	0.9999	78-600	0.09	0.999	82-600

			Julien			Yang		
Q (m^3/s)	d_s (mm)	f	q	r^2	range	q	r^2	range
139	1.5	0.03	0.3	1.000	160-600	0.32	0.9999	105-600
97	1.5	0.03	0.3	1.000	140-600	0.33	0.9999	95-600
35	1.5	0.03	0.3	1.000	95-600	0.36	0.9995	76-389

			A and W			E and H		
Q (m^3/s)	d_s (mm)	f	q	r^2	range	q	r^2	range
139	1.5	0.03	--	--	--	0.4	1.000	93-600
97	1.5	0.03	--	--	--	0.4	1.000	80-600
35	1.5	0.03	--	--	--	0.4	1.000	53-600

			Brownlie			M and W		
Q (m^3/s)	d_s (mm)	f	q	r^2	range	q	r^2	range
139	1.5	0.03	0.4	0.9999	121-600	0.06	0.9986	112-570
97	1.5	0.03	0.4	0.9999	109-600	0.06	0.9987	97-455
35	1.5	0.03	0.4	0.9999	83-600	0.05	0.9959	66-249

Table C.6: Summary of the exponent q for all sediment transport equations and Darcy-Weisbach resistance equation for $f = 0.03$ and $d_s = 0.3$ mm and 1.5 mm. r^2 represents the correlation coefficient of the linear regression. The numbers in the Range column represent the range of widths from which the regression was generated. Missing values (–) could not be estimated.

			Julien			Yang		
Q (m^3/s)	d_s (mm)	n	q	r^2	range	q	r^2	range
139	0.3	0.023	0.14	1	171-600	0.34	0.9999	119-600
97	0.3	0.023	0.14	1	151-600	0.35	0.9999	110-600
35	0.3	0.023	0.14	1	106-600	0.36	1	111-200

			A and W			E and H		
Q (m^3/s)	d_s (mm)	n	q	r^2	range	q	r^2	range
139	0.3	0.023	---	---	---	0.42	1	116-600
97	0.3	0.023	---	---	---	0.42	1	101-600
35	0.3	0.023	---	---	---	0.42	1	68-600

			Brownlie			M and W		
Q (m^3/s)	d_s (mm)	n	q	r^2	range	q	r^2	range
139	0.3	0.023	0.49	1	166-600	0.33	1	157-600
97	0.3	0.023	0.49	1	150-600	0.33	1	137-600
35	0.3	0.023	0.51	1	117-600	0.32	0.9999	94-600

			Julien			Yang		
Q (m^3/s)	d_s (mm)	n	q	r^2	range	q	r^2	range
139	1.5	0.023	0.14	1	154-600	---	---	---
97	1.5	0.023	0.14	1	136-600	---	---	---
35	1.5	0.023	0.14	1	95-600	---	---	---

			A and W			E and H		
Q (m^3/s)	d_s (mm)	n	q	r^2	range	q	r^2	range
139	1.5	0.023	---	---	---	0.42	1	98-600
97	1.5	0.023	---	---	---	0.42	1	85-600
35	1.5	0.023	---	---	---	0.42	1	57-600

			Brownlie			M and W		
Q (m^3/s)	d_s (mm)	n	q	r^2	range	q	r^2	range
139	1.5	0.023	0.52	1	187-600	0.29	1	128-491
97	1.5	0.023	0.52	1	179-600	0.28	1	112-401
35	1.5	0.023	0.56	1	238-351	0.27	1	76-230

Table C.7: Summary of the exponent q for all sediment transport equations and Manning resistance equation for $n = 0.023$ and $d_s = 0.3$ mm and 0.5 mm. r^2 represents the correlation coefficient of the linear regression. The numbers in the Range column represent the range of widths from which the regression was generated. Missing values (–) could not be estimated.

			Julien			Yang		
Q (m^3/s)	d_s (mm)	n	q	r^2	range	q	r^2	range
139	0.3	0.01	0.14	1	111-600	0.33	0.9999	85-600
97	0.3	0.01	0.14	1	98-600	0.34	0.9999	76-600
35	0.3	0.01	0.14	1	68-600	0.35	0.9998	59-437

			A and W			E and H		
Q (m^3/s)	d_s (mm)	n	q	r^2	range	q	r^2	range
139	0.3	0.01	---	---	---	0.42	1	89-600
97	0.3	0.01	---	---	---	0.42	1	77-600
35	0.3	0.01	---	---	---	0.42	1	52-600

			Brownlie			M and W		
Q (m^3/s)	d_s (mm)	n	q	r^2	range	q	r^2	range
139	0.3	0.01	0.48	1	136-600	0.33	1	157-600
97	0.3	0.01	0.49	1	122-600	0.33	1	137-600
35	0.3	0.01	0.5	1	92-600	0.32	0.9999	94-600

			Julien			Yang		
Q (m^3/s)	d_s (mm)	n	q	r^2	range	q	r^2	range
139	0.3	0.04	0.14	1	229-600	0.35	0.9999	161-600
97	0.3	0.04	0.14	1	202-600	0.35	0.9999	159-495
35	0.3	0.04	0.14	1	142-600	---	---	---

			A and W			E and H		
Q (m^3/s)	d_s (mm)	n	q	r^2	range	q	r^2	range
139	0.3	0.04	---	---	---	0.42	1	89-600
97	0.3	0.04	---	---	---	0.42	1	120-600
35	0.3	0.04	---	---	---	0.42	1	81-600

			Brownlie			M and W		
Q (m^3/s)	d_s (mm)	n	q	r^2	range	q	r^2	range
139	0.3	0.04	0.49	1	190-600	0.33	1	157-600
97	0.3	0.04	0.5	1	173-600	0.33	1	137-600
35	0.3	0.04	0.52	1	140-600	0.32	0.9999	94-600

Table C.8: Summary of the exponent q for all sediment transport equations and Manning resistance equation for $n = 0.010$ and $n = 0.040$ and $d_s = 0.3$ mm. r^2 represents the correlation coefficient of the linear regression. The numbers in the Range column represent the range of widths from which the regression was generated. Missing values (–) could not be estimated.

			Julien			Yang		
Q (m^3/s)	d_s (mm)	f	p	r^2	range	p	r^2	range
139	0.3	0.03	0.14	1	87-2270	0.15	0.9996	24-2480
97	0.3	0.03	0.14	1	87-2885	0.16	0.9996	24-3190
35	0.3	0.03	0.14	1	87-5666	0.17	0.9994	25-6556

			A and W			E and H		
Q (m^3/s)	d_s (mm)	f	p	r^2	range	p	r^2	range
139	0.3	0.03	0.15	0.999	149-2275	0.22	0.9999	36-2415
97	0.3	0.03	0.14	0.998	157-2929	0.22	0.9999	35-3141
35	0.3	0.03	0.19	0.999	181-6109	0.22	0.9999	35-6615

			Brownlie			M and W		
Q (m^3/s)	d_s (mm)	f	p	r^2	range	p	r^2	range
139	0.3	0.03	0.19	1	32-2296	0.06	0.9998	74-2143
97	0.3	0.03	0.19	1	32-2968	0.06	0.9998	73-2650
35	0.3	0.03	0.20	1	34-6184	0.05	0.9995	73-4820

			Julien			Yang		
Q (m^3/s)	d_s (mm)	f	p	r^2	range	p	r^2	range
139	1.5	0.03	0.14	1	87-2776	0.18	0.9997	29-2703
97	1.5	0.03	0.14	1	86-3524	0.18	0.9996	29-3475
35	1.5	0.03	0.14	1	86-6929	0.2	0.9992	32-7178

			A and W			E and H		
Q (m^3/s)	d_s (mm)	f	p	r^2	range	p	r^2	range
139	1.5	0.03	---	---	---	0.22	0.9999	36-3332
97	1.5	0.03	---	---	---	0.22	0.9999	36-4334
35	1.5	0.03	---	---	---	0.22	0.9999	34-9127

			Brownlie			M and W		
Q (m^3/s)	d_s (mm)	f	p	r^2	range	p	r^2	range
139	1.5	0.03	0.20	1	34-3079	0.04	0.9989	68-2447
97	1.5	0.03	0.21	1	35-4001	0.03	0.9977	69-3011
35	1.5	0.03	0.22	1	36-8471	0.02	0.9833	66-5388

Table C.9: Summary of the exponent p for all sediment transport equations and Darcy-Weisbach resistance equation for $f = 0.03$ and $d_s = 0.3$ mm and 1.5 mm. r^2 represents the correlation coefficient of the linear regression. The numbers in the Range column represent the range of widths from which the regression was generated. Missing values (–) could not be estimated.

			Julien			Yang		
Q (m^3/s)	d_s (mm)	n	p	r^2	range	p	r^2	range
139	0.3	0.023	0.09	0.9993	75-1633	0.2	0.9997	33-2070
97	0.3	0.023	0.09	0.9993	74-2004	0.2	0.9996	34-2613
35	0.3	0.023	0.09	0.9995	75-3576	0.21	0.9994	25-5099

			A and W			E and H		
Q (m^3/s)	d_s (mm)	n	p	r^2	range	p	r^2	range
139	0.3	0.023	0.23	0.9997	155-2048	0.24	0.9999	40-1947
97	0.3	0.023	0.24	0.9997	160-2599	0.24	0.9999	41-2473
35	0.3	0.023	0.26	0.9996	174-5182	0.24	0.9999	39-4867

			Brownlie			M and W		
Q (m^3/s)	d_s (mm)	n	p	r^2	range	p	r^2	range
139	0.3	0.023	0.27	0.9999	50-2060	0.19	1	100-2143
97	0.3	0.023	0.28	0.9999	51-2633	0.19	1	99-2650
35	0.3	0.023	0.29	0.9998	52-5314	0.19	1	96-4820

			Julien			Yang		
Q (m^3/s)	d_s (mm)	n	p	r^2	range	p	r^2	range
139	1.5	0.023	0.09	0.9994	75-1940	0.22	0.9996	41-2251
97	1.5	0.023	0.09	0.9994	75-2368	0.23	0.9995	43-2847
35	1.5	0.023	0.09	0.9995	74-4250	0.25	0.999	49-5628

			A and W			E and H		
Q (m^3/s)	d_s (mm)	n	p	r^2	range	p	r^2	range
139	1.5	0.023	---	---	---	0.24	0.9999	40-2609
97	1.5	0.023	---	---	---	0.24	0.9999	40-3314
35	1.5	0.023	---	---	---	0.24	1	39-6522

			Brownlie			M and W		
Q (m^3/s)	d_s (mm)	n	p	r^2	range	p	r^2	range
139	1.5	0.023	0.29	0.9998	55-2732	0.17	1	92-2447
97	1.5	0.023	0.29	0.9998	56-3511	0.17	0.9999	90-3011
35	1.5	0.023	0.31	0.9998	61-7213	0.16	0.9996	88-5388

Table C.10: Summary of the exponent p for all sediment transport equations and Manning resistance equation for $n = 0.023$ and $d_s = 0.3$ mm and 1.5 mm. r^2 represents the correlation coefficient of the linear regression. The numbers in the Range column represent the range of widths from which the regression was generated. Missing values (–) could not be estimated.

			Julien			Yang		
Q (m^3/s)	d_s (mm)	n	p	r^2	range	p	r^2	range
139	0.3	0.01	0.09	0.9994	74-3335	0.19	0.9997	31-3020
97	0.3	0.01	0.09	0.9995	73-4092	0.19	0.9997	31-3811
35	0.3	0.01	0.09	0.9996	75-7303	0.2	0.9995	32-7412

			A and W			E and H		
Q (m^3/s)	d_s (mm)	n	p	r^2	range	p	r^2	range
139	0.3	0.01	0.24	0.9997	167-2578	0.24	0.9999	40-3067
97	0.3	0.01	0.25	0.9996	171-3289	0.24	0.9999	41-3895
35	0.3	0.01	0.28	0.9996	185-6663	0.24	1	40-7667

			Brownlie			M and W		
Q (m^3/s)	d_s (mm)	n	p	r^2	range	p	r^2	range
139	0.3	0.01	0.27	0.9999	49-2603	0.19	1	100-2143
97	0.3	0.01	0.28	0.9999	49-3324	0.19	1	99-2650
35	0.3	0.01	0.28	0.9998	51-6684	0.19	1	96-4820

			Julien			Yang		
Q (m^3/s)	d_s (mm)	n	p	r^2	range	p	r^2	range
139	0.3	0.04	0.09	0.9992	75-1016	0.2	0.9996	35-1614
97	0.3	0.04	0.09	0.9993	75-1247	0.2	0.9996	35-2038
35	0.3	0.04	0.09	0.9994	74-2226	0.22	0.9993	38-3990

			A and W			E and H		
Q (m^3/s)	d_s (mm)	n	p	r^2	range	p	r^2	range
139	0.3	0.04	0.22	0.9997	149-1766	0.24	0.9999	40-3067
97	0.3	0.04	0.23	0.9997	153-2234	0.24	0.9999	40-1828
35	0.3	0.04	0.25	0.9996	166-4411	0.24	0.9999	40-3599

			Brownlie			M and W		
Q (m^3/s)	d_s (mm)	n	p	r^2	range	p	r^2	range
139	0.3	0.04	0.28	0.9999	52-1764	0.19	1	100-2143
97	0.3	0.04	0.28	0.9999	52-2257	0.19	1	99-2650
35	0.3	0.04	0.29	0.9998	54-4567	0.19	1	96-4820

Table C.11: Summary of the exponent p for all sediment transport equations and Manning resistance equation for $n = 0.010$ and $n = 0.040$ and $d_s = 0.3$ mm. r^2 represents the correlation coefficient of the linear regression. The numbers in the Range column represent the range of widths from which the regression was generated.

			Width at minimum slope					
Q_s (ppm)	d_s (mm)	f	Julien	Yang	A and W	E and H	Brownlie	M and W
1179	0.3	0.03	30	11	32	13	13	44
416	0.3	0.03	34	13	35	14	14	52

			Width to depth ration at minimum slope					
Q_s (ppm)	d_s (mm)	f	Julien	Yang	A and W	E and H	Brownlie	M and W
1179	0.3	0.03	12	1.84	13.49	2.13	2.16	24.95
416	0.3	0.03	12	2.03	12.47	1.97	1.95	23.93

Table C.12: Summary of the width-depth ratios and widths at minimum slope for all sediment transport equations, Darcy-Weisbach resistance equation, and two different sediment concentrations.

			q			
			Julien	Yang		
Q_s (ppm)	d_s (mm)	f	q	q	r^2	range
1179	0.3	0.03	0.25	0.27	0.9999	94-600
416	0.3	0.03	0.25	0.29	0.9999	115-600

			q			
			A and W	E and H		
Q_s (ppm)	d_s (mm)	f		q	r^2	range
1179	0.3	0.03	---	0.4	1	111-600
416	0.3	0.03	---	0.4	1	124-600

			q					
			Brownlie			M and W		
Q_s (ppm)	d_s (mm)	f	q	r^2	range	q	r^2	range
1179	0.3	0.03	0.35	1	122-600	0.10	0.9999	136-600
416	0.3	0.03	0.36	1	156-600	0.10	1	166-600

			p			
			Julien	Yang		
Q_s (ppm)	d_s (mm)	f	p	p	r^2	range
1179	0.3	0.03	0.14	0.15	0.9996	24-2480
416	0.3	0.03	0.14	0.16	0.9996	26-2059

			p					
			A and W			E and H		
Q_s (ppm)	d_s (mm)	f	p	r^2	range	p	r^2	range
1179	0.3	0.03	0.15	0.999	149-2275	0.22	0.9999	36-2415
416	0.3	0.03	0.18	0.9993	184-1877	0.22	0.9999	37-1961

			p					
			Brownlie			M and W		
Qs ppm	ds (mm)	f	p	r^2	range	p	r^2	range
1179	0.3	0.03	0.19	0.9998	32-2296	0.06	0.9998	74-2143
416	0.3	0.03	0.2	0.9997	35-1862	0.06	0.9997	74-1552

Table C.13: Summary of the exponents p and q for all sediment transport equations, Darcy-Weisbach resistance equation, and two different sediment concentrations. r^2 represents the correlation coefficient of the linear regression. The numbers in the Range column represent the range of widths from which the regression was generated.

			Width at minimum slope					
Q_s (ppm)	d_s (mm)	n	Julien	Yang	A and W	E and H	Brownlie	M and W
1179	0.3	0.023	39	11	27	12	12	26
416	0.3	0.023	45	13	29	14	14	32

			Width to depth ration at minimum slope					
Q_s (ppm)	d_s (mm)	n	Julien	Yang	A and W	E and H	Brownlie	M and W
1179	0.3	0.023	18	1.86	9.97	1.85	1.85	10.15
416	0.3	0.023	18	2.07	8.98	2.03	1.98	10.43

Table C.14: Summary of the width-depth ratios and widths at minimum slope for all sediment transport equations, Manning resistance equation, and two different sediment concentrations.

			q			
			Julien	Yang		
Q_s (ppm)	d_s (mm)	n	q	q	r^2	range
1179	0.3	0.023	0.14	0.34	0.9999	119-600
416	0.3	0.023	0.14	0.36	0.9999	159-600

			q			
			A and W	E and H		
Q_s (ppm)	d_s (mm)	n		q	r^2	range
1179	0.3	0.023	---	0.42	1	116-600
416	0.3	0.023	---	0.42	1	129-600

			q					
			Brownlie			M and W		
Q_s (ppm)	d_s (mm)	n	q	r^2	range	q	r^2	range
1179	0.3	0.023	0.49	1	166-600	0.33	1	157-600
416	0.3	0.023	0.51	1	232-600	0.34	1	192-600

			p			
			Julien	Yang		
Q_s (ppm)	d_s (mm)	n	p	p	r^2	range
1179	0.3	0.023	0.08	0.2	0.9997	33-2070
416	0.3	0.023	0.08	0.21	0.9997	36-1740

			p					
			A and W			E and H		
Q_s (ppm)	d_s (mm)	n	p	r^2	range	p	r^2	range
1179	0.3	0.023	0.23	0.9997	155-204	0.24	0.9999	40-1947
416	0.3	0.023	0.25	0.9997	179-169	0.24	0.9999	40-1611

			p					
			Brownlie			M and W		
Q_s (ppm)	d_s (mm)	n	p	r^2	range	p	r^2	range
1179	0.3	0.023	0.27	0.9999	50-2060	0.19	1	100-2143
416	0.3	0.023	0.24	0.9999	319-1689	0.20	1	100-1552

Table C.15: Summary of the exponents p and q for all sediment transport equations,Manning resistance equation, and two different sediment concentrations.r^2 represents the correlation coefficient of the linear regression. The numbers in the Range column represent the range of widths from which the regression was generated.

	Input Variables	ds = 0.3	ds = 0.3	Q = 139	Q = 97	ds = 0.3
		f = 0.03	f = 0.03	f = 0.03	f = 0.03	f = 0.03
	Modified Variable	Q (m^3/s)	Q (m^3/s)	ds (mm)	ds (mm)	Qs (ppm)
	Initial Value	139	97	0.3	0.3	1179
	Modified Value (New)	97	35	1.5	1.5	416
		Julien Eq.				
Response Variables	Width at min S	0.441	0.481	-0.025	-0.029	-0.206
	W/h at min S	0.000	0.000	0.000	0.000	0.000
	q	0.000	0.000	0.000	0.000	0.000
	p	0.000	0.000	0.000	0.000	0.000
		Yang Eq.				
	Width at min S	0.301	0.469	0.000	0.000	-0.281
	W/h at min S	-0.324	-0.132	0.011	0.009	-0.160
	q	-0.123	-0.112	0.001	0.045	-0.114
	p	-0.221	-0.098	0.050	0.031	-0.103
		Ackers and White Eq.				
	Width at min S	0.310	0.593	2.633	1.672	-0.145
	W/h at min S	-0.223	0.221	23.201	11.433	0.117
	q	--	--	--	--	--
	p	0.221	-0.559	--	--	-0.309
		Engelund and Hanse Eq.				
	Width at min S	0.509	0.569	-0.038	-0.045	-0.119
	W/h at min S	0.124	0.114	0.007	-0.011	0.116
	q	0.000	0.000	0.000	0.000	0.000
	p	0.000	0.000	0.000	0.000	0.000
		Brownlie Eq.				
	Width at min S	0.509	0.569	-0.038	-0.045	-0.119
	W/h at min S	0.153	0.144	-0.007	-0.022	0.150
	q	0.000	-0.045	0.014	0.014	-0.044
	p	0.000	-0.082	0.013	0.026	-0.081
		Molinas and Wu Eq.				
	Width at min S	0.376	0.441	0.017	0.019	-0.281
	W/h at min S	-0.032	-0.069	0.080	0.084	0.063
	q	0.000	0.156	-0.100	-0.100	0.000
	p	0.000	0.261	-0.083	-0.125	0.000

Table C.16: Jacobian matrixes for all sediment transport equations and Darcy-Weisbach resistance equation. The four rows at the top of the table contain the input values to the model. Each element of the matrix represents the partial derivative of the response variable with respect to the reference solution obtained with the data in the first three rows of the table.

	Input Variables	d_s = 0.3 mm	d_s = 0.3 mm	d_s = 0.3 mm	ds = 0.3 mm	Q = 139 m^3/s	Q = 97 m^3/s	Q = 139 m^3/s	Q = 97 m^3/s	Q = 139 m^3/s	Q = 97 m^3/s	d_s = 0.3 mm
		n= 0.023	n= 0.023	n= 0.010	n= 0.010	n = 0.023	n = 0.023	d_s = 0.3 mm	d_s = 0.3 mm	d_s = 0.3 mm	d_s = 0.3 mm	n = 0.023
	Modified Variable	Q (m^3/s)	Q (m^3/s)	Q (m^3/s)	Q (m^3/s)	d_s	d_s	n	n	n	n	Q_s (ppm)
	Initial Value	139	97	139	97	0.3	0.3	0.01	0.01	0.023	0.023	1179
	Modified Value (New)	97	35	97	35	1.5	1.5	0.023	0.023	0.04	0.04	416
		Julien Eq.										
Response Variable	Width at min S	0.339	0.492	0.397	0.427	-0.026	-0.029	0.431	0.455	0.451	0.425	-0.238
	W/h at min S	0.000	0.000	0.000	0.000	0.000	0.000	0.000	0.000	0.000	0.000	0.000
	q	0.000	0.000	0.000	0.000	0.000	0.000	0.000	0.000	0.000	0.000	0.000
	p	0.000	0.000	0.000	0.000	0.000	0.000	0.000	0.000	0.000	0.000	0.000
		Yang Eq.										
	Width at min S	0.301	0.469	0.368	0.587	0.000	0.000	0.171	0.192	0.246	0.271	-0.281
	W/h at min S	-0.267	-0.070	-0.119	0.256	0.009	0.009	-0.036	-0.004	0.044	0.088	-0.174
	q	-0.097	-0.045	-0.100	-0.046			0.023	0.023	0.040	0.000	-0.091
	p	0.000	-0.078	0.000	-0.082	0.025	0.038	0.040	0.040	0.000	0.000	-0.077
		Ackers and White Eq.										
	Width at min S	0.490	0.544	0.432	0.548	0.222	0.196	0.134	0.115	0.100	0.176	-0.114
	W/h at min S	0.153	0.127	0.032	0.126	0.961	0.824	0.055	0.024	-0.016	0.104	0.153
	q											
	p	-0.144	-0.130	-0.138	-0.188			-0.032	-0.031	-0.059	-0.056	-0.134
		Engelund and Hanse Eq.										
	Width at min S	0.276	0.569	0.662	0.391	-0.021	-0.045	0.154	0.288	0.338	0.246	-0.258
	W/h at min S	-0.376	0.182	0.516	-0.366	0.046	-0.016	-0.116	0.092	0.139	-0.026	-0.150
	q	0.000	0.000	0.000	0.000	0.000	0.000	0.000	0.000	0.000	0.000	0.000
	p	0.000	0.000	0.000	0.000	0.000	0.000	0.000	0.000	0.000	0.000	0.000
		Brownlie Eq.										
	Width at min S	0.276	0.569	0.602	0.522	-0.021	-0.045	0.070	0.171	0.225	0.123	-0.258
	W/h at min S	-0.376	0.175	0.402	0.043	0.035	-0.024	-0.078	0.106	0.190	-0.007	-0.109
	q	0.000	-0.064	-0.069	-0.032	0.015	0.015	0.016	0.000	0.000	0.028	-0.063
	p	-0.123	-0.056	-0.123	0.000	0.019	0.009	0.000	0.000	0.050	0.000	0.172
		Molinas and Wu Eq.										
	Width at min S	0.382	0.476	0.382	0.476	-0.010	-0.011	0.000	0.000	0.000	0.000	-0.357
	W/h at min S	-0.020	0.015	-0.020	0.015	0.027	0.024	0.000	0.000	0.000	0.000	-0.043
	q	0.000	0.047	0.000	0.047	-0.030		0.000	0.000	0.000	0.000	-0.047
	p	0.000	0.000	0.000	0.000	-0.026	-0.026	0.000	0.000	0.000	0.000	-0.081

Table C.17: Jacobian matrixes for all sediment transport equations and Manning resistance equation. The four rows at the top of the table contain the input values to the model. Each element of the matrix represents the partial derivative of the response variable with respect to the reference solution obtained with the data in the first three rows of the table.

Appendix D

Effect of Sediment Concentration

The effect of sediment concentration on the time to equilibrium can be tested with the simulations performed to design the temporarily channel at the downstream end of the middle Rio Grande, that conveys the water into Elephant Butte Reservoir. The temporarily channel consists of a wide middle reach (Subreach 2), located between to narrow reaches (Subreach 1 (upstream) and Subreach 2 (downstream)). Table D.1 summarizes the geometric characteristics of the channel, the sediment size, and the roughness coefficient used in the simulations. The change in width between Subreaches 1 and 2 and between Subreaches 2 and 3 were simulated with a transition of 200 m. The upstream and downstream nodes were fixed for this simulation, in order to control the downstream degradation.

Two different cases (A and B) were studied. In case A, the incoming sediment transport to the model was not specified. In case B, the incoming sediment load to the channel at the first upstream node was estimated with a sediment rating curve.

Subreach	Width (m)	Length (m)	Initial Slope (m/m)	n	d_s (mm)
1 (narrow-upstream)	76	4200	0.00143	0.024	0.22
2 (wide-middle)	91	400	0.00145	0.024	0.22
3 (narrow-upstream)	76	6200	0.00172	0.024	0.22

Table D.1: Summary of data input into the quasi-steady state model to design the temporarily channel upstream from Elephant Butte Reservoir.

In both cases, the sediment transport along the channel was computed with Yang's (1973) equation. The sediment rating curve used is $Q_s = 0.05Q^{1.6224}$, where Q is the discharge in cubic feet per second and Q_s is the sediment load in metric-tons per day.

The mean daily flows at the San Marcial gage from 1/1/95 to 12/31/99 were routed along the channel. Figure D.1 shows the bed elevation profiles for 0, 2 and 5 years for case A (a) and case B (b). In case A, the channel degraded until equilibrium was achieved. In case B, the excess of sediment concentration upstream, caused aggradation in the channel, increase of the slope, and subsequence degradation.

Figures D.2 D.3 show the changes in reach-averaged slopes with time at the three subreaches for cases A and B respectively. The changes in slope with time for case B are more variables than for case A, due to the impulses of sediment input into the channel during high flows. The wide channel (Subreach 2) developed at steeper slope than the two narrow reaches (1 and 3). The equilibrium slope for subreaches 1 and 3 should be the same, since they both have the same width. Subreach 1 and 3 developed the same slope in less than one year in case B, and in about 2.5 years in case A. This means that the increase in sediment concentration increases the rate of change in slope.

Figure D.4 shows the comparison of the change in reach-averaged slope with time at each subreach and for both cases. The rate of change in slope with time is faster when the channel is overload with sediment, as in case B. In the case of subreach 3, the initial rates of change in slope with time is the same for both cases and then decreases less rapidly for case B than case A. This response might be due to the decrease in supply of sediment from the upstream reaches (1 and 2), where the input sediment has been deposited.

From this analysis, it can be concluded that the increase in sediment concentration in a channel, induces the channel to change the slope at a faster rate than without the increase in sediment concentration.

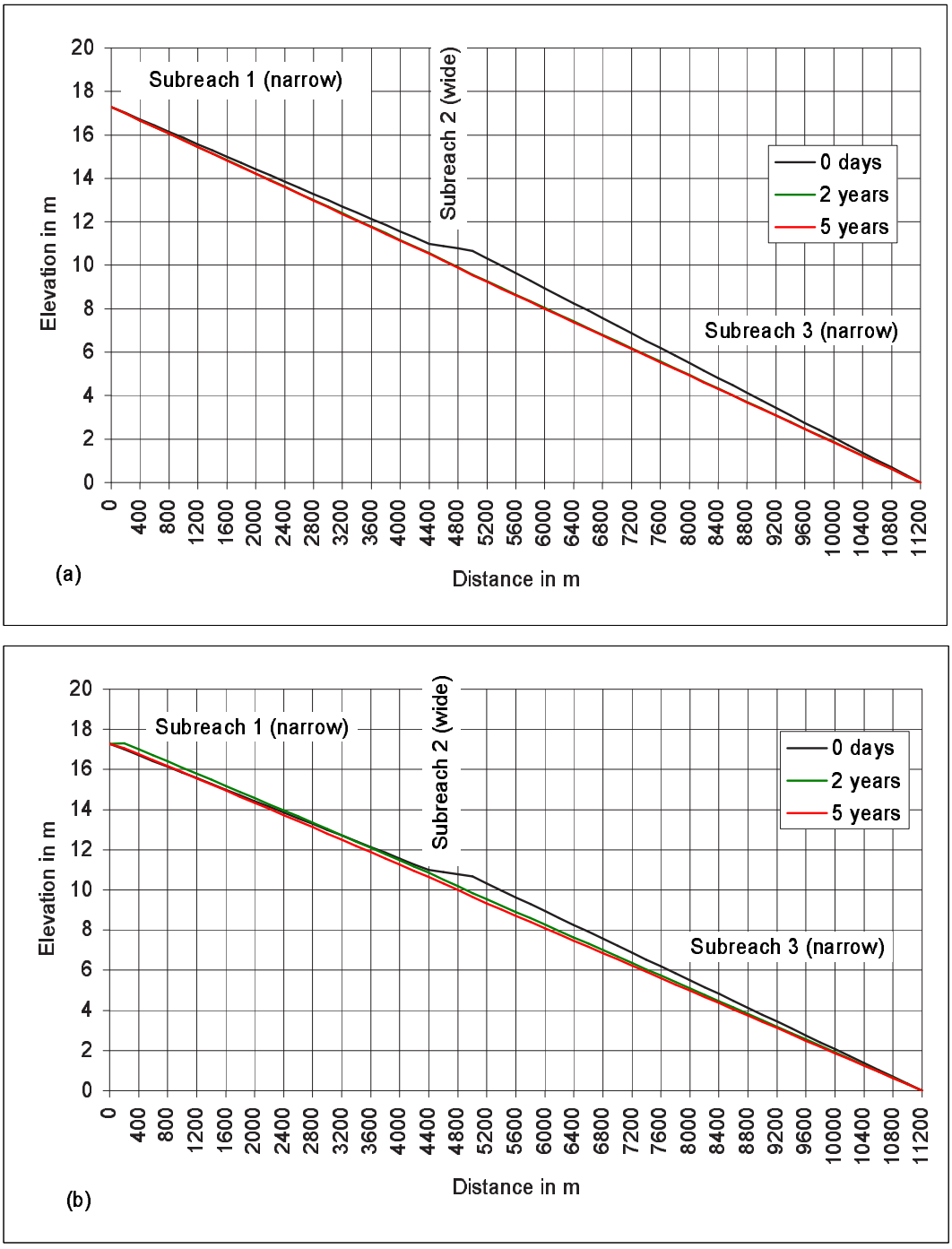

Figure D.1: Bed elevation profiles of the temporarily channel (a) Elevation profiles for case A. (b) Elevation profiles for case B.

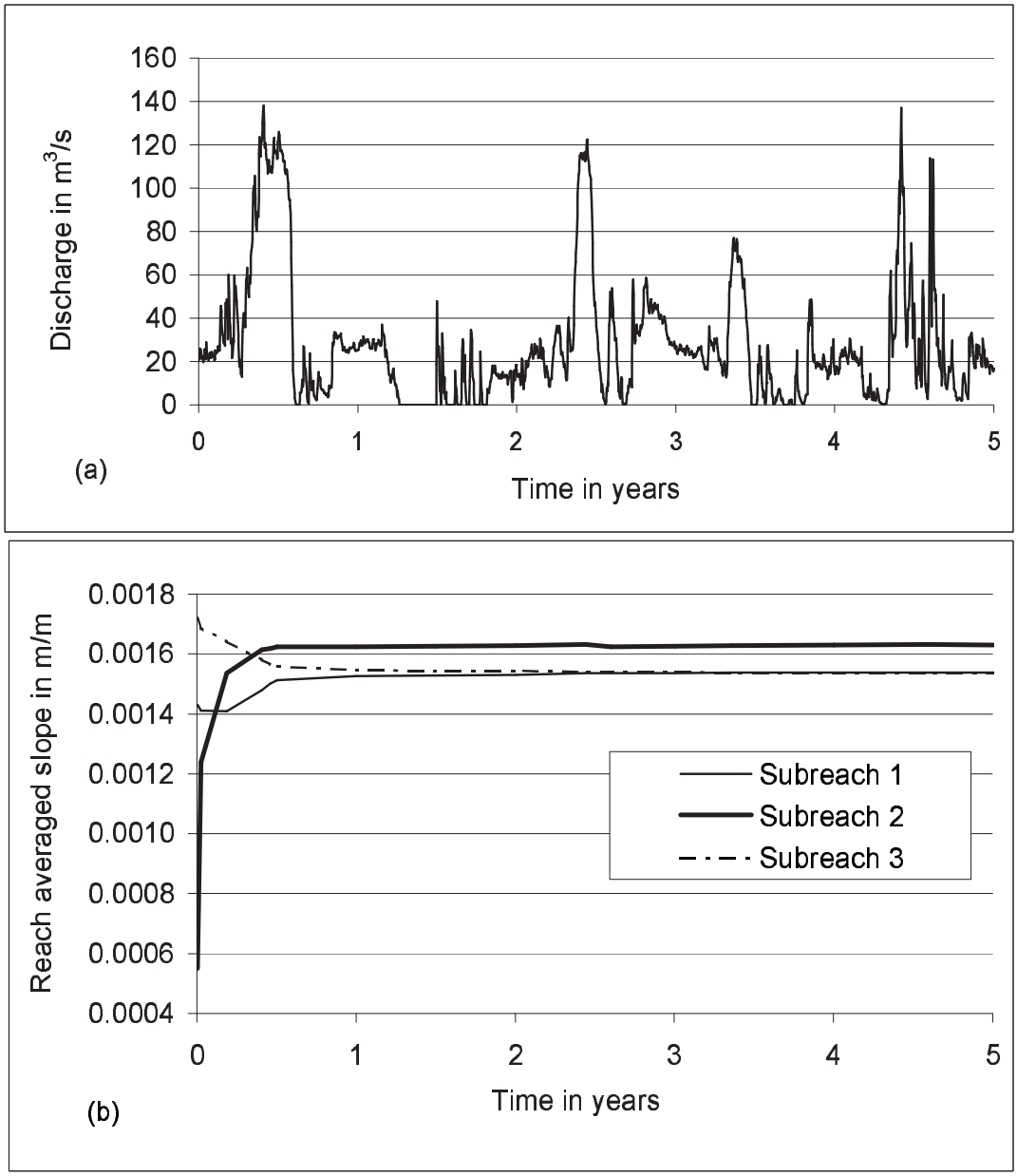

Figure D.2: Changes in reach-averaged slopes with time. (a) Mean daily flow discharges at San Marcial gage input into the model. (b) Reach-averaged slopes for case A.

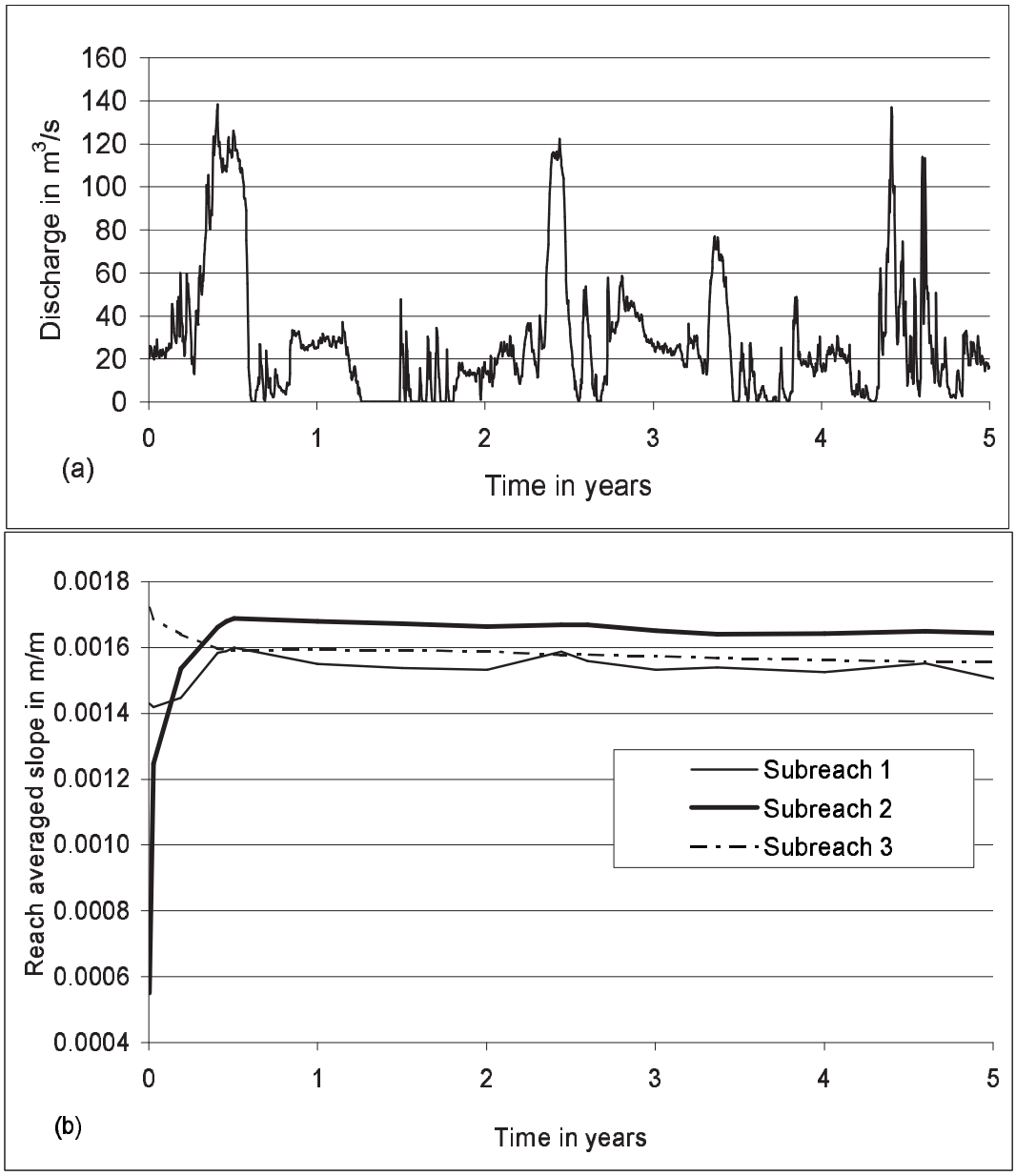

Figure D.3: Changes in reach-averaged slopes with time. (a) Mean daily flow discharges at San Marcial gage input into the model. (b) Reach-averaged slopes for case B.

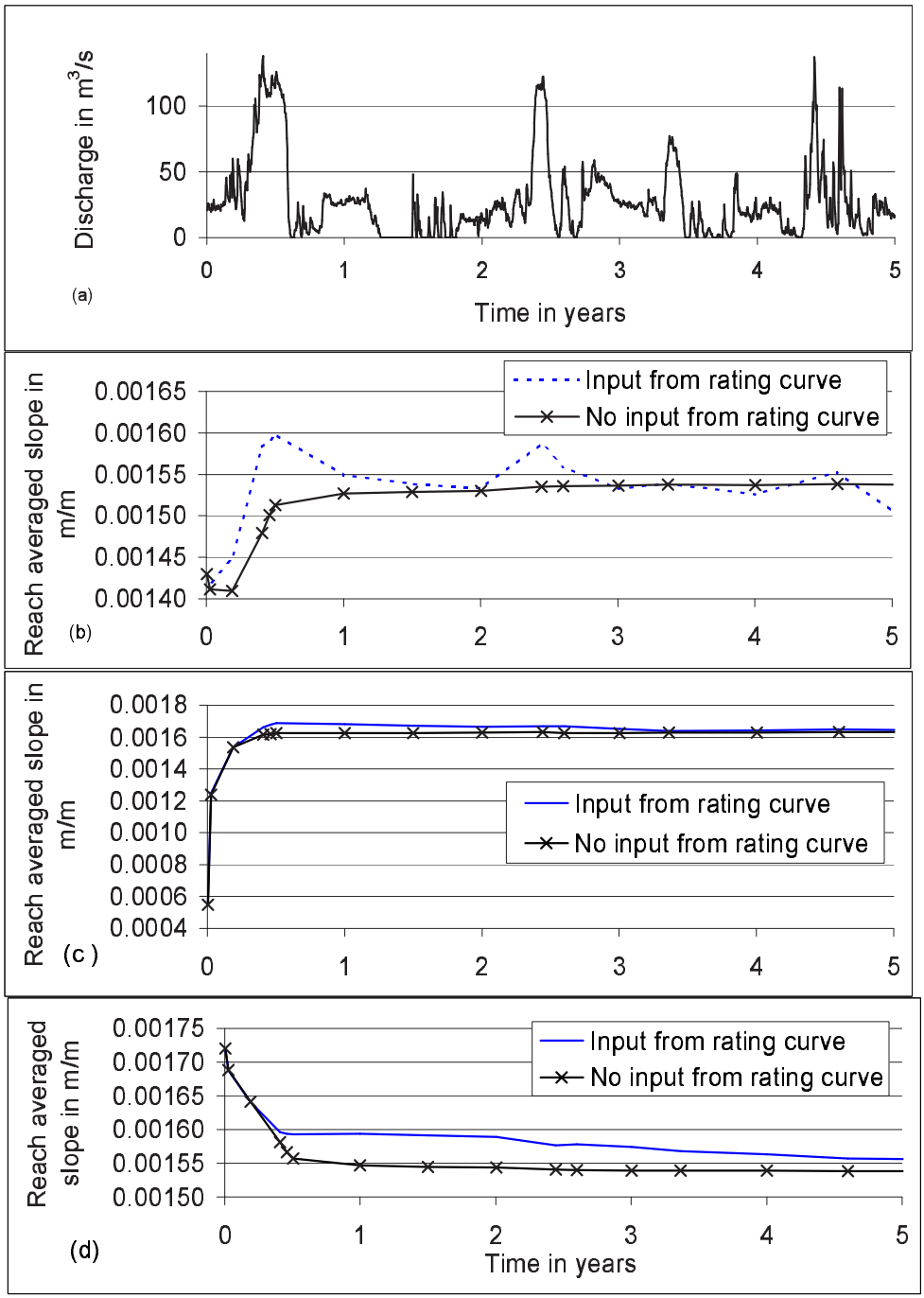

Figure D.4: Changes in reach-averaged slopes with time at each subreach for cases A and B. (a) Mean daily flow discharges at San Marcial gage input into the model. (b) Reach-averaged slope for Subreach 1. (c) Reach-averaged slope for Subreach 2. (d) Reach-averaged slope for Subreach 3.

Appendix E

Flow Duration Curves at San Acacia Gage

This appendix contains the flow duration curves developed at the San Acacia gage during the periods 1986-2000 and 1978-2000. According to the water discharge mass curve (Figure 3.2) presented in Chapter 3, the water regime has not change between 1978 and 2000. However, another flow duration curve was developed to account for the cessation of diversion to the Low Flow Conveyance Channel in 1985.

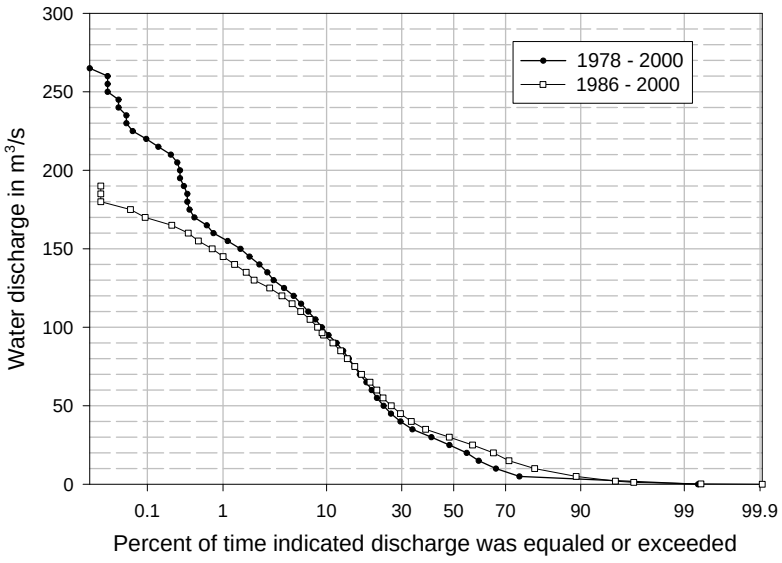

Figure E.1: Flow duration curves at the San Acacia gage for the 1978 to 2000 and 1986 to 2000 periods.

Appendix F

Sensitivity Analysis of Time to Equilibrium

This appendix contains the results of the numerical model with constant discharge for different values of channel length, sediment size, and roughness coefficient. The effect of different discharges on the time to reach equilibrium is also tested. In addition, an exponential model is fit to the transient solution of the slope to describe changes in reach-averaged slope with time.

F.1 Effect of Channel Length

In order to test the change in time to reach equilibrium due to changes in channel length, two runs were performed with a channel length of 32 kilometers and 52 kilometers. A constant flow discharge of $Q = 36\ m^3/s$ was routed. The roughness coefficient was 0.023, the sediment size was 0.50 mm and the initial slope was 0.0008 m/m for both runs. The geometry data input into the model are summarized in Table F.1. The length of the transition between the narrow and the wide reaches was 200 m. In addition, the time step used was 0.2 days. Figure F.1 presents the change in reach-averaged slope with time in the upstream (narrow) and downstream (wide) reaches.

Figure F.1 shows that the channel reached equilibrium faster in the shorter reach, which is an expected result, because the final volume of sediment comprised between the initial and final bed profiles is less when the channel is shorter. The time to equilibrium is expected to vary with the square of the reach length (L^2).

Run	Length (km)	d_x (m)	W_1 (m)	W_2 (m)	L_1 (km)	L_2 (km)
1	32	200	100	200	12.2	19.6
2	52	200	100	200	26.8	25.0

Table F.1: Geometry data input into the numerical model to test the effect of channel length on the time to reach equilibrium.

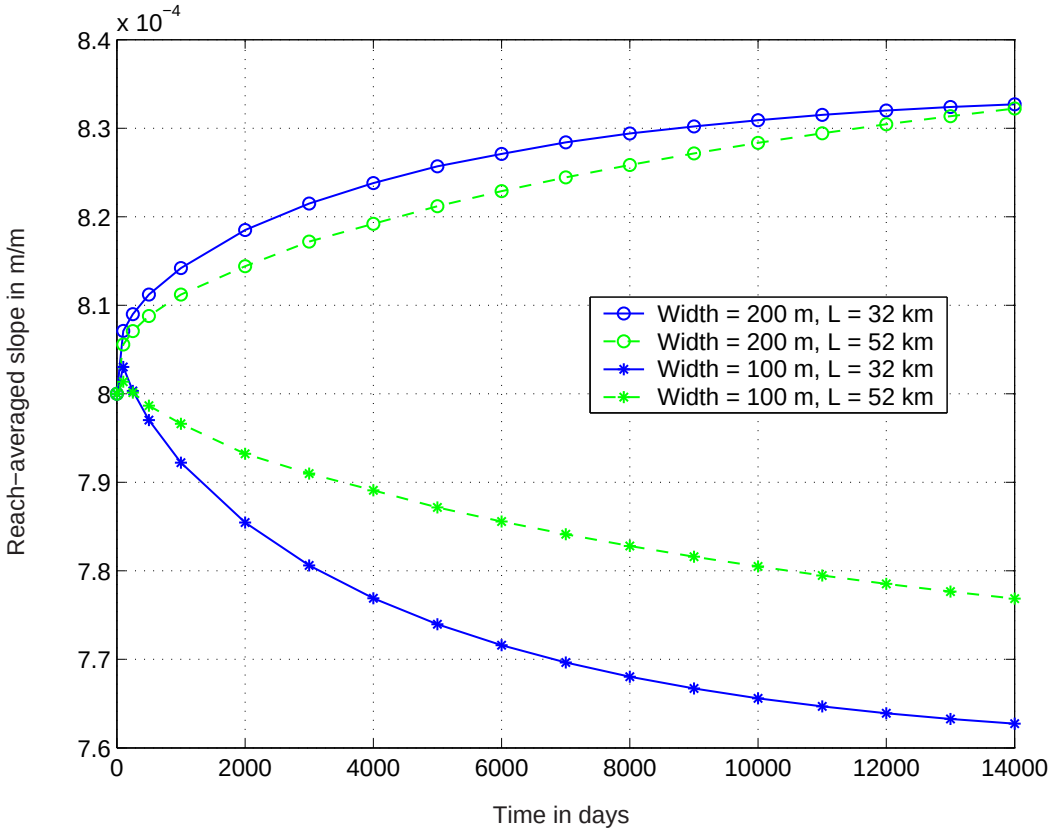

Figure F.1: Change in reach-averaged slope with time in a narrow (upstream) and wide (downstream) reaches of a channel, for two different channel lengths.

F.2 Effect of Sediment Size

Two model runs were performed to study the change in time to reach equilibrium due to the size of the sediment particles. Table F.2 summarizes the data input into

Run	d_s (mm)	Q (m^3/s)	n	d_x (m)	$d_t(day)$	W_1 (m)	W_2 (m)
1	1.00	142	0.03	200	0.2	100	200
2	0.50	142	0.03	200	0.2	100	200

Table F.2: Data input into the model to test the effect of the sediment size on the time to reach equilibrium.

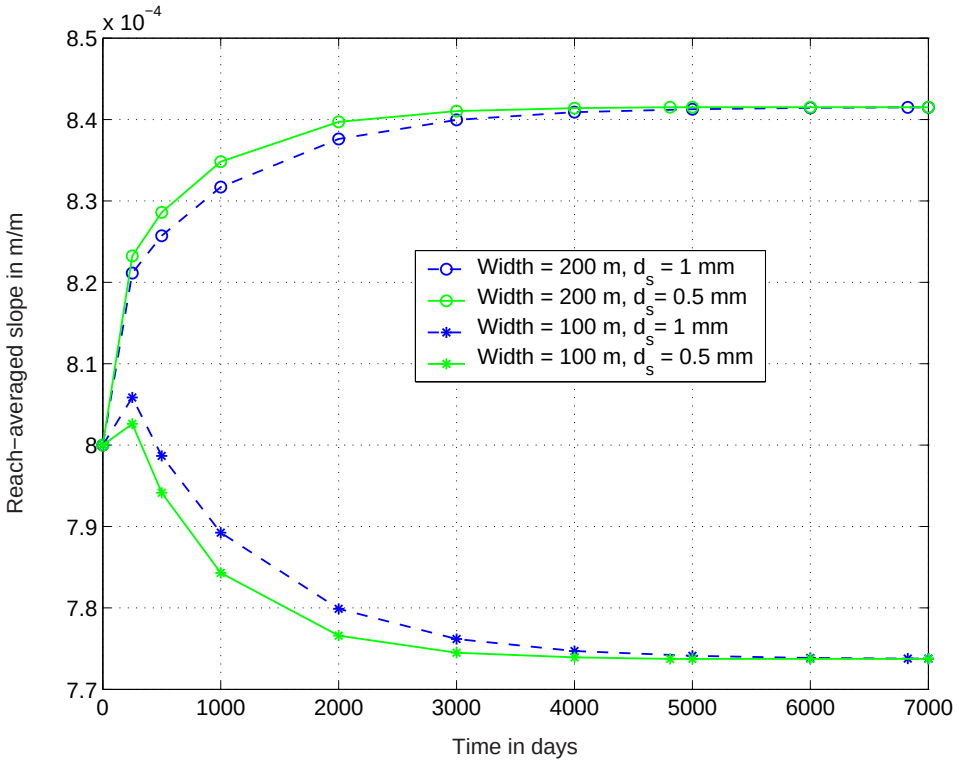

Figure F.2: Change in reach-averaged slope with time in a narrow (upstream) and wide (downstream) reaches of a channel, for two different sediment sizes.

the model. The total length of the channel was 32 Km with a constant initial slope of 0.0008 m/m for all the runs. Figure F.2 shows the change in reach-averaged slope with time of the upstream (narrow) and downstream (wide) reaches.

Time to equilibrium is reached faster with finer sediment. The rate of change in

slope with time is greater when the sediment is finer. For these examples, the time to equilibrium was about 3,000 days, when the sediment size was $d_s = 0.5\ mm$, while it increased to about 5,000 days when the sediment size was increased to $d_s = 1.00\ mm$. Finer sediments are easier to entrain. Therefore, the adjustment of slope occurs faster with fine sediment than with coarser sediment. However, finer sediments decrease the trap efficiency and could decrease the aggradation/degradation of the channel. For this case, it does not happens, because the trap efficiency is 100 % in both cases.

F.3 Effect of Manning Roughness Coefficient

Two runs were performed with different Manning n roughness coefficients to test the change in the time to reach equilibrium. Table F.3 summarizes the data input into the model. The total length of the channel was 32 Km with a constant initial slope of 0.0008 m/m for all the runs. Figure F.3 shows the change in reach-averaged slope with time of the upstream (narrow) and downstream (wide) reaches.

Sediment transport equilibrium is reached faster with larger friction factor. An increase in roughness produces an increase in flow depth and consequently an increase in bed shear stress.

Run	n	Q (m^3/s)	d_s (mm)	d_x (m)	$d_t(day)$	W_1 (m)	W_2 (m)
1	0.030	142	0.50	200	0.2	100	200
2	0.023	142	0.50	200	0.2	100	200

Table F.3: Data input into the model to test the effect of the Manning roughness coefficient on the time to reach equilibrium.

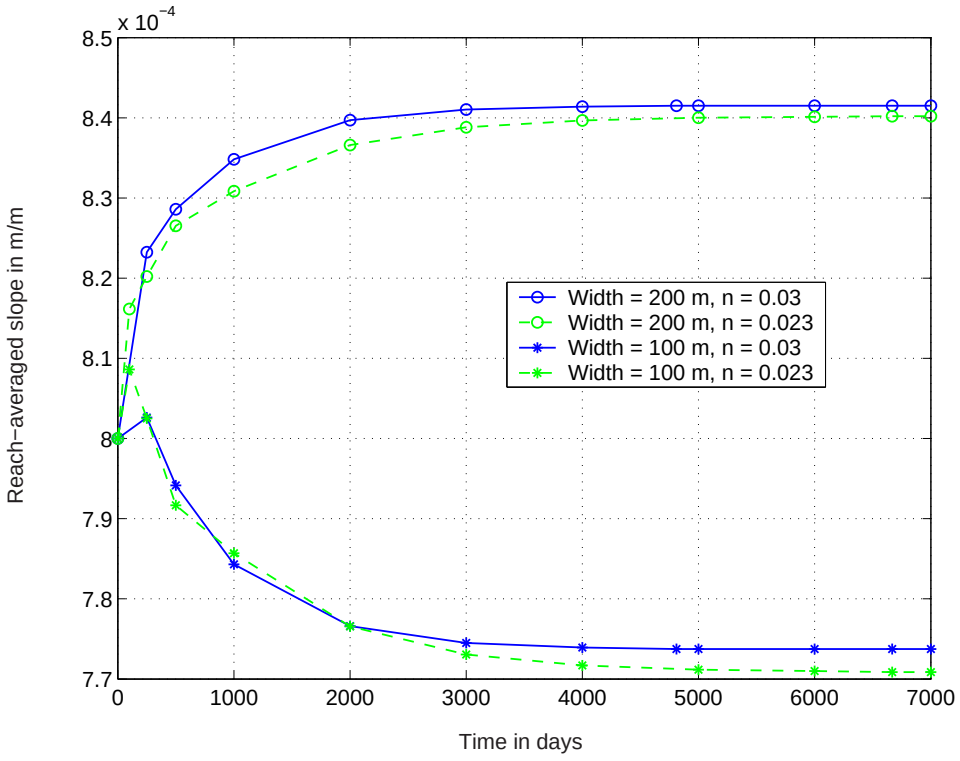

Figure F.3: Change in reach-averaged slope with time in a narrow (upstream) and wide (downstream) reaches of a channel, for two different Manning roughness coefficients.

F.4 Effect of Discharge on the Equilibrium Time

Two runs were performed with different constant flow discharges to test the change in the equilibrium time. Table F.4 summarizes the data input into the model. The total length of the channel was 32 Km with a constant initial slope of 0.0008 m/m for all the runs. Figure F.4 shows the change in reach-averaged slope with time of the upstream (narrow) and downstream (wide) reaches.

The reach-averaged slope changes rapidly with larger flows. Also, the equilibrium slopes for both reaches are larger for large discharges than for low flows. The increase in flow discharge increases the sediment concentration and therefore, the equilibrium

Run	Q (m^3/s)	n	d_s (mm)	W_1 (m)	W_2 (m)
1	142	0.023	0.50	100	200
2	36	0.023	0.50	100	200

Table F.4: Data input into the model to test the effect of water discharge on the time to reach equilibrium.

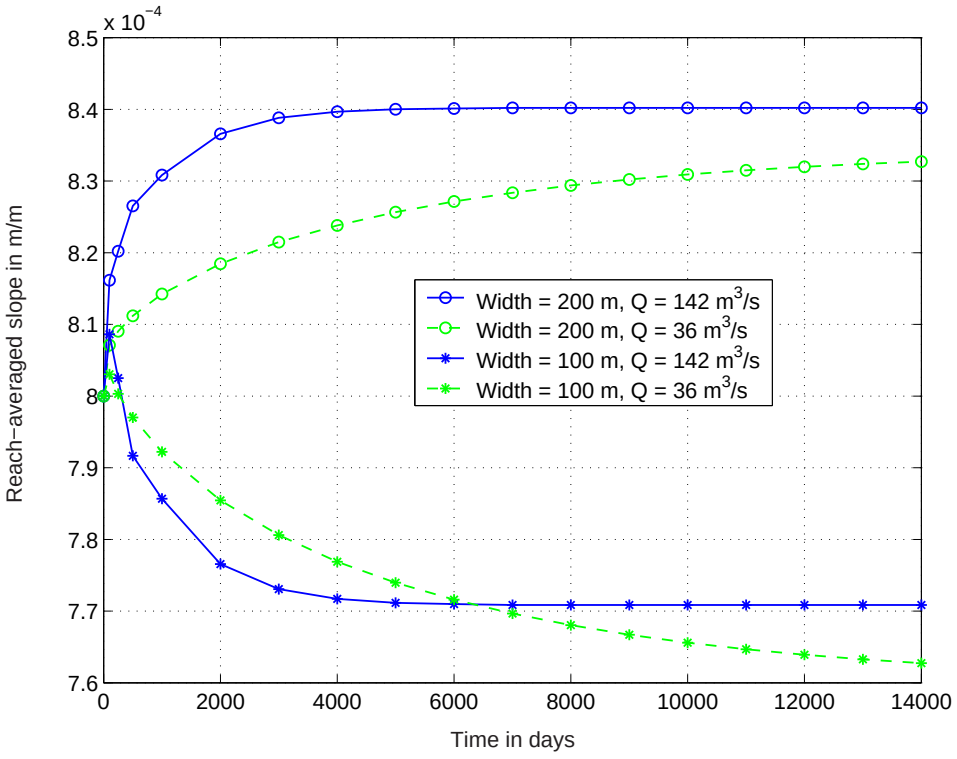

Figure F.4: Change in reach-averaged slope with time in a narrow (upstream) and wide (downstream) reaches of a channel, for two different water discharges.

slope.

F.5 Exponential Model

An exponential model was fit to the transient solution of the slope. This model is based on the concept that the slope changes more rapidly, the further it is from the

equilibrium state. The same type of model have been applied to describe the changes in channel width with time in the Rio Grande (Richard, 2001). The hypothesis of the model is that the magnitude of the slope of the slope versus time curve increases with deviation from the equilibrium slope (S_e).

$$\frac{\Delta S}{\Delta t} = -k(S - S_e) \tag{F.1}$$

Where ΔS is the change in slope during the time period Δt; and Δt is the time period in days.

Differentiating F.1 the following equation is obtained:

$$\frac{dS}{dt} = -k(S - S_e) \tag{F.2}$$

Then, rearranging and integrating equation F.2:

$$\int_{S_o}^{S} \frac{dS}{S - S_e} = \int_{0}^{t} -k dt$$

$$\ln(S - S_e) - \ln(S_o - S_e) = -kt + 0$$

$$\ln\left(\frac{S - S_e}{S_o - S_e}\right) = e^{-kt} \tag{F.3}$$

The resulting exponential function is:

$$S = S_e + (S_o - S_e).e^{-kt}$$

Where k is a constant, S_e is the equilibrium channel slope, S_o is the channel slope at time t_o; and S is the channel slope at time, t.

The exponential model was fit to the simulation results of Chapter 4, Section 4.2.3. The equilibrium channel slope (S_e was obtained from the numerical simulations, and the constant k was obtained by minimizing the sum of square errors (SSE). The exponential model was fit from the day 100, when the slope of the narrow

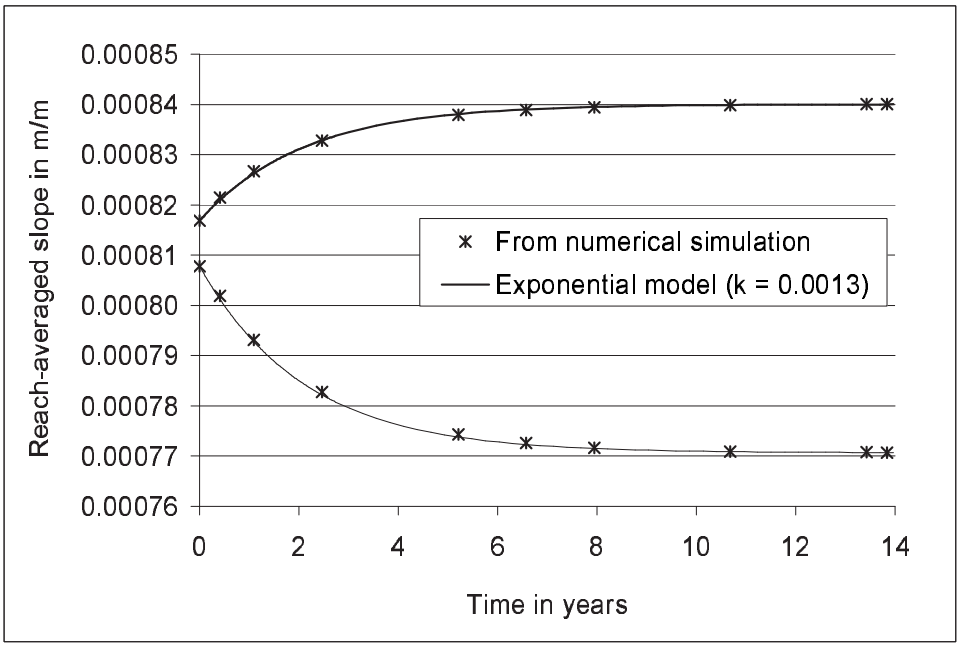

Figure F.5: Change in reach-averaged slope with time in a narrow (upstream) and wide (downstream) reaches of a channel as predicted with the numerical simulations and with the exponential model.

reach started to decline. Figure F.5 shows the exponential model fit to the data as well as the data from the simulation. This plot shows the time scale in years, however, the regression was performed with the time in days. The exponential model is in good agreement with the results from the simulation. The coefficient k might be a function of the reach length, the sediment size, the flow discharge and the roughness coefficient.

Appendix G

Flow Charts and Computer Codes

This appendix contains the flow charts of the numerical models for constant and variable discharges.

G.1 Flow Chart of Numerical Model for Constant Discharge

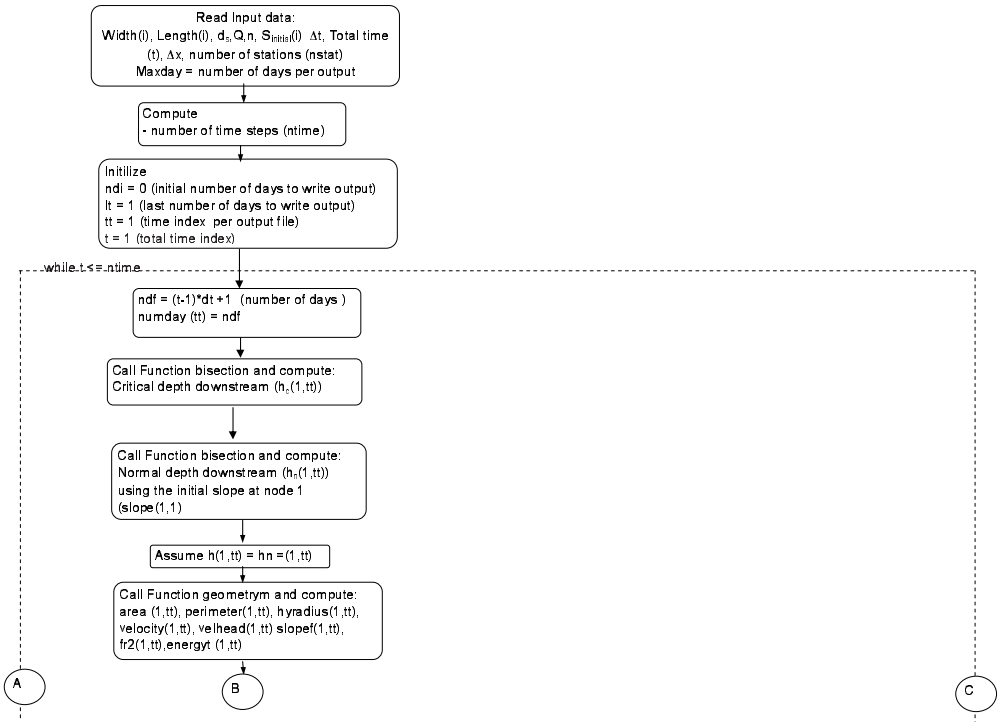

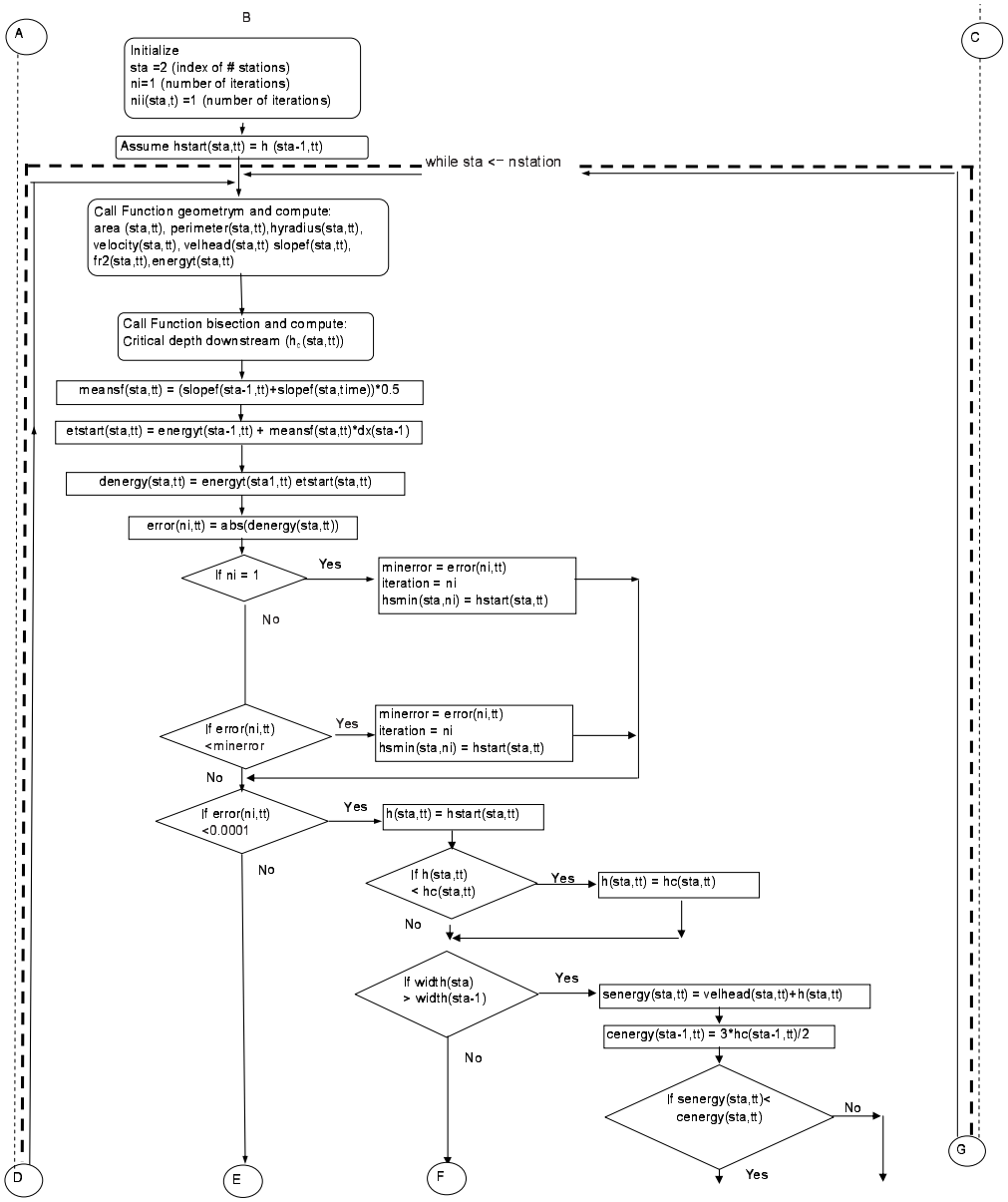
A
B
C
D
E
F
G
Initialize
sta =2 (index of # stations)
ni=1 (number of iterations)
nii(sta,t) =1 (number of iterations)
Assume hstart(sta,tt) = h (sta-1,tt)
while sta <= nstation
Call Function geometrym and compute:
area (sta,tt), perimeter(sta,tt),hyradius(sta,tt),
velocity(sta,tt), velhead(sta,tt) slopef(sta,tt),
fr2(sta,tt),energyt(sta,tt)
Call Function bisection and compute:
Critical depth downstream (h, (sta,tt))
meansf(sta,tt) = (slopef(sta-1,tt)+slopef(sta,time))*0.5
etstart(sta,tt) = energyt(sta-1,tt) + meansf(sta,tt)*dx(sta-1)
denergy(sta,tt) = energyt(sta1,tt) etstart(sta,tt)
error(ni,tt) = abs(denergy(sta,tt))
If ni = 1
Yes
minerror = error(ni,tt)
iteration = ni
hsmin(sta,ni) = hstart(sta,tt)
No
If error(ni,tt)
<minerror
Yes
minerror = error(ni,tt)
iteration = ni
hsmin(sta,ni) = hstart(sta,tt)
No
If error(ni,tt)
<0.0001
Yes
h(sta,tt) = hstart(sta,tt)
No
If h(sta,tt)
< hc(sta,tt)
Yes
h(sta,tt) = hc(sta,tt)
No
If width(sta)
> width(sta-1)
Yes
senergy(sta,tt) = velhead(sta,tt)+h(sta,tt)
cenergy(sta-1,tt) = 3*hc(sta-1,tt)/2
No
If senergy(sta,tt)<
cenergy(sta,tt)
No
Yes

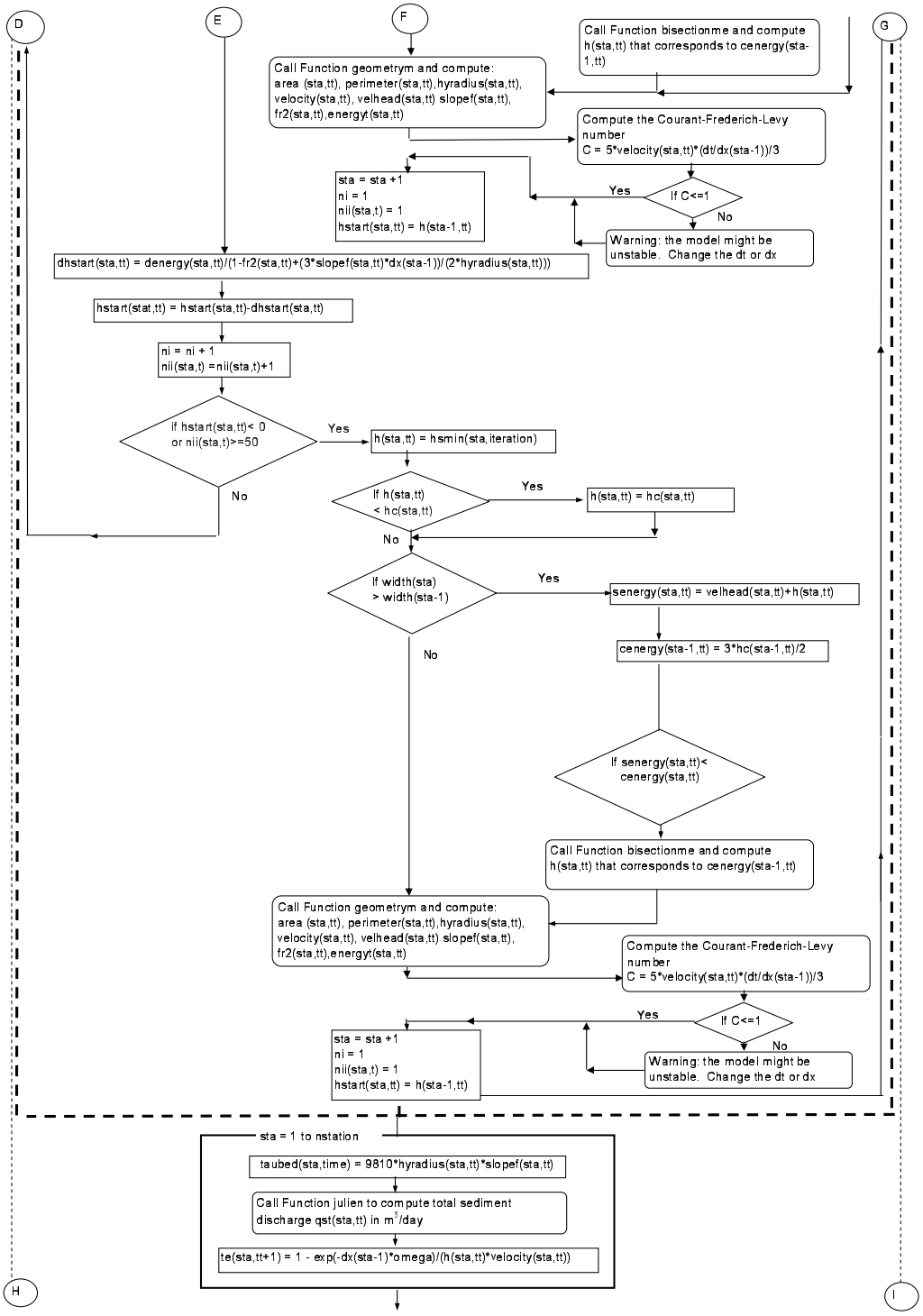
D
E
F
G
H
I
Call Function bisectionme and compute h(sta,tt) that corresponds to cenergy(sta-1,tt)
Call Function geometrym and compute: area (sta,tt), perimeter(sta,tt),hyradius(sta,tt), velocity(sta,tt), velhead(sta,tt) slopef(sta,tt), fr2(sta,tt),energyt(sta,tt)
Compute the Courant-Frederich-Levy number C = 5*velocity(sta,tt)*(dt/dx(sta-1))/3
sta = sta +1
ni = 1
nii(sta,t) = 1
hstart(sta,tt) = h(sta-1,tt)
If C<=1
Yes
No
Warning: the model might be unstable. Change the dt or dx
dhstart(sta,tt) = denergy(sta,tt)/(1-fr2(sta,tt)+(3*slopef(sta,tt)*dx(sta-1))/(2*hyradius(sta,tt)))
hstart(stat,tt) = hstart(sta,tt)-dhstart(sta,tt)
ni = ni + 1
nii(sta,t) =nii(sta,t)+1
if hstart(sta,tt)< 0 or nii(sta,t)>=50
Yes
No
h(sta,tt) = hsmin(sta,iteration)
If h(sta,tt) < hc(sta,tt)
Yes
No
h(sta,tt) = hc(sta,tt)
If width(sta) > width(sta-1)
Yes
No
senergy(sta,tt) = velhead(sta,tt)+h(sta,tt)
cenergy(sta-1,tt) = 3*hc(sta-1,tt)/2
If senergy(sta,tt)< cenergy(sta,tt)
Call Function bisectionme and compute h(sta,tt) that corresponds to cenergy(sta-1,tt)
Call Function geometrym and compute: area (sta,tt), perimeter(sta,tt),hyradius(sta,tt), velocity(sta,tt), velhead(sta,tt) slopef(sta,tt), fr2(sta,tt),energyt(sta,tt)
Compute the Courant-Frederich-Levy number C = 5*velocity(sta,tt)*(dt/dx(sta-1))/3
If C<=1
Yes
No
Warning: the model might be unstable. Change the dt or dx
sta = sta +1
ni = 1
nii(sta,t) = 1
hstart(sta,tt) = h(sta-1,tt)
sta = 1 to nstation
taubed(sta,time) = 9810*hyradius(sta,tt)*slopef(sta,tt)
Call Function julien to compute total sediment discharge qst(sta,tt) in m3/day
te(sta,tt+1) = 1 - exp(-dx(sta-1)*omega)/(h(sta,tt)*velocity(sta,tt))

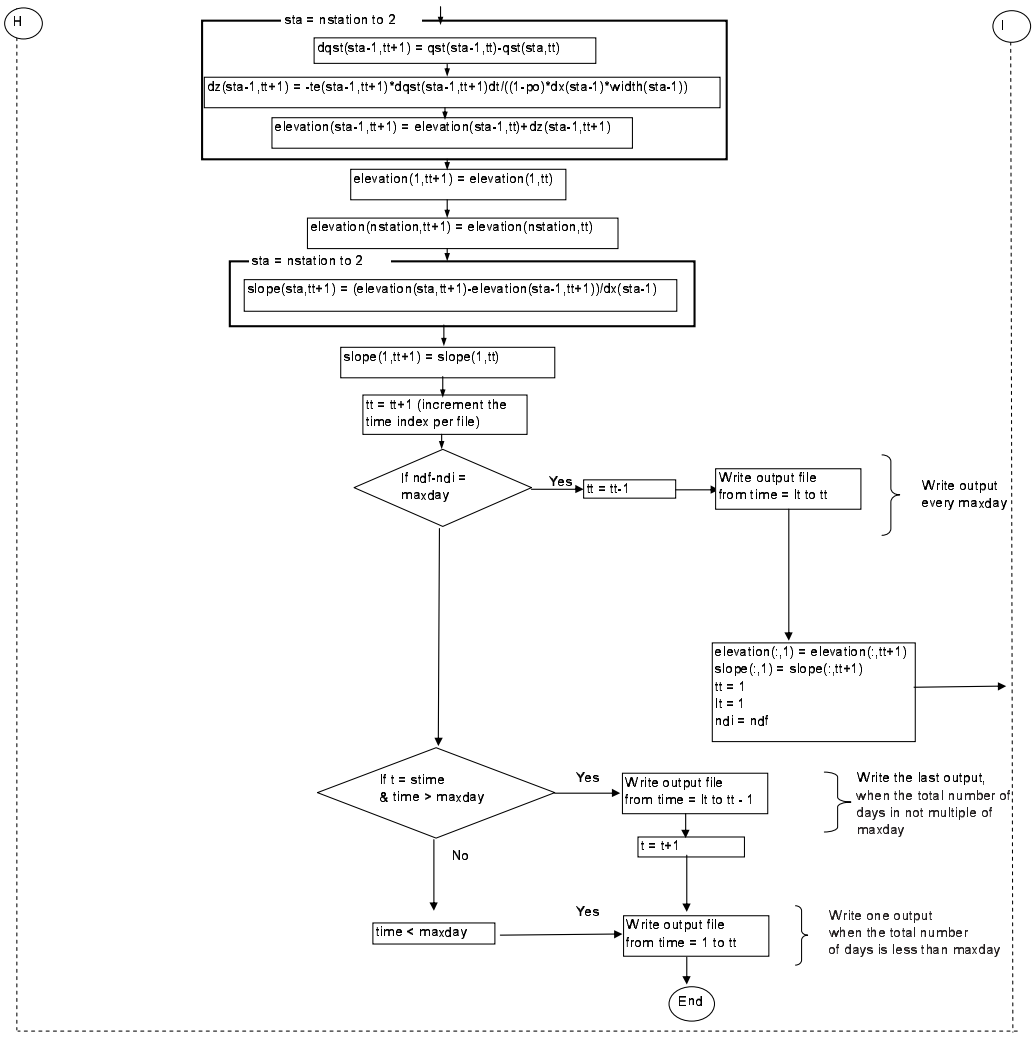
H
I
sta = nstation to 2
dqst(sta-1,tt+1) = qst(sta-1,tt)-qst(sta,tt)
dz(sta-1,tt+1) = -te(sta-1,tt+1)*dqst(sta-1,tt+1)dt/((1-po)*dx(sta-1)*width(sta-1))
elevation(sta-1,tt+1) = elevation(sta-1,tt)+dz(sta-1,tt+1)
elevation(1,tt+1) = elevation(1,tt)
elevation(nstation,tt+1) = elevation(nstation,tt)
sta = nstation to 2
slope(sta,tt+1) = (elevation(sta,tt+1)-elevation(sta-1,tt+1))/dx(sta-1)
slope(1,tt+1) = slope(1,tt)
tt = tt+1 (increment the time index per file)
If ndf-ndi = maxday
Yes
tt = tt-1
Write output file from time = lt to tt
Write output every maxday
elevation(:,1) = elevation(:,tt+1)
slope(:,1) = slope(:,tt+1)
tt = 1
lt = 1
ndi = ndf
If t = stime & time > maxday
Yes
Write output file from time = lt to tt - 1
Write the last output, when the total number of days in not multiple of maxday
t = t+1
No
time < maxday
Yes
Write output file from time = 1 to tt
Write one output when the total number of days is less than maxday
End

G.2 Code of the Numerical Model for Constant Discharge

```
%Script file: steady.m
%
%Purpose:
%This program computes backwater profiles in a sequence of channel
%reaches under steady flow conditions.  Then the aggradation
%and degradation of the channel bed is calculated using
%Julien's sediment transport equation. The resistance equation
%is Manning and the energy equation is solved using Henderson's method
%
%Define variables
%Input data:
%
%time = total time in days
%dt = delta time in days
%disc = flow discharge in m3/s
%nstation = number of stations along the channel
%station = station number
%length = channel length in m
%slope = channel slope
%width = channel width in m
%n = friction factor
%ds = sediment diameter in m
%vis = Kinematic viscosity in m2/s
%po = sediment porosity
%z = side slope
%
%Other variables
```

```
%ntime = number of time steps
%h = known flow depth in m at a station along the channel
%hstart = guessed flow depth in m at a station along the channel
%area = cross section area in m2 (rectangular section)
%perimeter = wetted perimeter in m (rectangular section)
%hyradius = hydraulic radius in m (rectangular section)
%velocity = mean flow velocity in m/s
%velhead = velocity head in m
%energyt = total energy in m
%slopef = friction slope
%fr2 = Froude number squared
%taubed = bed shear stress in N/m2
%meansf = average of friction slope between two adjacent stations
%etstart = total energy start in m
%denergy = delta energy in m
%dhstart = flow depth increment in m
%omega = fall velocity in m/s
%ndi = initial day of output file
%ndf = last day of output file
%lt = last time step an output file was written
%tt = time step per output file
%t = total time
%hn = normal depth m
%hc = critical depth m
%hmin = minimum initial bound input into the bisection method
%       to compute the normal depth and critical depth in the case of
%       non-rectangular sections
%hmax = maximum initial bound input into the bisection method
```

```
%      to compute the normal depth and critical depth in the case of
%      non-rectangular sections
%qbv = unit sediment discharge in m2/s
%qst = sediment discharge in m3/day
%dqst = change in sediment discharge between two adjacent
%       stations in m3/day
%maxday = number of days per output file
%iteration = is the iteration number where the minimum error happens
%hsmin = is the flow depth in m that produces the minimum error
%minerror = is the minimum error of specific energy in m
%senergy = specific energy in m
%cenergy = critical energy in m
%
clear all
%Get input data
%
 time = 3;
 dt = 0.01;
 n = 0.023;
 disc = 2;
 ds = 0.0003;
 vis=0.000001;
 po = 0.43;
 z = 0;
 maxday = 3;
%
%Opening the input file
 disp('Enter the name of the input file that contains the);
```

```
 disp('channel characteristics. The input file must);
 disp('contain five columns with the following data:);
 disp('Column 1 = Station #, Column 2 = length,);
 disp('Column 3 = Slope, Column 4 =');
 disp('Elevation and Column 5 = Width. The first row);
 disp('must contain the column headings:  '  );
 filename = input('  ','s');
%
%Calling function to read input data
 [nstation, station,length,slope,elevation,width,...
 dx] = openfile1(filename);
%
if time < maxday
    %Enter name of output file
    disp('Enter the name of the output file:   ');
    ofilename = input('   ','s');
end
%
t0 = clock;
%Creating slope and elevation matrixes.  The first index (x)
%corresponds to the station along the channel.  The second index
%corresponds to time.  Time = 1 is the first day
x = 1:1:nstation;
slope(x,1) = slope(x); elevation(x,1) = elevation(x);
%
%Calculate the number of time steps.  Time=1
%corresponds to the initial conditions (time = 0):
%initial slope, discharge, d/s flow depth, etc.  Time = 2 will be
```

```
%0 + dt, time = 3 will be 0 + 2*dt and so on...tn = t0 + (n-1)*dt
ntime = 1+ time/dt;
%
%Call function to calculate the fall velocity of ds
omega = fallv(vis,ds);
%
%Calculate the backwater
ndi = 0; %initial number of days
lt =1; %last time an output file was written
tt = 1; %index from 1  to 365 days
t = 1; %initilize time
%
while t <= ntime
ndf = (t-1)*dt; %number of days
numday(tt) = ndf;
disp(['day # :' num2str(ndf)]);
%Compute the normal depth at station 1 and assume
%d/s depth (sta 1) = normal depth
 if slope(1,tt)< 0;
 error('slope < 0, normal depth does not exist');
 else
 hmin = 0;  %hmin and hmax are the min and max
           %initial bounds for the bisection method iterations
 hmax = 30;
 flag = 1; %flag = 1 indicates the bisection function
          %to compute the normal depth
 hn(1,tt)] =bisection(disc,slope(1,1),n,width(1),z,hmin,hmax,flag);
 h(1,tt) = hn(1,tt);
```

```
 end
%Calculate the critical depth at station 1
if z == 0
%hc for rectangular section
hc(1,tt) = ((disc^2)/(9.81*width(1)^2))^(1/3); else
hmin = 0;  %hmin and hmax are the min and max initial
           %bounds for the bisection method iterations
hmax = 2*((disc^2)/(9.81*width(1)^2))^(1/3);
flag = 2;  %flag = 2 indicates the bisection function
           %to compute the critical depth
[hc(1,tt)]=bisection(disc,slope(1,tt),n,width(1),z...
,hmin,hmax,flag);
end
%Calling function geometry to compute the area, perimeter,
%hydraulic radius, velocity, velocity head,total energy and
%friction slope at station 1 (downstream end of the channel),
%based on the flow depth at sta 1, flow discharge, width,
%elevation and friction factor (f)
[area(1,tt),perimeter(1,tt),hyradius(1,tt),velocity(1,tt)...
,velhead(1,tt),energyt(1,tt),slopef(1,tt),fr2(1,tt)] =...
geometrym(width(1),h(1,tt),disc,elevation(1,tt), n,z);

%Calculate the bed shear stress in N/m2 at station 1
taubed(1,tt) = 9810*hyradius(1,tt)*slopef(1,tt);

%Initializing the counter 'sta' to start computing
%the backwater profile
sta = 2;
```

```
%Assuming the u/s depth (sta = 2) equal to the
%d/s depth (sta = 1)
hstart(sta,tt) = h(sta-1,tt);

%number of iterations
ni =1; nii(sta,t) = 1;
while sta <= nstation
%Calling function geometry
[area(sta,tt),perimeter(sta,tt),hyradius(sta,tt)...
,velocity(sta,tt),velhead(sta,tt),energyt(sta,tt)...
,slopef(sta,tt),fr2(sta,tt)] =...
geometrym(width(sta),hstart(sta,tt),disc,elevation(sta,tt), n,z);
if z == 0
%hc for rectangular section
hc(sta,tt) = ((disc^2)/(9.81*width(sta)^2))^(1/3);
else
hmin = 0;  %hmin and hmax are the min and max initial
           %bounds for the bisection method iterations
hmax = 1.1*((disc^2)/(9.81*width(sta)^2))^(1/3);
flag = 2;  %flag = 2 indicates the bisection function
           %to compute the critical depth
[hc(sta,tt)]=bisection(disc,slope(sta,tt),n...
,width(sta),z,hmin,hmax,flag);
end
%Compute the average friction slope between stations
%sta and sta-1
meansf(sta,tt) = (slopef(sta-1,tt)+slopef(sta,tt))*0.5;
```

```
%Compute the total energy at the u/s station (sta)
%as the total energy d/s plus
%the head lost between both stations = meansf * dx
etstart(sta,tt) = energyt(sta-1,tt) + meansf(sta,tt)*dx(sta-1);

%Compute the difference in total energy in station sta by
%subtracting the
%total energy start (etstart)and the total energy computed with the
%function geometry energyt
denergy(sta,tt) = energyt(sta,tt)-etstart(sta,tt);
error(ni,tt)=abs(denergy(sta,tt)); if ni == 1
minerror=error(ni,tt); iteration=ni; hsmin(sta,ni)=hstart(sta,tt);
elseif error(ni,tt)< minerror
minerror=error(ni,tt);
iteration=ni;
hsmin(sta,ni)=hstart(sta,tt);
end
%Check if denergy is less than an especified error.  If so,
%the assumed elevation at the u/s station is rigth and
%we proceed to the next u/s station.  If not, a new
%value will be assumed. dhstart is added to the previous assummed
%depth to compute the new assummed depth. dhstart equation
%comes from Henderson (1966) book pp.143
if abs(denergy(sta,tt)) <=0.001
h(sta,tt) = hstart(sta,tt);
 %If h(sta,t) is in the wrong side of hc, h is set to hc
if h(sta,tt) < hc(sta,tt)
```

```
h(sta,tt)=hc(sta,tt);

disp('Msg 1:h is set to hc');
disp(t);
disp(sta);
end
if width(sta) > width(sta-1)%there is a contraction
%check if the specific energy is less than the critical
%energy at the constriction
%Specific energy at sta
senergy(sta,tt) = velhead(sta,tt)+h(sta,tt);
%critical energy at the next downstream station
cenergy(sta-1,tt) = 3*hc(sta-1,tt)/2;
%If energy < critical energy, the water has to backup
%until it gets sufficient energy to pass
 if senergy(sta,tt) < cenergy(sta-1,tt)
 hmin = hc(sta,tt);
 hmax=1.5*h(sta,tt);
 h(sta,tt)=bisectionme(hmin,hmax,discharge(tt)...
 ,cenergy(sta-1,tt),width(sta),z);
 disp('Msg2: h corresponds to critical energy downstream');
 disp(sta);
 disp(t);
end
end
%Calling function geometrym
[area(sta,tt),perimeter(sta,tt),hyradius(sta,tt),velocity(sta,tt)...
,velhead(sta,tt),energyt(sta,tt),slopef(sta,tt),fr2(sta,tt)] =...
```

```
geometrym (width(sta),h(sta,tt),disc,elevation(sta,tt), n,z);

%Compute the Courant-Friedrich-Levy number and check stability
 courant(sta,tt) = dt*5*velocity(sta,tt)/(3*dx(sta-1));
 if courant(sta,tt)>1
 disp('the model is unstable');
 end

%Increase the counter to compute the flow depth in
%the next upstream station
sta = sta + 1;

%Initialized the number of iterations to 1 in the next station
ni = 1;
nii(sta,t) = 1;

%Assume a new hstart(sta) value equal to the
%d/s depth just calculated at 'sta'
hstart(sta,tt) = h(sta-1,tt);

else
%Calculate the flow increment (dhstart)
dhstart(sta,tt)=denergy(sta,tt)/(1-fr2(sta,tt)...
+(3*slopef(sta,tt)*dx(sta-1))/(2*hyradius(sta,tt)));

%Add the flow increment to the assumed flow depth hstart
hstart(sta,tt) = hstart(sta,tt)- dhstart(sta,tt);
```

```
%Increase the number of iterations
 ni = ni + 1;
 nii(sta,t) = nii(sta,t) +1;
 if hstart(sta,tt) < 0 |
 nii(sta,t) >= 50
%If hstart is negative, the solution will be the minimum error wse
 h(sta,tt) = hsmin(sta,iteration);
 disp('Msg 3:No solution for the energy equation was found.
 h is set to the minimum error h');
 disp(sta);
 disp(t);

if width(sta) > width(sta-1) %there is a contraction
%check if the specific energy is less than the critical
%energy at the constriction
%Specific energy at sta
senergy(sta,tt) = velhead(sta,tt)+h(sta,tt);
%critical energy at the next downstream station
cenergy(sta-1,tt) = 3*hc(sta-1,tt)/2;
%If energy < critical energy, the water has to backup
%until it gets sufficient energy to pass
if senergy(sta,tt) < cenergy(sta-1,tt)
 hmin = hc(sta,tt);
 hmax = 3;
 h(sta,tt) = bisectionme(hmin,hmax,disc...
 ,cenergy(sta-1,tt),width(sta),z);
 disp('Msg 4:h corresponds to critical energy downstream');
 disp(sta);
```

```
 disp(t);


end
 else
%if the minimum error wse < critical depth, h is set to critical
if h(sta,tt) < hc(sta,tt)
 h(sta,tt) = hc(sta,tt);
 disp('Msg 5:h is set to hc');
 disp(sta);
 disp(t);
end
end
%Compute the channel characteristics with the new depth
[area(sta,tt),perimeter(sta,tt),hyradius(sta,tt),velocity(sta,tt)...
,velhead(sta,tt),energyt(sta,tt),slopef(sta,tt),fr2(sta,tt)] =...
geometrym (width(sta),h(sta,tt),disc,elevation(sta,tt), n,z);
%Compute the Courant-Friedrich-Levy number and check stability
courant(sta,tt) = dt*5*velocity(sta,tt)/(3*dx(sta-1));
 if courant(sta,tt)>1
 disp('the model is unstable');
 end
%Increse the number of stations
sta = sta+1;
%Set number of iterations to 1
 ni = 1;
 nii(sta,t) = 1;
%New assumed depth equal to previous depth
 hstart(sta,tt) = h(sta-1,tt);
```

```
 end
 end
end
%Compute the bed shear stress in N/m2 based on the friction
%slope at each node
 i = 1:nstation;
 taubed(i,tt) = 9810*hyradius(i,tt).*slopef(i,tt);
%%%%%%%% - SEDIMENT TRANSPORT - AGGRADATION/DEGRADATION - %%%%%
%Calculate the sediment discharge at each station
%using Julien's equation
for sta = nstation:-1:1
 %Unit sediment discharge in m2/sec
 qbv(sta,tt) = julien(ds,taubed(sta,tt));
 %Sediment discharge in m3/day
 qst(sta,tt) = qbv(sta,tt)*width(sta)*86400;
end
for sta = nstation:-1:2
%Change in sediment discharge between 2 adjacent stations
 dqst(sta-1,tt+1) = qst(sta-1,tt) - qst(sta,tt);
%Trap efficiency at time t+1 based on h and velocity
%computed at time = t
 te(sta-1,tt+1) = 1-exp(-dx(sta-1)*omega/(h(sta-1,tt)...
 *velocity(sta-1,tt)));
%Change in bed elevation at time t+1
 dz(sta-1,tt+1) = -te(sta-1,tt+1)*dqst(sta-1,tt+1)...
 *dt/((1-po)*dx(sta-1)*width(sta-1));
%New bed elevation at time t+1
 elevation(sta-1,tt+1) = elevation(sta-1,tt)+dz(sta-1,tt+1);
```

```
end
%Fix elevation at the u/s stations
elevation(nstation,tt+1) = elevation(nstation,tt);
 for sta = nstation:-1:2
 %Calculate the new bed channel slope
 slope(sta,tt+1) = (elevation(sta,tt+1)...
 -elevation(sta-1,tt+1))/dx(sta-1);
 end
 %Slope at first downstream node equal to the slope
 at the node upstream from it
 slope(1,tt+1) = slope(2,tt+1);
tt = tt+1; %increment the time index tt
%Printing out the results every maxdays days
if ndf - ndi == maxday
 tt = tt-1;
 numfile = int2str(ndf);
 fileout=strcat(numfile,'.out');
 fid = fopen(fileout,'wt');
 fprintf(fid,'%-15s %-11s %-12s %-12s %-15s %-12s %-12s...
  %-12s %-12s %-12s %-15s %-12s\n','day','Station','Length'...
  ,'Slope','Elevation','Width','Q','h','Sf','Fr2', 'hc','qst');
 for k = lt:tt
   ddiff = numday(k) - round(numday(k));
    if ddiff == 0
    for s = 1:nstation
    fprintf(fid,'%6.1f\t %11d\t %11.2f\t %10.6e\t %11.6e\t
    %11.2f\t %11.2f\t %6.4f\t %10.2e\t %10.4e\t %6.4f\t %6.4f\n',...
    numday(k), station(s), length(s),slope(s,k),elevation(s,k),
```

```
   width(s), disc,h(s,k),slopef(s,k),fr2(s,k),hc(s,k),qst(s,k));
   end
   end
end
fclose(fid);
elevation(:,1) = elevation(:,tt+1);
slope(:,1) = slope(:,tt+1);
tt = 1;
lt = 1;
ndi = ndf;
elseif t == ntime & time > maxday  %printing out the results
numfile = int2str(ndf);
fileout=strcat(numfile,'.out');
fid = fopen(fileout,'wt');
fprintf(fid,'%-15s %-11s %-12s %-12s %-15s %-12s %-12s...
   %-12s %-12s %-12s %-15s %-12s\n','day','Station','Length'...
   ,'Slope','Elevation', 'Width','Q','h','Sf','Fr2','hc','qst');
for k = lt:tt-1
  ddiff = numday(k) - round(numday(k));
  if ddiff == 0
  for s = 1:nstation
  fprintf(fid,'%6.1f\t %11d\t %11.2f\t %10.6e\t %11.6e\t..
  %11.2f\t %11.2f\t %6.4f\t %10.2e\t %10.4e\t %6.4f\t %6.4f\n',...
  numday(k), station(s), length(s),slope(s,k),elevation(s,k),...
  width(s),disc,h(s,k),slopef(s,k),fr2(s,k),hc(s,k),qst(s,k));
end
end
end
```

```
fclose(fid);
end
    t = t +1; %increment the total time index
end
%%%%%%%% - WRITING OUTPUT - %%%%%%%%%%%%%%%%%%%%%%%%%%%%%%%%%%%%
%Printing out the results if the total time is less than maxday
if time < maxday fid = fopen(ofilename,'wt');
fprintf(fid,'%-15s %-11s %-12s %-12s %-15s %-12s %-12s...
    %-12s %-12s %-12s %-15s %-12s\n',
    'day','Station','Length', 'Slope','Elevation', 'Width','Q'...
    ,'h','Sf','Fr2', 'hc','Qs');
 for k = 1:tt
 ddiff = numday(k) - round(numday(k));
 if ddiff == 0
 for s = 1:nstation
 fprintf(fid,'%6.1f\t %11d\t %11.2f\t %10.6e\t %11.6f\t...
 %11.2f\t %11.2f\t %6.4f\t %10.2e\t %10.4e\t %6.4f\t...
 %11.2f\n',numday(k), station(s), length(s),slope(s,k),
 elevation(s,k),width(s),disc, h(s,k),slopef(s,k),...
 fr2(s,k),hc(s,k),qst(s,k));
 end
 end
 end
fclose(fid); end elapsedtime = etime(clock,t0);
%
%Counts the total running time
%
fprintf('The elapsed time in seconds is = %6.3f\n',elapsedtime);
```

G.3 Flow Chart of Numerical Model for Variable Discharge with no Control of Degradation along the Channel

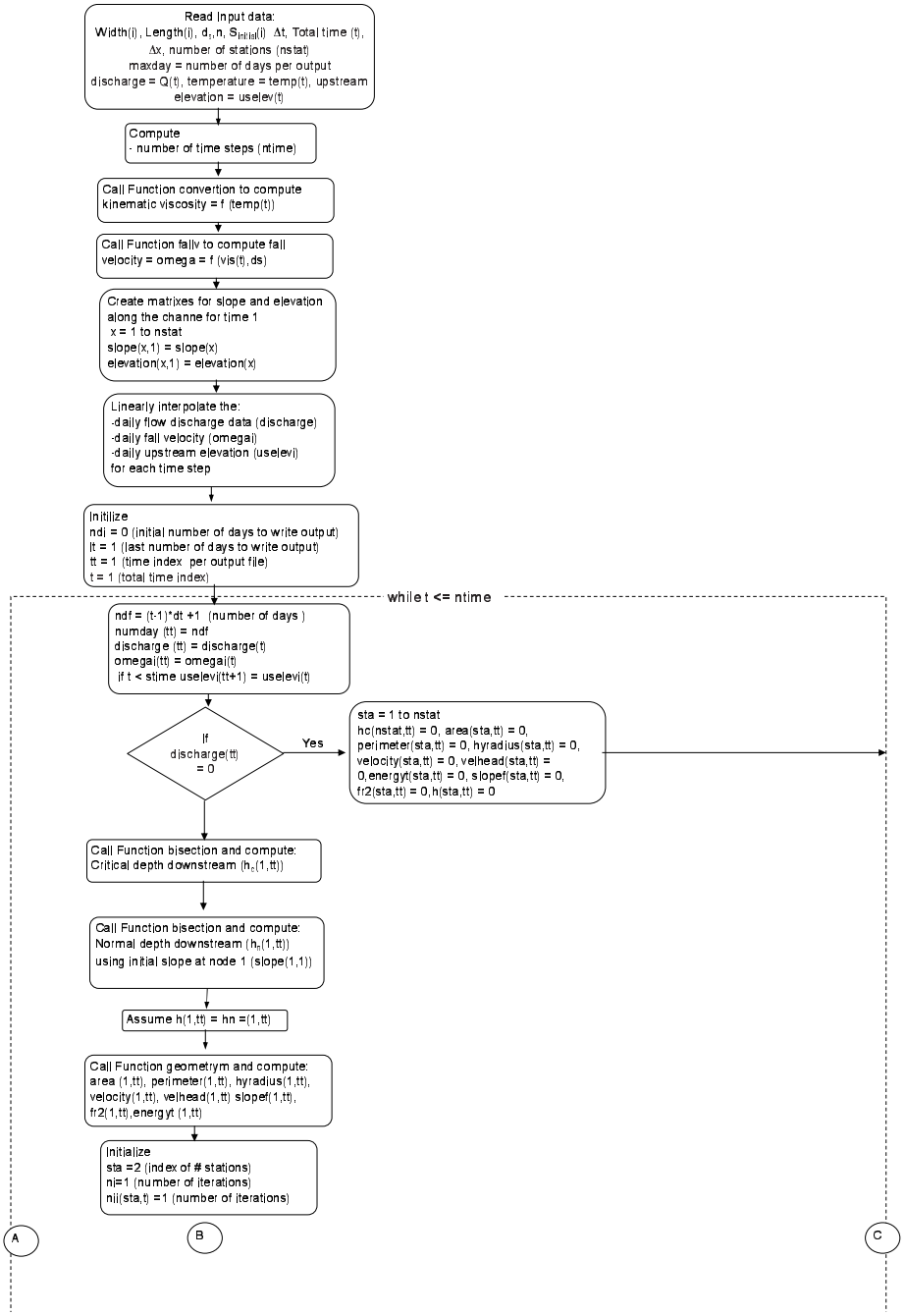

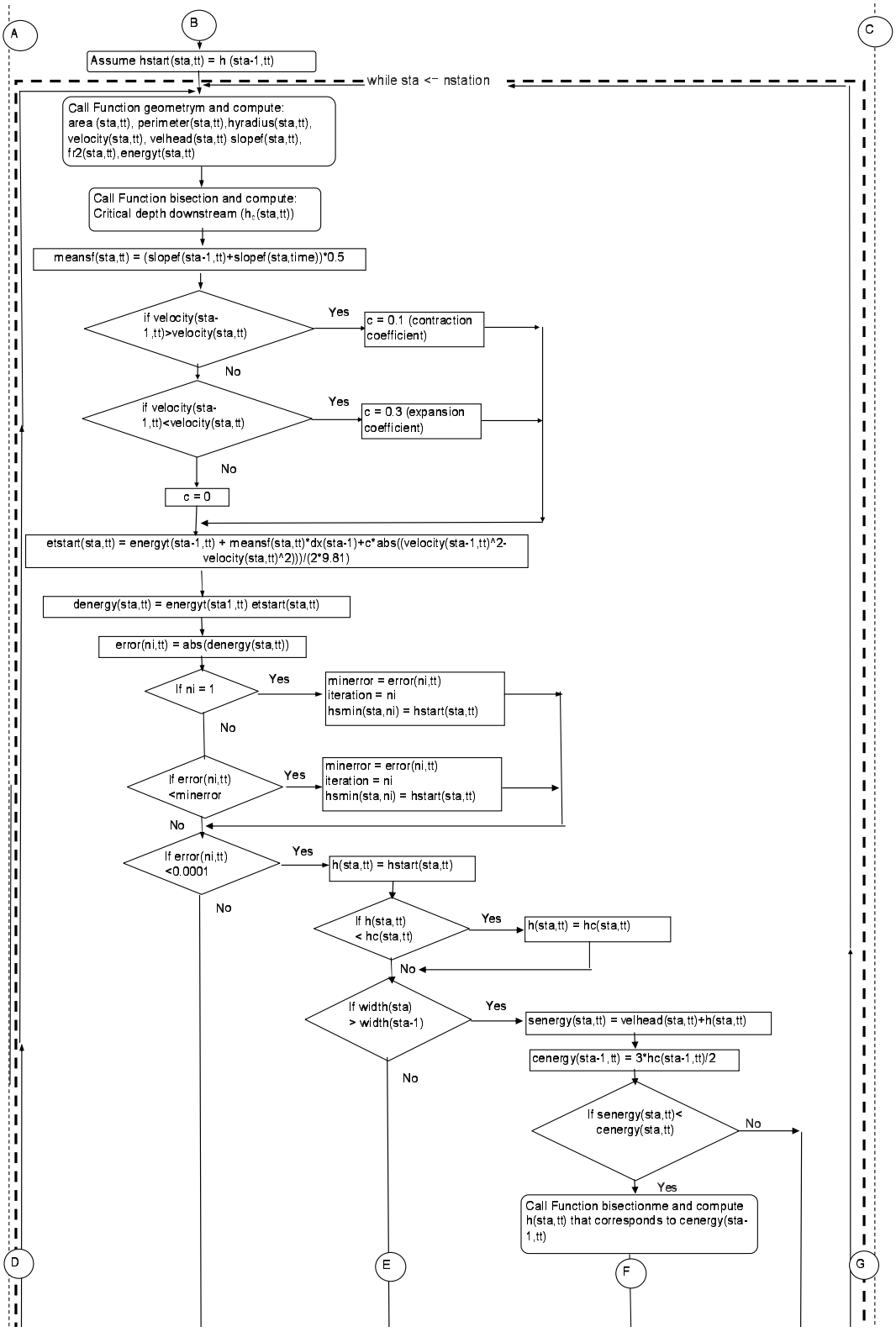
A
B
C
Assume hstart(sta,tt) = h (sta-1,tt)
while sta <= nstation
Call Function geometrym and compute:
area (sta,tt), perimeter(sta,tt),hyradius(sta,tt),
velocity(sta,tt), velhead(sta,tt) slopef(sta,tt),
fr2(sta,tt),energyt(sta,tt)
Call Function bisection and compute:
Critical depth downstream (hc(sta,tt))
meansf(sta,tt) = (slopef(sta-1,tt)+slopef(sta,time))*0.5
if velocity(sta-1,tt)>velocity(sta,tt)
Yes
c = 0.1 (contraction coefficient)
No
if velocity(sta-1,tt)<velocity(sta,tt)
Yes
c = 0.3 (expansion coefficient)
No
c = 0
etstart(sta,tt) = energyt(sta-1,tt) + meansf(sta,tt)*dx(sta-1)+c*abs((velocity(sta-1,tt)^2-velocity(sta,tt)^2)))/(2*9.81)
denergy(sta,tt) = energyt(sta1 ,tt) etstart(sta,tt)
error(ni,tt) = abs(denergy(sta,tt))
If ni = 1
Yes
minerror = error(ni,tt)
iteration = ni
hsmin(sta,ni) = hstart(sta,tt)
No
If error(ni,tt) <minerror
Yes
minerror = error(ni,tt)
iteration = ni
hsmin(sta,ni) = hstart(sta,tt)
No
If error(ni,tt) <0.0001
Yes
h(sta,tt) = hstart(sta,tt)
No
If h(sta,tt) < hc(sta,tt)
Yes
h(sta,tt) = hc(sta,tt)
No
If width(sta) > width(sta-1)
Yes
senergy(sta,tt) = velhead(sta,tt)+h(sta,tt)
cenergy(sta-1,tt) = 3*hc(sta-1,tt)/2
No
If senergy(sta,tt)< cenergy(sta,tt)
No
Yes
Call Function bisectionme and compute h(sta,tt) that corresponds to cenergy(sta-1,tt)
D
E
F
G

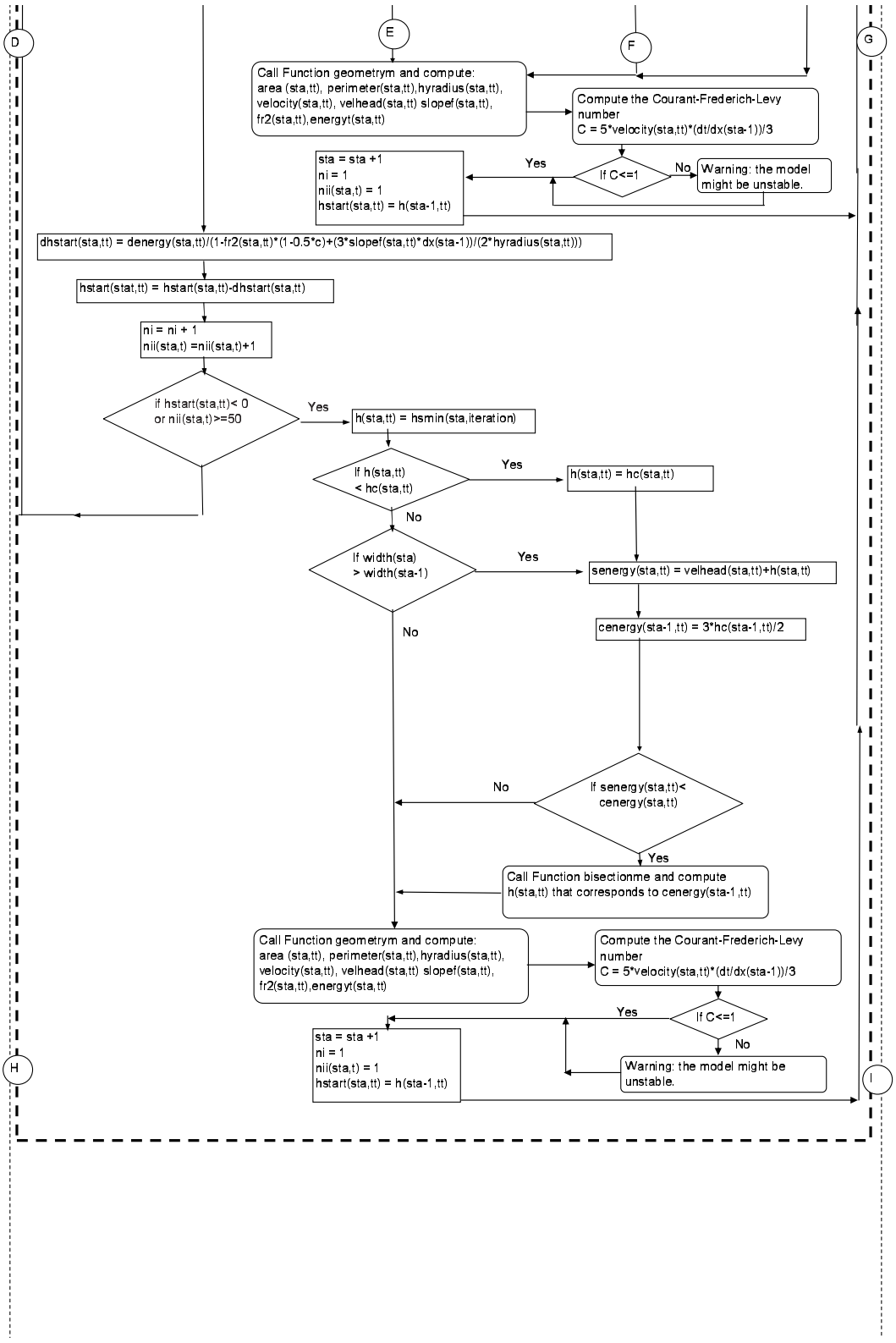
D
E
F
G
H
I
Call Function geometrym and compute:
area (sta,tt), perimeter(sta,tt),hyradius(sta,tt),
velocity(sta,tt), velhead(sta,tt) slopef(sta,tt),
fr2(sta,tt),energyt(sta,tt)
Compute the Courant-Frederich-Levy
number
C = 5*velocity(sta,tt)*(dt/dx(sta-1))/3
If C<=1
Yes
No
Warning: the model
might be unstable.
sta = sta +1
ni = 1
nii(sta,t) = 1
hstart(sta,tt) = h(sta-1,tt)
dhstart(sta,tt) = denergy(sta,tt)/(1-fr2(sta,tt)*(1-0.5*c)+(3*slopef(sta,tt)*dx(sta-1))/(2*hyradius(sta,tt)))
hstart(stat,tt) = hstart(sta,tt)-dhstart(sta,tt)
ni = ni + 1
nii(sta,t) =nii(sta,t)+1
if hstart(sta,tt)< 0
or nii(sta,t)>=50
Yes
h(sta,tt) = hsmin(sta,iteration)
If h(sta,tt)
< hc(sta,tt)
Yes
h(sta,tt) = hc(sta,tt)
No
If width(sta)
> width(sta-1)
Yes
senergy(sta,tt) = velhead(sta,tt)+h(sta,tt)
cenergy(sta-1,tt) = 3*hc(sta-1,tt)/2
No
If senergy(sta,tt)<
cenergy(sta,tt)
No
Yes
Call Function bisectionme and compute
h(sta,tt) that corresponds to cenergy(sta-1,tt)
Call Function geometrym and compute:
area (sta,tt), perimeter(sta,tt),hyradius(sta,tt),
velocity(sta,tt), velhead(sta,tt) slopef(sta,tt),
fr2(sta,tt),energyt(sta,tt)
Compute the Courant-Frederich-Levy
number
C = 5*velocity(sta,tt)*(dt/dx(sta-1))/3
If C<=1
Yes
No
Warning: the model might be
unstable.
sta = sta +1
ni = 1
nii(sta,t) = 1
hstart(sta,tt) = h(sta-1,tt)

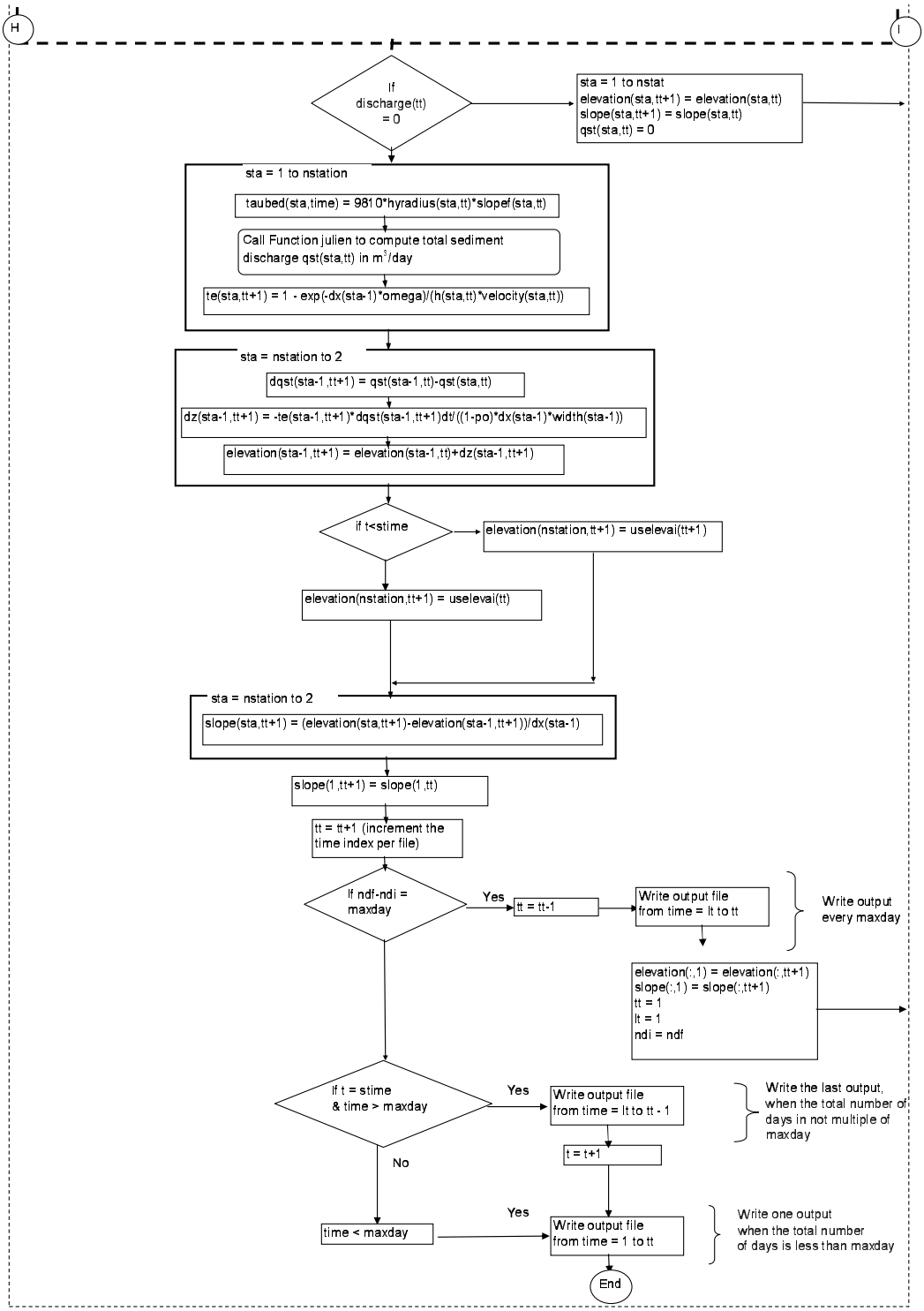
H
I
If discharge(tt) = 0
sta = 1 to nstat
elevation(sta,tt+1) = elevation(sta,tt)
slope(sta,tt+1) = slope(sta,tt)
qst(sta,tt) = 0
sta = 1 to nstation
taubed(sta,time) = 9810*hyradius(sta,tt)*slopef(sta,tt)
Call Function julien to compute total sediment discharge qst(sta,tt) in m3/day
te(sta,tt+1) = 1 - exp(-dx(sta-1)*omega)/(h(sta,tt)*velocity(sta,tt))
sta = nstation to 2
dqst(sta-1,tt+1) = qst(sta-1,tt)-qst(sta,tt)
dz(sta-1,tt+1) = -te(sta-1,tt+1)*dqst(sta-1,tt+1)dt/((1-po)*dx(sta-1)*width(sta-1))
elevation(sta-1,tt+1) = elevation(sta-1,tt)+dz(sta-1,tt+1)
if t<stime
elevation(nstation,tt+1) = uselevai(tt+1)
elevation(nstation,tt+1) = uselevai(tt)
sta = nstation to 2
slope(sta,tt+1) = (elevation(sta,tt+1)-elevation(sta-1,tt+1))/dx(sta-1)
slope(1,tt+1) = slope(1,tt)
tt = tt+1 (increment the time index per file)
If ndf-ndi = maxday
Yes
tt = tt-1
Write output file from time = lt to tt
Write output every maxday
elevation(:,1) = elevation(:,tt+1)
slope(:,1) = slope(:,tt+1)
tt = 1
lt = 1
ndi = ndf
If t = stime & time > maxday
Yes
Write output file from time = lt to tt - 1
Write the last output, when the total number of days in not multiple of maxday
t = t+1
No
time < maxday
Yes
Write output file from time = 1 to tt
Write one output when the total number of days is less than maxday
End

G.4 Code of the Numerical Model for Variable Discharge with no Control of Degradation along the Channel

```
%Script file: unsteady.m
%
%Purpose:
%This program computes the aggradation/degradation in
%a sequence of channel reaches under unsteady flow conditions.
%The energy equation is solved with Henderson's equation
%The model works with trapezoidal cross sections
%The model uses Manning resistance equation
%The normal depth is computed with the bisection method.
%The critical depth is computed with the bisection method.
%If the cross section is rectangular, the critical depth is
%computed without any iteration.
%When the energy equation does not converge, the flow depth
%is set to the minimum error elevation.  If the minimum error
%elevation is in the wrong side of the critical depth, the
%elevation is set to critical.
%When there is a contraction, the programs checks if the flow
%is chocked.  If so, the program computes the flow depth that
%will produce an energy equal to the minimum energy o
%critical energy downstream at the constriction
%
%Define variables
%Input data:
%
%time = total time in days
%dt = delta time in days
```

```
%disc = flow discharge in m3/s from input file
%discharge = interpolated flow discharge in m3/s
%nstation = number of stations along the channel
%station = station number
%length = channel length in m
%slope = channel slope
%width = channel width in m
%n = friction factor
%ds = sediment diameter in m
%vis = Kinematic viscosity in m2/s
%po = sediment porosity
%z = side slope
%
%Other variables
%ntime = number of time steps
%h = known flow depth in m at a station along the channel
%hstart = guessed flow depth in m at a station along the channel
%area = cross section area in m2 (rectangular section)
%perimeter = wetted perimeter in m (rectangular section)
%hyradius = hydraulic radius in m (rectangular section)
%velocity = mean flow velocity in m/s
%velhead = velocity head in m
%energyt = total energy in m
%slopef = friction slope
%fr2 = Froude number squared
%taubed = bed shear stress in N/m2
%meansf = average of friction slope between two adjacent stations
%etstart = total energy start in m
```

```
%denergy = delta energy in m
%dhstart = flow depth increment in m
%omega = fall velocity in m/s
%ndi = initial day of output file
%ndf = last day of output file
%lt = last time step an output file was written
%tt = time step per output file
%t = total time
%hn = normal depth m
%hc = critical depth m
%hmin = minimum initial bound input into the bisection method
%       to compute the normal depth and
%       critical depth in the case of non-rectangular sections
%hmax = maximum initial bound input into the bisection method
%       to compute the normal depth and
%       critical depth in the case of non-rectangular sections
%qbv = unit sediment discharge in m2/s
%qst = sediment discharge in m3/day
%dqst = change in sediment discharge between two adjacent
%       stations in m3/day
%maxday = number of days per output file
%iteration = is the iteration number where the minimum error
%            happens
%hsmin = is the flow depth that produces the minimum error
%minerror = is the minimum error of specific energy in m
%senergy = specific energy in m
%cenergy = critical energy in m
%
```

```
clear all
%%%%% Get input data %%%%%%%%%%%%%%%%%%%%%%%%%%%%%%%%%%%%
 n = 0.023; %Manning friction factor
 z = 0; %cross section side slope
 ds = 0.0003;
 vis = 0.000001;
 po = 0.43;
 maxday = 50;
%Opening the input file that contains the channel
%characteristics
 disp('Enter the name of the input file that contains the);
 disp('channel characteristics. The input file must);
 disp('contain five columns with the following data:);
 disp('Column 1 = Station #, Column 2 = length,);
 disp('Column 3 = Slope, Column 4 =');
 disp('Elevation and Column 5 = Width. The first row);
 disp('must contain the column headings:  '  );
 filename = input('  ','s');

%Calling function to read input data and compute nstation and dx
[nstation, station,length,slope,elevation,width,dx] = openfile1
(filename);

%Opening the input file that contains the flow discharge data
 disp('Enter the name of the input file that contains');
 disp('the flow discharge data, temperature data,');
 disp('bed elevation in the upstream node for the');
 disp('whole record. This input file must contain');
```

```
 disp('four columns.  The first column has the time');
 disp('in days, the second column has the flow discharge);
 disp('in m3/s, the third column contains the temperature,');
 disp('and the fourth columns has the bed elevation in the');
 disp('most upstream node. The first row must contain the');
 disp('column headings:   ');
filename2 = input('   ','s');
%Calling function to read input data and determine
%total time (time)
 [time,day,disc,temp,uselev] = openfile2 (filename2);
 if time < maxday
    %Enter name of output file
    disp('Enter the name of the output file:   ');
    ofilename = input('   ','s');
 end
%Print the total time obtained from filename2
fprintf('Total time is: %f\n',time);

%Get dt
dt = input('Enter delta t =  ');

%Initializing time
t0 = clock;

%Compute the kinematic viscosity for each water temperature
vis = conversion(temp);

%Call function to calculate the fall velocity of ds
```

```
omega = fallv(vis,ds);

%Creating slope and elevation matrixes for the first day.
%The first index (x) corresponds to the stations along
%the channel.  The second index corresponds to time.
%Time = 1 is the first day
x = 1:1:nstation; slope(x,1) = slope(x); elevation(x,1) =
elevation(x);
%Calculate the total time the model will run.  Time=1
%corresponds to the initial conditions (time = day 1):
%initial slope, discharge, d/s flow depth, etc.
%Time = 2 will be 1day + dt, time = 3 will be 1day
%+ 2*dt and so on...tn = 1dat + (n-1)*dt

 if time == 1
  stime = 1;
  fprintf('Total time is 1 day.  The model will run
  for %f\t day', time);
 else
  counter = 0;
  cumtime = 0;
 while cumtime <= time
  cumtime = 1+counter*dt;
  counter = counter + 1;
 end
 fprintf('The model will run for %f\t days',cumtime - dt);
 stime = counter -1;
end
```

```
%Create a matrix with all the time step - discharge pairs
% by interpolating the discharge data. The interpolation
%will be linear
 timestep = 1:dt:time;
 discharge = interp1(day, disc,timestep);

%Compute the fall velocity for each time step with a
%linear interpolation
 timestep = 1:dt:time;
 omegai = interp1(day, omega,timestep);

%Compute the upstream bed elevation for each time step using
%linear interpolation
 timestep = 1:dt:time;
 uselevi = interp1(day, uselev,timestep);

%%%%%%    Calculate the backwater  %%%%
%Calculate the critical depth along the channel
ndi = 0; %initial number of days
lt =1; %last time an output file was written
tt = 1; %index from 1  to 365 days
t = 1; %initilize time

while t <= stime
 ndf = (t-1)*dt+1; %number of days
 numday(tt) = ndf;
 discharge(tt) = discharge(t);
```

```
 disp(['day # :' num2str(ndf)]);
 omegai(tt) = omegai(t);
 if t < stime
    uselevi(tt+1) = uselevi(t+1);
 end
%Checking for zero discharge.  If Q = 0, everything else is 0
 if discharge(tt) == 0
 sta = 1:nstation;
 hn(sta,tt) = 0;
 hc(sta,tt) = 0;
 area (sta,tt) = 0; perimeter(sta,tt) = 0; hyradius(sta,tt) = 0;
 velocity(sta,tt) = 0; velhead(sta,tt) = 0; energyt(sta,tt) = 0;
 slopef(sta,tt) = 0; fr2(sta,tt) = 0;
 else
 %Compute the normal depth at station 1 and assume
 %d/s depth (sta 1) = normal depth
 if slope(1,tt)< 0
 error('Slope < 0, normal depth does not exist');
 else
 hmin = 0;  %hmin and hmax are the min and max
            %initial bounds for the bisection method iterations
 hmax = 10;
 flag = 1; %flag = 1 indicates the bisection function
           %to compute the normal depth
 [hn(1,tt)] = bisection(discharge(tt),slope(1,tt)...
 ,n,width(1),z,hmin,hmax,flag);
 h(1,tt) = hn(1,tt);
 end
```

```
 %Calculate the critical depth at station 1
 if z == 0
 %hc for rectangular section
 hc(1,tt) = ((discharge(tt)^2)/(9.81*width(1)^2))^(1/3);
 else
 hmin = 0;  %hmin and hmax are the min and max initial
            %bounds for the bisection method iterations
 hmax = 1.1*((discharge(tt)^2)/(9.81*width(1)^2))^(1/3);
 flag = 2;  %flag = 2 indicates the bisection function
            %to compute the critical depth
 [hc(1,tt)] = bisection(discharge(tt),slope(1,tt),n...
 ,width(1),z,hmin,hmax,flag);
 end
%Calling function geometrym to compute the area,
%perimeter,hydraulic radius, velocity, velocity head,
%total energy and friction slope at station 1
%(downstream end of the channel), based on the flow
%depth specified, flow discharge, width, elevation
%and friction factor (f)

[area(1,tt),perimeter(1,tt),hyradius(1,tt),velocity(1,tt)...
,velhead(1,tt),energyt(1,tt),slopef(1,tt)...
,fr2(1,tt)]=geometrym(width(1),h(1,tt),discharge(tt)...
,elevation(1,tt),n,z);

%Calculate the bed shear stress in N/m2 at station 1
taubed(1,tt) = 9810*hyradius(1,tt)*slopef(1,tt);
```

```
%Initializing the counter 'sta' to start computing the
%backwater profile
sta = 2;

%Assuming the u/s depth (sta = 2) equal to the d/s depth (sta = 1)
hstart(sta,tt) = h(sta-1,tt);

%number of iterations
 ni =1;
 nii(sta,t) = 1;

while sta <= nstation
%Calling function geometrym
[area(sta,tt),perimeter(sta,tt),hyradius(sta,tt),velocity(sta,tt)...
,velhead(sta,tt),energyt(sta,tt),slopef(sta,tt),fr2(sta,tt)]=...
geometrym(width(sta),hstart(sta,tt),discharge(tt),...
elevation(sta,tt),n,z);

%Calculate the critical depth along the channel
if z == 0
 %hc for rectangular section
 hc(sta,tt) = ((discharge(tt)^2)/(9.81*width(sta)^2))^(1/3);
 else
%hmin and hmax are the min and max initial bounds for the
%bisection method iterations
 hmin = 0;
 hmax = 1.1*((discharge(tt)^2)/(9.81*width(sta)^2))^(1/3);
 flag = 2;  %flag = 2 indicates the bisection function to
```

```
            %compute the critical depth
 [hc(sta,tt)] = bisection(discharge(tt),slope(sta,tt),n...
 ,width(sta),z,hmin,hmax,flag);
end

%Compute the average friction slope between stations
%sta and sta-1
meansf(sta,tt) = (slopef(sta-1,tt)+slopef(sta,tt))*0.5;

 if velocity(sta-1,tt) > velocity(sta,tt)
 %if the downstream velocity is greater than the upstream
 %velocity an contraction occurs.
 %Minor losses are summed to the total energy loss
 c = 0.1; %From Hec-Ras manual. Chapter 3
 elseif velocity(sta-1,tt) < velocity (sta,tt)
 %if the downstream velocity is less than the upstream
 %velocity an expansion occurs.
 %Minor losses are summed to the total energy loss
 c = 0.3; %From Hec-Ras manual. Chapter 3
 else
 c = 0;
 end
%Compute the total energy at the u/s station (sta)
%as the total energy d/s plus
%the head lost between both stations = meansf * dx plus
%minor losses
 etstart(sta,tt) = energyt(sta-1,tt) + ...
 meansf(sta,tt)*dx(sta-1) + c*abs((velocity(sta-1,tt)^(2)...
```

```
 -velocity(sta,tt)^(2)))/(2*9.81);

%Compute the difference in total energy in station
%sta by sustracting the
%total energy start (etstart)and the total energy computed
%with the function geometry energyt
 denergy(sta,tt) = energyt(sta,tt)-etstart(sta,tt);
 error(ni,tt) = abs(denergy(sta,tt));
 if ni == 1
    minerror = error(ni,tt);
    iteration  = ni;
    hsmin(sta,ni) = hstart(sta,tt);
    elseif error(ni,tt)< minerror
    minerror = error(ni,tt);
    iteration = ni;
    hsmin(sta,ni) = hstart(sta,tt);
 end
%Check if denergy is less than an specified error.  If so,
%the assumed elevation at the u/s station is right and we
%proceed to the next u/s station.  If not, a new
%value will be assumed. dhstart is added to the previous
%assumed depth to compute the new assumed depth.
%dhstart equation comes from Henderson (1966) book pp.143
 if abs(denergy(sta,tt)) <=0.001
   h(sta,tt) = hstart(sta,tt);
 %If h(sta,t) is in the wrong side of hc, h is set to hc
 if h(sta,tt) < hc(sta,tt)
 h(sta,tt) = hc(sta,tt);
```

```
 disp('Msg 1: h is set to hc');
 disp(sta);
 disp(t);
 end
if width(sta) > width(sta-1) %there is a contraction
%check if the specific energy is less than the
%critical energy at the constriction
%Specific energy at sta
 senergy(sta,tt) = velhead(sta,tt)+h(sta,tt);
 %Critical energy at the next downstream station
 cenergy(sta-1,tt) = 3*hc(sta-1,tt)/2;
 %If energy < critical energy, the water has to backup
 %until it gets sufficient energy to pass
 if senergy(sta,tt) < cenergy(sta-1,tt)
 hmin = hc(sta,tt);
 hmax = 1.5*h(sta,tt);
 h(sta,tt) = bisectionme(hmin,hmax,discharge(tt)...
 ,cenergy(sta-1,tt),width(sta),z);
 disp('Msg2: h corresponds to critical energy downstream');
 disp(sta);
 disp(t);
 end
 end
%Calling function geometrym
[area(sta,tt),perimeter(sta,tt),hyradius(sta,tt)...
,velocity(sta,tt),velhead(sta,tt),energyt(sta,tt)...
,slopef(sta,tt),fr2(sta,tt)]=geometrym(width(sta)...
,h(sta,tt),discharge(tt),elevation(sta,tt),n,z);
```

```
%Compute the Courant-Friedrich-Levy number and check stability
 courant(sta,tt) = dt*5*velocity(sta,tt)/(3*dx(sta-1));
 if courant(sta,tt)>1
   disp('the model is unstable');
 end

%increase the counter to compute the flow depth in the next
%upstream station
 sta = sta + 1;

%Initialized the number of iterations to 1 in the next station
 ni = 1;
 nii(sta,t) = 1;

%Assume a new hstart(sta) value equal to the d/s depth just
%calculated at 'sta'
 hstart(sta,tt) = h(sta-1,tt);

 else
%Calculate the flow increment (dhstart)
 dhstart(sta,tt) = denergy(sta,tt)/(1-fr2(sta,tt)*(1-0.5*c)+...
 (3*slopef(sta,tt)*dx(sta-1))/(2*hyradius(sta,tt)));

%Add the flow increment to the assumed flow depth hstart
 hstart(sta,tt) = hstart(sta,tt)- dhstart(sta,tt);

%Increase the number of iterations
```

```
 ni = ni + 1;
 nii(sta,t) = nii(sta,t) +1;

 if hstart(sta,tt) < 0 | nii(sta,t) >= 50
%If hstart is negative, the solution will be the minimum
%error wse
 h(sta,tt) = hsmin(sta,iteration);
 disp('Msg 3:No solution for the energy equation was found.);
 disp('h is set to the minimum error h');
 disp(sta)
 disp(t)
if width(sta) > width(sta-1) %there is a contraction
 %check if the specific energy is less than the critical
 %energy at the constriction
 %Specific energy at sta
 senergy(sta,tt) = velhead(sta,tt)+h(sta,tt);
 %Critical energy at the next downstream station
 cenergy(sta-1,tt) = 3*hc(sta-1,tt)/2;
 %If energy < critical energy, the water has to backup
 %until it gets sufficient energy to pass
 if senergy(sta,tt) < cenergy(sta-1,tt)
 hmin = hc(sta,tt);
 hmax = 3;
 h(sta,tt) = bisectionme(hmin,hmax,discharge(tt)...
 ,cenergy(sta-1,tt),width(sta),z);
 disp('Msg 4:h corresponds to critical energy downstream');
 disp(sta);
 disp(t);
```

```
 end
 else
 %if the minimum error wse < critical depth, h is set to critical
 if h(sta,tt) < hc(sta,tt)
 h(sta,tt) = hc(sta,tt);
 disp('Msg 5:h is set to hc');
 disp(sta);
 disp(t);
 end
 end
%Compute the channel characteristics with the new depth
[area(sta,tt),perimeter(sta,tt),hyradius(sta,tt)...
,velocity(sta,tt),velhead(sta,tt),energyt(sta,tt)...
,slopef(sta,tt),fr2(sta,tt)]=geometrym(width(sta)...
,h(sta,tt),discharge(tt),elevation(sta,tt),n,z);

%Compute the Courant-Friedrich-Levy number and check stability
 courant(sta,tt) = dt*5*velocity(sta,tt)/(3*dx(sta-1));
 if courant(sta,tt)>1
   disp('the model is unstable');
 end

%Increase the number of stations
 sta = sta+1;
%Set number of iterations to 1
 ni = 1;
 nii(sta,t) = 1;
%New assumed depth equal to previous depth
```

```
 hstart(sta,tt) = h(sta-1,tt);
 end
 end
 end
 end
%Compute the bed shear stress in N/m2 based on the
%friction slope at each node
 i = 1:nstation;
 taubed(i,tt) = 9810*hyradius(i,tt).*slopef(i,tt);
 wselevation(i,tt) = elevation(i,tt)+h(i,tt);
%%%%%% - SEDIMENT TRANSPORT - AGGRADATION/DEGRADATION - %%%%%%%
%Calculate the sediment discharge at each
%station using Julien's equation
%If discharge is zero, then the bed elevation and
%slope do not change
 if discharge(t) == 0
 sta = 1:nstation;
 elevation(sta,tt+1) = elevation(sta,tt);
 slope(sta,tt+1) = slope(sta,tt);
 else
 for sta = nstation:-1:1
 %Unit sediment discharge
 qbv(sta,tt) = julien(ds,taubed(sta,tt));
 %Sediment discharge in m3/day
 qst(sta,tt) = qbv(sta,tt)*width(sta)*86400;
 end
%Computing from upstream to downstream.  nstation is upstream
 for sta = nstation:-1:2
```

```
 %Change in sediment discharge between 2 adjacent stations
 %backward difference approximation
 dqst(sta-1,tt+1) = qst(sta-1,tt)-qst(sta,tt);
 %Trap efficiency at time t+1 based on h and velocity
 %computed at time = t
 te(sta-1,tt+1) = 1-exp(-dx(sta-1)*omegai(tt)...
 /(h(sta-1,tt)*velocity(sta-1,tt)));
 %Change in bed elevation at time t+1
 dz(sta-1,tt+1) = -te(sta-1,tt+1)*dqst(sta-1,tt+1)*dt...
 /((1-po)*dx(sta-1)*width(sta-1));
 %New bed elevation at time t+1
 %backward difference approximation in space and forward
 %difference in time
 elevation(sta-1,tt+1) = elevation(sta-1,tt)...
 + dz(sta-1,tt+1);
 end
 if t < stime
%Elevation upstream is given as a boundary condition
 elevation(nstation,tt+1) = uselevi(tt+1);
 else
 %The computations end at t = stime.  The elevation
 %at t = stime was computed in the previous time step
 elevation(nstation,tt+1) = elevation(nstation,tt);
 end
%Fix elevation at the d/s stations
 elevation(1,tt+1) = elevation(1,tt);
 for sta = nstation:-1:2
%Calculate the new bed channel slope
```

```
 slope(sta,tt+1) = (elevation(sta,tt+1)...
 -elevation(sta-1,tt+1))/dx(sta-1);
 end
 slope(1,tt+1) = slope(1,tt);
 end
 tt = tt+1; %increment the time index tt
%Printing out the results every maxday days
 if ndf - ndi == maxday
 tt = tt-1;
 numfile = int2str(ndf);
 fileout=strcat(numfile,'.out');
 fid = fopen(fileout,'wt');
 fprintf(fid,'%-15s %-11s %-12s %-12s %-15s...
 %-12s %-12s %-12s %-12s %-12s %-15s %-12s\n',...
 'days','Station','Length', 'Slope','Elevation'...
 ,'Width','Q','h','Sf','Fr2','hc','qst');
 for k = lt:tt
 ddiff = numday(k) - round(numday(k));
 if ddiff == 0
 for s = 1:nstation
 fprintf(fid,'%6.1f\t %11d\t %11.2f\t %10.6e\t %11.6e\t...
 %11.2f\t %11.2f\t %6.4f\t %10.2e\t %10.4e\t %6.4f\t %6.4f\n',...
 numday(k), station(s), length(s),slope(s,k),elevation(s,k),...
 width(s),discharge(k),h(s,k),slopef(s,k),fr2(s,k),hc(s,k),...
 qst(s,k));
 end
 end
 end
```

```
fclose(fid);
elevation(:,1) = elevation(:,tt+1);
slope(:,1) = slope(:,tt+1);
tt = 1;
lt = 1;
ndi = ndf;
elseif t == stime & time > maxday
numfile = int2str(ndf);
fileout=strcat(numfile,'.out');
fid = fopen(fileout,'wt');
fprintf(fid,'%-15s %-11s %-12s %-12s %-15s %-12s...
%-12s %-12s %-12s %-12s %-15s %-12s\n',...
'Station','Length', 'Slope','Elevation',...
 'Width','Q','h','Sf','Fr2','hc','qst');
for k = lt:tt-1
ddiff = numday(k) - round(numday(k));
if ddiff == 0
for s = 1:nstation
fprintf(fid,'%6.1f\t %11d\t %11.2f\t %10.6e\t...
%11.6e\t %11.2f\t %11.2f\t %6.4f\t %10.2e\t...
%10.4e\t %6.4f\t %6.4f\n', numday(k),...
station(s), length(s),slope(s,k),elevation(s,k),...
width(s), discharge(k),h(s,k),slopef(s,k),...
fr2(s,k),hc(s,k),qst(s,k));
end
end
end
fclose(fid);
```

```
 end
 t = t +1; %increment the total time index
end
%%%%%%%%% Writing the results into a file %%%%%%%%%
%Printing out the results if the total time is less
%than maxday days
if time < maxday fid = fopen(ofilename,'wt');
 fprintf(fid,'%-15s %-11s %-12s %-12s %-15s %-12s...
 %-12s %-12s %-12s %-12s %-15s %-12s\n',...
 'Slope','Elevation', 'Width','Q','h','Sf','Fr2',...
 'hc','qst');
 for k = 1:tt;
 ddiff = numday(k) - round(numday(k));
 if ddiff == 0
 for s = 1:nstation
 fprintf(fid,'%6.1f\t %11d\t %11.2f\t %10.6e\t...
 %11.6e\t %11.2f\t %11.2f\t %6.4f\t %10.2e\t...
 %10.4e\t %6.4f\t %6.4f\n', numday(k),...
 station(s), length(s),slope(s,k),elevation(s,k),...
 width(s), discharge(k),h(s,k), slopef(s,k),...
 fr2(s,k),hc(s,k),qst(s,k));
 end
 end
 end
 fclose(fid);
 end
 elapsedtime = etime(clock,t0);
 fprintf('The elapsed time in seconds is = %6.3f\n',elapsedtime);
```

G.5 Flow Chart of Numerical Model for Variable Discharge with Control of Degradation along the Channel

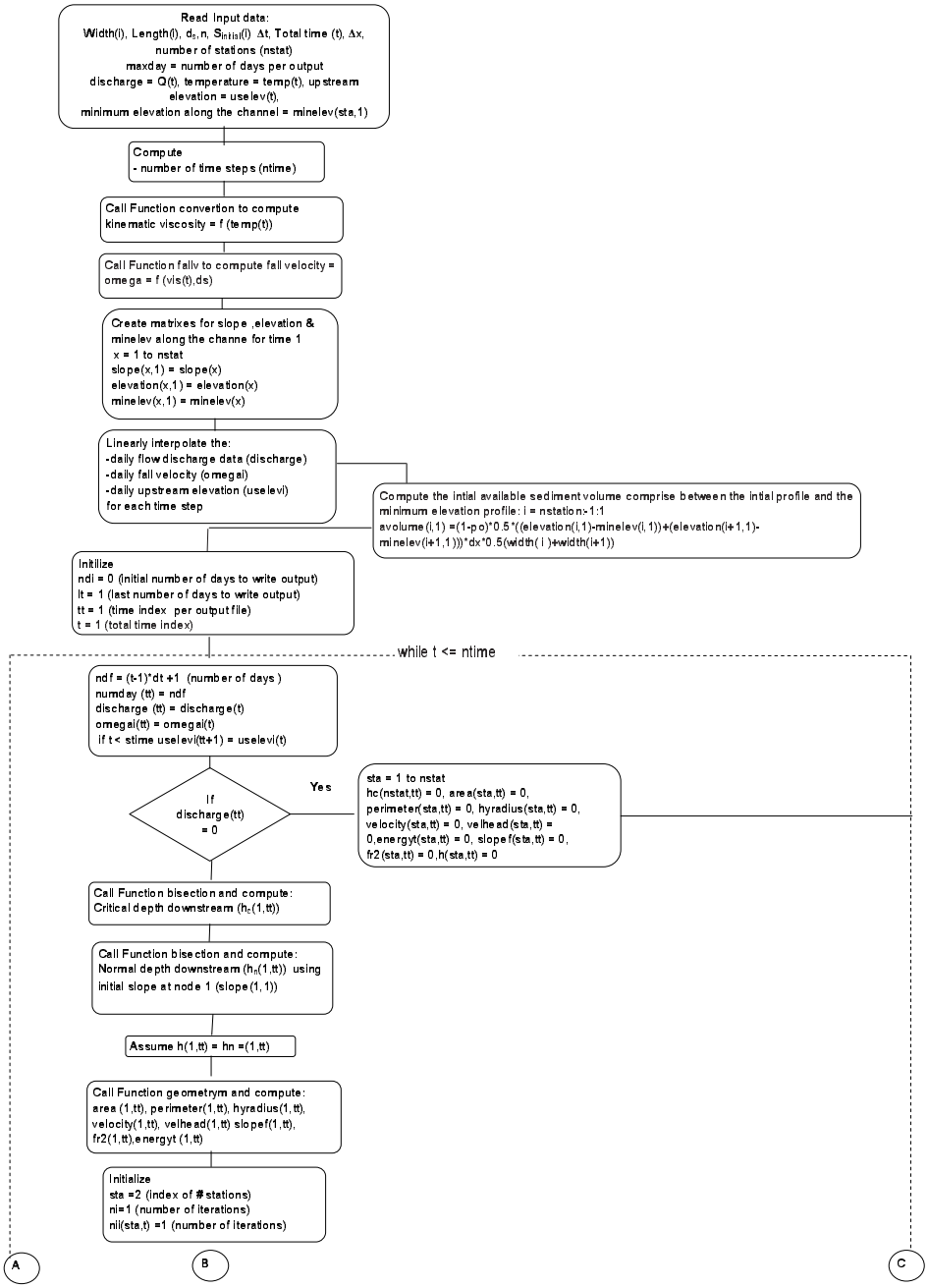

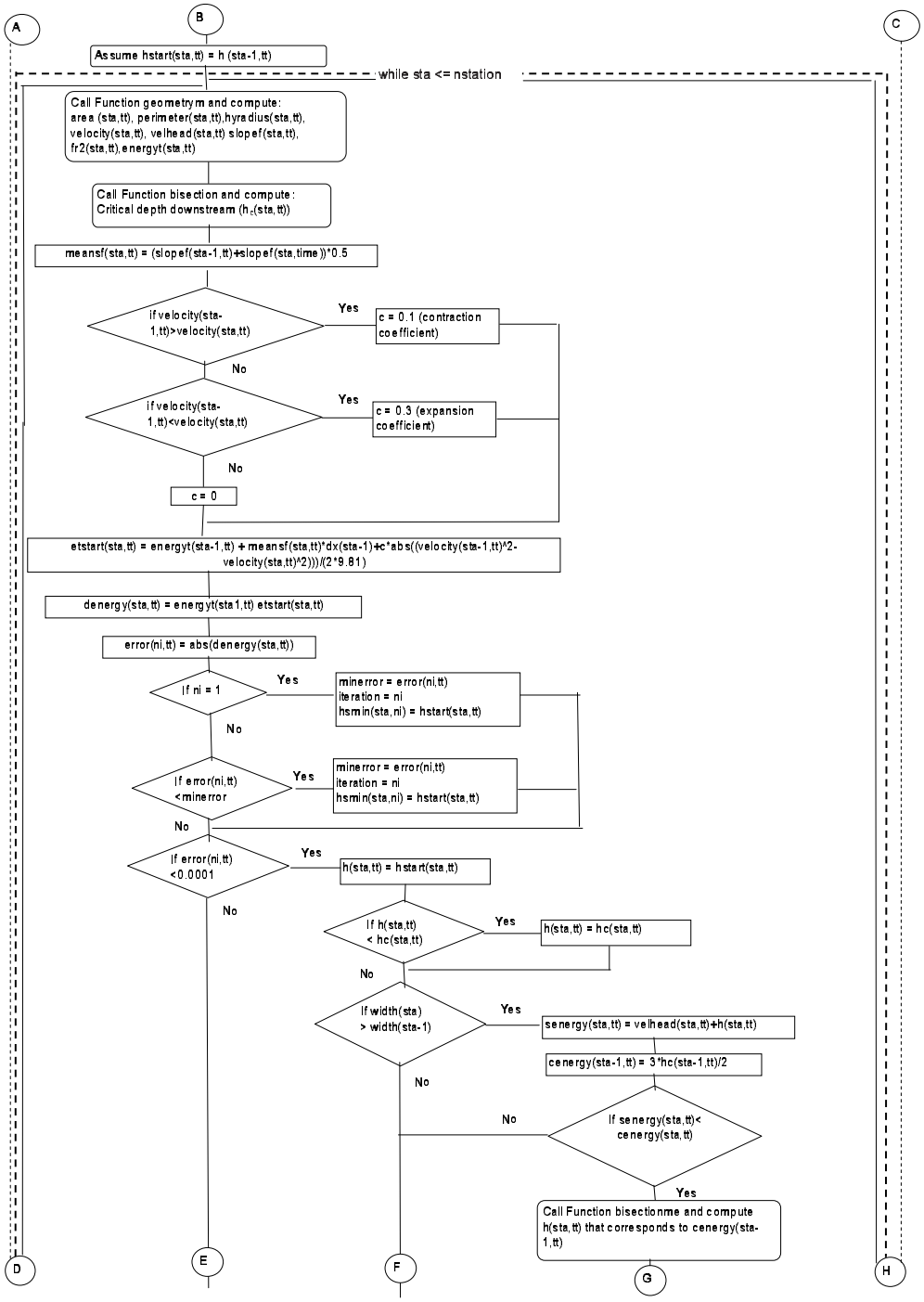
A
B
C
Assume hstart(sta,tt) = h (sta-1,tt)
while sta <= nstation
Call Function geometrym and compute:
area (sta,tt), perimeter(sta,tt),hyradius(sta,tt),
velocity(sta,tt), velhead(sta,tt) slopef(sta,tt),
fr2(sta,tt),energyt(sta,tt)
Call Function bisection and compute:
Critical depth downstream (hc(sta,tt))
meansf(sta,tt) = (slopef(sta-1,tt)+slopef(sta,time))^0.5
If velocity(sta-1,tt)>velocity(sta,tt)
Yes
c = 0.1 (contraction coefficient)
No
If velocity(sta-1,tt)<velocity(sta,tt)
Yes
c = 0.3 (expansion coefficient)
No
c = 0
etstart(sta,tt) = energyt(sta-1,tt) + meansf(sta,tt)*dx(sta-1)+c*abs((velocity(sta-1,tt)^2-velocity(sta,tt)^2)))/(2*9.81)
denergy(sta,tt) = energyt(sta1,tt) etstart(sta,tt)
error(ni,tt) = abs(denergy(sta,tt))
If ni = 1
Yes
minerror = error(ni,tt)
iteration = ni
hsmin(sta,ni) = hstart(sta,tt)
No
If error(ni,tt) <minerror
Yes
minerror = error(ni,tt)
iteration = ni
hsmin(sta,ni) = hstart(sta,tt)
No
If error(ni,tt) <0.0001
Yes
h(sta,tt) = hstart(sta,tt)
No
If h(sta,tt) < hc(sta,tt)
Yes
h(sta,tt) = hc(sta,tt)
No
If width(sta) > width(sta-1)
Yes
senergy(sta,tt) = velhead(sta,tt)+h(sta,tt)
cenergy(sta-1,tt) = 3*hc(sta-1,tt)/2
No
No
If senergy(sta,tt)< cenergy(sta,tt)
Yes
Call Function bisectionme and compute h(sta,tt) that corresponds to cenergy(sta-1,tt)
D
E
F
G
H

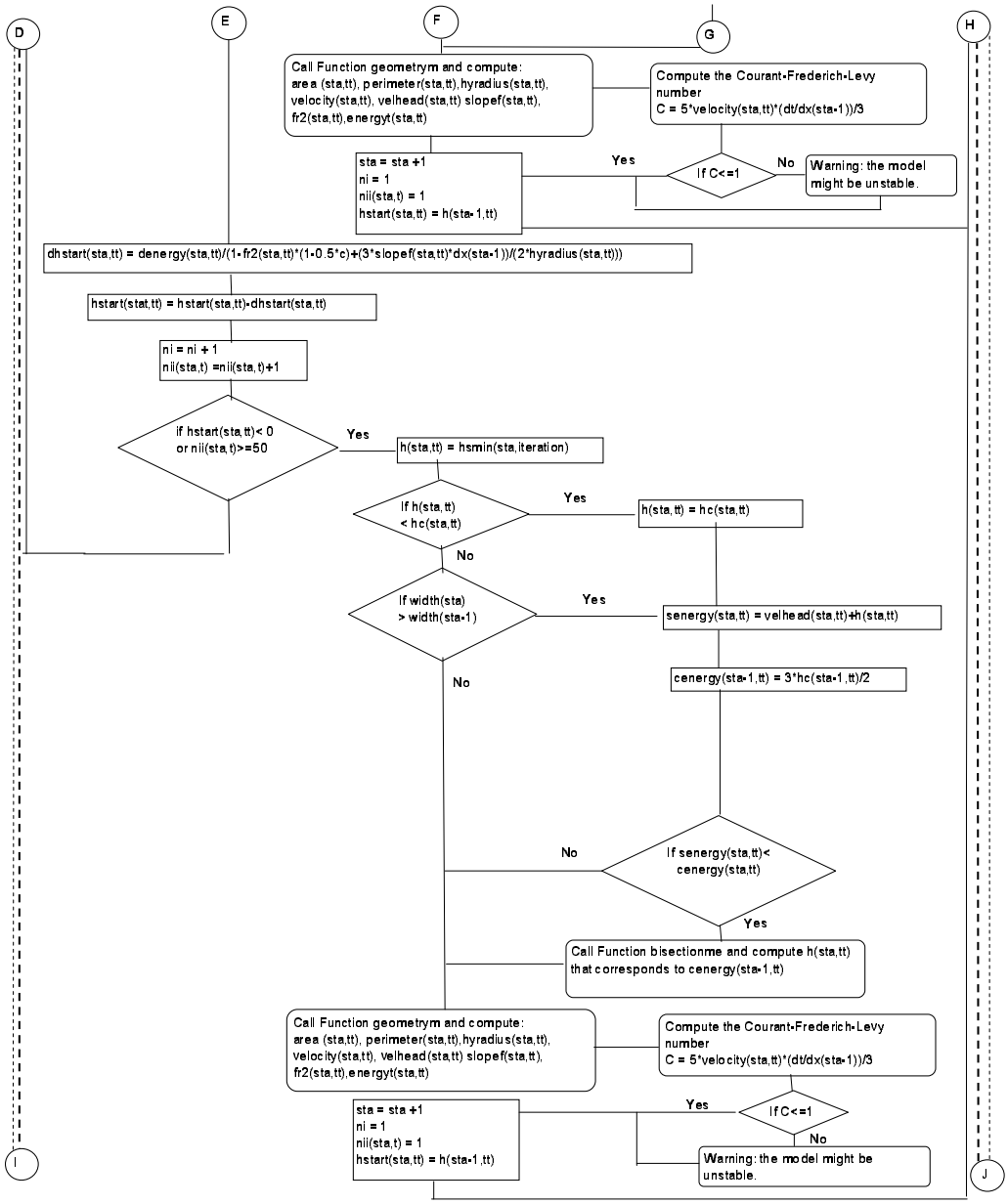
D
E
F
G
H
Call Function geometrym and compute:
area (sta,tt), perimeter(sta,tt),hyradius(sta,tt),
velocity(sta,tt), velhead(sta,tt) slopef(sta,tt),
fr2(sta,tt),energyt(sta,tt)
Compute the Courant-Frederich-Levy
number
C = 5*velocity(sta,tt)*(dt/dx(sta-1))/3
sta = sta +1
ni = 1
nii(sta,t) = 1
hstart(sta,tt) = h(sta-1,tt)
Yes
If C<=1
No
Warning: the model
might be unstable.
dhstart(sta,tt) = denergy(sta,tt)/(1-fr2(sta,tt)*(1-0.5*c)+(3*slopef(sta,tt)*dx(sta-1))/(2*hyradius(sta,tt)))
hstart(stat,tt) = hstart(sta,tt)-dhstart(sta,tt)
ni = ni + 1
nii(sta,t) =nii(sta,t)+1
If hstart(sta,tt)< 0
or nii(sta,t)>=50
Yes
h(sta,tt) = hsmin(sta,iteration)
If h(sta,tt)
< hc(sta,tt)
Yes
h(sta,tt) = hc(sta,tt)
No
If width(sta)
> width(sta-1)
Yes
senergy(sta,tt) = velhead(sta,tt)+h(sta,tt)
cenergy(sta-1,tt) = 3*hc(sta-1,tt)/2
No
No
If senergy(sta,tt)<
cenergy(sta,tt)
Yes
Call Function bisectionme and compute h(sta,tt)
that corresponds to cenergy(sta-1,tt)
Call Function geometrym and compute:
area (sta,tt), perimeter(sta,tt),hyradius(sta,tt),
velocity(sta,tt), velhead(sta,tt) slopef(sta,tt),
fr2(sta,tt),energyt(sta,tt)
Compute the Courant-Frederich-Levy
number
C = 5*velocity(sta,tt)*(dt/dx(sta-1))/3
sta = sta +1
ni = 1
nii(sta,t) = 1
hstart(sta,tt) = h(sta-1,tt)
Yes
If C<=1
No
Warning: the model might be
unstable.
I
J

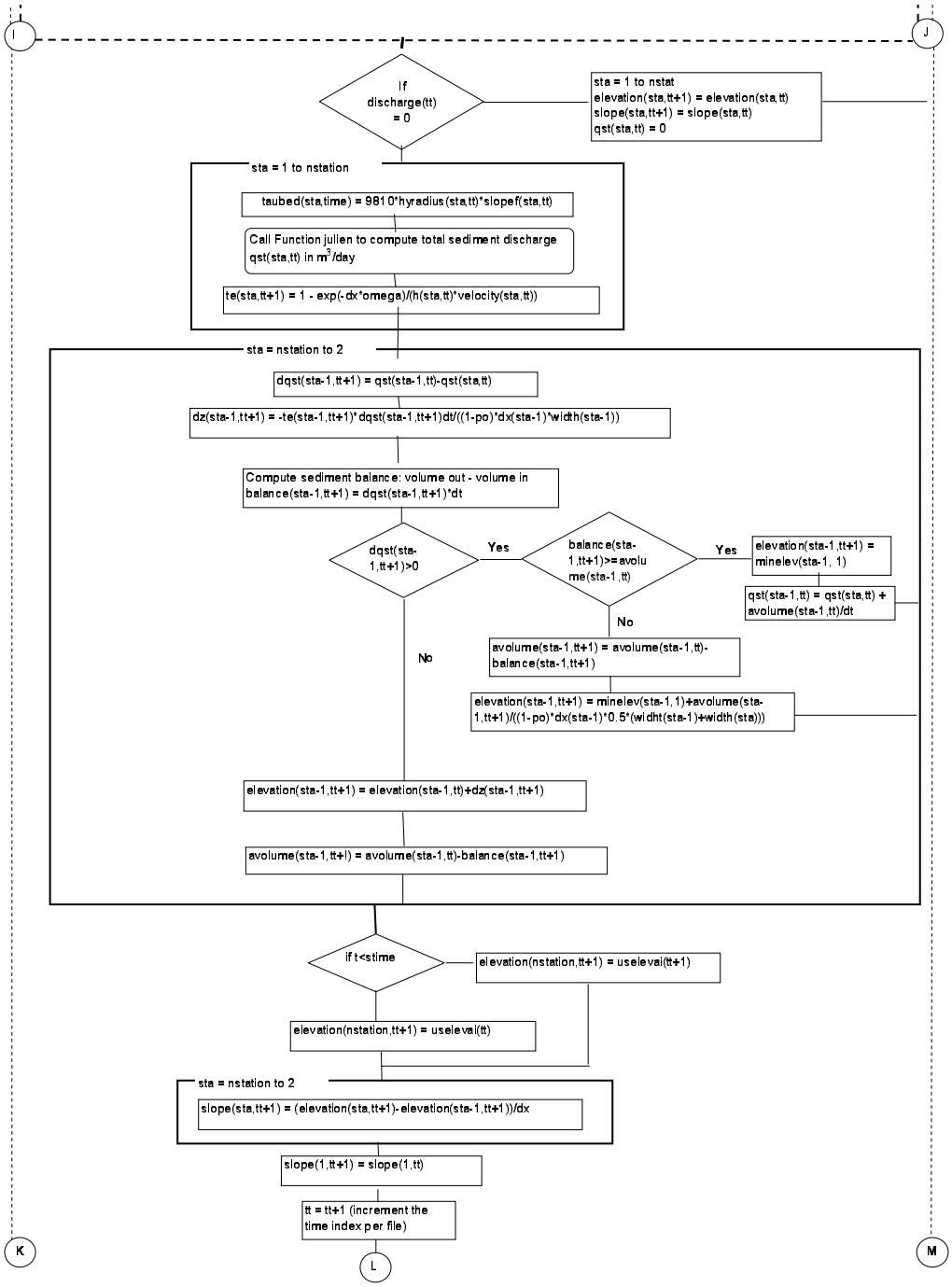
I
J
If discharge(tt) = 0
sta = 1 to nstat
elevation(sta,tt+1) = elevation(sta,tt)
slope(sta,tt+1) = slope(sta,tt)
qst(sta,tt) = 0
sta = 1 to nstation
taubed(sta,time) = 9810*hyradius(sta,tt)*slopef(sta,tt)
Call Function julien to compute total sediment discharge qst(sta,tt) in m3/day
te(sta,tt+1) = 1 - exp(-dx*omega)/(h(sta,tt)*velocity(sta,tt))
sta = nstation to 2
dqst(sta-1,tt+1) = qst(sta-1,tt)-qst(sta,tt)
dz(sta-1,tt+1) = -te(sta-1,tt+1)*dqst(sta-1,tt+1)dt/((1-po)*dx(sta-1)*width(sta-1))
Compute sediment balance: volume out - volume in
balance(sta-1,tt+1) = dqst(sta-1,tt+1)*dt
dqst(sta-1,tt+1)>0
Yes
balance(sta-1,tt+1)>=avolume(sta-1,tt)
Yes
elevation(sta-1,tt+1) = minelev(sta-1, 1)
qst(sta-1,tt) = qst(sta,tt) + avolume(sta-1,tt)/dt
No
avolume(sta-1,tt+1) = avolume(sta-1,tt)-balance(sta-1,tt+1)
No
elevation(sta-1,tt+1) = minelev(sta-1,1)+avolume(sta-1,tt+1)/((1-po)*dx(sta-1)*0.5*(widht(sta-1)+width(sta)))
elevation(sta-1,tt+1) = elevation(sta-1,tt)+dz(sta-1,tt+1)
avolume(sta-1,tt+l) = avolume(sta-1,tt)-balance(sta-1,tt+1)
if t<stime
elevation(nstation,tt+1) = useleval(tt+1)
elevation(nstation,tt+1) = useleval(tt)
sta = nstation to 2
slope(sta,tt+1) = (elevation(sta,tt+1)-elevation(sta-1,tt+1))/dx
slope(1,tt+1) = slope(1,tt)
tt = tt+1 (increment the time index per file)
K
L
M

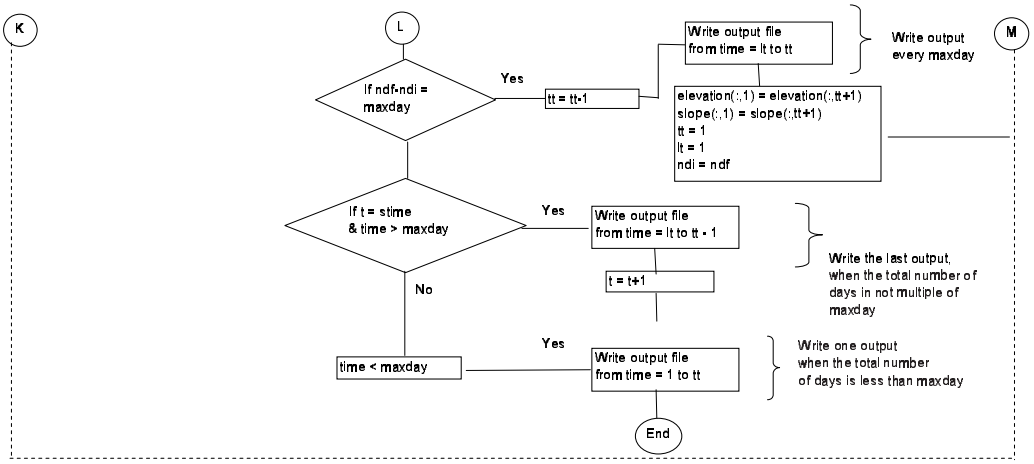
K
L
M
If ndf-ndi = maxday
Yes
tt = tt+1
Write output file from time = lt to tt
Write output every maxday
elevation(:,1) = elevation(:,tt+1)
slope(:,1) = slope(:,tt+1)
tt = 1
lt = 1
ndi = ndf
If t = stime & time > maxday
Yes
Write output file from time = lt to tt - 1
t = t+1
Write the last output, when the total number of days in not multiple of maxday
No
time < maxday
Yes
Write output file from time = 1 to tt
Write one output when the total number of days is less than maxday
End

G.6 Code of the Numerical Model for Variable Discharge with Control of Degradation along the Channel

```
%Script file: unsteady_2.m
%
%Purpose:
%This program computes the aggradation/degradation in a sequence
%of channel reaches under unsteady flow conditions.  The energy
%equation is solved with Henderson's equation. The model works
%with trapezoidal cross sections. The model uses Manning
%resistance equation. The normal depth is computed with the
%bisection method.  The critical depth is computed with the
%bisection method.  If the cross section is rectangular, the
%critical depth is computed without any iteration. When the
%energy equation does not converge, the flow depth is set to
%the minimum error elevation.  If the minimum error elevation
%is in the wrong side of the critical depth, the elevation is
%set to critical. When there is a contraction, the programs checks
%if the flow is chocked.  If so, the program computes
%the flow depth that will produce an energy equal to the minimum
%energy o critical energy downstream at the constriction
%
%Define variables
%Input data:
%
%time = total time in days
%dt = delta time in days
%disc = flow discharge in m3/s from input file
%discharge = interpolated flow discharge in m3/s
```

```
%nstation = number of stations along the channel
%station = station number
%length = channel length in m
%slope = channel slope
%width = channel width in m
%n = friction factor
%ds = sediment diameter in m
%vis = Kinematic viscosity in m2/s
%po = sediment porosity
%z = side slope
%
%Other variables
%ntime = number of time steps
%h = known flow depth in m at a station along the channel
%hstart = guessed flow depth in m at a station along the channel
%area = cross section area in m2 (rectangular section)
%perimeter = wetted perimeter in m (rectangular section)
%hyradius = hydraulic radius in m (rectangular section)
%velocity = mean flow velocity in m/s
%velhead = velocity head in m
%energyt = total energy in m
%slopef = friction slope
%fr2 = Froude number squared
%taubed = bed shear stress in N/m2
%meansf = average of friction slope between two adjacent stations
%etstart = total energy start in m
%denergy = delta energy in m
%dhstart = flow depth increment in m
```

```
%omega = fall velocity in m/s
%ndi = initial day of output file
%ndf = last day of output file
%lt = last time step an output file was written
%tt = time step per output file
%t = total time
%hn = normal depth m
%hc = critical depth m
%hmin = minimum initial bound input into the bisection method
%       to compute the normal depth and
%       critical depth in the case of non-rectangular sections
%hmax = maximum initial bound input into the bisection method
%       to compute the normal depth and
%       critical depth in the case of non-rectangular sections
%qbv = unit sediment discharge in m2/s
%qst = sediment discharge in m3/day
%dqst = change in sediment discharge between two adjacent
%       stations in m3/day
%maxday = number of days per output file
%iteration = is the iteration number where the minimum error
%         happens
%hsmin = is the flow depth that produces the minimum error
%minerror = is the minimum error of specific energy in m
%senergy = specific energy in m
%cenergy = critical energy in m
%
clear all
%%%%%%%%%%%%%%%% Get input data %%%%%%%%%%%%%%%%%%%%%%%
```

```
 n = 0.023; %Manning friction factor
 z = 0; %cross section side slope
 ds = 0.0003;
 vis = 0.000001;
 po = 0.43;
 maxday = 50;

%Opening the input file that contains the channel characteristics
 disp('Enter the name of the input file that contains the channel');
 disp('characteristics. The input file must contain five columns');
 disp('with the following data: Column 1 = Station number,');
 disp('Column 2 = length, Column 3 = Slope, Column 4 =Elevation');
 disp('and Column 5 = Width, Column 6 = minimum elevation.');
 disp('The first row must contain the column headings:  ' );
 filename =input(' ','s');

%Calling function to read input data and compute nstation and dx
 [nstation, station,length,slope,elevation,width,...
 dx,minelev] = openfile3(filename);
%Opening the input file that contains the flow discharge data
 disp('Enter the name of the input file that contains the flow');
 disp('discharge data, temperature data,bed elevation in the');
 disp('upstream node for the whole record. This input file must');
 disp('contain four columns.  The first column has the time in');
 disp('days, the second column has the flow discharge in m3/s,');
 disp('the third column contains the temperature,and the fourth');
 disp('columns has the bed elevation in the most upstream node');
 disp('The first row must contain the column headings:   ');
```

```
 filename2 = input('   ','s');

 %Calling function to read input data and determine
 %total time (time)
 [time,day,disc,temp,uselev] = openfile2 (filename2);

if time < maxday
    %Enter name of output file
    disp('Enter the name of the output file:   ');
    ofilename = input('   ','s');
end

%Print the total time obtained from filename2
fprintf('Total time is: %f\n',time);

%Get dt
dt = input('Enter delta t =  ');

%Initializing time
t0 = clock;

%Compute the kinematic viscosity for each water temperature
vis = conversion(temp);

%Call function to calculate the fall velocity of ds
omega = fallv(vis,ds);

%Creating slope and elevation matrixes for the first day.
```

```
%The first index (x) corresponds to the stations along
%the channel.  The second index corresponds
%to time.  Time = 1 is the first day
 x = 1:1:nstation;
 slope(x,1) = slope(x);
 elevation(x,1) = elevation(x);
 minelev(x,1)=minelev(x);

%Calculate the total time the model will run.  Time=1
%corresponds to the initial conditions (time = day 1):
%initial slope, discharge, d/s flow depth, etc.  Time = 2
%will be 1day + dt, time = 3 will be 1day + 2*dt and so on...
%tn = 1dat + (n-1)*dt
if time == 1
 stime = 1;
 fprintf('Total time is 1 day. The model will run
 for %f\t day', time);
else
    counter = 0;
    cumtime = 0;
    while cumtime <= time
        cumtime = 1+counter*dt;
        counter = counter + 1;
    end
    fprintf('The model will run for %f\t days',cumtime - dt);
    stime = counter -1;
end
%Create a matrix with all the time step - discharge pairs
```

```
%by interpolating the discharge data
%The interpolation will be linear
timestep = 1:dt:time; discharge = interp1(day, disc,timestep);

%Compute the fall velocity for each time step with a
%linear interpolation
timestep = 1:dt:time; omegai = interp1(day, omega,timestep);

%Compute the upstream bed elevation for each time step using
%linear interpolation
timestep = 1:dt:time; uselevi = interp1(day, uselev,timestep);

%Initialize the accumulated volume of sediment in the channel
%at time 1
for i = nstation-1:-1:1; avolume (i,1) =
(1-po)*0.5*((elevation(i,1) -
minelev(i,1))+(elevation(i+1,1)-minelev(i+1,1)))...
*dx(i).*0.5*(width(i)+width(i+1));
end
%%%%%%    Calculate the backwater  %%%%%%%%%%%%%%%%%%%%%%
%Calculate the critical depth along the channel
ndi = 0; %initial number of days
lt =1; %last time an output file was written
tt = 1; %index from 1  to 365 days
t = 1; %initilize time

while t <= stime
    ndf = (t-1)*dt+1; %number of days
```

```
    numday(tt) = ndf;
    discharge(tt) = discharge(t);
    disp(['day # :' num2str(ndf)]);
    omegai(tt) = omegai(t);
    if t < stime
        uselevi(tt+1) = uselevi(t+1);
    end
%Checking for zero discharge. If Q = 0, everything else is 0
 if discharge(tt) == 0
 sta = 1:nstation;
 hn(sta,tt) = 0;
 hc(sta,tt) = 0;
 area (sta,tt) = 0; perimeter(sta,tt) = 0; hyradius(sta,tt) = 0;
 velocity(sta,tt) = 0; velhead(sta,tt) = 0; energyt(sta,tt) = 0;
 slopef(sta,tt) = 0; fr2(sta,tt) = 0;
 else
%Compute the normal depth at station 1 and assume d/s depth
%(sta 1) = normal depth
 if slope(1,tt)<0
 error('Slope < 0, there is not normal depth');
 else
 hmin = 0;  %hmin and hmax are the min and max initial bounds
            %for the bisection method iterations
 hmax = 10;
 flag = 1; %flag = 1 indicates the bisection function to compute
           %the normal depth
 [hn(1,tt)] = bisection(discharge(tt),slope(1,1),n,width(1),...
 z,hmin,hmax,flag);
```

```
 h(1,tt) = hn(1,tt);
 end
 %Calculate the critical depth at station 1
 if z == 0
 %hc for rectangular section
 hc(1,tt) = ((discharge(tt)^2)/(9.81*width(1)^2))^(1/3);
 else
%hmin and hmax are the min and max initial bounds for the bisection
%method iterations
 hmin = 0;
 hmax = 1.1*((discharge(tt)^2)/(9.81*width(1)^2))^(1/3);
 flag = 2;  %flag = 2 indicates the bisection function to compute
            %the critical depth
 [hc(1,tt)] = bisection(discharge(tt),slope(1,tt),n,width(1),...
 z,hmin,hmax,flag);
end
%Calling function geometrym to compute the area, perimeter,hydraulic
%radius, velocity, velocity head,total energy and friction slope at
%station 1 (downstream end of the channel), based on the flow depth
%specified, flow discharge, width, elevation and friction factor (f)

 [area(1,tt),perimeter(1,tt),hyradius(1,tt),velocity(1,tt),...
 velhead(1,tt),energyt(1,tt),slopef(1,tt),...
 fr2(1,tt)] = geometrym(width(1),h(1,tt),discharge(tt),...
 elevation(1,tt), n,z);

%Calculate the bed shear stress in N/m2 at station 1
 taubed(1,tt) = 9810*hyradius(1,tt)*slopef(1,tt);
```

```
%Initializing the counter 'sta' to start computing the backwater
%profile
 sta = 2;

%Assuming the u/s depth (sta = 2) equal to the d/s depth (sta = 1)
 hstart(sta,tt) = h(sta-1,tt);

%number of iterations
 ni =1;
 nii(sta,t) = 1;
while sta <= nstation

%Calling function geometrym
[area(sta,tt),perimeter(sta,tt),hyradius(sta,tt),...
velocity(sta,tt),velhead(sta,tt),energyt(sta,tt),slopef(sta,tt),...
fr2(sta,tt)]=geometrym(width(sta),hstart(sta,tt),discharge(tt),...
elevation(sta,tt),n,z);

%Calculate the critical depth along the channel
 if z == 0
  %hc for rectangular section
  hc(sta,tt) = ((discharge(tt)^2)/(9.81*width(sta)^2))^(1/3);
 else
  %hmin and hmax are the min and max initial bounds for the
  %bisection method iterations
  hmin = 0;
  hmax = 1.1*((discharge(tt)^2)/(9.81*width(sta)^2))^(1/3);
```

```
  %flag = 2 indicates the bisection function to compute
  %the critical depth
  flag = 2;
  [hc(sta,tt)] = bisection(discharge(tt),slope(sta,tt),n,width(sta),...
  z,hmin,hmax,flag);
 end

%Compute the average friction slope between stations sta and sta-1
 meansf(sta,tt) = (slopef(sta-1,tt)+slopef(sta,tt))*0.5;

 if velocity(sta-1,tt) > velocity(sta,tt)
%if the downstream velocity is greater than the upstream velocity
%an contraction occurs. Minor losses are summed to the total energy
%loss
 c = 0.1; %From Hec-Ras manual. Chapter 3
 elseif velocity(sta-1,tt) < velocity (sta,tt)
%if the downstream velocity is less than the upstream velocity
%an expansion occurs.
%Minor losses are summed to the total energy loss
 c = 0.3; %From Hec-Ras manual. Chapter 3
 else
 c = 0;
 end
%Compute the total energy at the u/s station (sta) as the
%total energy d/s plus the head lost between both stations plus
%minor losses
etstart(sta,tt) = energyt(sta-1,tt) + meansf(sta,tt)*dx(sta-1)+...
c*abs((velocity(sta-1,tt)^(2)-velocity(sta,tt)^(2)))/(2*9.81);
```

```
%Compute the difference in total energy in station sta by
%subtracting the total energy start (etstart)and the total
%energy computed with the function geometry energyt
 denergy(sta,tt) = energyt(sta,tt)-etstart(sta,tt);
 error(ni,tt) = abs(denergy(sta,tt));
 if ni == 1
    minerror = error(ni,tt);
    iteration  = ni;
    hsmin(sta,ni) = hstart(sta,tt);
    elseif error(ni,tt)< minerror
    minerror = error(ni,tt);
    iteration = ni;
    hsmin(sta,ni) = hstart(sta,tt);
 end
%Check if denergy is less than an specified error.  If so,
%the assumed elevation at the u/s station is right and we proceed
%to the next u/s station.  If not, a new value will be assumed.
%dhstart is added to the previous assumed depth to compute the
%new assumed depth. dhstart equation comes from Henderson (1966)
%book pp.143
 if abs(denergy(sta,tt)) <=0.001
 h(sta,tt) = hstart(sta,tt);
 %If h(sta,t) is in the wrong side of hc, h is set to hc
 if h(sta,tt) < hc(sta,tt)
 h(sta,tt) = hc(sta,tt);
 disp('Msg 1: h is set to hc');
 disp(sta);
 disp(t);
```

```
 end
 if width(sta) > width(sta-1) %there is a contraction
 %check if the specific energy is less than the critical
 %energy at the constriction
 %Specific energy at sta
 senergy(sta,tt) = velhead(sta,tt)+h(sta,tt);
 %critical energy at the next downstream station
 cenergy(sta-1,tt) = 3*hc(sta-1,tt)/2;
 %If energy < critical energy, the water has to backup
 %until it gets sufficient energy to pass
 if senergy(sta,tt) < cenergy(sta-1,tt)
 hmin = hc(sta,tt);
 hmax = 1.5*h(sta,tt);
 h(sta,tt) = bisectionme(hmin,hmax,discharge(tt),...
 cenergy(sta-1,tt),width(sta),z);
 disp('Msg2: h corresponds to critical energy downstream');
 disp(sta);
 disp(t);
 end
 end
 %Calling function geometrym
 [area(sta,tt),perimeter(sta,tt),hyradius(sta,tt),...
 velocity(sta,tt),velhead(sta,tt),energyt(sta,tt),...
 slopef(sta,tt),fr2(sta,tt)] =geometrym (width(sta),...
 h(sta,tt),discharge(tt),elevation(sta,tt), n,z);

%Compute the Courant-Friedrich-Levy number and check stability
courant(sta,tt) = dt*5*velocity(sta,tt)/(3*dx(sta-1));
```

```
  if courant(sta,tt)>1
    disp('the model is unstable');
  end

%increase the counter to compute the flow depth in the next
%upstream station
 sta = sta + 1;

%Initialized the number of iterations to 1 in the next station
 ni = 1;
 nii(sta,t) = 1;

%Assume a new hstart(sta) value equal to the d/s depth just
%calculated at 'sta'
 hstart(sta,tt) = h(sta-1,tt);
else
%Calculate the flow increment (dhstart)
 dhstart(sta,tt) = denergy(sta,tt)/(1-fr2(sta,tt)*(1-0.5*c)+...
 (3*slopef(sta,tt)*dx(sta-1))/(2*hyradius(sta,tt)));

%Add the flow increment to the assumed flow depth hstart
 hstart(sta,tt) = hstart(sta,tt)- dhstart(sta,tt);

%Increase the number of iterations
 ni = ni + 1;
 nii(sta,t) = nii(sta,t) +1;

%If hstart is negative, the solution will be
```

```
%the minimum error wse
 if hstart(sta,tt) < 0 | nii(sta,t) >= 50
 h(sta,tt) = hsmin(sta,iteration);
 disp('Msg 3:No solution for the energy equation was found.');
 disp('h is set to the minimum error h');
 disp(sta);
 disp(t);
 if width(sta) > width(sta-1) %there is a contraction
 %check if the specific energy is less than the critical energy
 %at the constriction
 %Specific energy at sta
 senergy(sta,tt) = velhead(sta,tt)+h(sta,tt);
 %Critical energy at the next downstream station
 cenergy(sta-1,tt) = 3*hc(sta-1,tt)/2;
 %If energy < critical energy, the water has to backup
 %until it gets sufficient energy to pass
 if senergy(sta,tt) < cenergy(sta-1,tt)
 hmin = hc(sta,tt);
 hmax = 3;
 h(sta,tt) = bisectionme(hmin,hmax,discharge(tt),...
 cenergy(sta-1,tt),width(sta),z);
 disp('Msg 4:h corresponds to critical energy downstream');
 disp(sta);
 disp(t);
 end
 else
 %if the minimum error wse < critical depth, h is set to critical
 if h(sta,tt) < hc(sta,tt)
```

```
 h(sta,tt) = hc(sta,tt);
 disp('Msg 5:h is set to hc');
 disp(sta);
 disp(t);
 end
 end
 %Compute the channel characteristics with the new depth
 [area(sta,tt),perimeter(sta,tt), hyradius(sta,tt),...
 velocity(sta,tt),velhead(sta,tt),energyt(sta,tt),...
 slopef(sta,tt),fr2(sta,tt)] =geometrym (width(sta),...
 h(sta,tt),discharge(tt),elevation(sta,tt), n,z);

 %Compute the Courant-Friedrich-Levy number and check stability
 courant(sta,tt) = dt*5*velocity(sta,tt)/(3*dx(sta-1));
   if courant(sta,tt)>1
      disp('the model is unstable');
   end

%Increase the number of stations
 sta = sta+1;
%Set number of iterations to 1
 ni = 1;
 nii(sta,t) = 1;
%New assumed depth equal to previous depth
 hstart(sta,tt) = h(sta-1,tt);
 end
 end
 end
```

```
 end
%Compute the bed shear stress in N/m2 based on the friction
%slope at each node
 i = 1:nstation;
 taubed(i,tt) = 9810*hyradius(i,tt).*slopef(i,tt);
 wselevation(i,tt) = elevation(i,tt)+h(i,tt);
%%%%%%%%% - SEDIMENT TRANSPORT - AGGRADATION/DEGRADATION - %%%%%%%
%Calculate the sediment discharge at each station using Julien's
%equation
%If discharge is zero, then the bed elevation and slope do not change
if discharge(t) == 0
 sta = 1:nstation;
 elevation(sta,tt+1) = elevation(sta,tt);
 slope(sta,tt+1) = slope(sta,tt);
 qst(sta,tt) = 0;
 else
 for sta = nstation:-1:1
 %Unit sediment discharge
 qbv(sta,tt) = julien(ds,taubed(sta,tt));
 %Sediment discharge in m3/day
 qst(sta,tt) = qbv(sta,tt)*width(sta)*86400;
 end
 for sta = nstation:-1:2
 %Change in sediment discharge between 2 adjacent stations
 dqst(sta-1,tt+1) = qst(sta-1,tt)-qst(sta,tt); %Out - in
 %Trap efficiency at time t+1 based on h and velocity computed at
 %time = t
 te(sta-1,tt+1) = 1-exp(-dx(sta-1)*omegai(tt)/(h(sta-1,tt)...
```

```
*velocity(sta-1,tt)));
%Change in bed elevation at time t+1
dz(sta-1,tt+1) = -te(sta-1,tt+1)*dqst(sta-1,tt+1)*dt/((1-po)...
*dx(sta-1)*0.5*(width(sta-1)+width(sta)));
%Volume out - volume in = sediment balance
balance(sta-1,tt+1) = dqst(sta-1,tt+1)*dt;
if dqst(sta-1,tt+1)>0 %there is degradation
%if the balance is >= available volume, everything will
%move downstream
if balance(sta-1,tt+1)>=avolume(sta-1,tt)
  %the new elevation is equal to the minimum elevation
   elevation(sta-1,tt+1) = minelev(sta-1,1);
  %Amount of sediment that goes into the next node = what comes
  %in in the previous one + the available volume
   ehqst(sta-1,tt) = qst(sta,tt)+ avolume(sta-1,tt)/dt;
  %the new available volume is zero, because everything was
  %moved out downstream
   avolume(sta-1,tt+1) = 0;
  else
  %if available volume is >balance, then only a part of the
  %available sediment is moved downstream
  avolume(sta-1,tt+1) = avolume(sta-1,tt)-balance(sta-1,tt+1);
  %compute new elevation at sta node due to the volume remaining
  elevation(sta-1,tt+1)=minelev(sta-1,1) + avolume(sta-1,tt+1)...
  /((1-po)*dx(sta-1)*(0.5*width(sta-1)+width(sta)));
  end
  else %there is aggradation
  elevation(sta-1,tt+1) = elevation(sta-1,tt) + dz(sta-1,tt+1);
```

```
   %Compute the available volume
   %balance is <0,when aggradation
   avolume(sta-1,tt+1) = avolume(sta-1,tt) - balance(sta-1,tt+1);
   end
   end
   if t < stime
      %Elevation upstream is given as a boundary condition
      elevation(nstation,tt+1) = uselevi(tt+1);
   else
      %The computations end at t = stime.  The elevation at t = stime
      %was computed in the previous time step
      elevation(nstation,tt+1) = elevation(nstation,tt);
   end
   for sta = nstation:-1:2
     %Calculate the new bed channel slope
     slope(sta,tt+1) = (elevation(sta,tt+1)...
     -elevation(sta-1,tt+1))/dx(sta-1);
   end
   slope(1,tt+1) = slope(1,tt);
   end
tt = tt+1; %increment the time index tt
%Printing out the results every maxday days
 if ndf - ndi == maxday
 tt = tt-1;
 numfile = int2str(ndf);
 fileout=strcat(numfile,'.out');
 fid = fopen(fileout,'wt');
 fprintf(fid,'%-15s %-11s %-12s %-12s %-15s...
```

```
%-12s %-12s %-12s %-12s %-12s %-15s %-12s\n',...
'days','Station','Length', 'Slope','Elevation'...
,'Width','Q','h','Sf','Fr2','hc','qst');
for k = lt:tt
ddiff = numday(k) - round(numday(k));
if ddiff == 0
for s = 1:nstation
fprintf(fid,'%6.1f\t %11d\t %11.2f\t %10.6e\t %11.6e\t...
%11.2f\t %11.2f\t %6.4f\t %10.2e\t %10.4e\t %6.4f\t %6.4f\n',...
numday(k), station(s), length(s),slope(s,k),elevation(s,k),...
width(s),discharge(k),h(s,k),slopef(s,k),fr2(s,k),hc(s,k),...
qst(s,k));
end
end
end
fclose(fid);
elevation(:,1) = elevation(:,tt+1);
slope(:,1) = slope(:,tt+1);
tt = 1;
lt = 1;
ndi = ndf;
elseif t == stime & time > maxday
numfile = int2str(ndf);
fileout=strcat(numfile,'.out');
fid = fopen(fileout,'wt');
fprintf(fid,'%-15s %-11s %-12s %-12s %-15s %-12s...
%-12s %-12s %-12s %-12s %-15s %-12s\n',...
'Station','Length', 'Slope','Elevation',...
```

```
  'Width','Q','h','Sf','Fr2','hc','qst');
 for k = lt:tt-1
 ddiff = numday(k) - round(numday(k));
 if ddiff == 0
 for s = 1:nstation
 fprintf(fid,'%6.1f\t %11d\t %11.2f\t %10.6e\t...
 %11.6e\t %11.2f\t %11.2f\t %6.4f\t %10.2e\t...
 %10.4e\t %6.4f\t %6.4f\n', numday(k),...
 station(s), length(s),slope(s,k),elevation(s,k),...
 width(s), discharge(k),h(s,k),slopef(s,k),...
 fr2(s,k),hc(s,k),qst(s,k));
 end
 end
 end
 fclose(fid);
 end
 t = t +1; %increment the total time index
end
%%%%%%%%% Writing the results into a file %%%%%%%%%
%Printing out the results if the total time is less
%than maxday days
if time < maxday fid = fopen(ofilename,'wt');
 fprintf(fid,'%-15s %-11s %-12s %-12s %-15s %-12s...
 %-12s %-12s %-12s %-12s %-15s %-12s\n',...
 'Slope','Elevation', 'Width','Q','h','Sf','Fr2',...
 'hc','qst');
 for k = 1:tt;
 ddiff = numday(k) - round(numday(k));
```

```
if ddiff == 0
for s = 1:nstation
fprintf(fid,'%6.1f\t %11d\t %11.2f\t %10.6e\t...
%11.6e\t %11.2f\t %11.2f\t %6.4f\t %10.2e\t...
%10.4e\t %6.4f\t %6.4f\n', numday(k),...
station(s), length(s),slope(s,k),elevation(s,k),...
width(s), discharge(k),h(s,k), slopef(s,k),...
fr2(s,k),hc(s,k),qst(s,k));
end
end
end
fclose(fid);
end
elapsedtime = etime(clock,t0);
fprintf('The elapsed time in seconds is = %6.3f\n',elapsedtime);
```

G.7 Code of Subroutines

G.7.1 Function: openfile1

```
function[nstation,station,length,slopei,elevationi,width,dx] =
openfile1(filedata)
%
%Purpose:
%This function opens the input file that contains the channel
%characteristic data.  The input variable is the
%filename and the output variables are number of stations,
%station number, length, initial slope, initial elevation,
%width and dx
%
```

```
if nargin < 1, error('Not input file name provided'), end
%%Reading the data
%
 fid = fopen(filedata,'rt');
%skip the first line;
 line = fgetl(fid);
%Assign the data to array T.  The input file must have 5
%columns (station, length, slope,elevation and width
 [T] = fscanf(fid,'%f',[5,inf]);
%T contains 5 rows. Row 1 = station, Row 2 = length and so
%on...T has to be transposed to obtain the same format as
%the input file. Column 1 = station, Column 2 = length, etc.
 T = T'; fclose(fid);
%N = the size of the array T.  The number of columns is known
%(5) but not the number of stations. The number of stations
%is the number of rows in matrix T
N = size(T);
%The number of stations is the first index of array N
 nstation = N(1);

 station = T(:,1);
 length = T(:,2);
 slopei = T(:,3);
 elevationi = T(:,4);
 width = T(:,5);

%Calculate delta x as the difference between the length of
%two adjacent stations
```

```
 i = 1:nstation-1; dx(i) = T(i+1,2) - T(i,2);
```

G.7.2 Function: openfile2

```
function [time,day, disc, temp,uselev] = openfile2(filedata)
%
%Purpose:
%This function opens the input file for the main script that
%contains the flow discharge data in m3/s ,the temperature in
%degrees Celsius, and the upstream elevation in m.
%The input variable is the filename and the output variables
%are time, discharge, temperature and elevation
%
if nargin < 1, error('Not input file name provided'), end
%%Reading the data
%
fid = fopen(filedata,'rt');
%skip the first line;
line = fgetl(fid);
%Assign the data to array T.  The input file must have 3
%columns (time, disc, temp)
%
[T] = fscanf(fid,'%f',[4,inf]);
%T contains 4 rows. Row 1 = time, Row 2 = discharge, Row 3 = temp,
%Row 4 = elev.  T has to be transposed to obtain the same format
%as the input file. Column 1 = time, Column 2 = discharge,
%Column 3 = temp,Column 4 = uselev
 T = T'; fclose(fid);
%N = the size of the array T.  The number of columns is known (3)
```

```
%but not the number of days.  The number of days is the number
%of rows in matrix T
N = size(T);
%The number of days is the first index of array N
time = N(1);

%The number of days is in the first column
day = T(:,1);

%The discharge is in the second column
disc = T(:,2);

%The temperature is in the third column
temp = T(:,3);

%The upstream elevation is in the fourth column
uselev = T(:,4);
```

G.7.3 Function: openfile3

```
function[nstation,station,length,slopei,elevationi,width,dx,minelev]
= openfile3(filedata)
%
%Purpose:
%This function opens the input file for the unsteady_2.m script.
%The input variable is the filename and the output variables
%are number of stations, station number, length, initial
%slope, initial elevation, width, minelev.
%
```

```
if nargin < 1, error('Not input file name provided'), end
%%Reading the data
%
%filedata = 'input.dat';
fid = fopen(filedata,'rt');
%skip the first line;
line = fgetl(fid);
%Assign the data to array T.  The input file must have 5 columns
%(station, length, slope,elevation and width)
[T] = fscanf(fid,'%f',[6,inf]);
%T contains 5 rows. Row 1 = station, Row 2 = length and so on...
%T has to be transposed to obtain the same format as the input
%file. Column 1 = station, Column 2 = length, etc.
T = T'; fclose(fid);
%N = the size of the array T.  The number of columns is known
%(5) but not the number of stations. The number of stations
%is the number of rows in matrix T
N = size(T);
%The number of stations is the first index of array N
 nstation = N(1);
 station = T(:,1);
 length = T(:,2);
 slopei = T(:,3);
 elevationi = T(:,4);
 width = T(:,5);
 minelev=T(:,6);
%Calculate delta x as the difference between the length of
%two adjacent stations
```

```
 i = 1:nstation-1;
 dx(i) = T(i+1,2) - T(i,2);
```

G.7.4 Function: bisection

```
function[hmean]=bisection(disc,slope,n,b,z,hmin,hmax,flag)
%Solving the f(x) = 0 using the bisection method.  This
%function computes the normal and the critical depth for a
%trapezoidal cross section
%
%Input data
%disch = flow discharge in m3/s
%slope = slope
%n = Manning friction factor
%b = Channel bottom width
%z = Channel side slope
%
%Other variables
%hmin = minimum depth for the initial iteration
%hmax = maximum depth for the initial iteration
%hmean = average depth between hmin and hmax
%range = error
%normal = function to compute the normal depth using
%Manning eq
 range = 1.e5;
   while range > 1.e-5
        hmean = 0.5*(hmin+hmax);
        if flag == 1;
```

```
if normal(disc,slope,n,b,z,hmin)*normal(disc,slope,n,b,z,hmean)<0
        hmax = hmean;
        range = abs(hmean - hmin);
            else
                hmin = hmean;
                range = abs(hmean-hmax);
            end
        else flag == 2;
if critical(disc,n,b,z,hmin)*critical(disc,n,b,z,hmean)<0
                hmax = hmean;
                range = abs(hmean - hmin);
            else
                hmin = hmean;
                range = abs(hmean-hmax);
            end
      end
 end
```

G.7.5 Function: normal

```
function [fhn] = normal(disc,slope,n,b,z,h)
%
%This function contains the equation to compute the normal
%depth using Manning Eq.
%Input data
%disch: discharge
%slope: slope
%n: Manning n
%b: Channel bottom width
```

```
%z: Side slope
%h: Flow depth
%g = gravitational acceleration in m/s2
%
g = 9.81;

%Compute area of trapezoidal section
area = ((b+z*h)*h);

%Compute perimeter of a trapezoidal section
per = b+2*h*sqrt(1+z^2);

%compute constant c1
c1 = ((disc*n)^(3/2))/slope^(3/4);

%Compute function of hn (normal depth)
fhn = ((area.^(5/2))./per)-c1;
```

G.7.6 Function: critical

```
function [fhc] = critical(disc,n,b,z,h)
%
%This function contains the equation to compute
%the normal depth using Manning Eq.
%Input data
%disch: discharge
%slope: slope
%n: Manning n
%b: Channel bottom width
```

```
%z: Side slope
%h: Flow depth
%g = gravitational acceleration in m/s2
%

g = 9.81;

%Compute area of trapezoidal section
area = ((b+z*h)*h);

%Compute top width of a trapezoidal section
t = b+2*z*h;

%Compute constant c1
c1 = disc/sqrt(g);

%Compute function of hn (normal depth)
fhc = area.^(3/2)./t^(1/2)-c1;
```

G.7.7 Function: conversion

```
function vis = conversion (t);
% convertion computes the kinematic viscosity of water as
% a function of temperature
% The input variable is
% t  -- water temperature in degrees Celsius
% The output variables is
% vis  -- kinematic viscosity in mš/s
```

```
% Calculate the kinematic viscosity.  This equation was
%generated from temperature-viscosity data from
% Fluid Mechanics book by Kundu (1990).  This equation is
%valid for 0<= temp <= 50 Celsius
vis = 4.496729E-10*t.^2 - 4.6205E-8 * t + 1.762786E-6;
```

G.7.8 Function: fallv

```
function omega = fallv (vis, d)
%fallv computes the fall velocity of sediment particles
%in m/s using Rubey's equation (from Julien 1995)
%The input variables are:
%vis    -- Kinematic viscosity in m2/s
%d      -- Sediment particle diameter in m
%Specific gravity G = 2.65 and gravity g = 9.81 m/sš

%The output and other variables are:
%omega      -- fall velocity in m/s

%Calculate a = (G-1)*g*d^3
%a = 1.65*9.81*d^3;
a = 1.65*9.81*d.^3;

%Calculate b = (G-s)*g*d
b = 1.65*9.81*d;

%Calculate fall velocity
 omega = (((2/3) + (36*vis.^2)./a).^(0.5)...
 -((36*vis.^2)./a).^0.5).*(b.^0.5);
```

G.8 Function:geometrym

```
function [area,perimeter,
hyradius,velocity,velhead,energyt,slopef,fr2]...
    = geometrym (width,h,disc,elevation, n,z);
%geometry computes the area, perimeter, hydraulic radius,
%velocity, velocity head, total energy and friction slope
%at a rectangular cross section.
%The input variables are:
%w      -- Channel width in m
%h      -- Flow depth in m
%discharge   -- Flow discharge in m3/s
%z      -- Channel elevation in m
%f      -- Friction factor

%Calculate the area in m2
area = (width+z*h)*h;
%Calculate the% wetted perimeter in m
perimeter = width + 2*h*sqrt(1+z^2);
%Calculate the hydraulic radius in m
hyradius = area./perimeter;
%Calculate the mean flow velocity m/s
velocity = disc./area;
%Calculate the velocity head in m
velhead = (velocity.^2)./(2*9.81);
%Calculate the total energy in m;
energyt = elevation + h + velhead;
%Calculate the friction slope in m/m, using D-W friction
%equation;
```

```
slopef = (disc.^2)*(n^2)./((area.^2).*(hyradius.^(4/3)));
%Calculate the Froude number squared
fr2 = (velocity.^2)./(9.81*h); %rectangular section
```

G.9 Function: bisectionm

```
function [hmean] = bisectionme(hmin,hmax,discharge,cenergy,b,z)
%Solving the f(x) = 0 using the bisection method.  This
%function solves the energy equation and outputs the flow
%depth
%
%Input data
%energyt = total energy at a previous station
%disc = flow discharge
%elevation = channel elevation at a downstream station
%n = Manning friction factor
%b = Channel bottom width
%z = Channel side slope
%h = known downstream depth
%
%Other variables
%hmin = minimum depth for the initial iteration
%hmax = maximum depth for the initial iteration
%hmean = average depth between hmin and hmax
%range = error
%minenergy = function to compute the energy equation
%in = number of iterations
    range = 1.e5;
    in = 1;
```

```
    while range > 1.e-10
        hmean = 0.5*(hmin+hmax);
 if minenergy(b,z,hmin,discharge,cenergy)*minenergy(b,...
              z,hmean,discharge,cenergy)<0
            hmax = hmean;
            range = abs(hmean - hmin);
        else
            hmin = hmean;
            range = abs(hmean-hmax);
        end
        in = in +1;
    end
```

G.9.1 Function: minenergy

```
function [fh] = minenergy(b,z,h,discharge,cenergy)
%
%This function contains the energy equation
%Input data
%cenergy = critical energy at the next downstream station
%discharge = flow discharge
%b = Channel bottom width
%z = Channel side slope
%h = unknown flow depth
%g = gravitational acceleration in m/s2
g = 9.81;
%Compute area
area = (b+z*h)*h;
%Compute the specific energy equation
```

```
fh = h - cenergy + (discharge^2)/(2*g*area^2);
```

G.9.2 Function: julien

```
function qbv = julien (d, taubed)
%julien computes the unit sediment discharge by volume in
%mš/s using Julien's (2001) sediment transport equation
%The input variables are:
%d      -- Sediment particle diameter in m
%taubed -- Bed shear stress in N/mš
%Specific gravity G = 2.65 and gravity = 9.81 m/sš

%The output and other variables are:
%taustart   -- Shields parameter
%qbv        -- unit sediment discharge by volume in mš/s

%Calculation of Shields parameter
taustart = (taubed/9810)./(1.65*d);

%Calculate the unit sediment discharge by volume
qbv = 18*sqrt(9.81)*(d.^(3/2)).*taustart.^2;
```

G.9.3 Function: yangs

```
function cmgl = yangs (vis, ds, taubed, v, sf, omega)
%yangs computes the concentration of sand in mg/l
%using Yang's (1973) sediment transport equation for sand
%particles.
%The input variables are:
%vis    -- Kinematic viscosity in mš/s
```

```
%ds      -- Sediment particle diameter in m
%taubed -- Bed shear stress in N/mš
%v      -- Mean flow velocity in m/s
%sf     -- Energy slope in m/m
%omega  -- Fall velocity in m/s of sediment particle of
%          diameter d

%Output and other variables:
%cmgl      -- Concentration in mg/l - output variable
%ustart    -- Shear velocity in m/s
%restart   -- Grain shear Reynolds number
%vcw       -- Dimensionless critical velocity
%a         -- ratio of shear velocity to fall velocity
%b         -- Fall velocity times diameter divided by
%             kinematic viscosity
%logcppm   -- Logarithm base 10 of concentration in ppm
%             according to Yang's equation
%cppm      -- concentration in ppm
%Water density = 1000 kg/m3
%Specific weight of sediment = 2.65
% Calculate shear velocity
ustart = (taubed./1000).^0.5;

% Calculate Grain shear Reynolds number
restart = ds.*ustart./vis;

% Calculate dimensionless critical velocity
if restart > 0 & restart < 70
```

```
    vcw = (2.5/(log10(restart)-0.06))+0.66;
elseif restart >= 70
    vcw = 2.05;
end
% Calculate the ratio of shear velocity to fall velocity
a = ustart./omega;
%Calculate the product of fall velocity times diameter,
%and divide it by viscosity
b = omega.*ds./vis;
% Calculate the product of vcw and sf
%c = vcw*sf;
    c = vcw.*sf;
% Calculate the product of v and sf and divide it by omega;
d = v.*sf./omega;

% Compare c and d.  If c > d, the sediment does not move
if c >= d
    cmgl = 0;
elseif c < d
%Calculate the logarithm (base 10)of the sediment concentration
%in ppm according to Yang's equation
logcppm = 5.435 -0.286*log10(b) - 0.457*log10(a) +...
(1.799-0.409*log10(b)-0.314*log10(a))*log10((d)-vcw.*sf);

%Convert the concentration in ppm to concentration in mg/l
 cppm = 10^logcppm;
 cmgl = 2.65*cppm./(2.65 +(1-2.65)*0.000001*cppm);
 end
```

G.9.4 Function: yangg

```
function cmgl = yangg (vis, d, taubed, v, sf, omega)
%yangg computes the concentration of gravel in mg/l
%using Yang's (1973) sediment transport equation for gravel
%particles.
%The input variables are:
%vis    -- Kinematic viscosity in mš/s
%d      -- Sediment particle diameter in m
%taubed -- Bed shear stress in N/mš
%v      -- Mean flow velocity in m/s
%sf     -- Energy slope in m/m
%omega  -- Fall velocity in m/s of sediment particle of
%          diameter d
%Output and other variables:
%cmgl      -- Concentration in mg/l - output variable
%ustart    -- Shear velocity in m/s
%restart   -- Grain shear Reynolds number
%vcw       -- Dimensionless critical velocity
%a         -- ratio of shear velocity to fall velocity
%b         -- Fall velocity times diameter divided by
%             kinematic viscosity
%logcppm   -- Logarithm base 10 of concentration in ppm
%             according to
%             Yang's equation
%cppm      -- concentration in ppm
%Water density = 1000 kg/m3
%Specific weight of sediment = 2.65
% Calculate shear velocity
```

```
ustart = (taubed./1000).^0.5;
% Calculate Grain shear Reynolds number
restart = ustart.*d./vis;
% Calculate dimensionless critical velocity
if restart > 0 & restart < 70
    vcw = (2.5/(log10(restart)-0.06))+0.66;
elseif restart >= 70
   vcw = 2.05;
end
%Calculate the ratio of shear velocity to fall velocity
a = ustart./omega;
%Calculate the product of fall velocity times diameter,
%and divide it by viscosity
b = omega.*d./vis;
% Calculate the product of vcw and sf
c = vcw.*sf;
% Calculate the product of v and sf and divide it by omega;
d = v.*sf./omega;

% Compare c and d.  If c > d, the sediment does not move
if c >= d
    cmgl = 0;
elseif c < d
%Calculate the logarithm (base 10)of the sediment
%concentration in ppm according to Yang's equation
logcppm = 6.681 -0.633*log10(b) - 4.816*log10(a) +...
2.784-0.305*log10(b)-0.282*log10(a))*...
log10((v.*sf./omega)-vcw.*sf);
```

```
%Convert the concentration in ppm to concentration in mg/l
 cppm = 10^logcppm;
 cmgl = 2.65*cppm./(2.65 +(1-2.65)*0.000001*cppm);
 end
```

G.10 Typical Input File

The input file consists of a text file (space delimited) with five columns. The first column contains the station number along the channel, the second column contains the accumulated channel length at each station, the third column lists the initial channel slope at each station, the fourth column contains the initial bed elevation at each station and the fifth column includes the channel width at each station. The input file is free format, which means that the widths of each column do not need to be specified. Also, the first row of the input file must contain the headings of each column. The second row of the file represents the first downstream station. All the units are metric. A typical input file follows.

Station	Length	Slope	Elevation	Width
500	0	0.00143	0	90
400	100	0.00143	0.143	90
300	200	0.00143	0.286	90
200	300	0.00143	0.429	90
100	400	0.00143	0.572	90
0	500	0.00143	0.715	90

G.11 Output File

The user of the program has to specify the number of days (maxday) that will be written out in each output file. The program will create a matrix that storages the variables that will be output for each day for the number of days specified by the

user. Each time the data are output and written to a file, the content of the matrix is replaced by the values that will be output in the next output file. Therefore, if the channel in consideration has many stations and the time step is very small, it is recommended to choose a small value for the variable maxday. In that way, the matrix will be small and the program will run faster. However, it will generate more output files. The output files are text files, which take small memory space. Also, they are named as <number>.out, where <number> is the last day printed on the file. For example, the file 20.out contains the output for the days 1 to 20.

The output file consists of 11 columns that contain the following: day number, station, length in m, slope in m/m, elevation in m, width in m, discharge in m^3/s, flow depth in m, energy slope in m/m, Froude number squared and sediment discharge in m^3/d.

Appendix H

Simulations with Different Sediment Sizes

This appendix presents the results of the simulations performed in the study reach of the Middle Rio Grande (described in Chapter 6) using three different bed material sizes to compute the sediment transport. The first simulation consists of computing the sediment transport with the median bed material size ($d_s = 0.26\ mm$) (see Figure 6.10 in Chapter 6). The second simulation consists of computing the sediment transport based on an equivalent diameter (Molinas and Wu, 1998), in order to compensate for size gradation. The third simulation consists of computing the sediment transport by size fractions without changing the gradation of the bed at each time step.

The equivalent diameter is equal to (Molinas and Wu, 1998):

$$D_e = \frac{1.8 D_{50}}{1 + 0.8(V_*/\omega_{50})^{0.1}(\sigma_g - 1)^2.2}$$

where, D_e is the equivalent diameter, D_{50} is the particle size for which 50 percent of bed material are finer by dry weight, V_*, is the shear velocity, ω_{50} is the fall velocity of a sediment particle size D_{50}, and σ_g is the standard deviation of the bed material defined by: $\sigma_g = \sqrt{D_{84}/D_{16}}$. D_{84} and D_{16} are the particle sizes for which 84 and 16 percent of bed material are finer by dry weight respectively.

Figure H.1 shows the comparison of the model results for the three cases. The bed degradation was controlled only in the last two downstream sections.

There are only some slight differences on the profiles in Figure H.1, which indicates that the bed material is almost uniform. The results obtained with d_{50} and D_e are almost the same for the upper and middle reaches. The results obtained

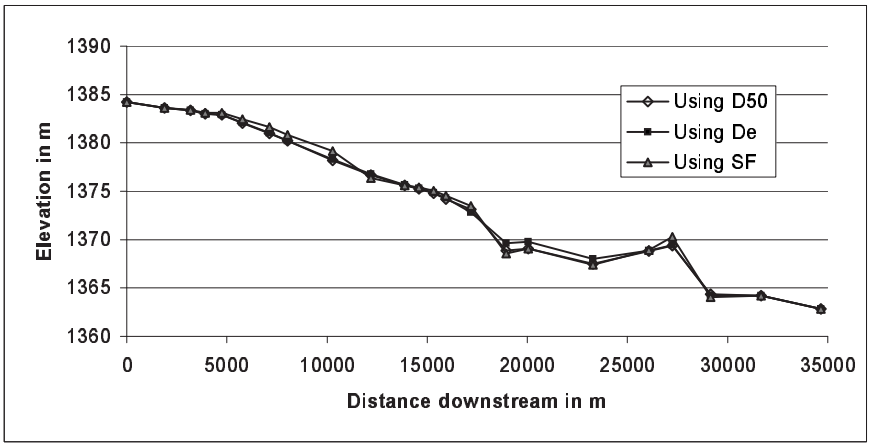

Figure H.1: Bed elevation profiles obtained by computing the sediment transport with a single diameter (d_{50} and D_e) and by size fraction.

by calculating the sediment transport by size fractions are similar to the results of the computations with the d_{50} in the downstream reach. Sediment transport estimations by size fractions are greater than the computations with a single diameter. The use of a single diameter such as d_{50} does not seem to introduce large errors in the simulations, given the close agreement between the simulations with d_{50}, D_e and size fraction.

Usually, erosion produces coarsening of the bed material. Therefore, the erosion obtained by size fractions without changing the gradation of the bed each time (as simulated in here) will be greater than the erosion obtained when changing the gradation of the bed. Rivera-Trejo and Soto-Cortés (2002) demonstrated that aggradation/degradation simulations calculated by size fractions and changing the gradation of the bed each time, produce an intermediate solution between the simulations performed with a single diameter and by size fractions without changing the gradation of the bed. The results presented in this appendix do not consider coarsening of the bed. However, the error of not considering such condition do not seem to be very large, given the good agreement between the three cases (d_{50},D_e and size fraction).

Appendix I

Intermediate Results of Model Validation

This appendix contains the comparison of the model results (see Chapter 6), with the field measurements in the middle Rio Grande in 1993, 1997 and 1998. In addition the field data collected in 1999 is compared to three different results from the numerical model: 1) using the unsteady flows from 1992 to 1999; 2) using the steady state flows equal to the mean annual flow during that period (Q = 39 m^3/s); and 3) using the dominant discharge equal to Q = 139 m^3/s.

I.1 Comparison of Model Simulations with 1993, 1997 and 1998 Field Measurements

Figures I.1, I.2 and I.3 show the plot of the measured bed elevation against distance for 1993, 1997 and 1998 respectively. The slopes of each subreach was estimated by fitting a regression line to the data and are indicated in the plots.

The slope of the wide reach is steeper than the slopes of the two narrow reaches for all the surveys. The surveys were performed in different months and therefore, in different points of the flow regime.

Figures I.4 (a) and (b), I.5 (a) and (b), and I.6 (a) and (b), presents the comparison of the model results with the field data. Model results are closer to the measurements, when the maximum degradation of the bed is controlled along the entire channel. However, in both cases (a and b), the model predicts the same trends. The wide reach develops steeper slopes than the slopes of the narrow reaches.

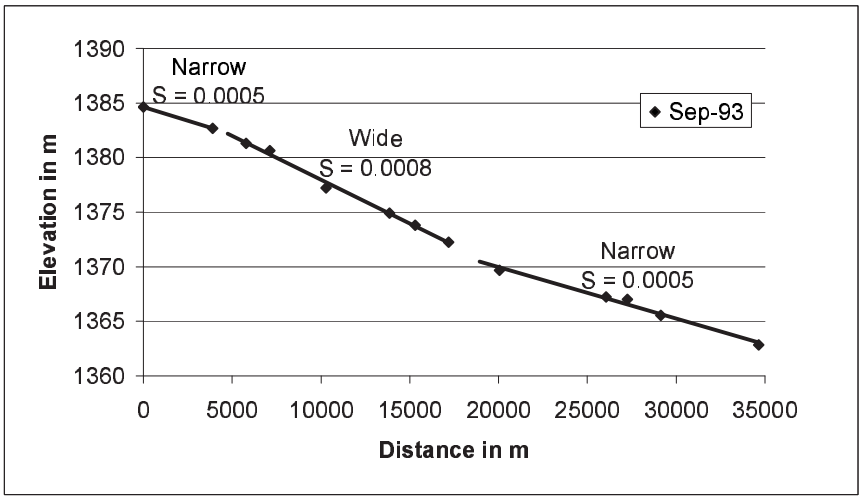

Figure I.1: Measured bed elevation against downstream distance for September 1993.

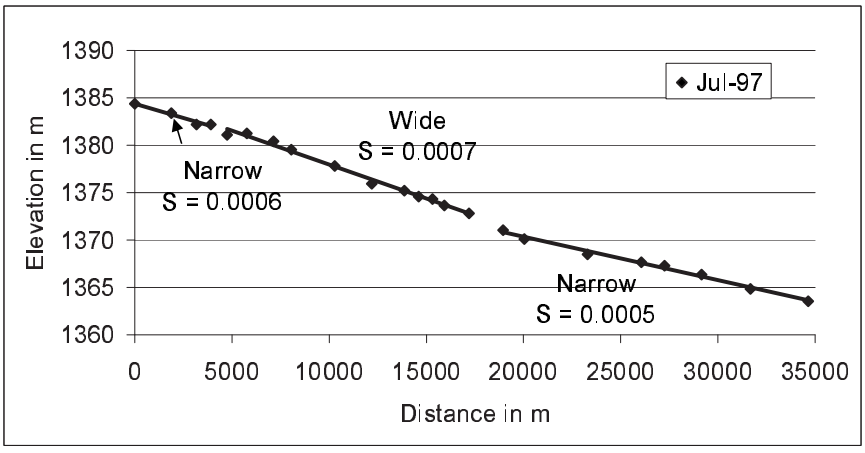

Figure I.2: Measured bed elevation against downstream distance for July 1997.

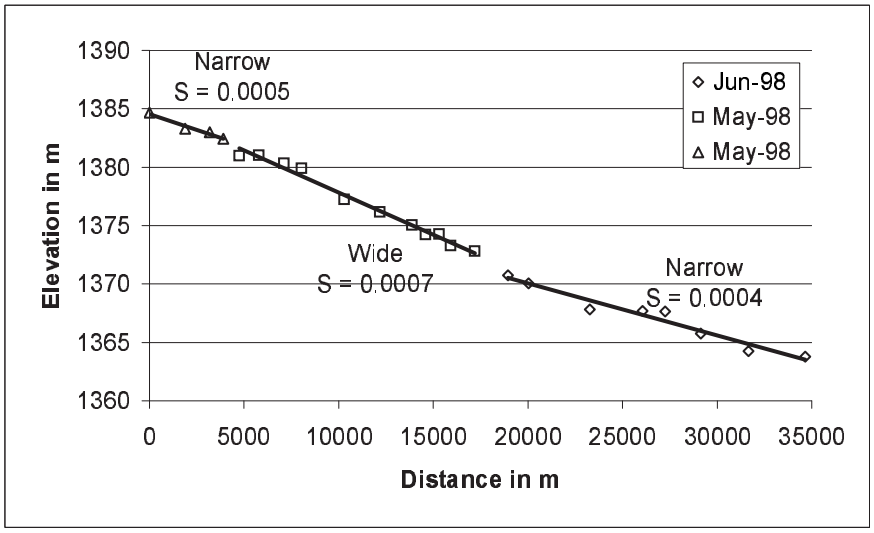

Figure I.3: Measured bed elevation against downstream distance for May-June 1998.

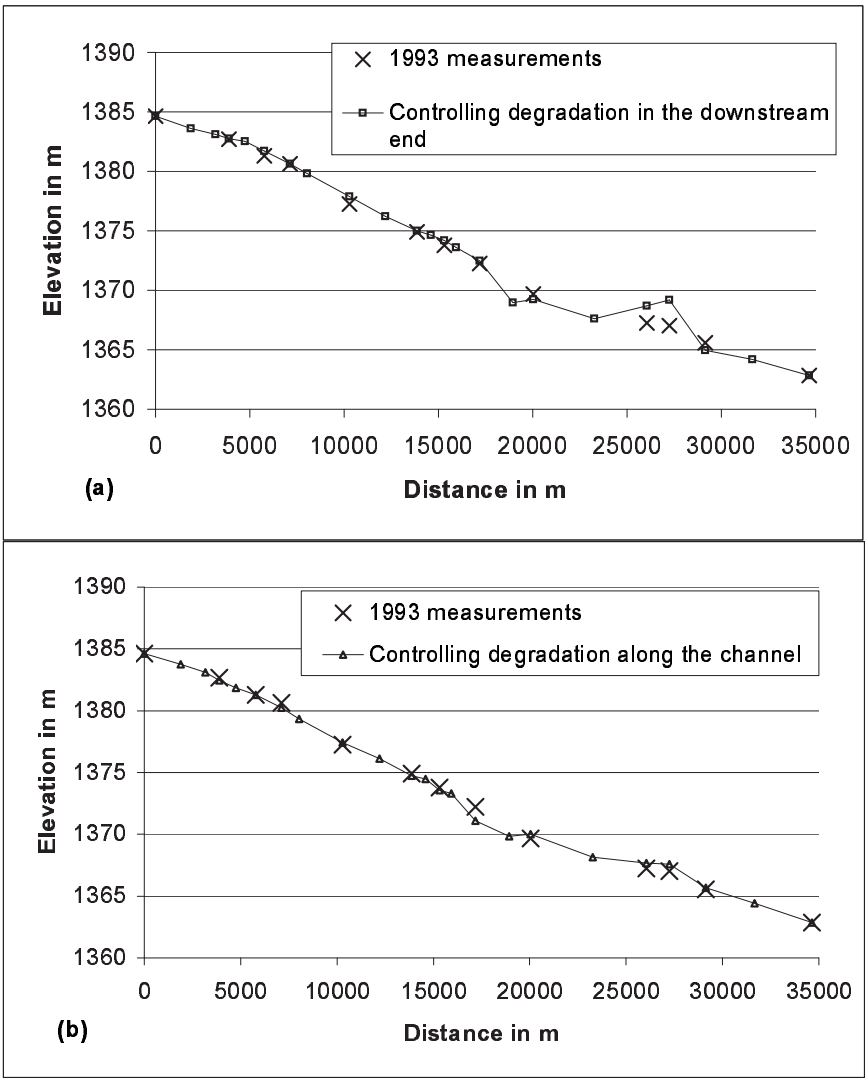

Figure I.4: Comparison of the resulting channel profile from the sediment transport model with the field data collected in 1993. (a) Channel degradation is controlled in the last two downstream nodes of the reach. (b) Channel degradation is controlled along the entire channel.

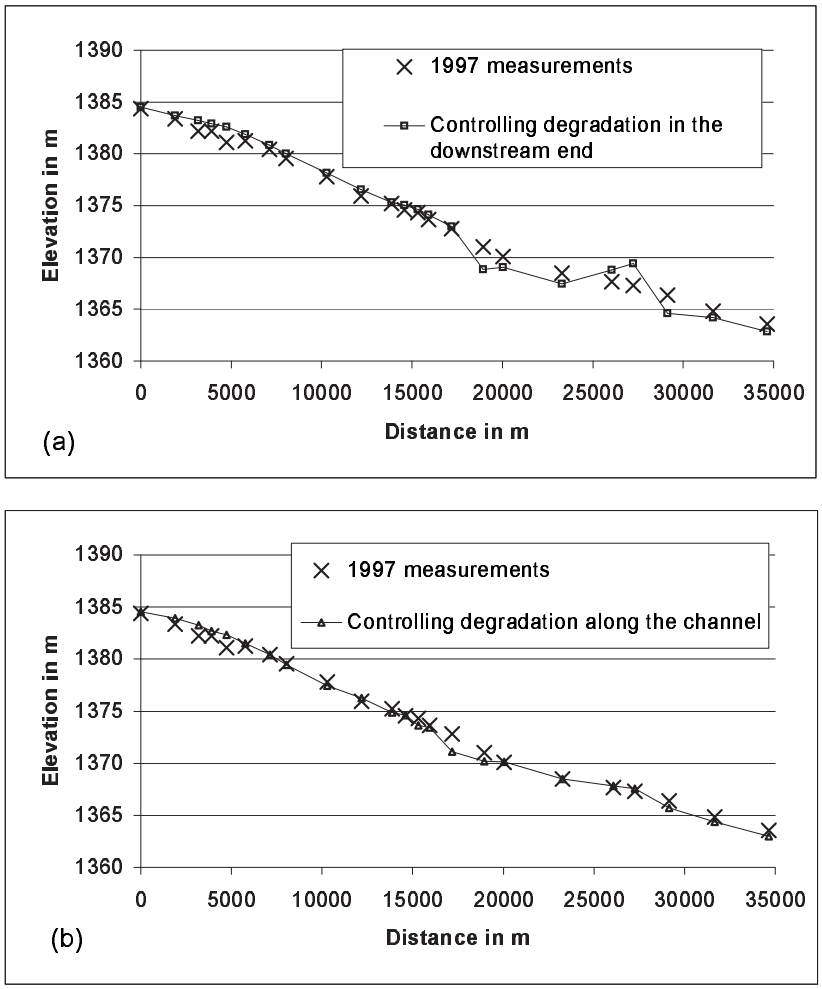

Figure I.5: Comparison of the resulting channel profile from the sediment transport model with the field data collected in 1997. (a) Channel degradation is controlled in the last two downstream nodes of the reach. (b) Channel degradation is controlled along the entire channel.

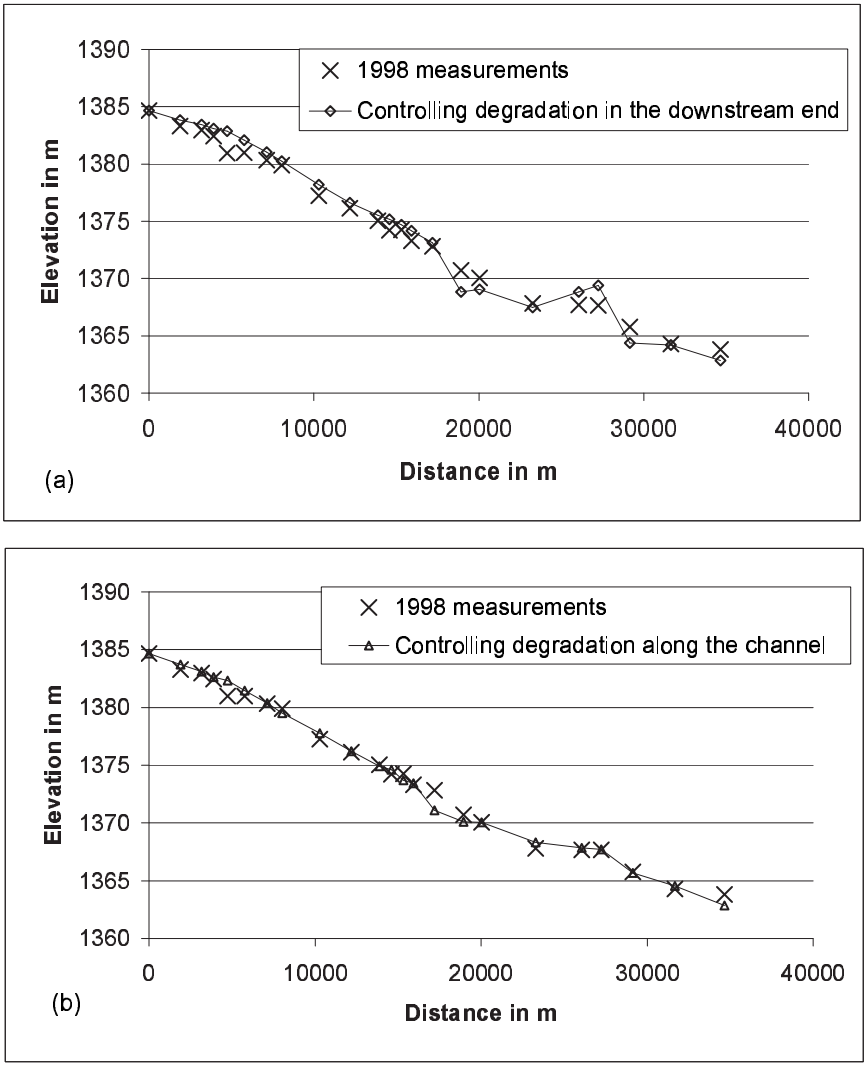

Figure I.6: Comparison of the resulting channel profile from the sediment transport model with the field data collected in 1998. (a) Channel degradation is controlled in the last two downstream nodes of the reach. (b) Channel degradation is controlled along the entire channel.